ABSTRACT

In this study, a basic mathematical model for the in-human host and in-mosquito dynamics of malaria parasite is formulated. A positive invariant region of the model was established, and a basic reproduction number $\mathcal{R}_0$, of the model was computed. Conditions for existence and stability of two equilibrium points: malaria free equilibrium (MFE) and malaria infection equilibrium (MIE) were established.

The impacts of model parameters on control of malaria infection were assessed through the sensitivity analysis of $\mathcal{R}_0$. Despite having lower sensitivity index compared to death rate of merozoites, and death rate of schizonts have greater impact on malaria control than that of merozoites.

The model was extended to incorporate the effect of immune responses using nonlinear bounded Michaelis- Menten-Monod functions to describe how immune responses interact with infected cells and parasites. Our results revealed that immunity has significant influence on reducing malaria infection at erythrocytic and sporogonic stages, but not at exo-erythrocytic stage.

We further extended the model to incorporate the antimalarial drug therapy, where four therapeutic classes of antimalarial drugs in various stages of entire life cycle of malaria parasite are included. In contrast to the immunity whose effect reduces infections on only two stages, drug therapy has the effect of reducing infection on all stages of the life cycle. Although its components do not appear in the expression of reproduction number, tissue schizonticidal drugs reveal a substantial effect on reducing the infection at each stage of malaria life cycle.

This study suggests that a combination therapy with all four classes of antimalarial drugs should be developed because of its prolific effect on controlling malaria, and for such case, an artemisinin derivatives-primaquine combination therapy is proposed.

DECLARATION

I, **MOHAMED ABDALLAH SELEMANI** do hereby declare to the Senate of Nelson Mandela African Institution of Science and Technology that this dissertation is my own original work and that it has neither been submitted nor being concurrently submitted for degree award in any other institution.

Mohamed Abdallah Selemani

Name and signature of candidate **Date**

The above declaration is confirmed

Prof. Livingstone Luboobi 17 December 2017

Name and signature of supervisor 1 **Date**

Dr. Yaw Nkansah-Gyekye 18-12-2017

Name and signature of supervisor 2 **Date**

COPYRIGHT

CERTIFICATION

The undersigned certify that they have read and hereby recommend for acceptance by the Nelson Mandela African Institution of Science and Technology (NM-AIST) in Arusha, the dissertation titled, ***Modelling the in-human Host and in-mosquito Dynamics of Malaria Parasite and Effect of Therapy***, in the partial fulfillment of the requirements for the degree of Doctor of Philosophy in Applied Mathematics and Computational Science of the NM-AIST.

Prof. Livingstone Luboobi _____ 17 December 2017

Name and signature of supervisor 1 **Date**

Dr. Yaw Nkansah-Gyekye _____ 18-12-2017

Name and signature of supervisor 2 **Date**

ACKNOWLEDGEMENTS

This work appears in its current form due to the assistance and guidance of several individuals. So, I would like to acknowledge them, each one in a unique way for making a successful completion of this work.

First and foremost, I sincerely thank my supervisors Prof. Livingstone Luboobi and Dr Yaw Nkansah-Gyekye, whose intellectual, professional guidance and supervision to the completion of this study are immeasurable and priceless. I have been extremely lucky to have supervisors who answered to my questions and queries so promptly, to ensure that this work is accomplished within allocated time-frame. Their commitment is extremely appreciated. I also thank all staff at Dean's office, school of Computational and Communication Sciences and Enginnering (CoCSE) who helped me in one way or another.

Great tribute to my sponsor, Tanzania Commission for Science and Technology (COSTECH) by providing me full financial support for my studies, and my employer, Sokoine University of Agriculture for granting me a three years study leave.

Thanks to my colleagues of PhD (Applied Mathematics) of the 2014-16 cohort at Nelson Mandela African Institution of Science and Technology (NM-AIST): Halid, Rigobert, Jairos, Selemani, Jacob and Adeline for the stimulating discussions, for the sleepless nights we were working together before deadlines, and for all the fun we have had in the three years of our stay at NM-AIST.

I am grateful to my parents and parents-in-law for their support, encouragement and persistent prayers they've made on my behalf. Their prayers for me are what sustained me thus far.

Last but not the least, a special thank and appreciate to my family for their patience and encouragement during the entire period of my studies. To my loving, supportive, encouraging, and patient wife Awetu whose faithful support during all stages of this PhD is so appreciated. To my two lovely little kids, Farhad and his sister Junainah, who missed out on a lot of their father's time during my absence for the entire period of three years.

However, none of the individuals mentioned above can be held accountable to any fault found in this study, so I remain solely responsible for all the deficiencies. May the Almighty God bless you all abundantly

DEDICATION

Awetu

&

Junainah and Farhad

To you, my precious wife and children I dedicate this work.

TABLE OF CONTENTS

LIST OF TABLES

LIST OF FIGURES

LIST OF APPENDICES

LIST OF ABBREVIATIONS

MFE	Malaria Free Equilibrium
MIE	Malaria Infection Equilibrium
HLCs	Hepatic Liver Cells
uHLCs	Uninfected Hepatic Liver Cells
iHLCs	Infected Hepatic Liver Cells
RBCs	Red Blood Cells
uRBCs	Uninfected Red Blood Cells
iRBCs	Infected Red Blood Cells
WHO	World Health Organization
NM-AIST	Nelson Mandela African Institution of Science and Technology
CoCSE	Computational and Communication Sciences and Enginnering
COSTECH	Commission for Science and Technology

CHAPTER ONE

Introduction

1.1 Background Information

Despite numerous efforts taken by both governments and non-governmental organizations to combat malaria, the impact of the disease on public health and economic growth is still high (Chamwali, 2013; White *et al.*, 2014). For instance, malaria constitutes 9-10 percent of the total of Africa's disease burden with dreadful economic consequences (Onyido *et al.*, 2010). Moreover, according to World malaria report (WHO, 2015), about 3.2 billion people worldwide are still at risk of contracting malaria and 80% of people who die of malaria are in Africa, and the incidence is high in sub-Saharan Africa. Between 2005 and 2014, the global expenditure on treatment and control of malaria increased from US$ 960 million to US$ 2.5 billion at rate of 4%.

Malaria is a communicable disease caused by a *Plasmodium* parasite and transmitted to humans through bites of female mosquitoes of genus *Anopheles*. Over 430 species of *Anopheles* exists, but only 30-40 of them can transmit malaria (Centers for Disease Control and Prevention, 2015). Moreover, out of a hundred plus species of *plasmodium* which can infect vertebrates, only four: *plasmodium falciparum, plasmodium vivax, plasmodium ovale* and *plasmodium malariae* infect humans (U. S. National Institute of Allergy and Infectious Diseases, 2007).

P.falciparum is the most pathogenic and highly fatal species of *plasmodium* that infects humans, which is prevailing in Africa. *P.vivax* is the widespread and predominant species that causes malaria in temperate regions (Latin America and Southeast Asia), but with less impact compared to *P.falciparum*. Two remaining species constitute a small percent of human malaria infection worldwide (Medicine for malaria venture, 2016). However, *plasmodium* parasites of all these species develop through almost the same life cycle.

1.1.1 Malaria Life Cycle

The life cycle of *plasmodium* is a complex and multi-stage, in which a parasite lives within two living organisms: a vertebrate host and a mosquito vector. To comprehend the cycle, we conceptulize it as set of three sub-cycles: the *exo-erythrocytic* cycle (A), the *erythrocytic* cycle (B) and the *sporogonic* cycle (C) as indicated in Fig. 1. The first two take place within human being and last-mentioned occurs in mosquito. In a definitive host (mosquito), *plasmodium* undergo

sexual reproduction while in a human (intermediate host), they undergo asexual reproduction, initially in hepatic liver cells (HLCs) and then repeatedly, in red blood cells (RBCs).

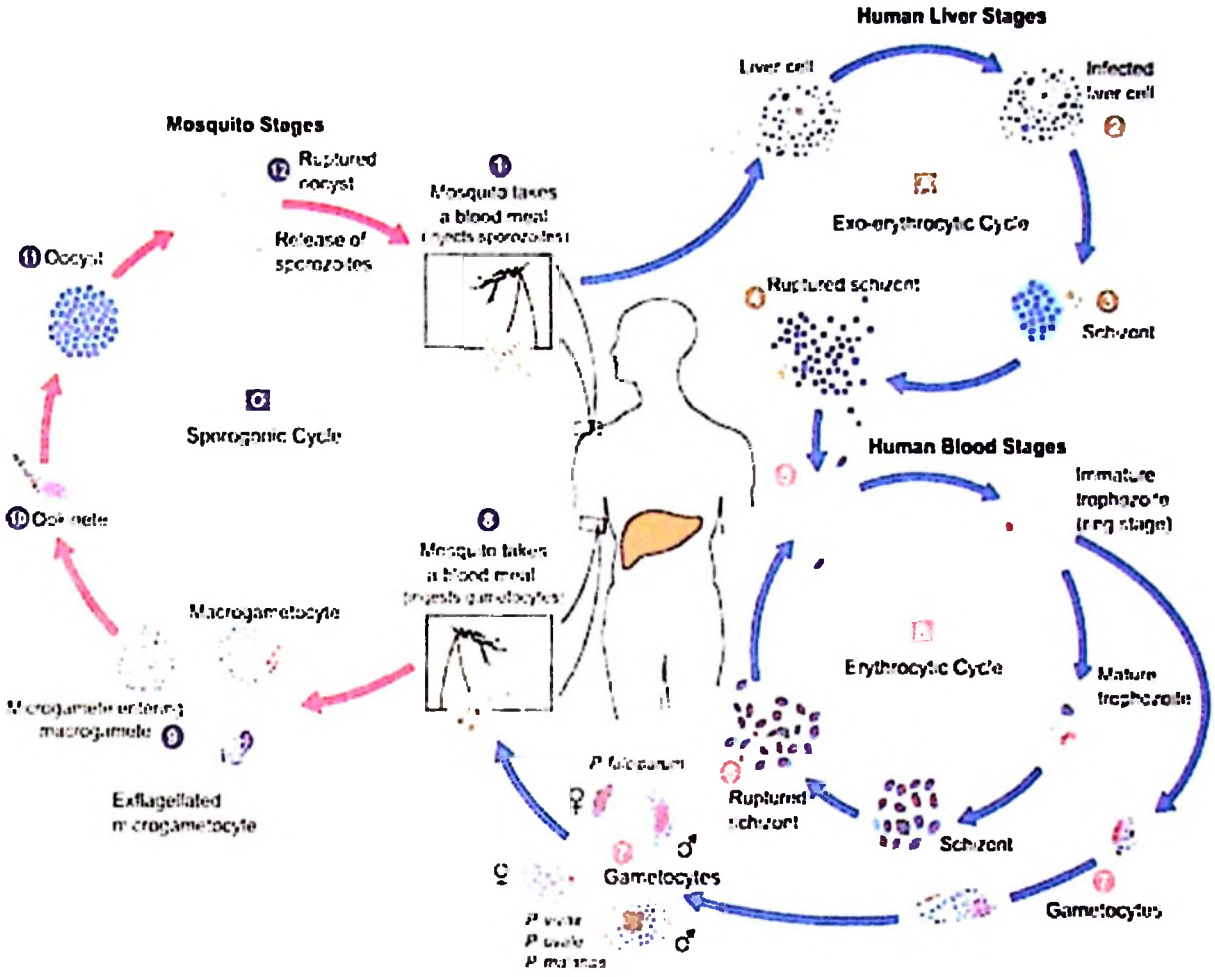

Figure 1: Malaria Life Cycle [Source: Centers for Disease Control and Prevention (2016)]

The exo-erythrocytic cycle is initiated by a bite from a parasite-carrying mosquito which seeks for blood to facilitate egg development, where sporozoites are injected into the bloodstream through the dermis (1). A number of injected sporozoites into human per bite is independent of sporozoites' population in mosquito's salivary gland (usually less than 25 sporozoites per bite), (Da *et al.*, 2015). Sporozoites quickly migrate to the liver and penetrate HLCs (2), where they develop to schizonts (3)-(4) that burst and give rise to thousands of merozoites (Corradin and Levitskaya, 2014) into the bloodstream marking the beginning of erythrocytic cycles. But for *P.vivax* and *P.ovale*, some of the liver stage parasites termed *hypnozoites* remain dormant in hepatic cells, where they may remain for months or even years before being activated and cause

relapses by attacking RBCs. Therefore, the asexual replication may be instigated without a new mosquito bite.

Merozoites invade RBCs (5), and initiate another mitotic replication within RBCs which is faster and less prolific compared to that in the liver (Chiyaka *et al.*, 2008). Then, they develop into erythrocytic schizonts (6) which finally burst and release an average of 16 merozoites (Garcia *et al.*, 2006; Tumwiine *et al.*, 2008) which re-invade new healthy RBCs. For still unknown reasons, some of these merozoites (approximately 1%) switch to the sexual form of parasites termed gametocytes (7) (Kiszewski, 2010; Delves *et al.*, 2012), a form of the parasite responsible for transmission to mosquito (Klein, 2013), and it takes place at or before the merozoites stage (Bannister and Sherman, 2009).

The sporogonic stage of parasite's life cycle begins when a parasite-free mosquito ingests the mature gametocytes (8), which are sexually dimorphic (microgametocytes and macrogametocytes) during its blood-meal, which then transform into gametes within the mosquito's midgut (9). The number of gametocytes ingested by mosquito per bite depends on gametocytes' density in bloodstream (Da *et al.*, 2015). Ingested gametocytes generate male and female gametes within the mosquito, which then fuse and further develop into oocysts (10)-(11). The oocysts rupture and release an average of 1000 sporozoites each (Nelson and Williams, 2014) that migrate to salivary glands ready for new mosquito-human transmission (12).

1.1.2 Malaria immunology

A major role of the human immune system is to defend a body against the infection-causing organisms, called pathogens like bacteria, virus, fungi and parasites. Human immune system has two main components termed as: innate (non-specific) immunity and adaptive (specific) immunity. Innate immune responses defend the body against any pathogenic invasion, while adaptive immune responses provide protection against a specific pathogen, and usually comes into action after the infections outrun the innate immunity. Innate immune responses include macrophages, interferon (IFN) and natural killer (NK) cells, while T-lymphocyte (cytotoxic T and helper T cells) and B-lymphocyte (B-cells) are some elements of adaptive immune responses. Cellular-mediated responses involves cell effectors such as cytotoxic T ($CD8^+$ T) and NK cells to kill intracellular pathogens while humoral responses involve effector molecules such as antibodies (secreted by B-cells) to clear free pathogens in body's fluid such as blood.

In malaria infection, both innate and adaptive immune responses are stimulated (Li *et al.*, 2011; Langhorne *et al.*, 2008) to obstruct parasites by either preventing the re-invasion of parasite or increasing the death rate of infected cells (Good, 2001; Stevenson and Riley, 2004; Li *et al.*, 2011), and both humoral and cell-mediated immune effector mechanisms are involved

in immunology of malaria (Langhorne *et al.*, 2008; Kinyanjui, 2012). Antibodies neutralize the sporozoites and merozoites and inhibit sporozoites' invasion to HLCs (Kinyanjui, 2012; Langhorne *et al.*, 2008) and merozoites' invasion to RBCs (Tumwiine *et al.*, 2008; Kinyanjui, 2012). They also restrain the parasite growth (Chiyaka *et al.*, 2008; Kinyanjui, 2012; Dent *et al.*, 2008). Macrophages are activated by NK cells to intensify phagocytosis and clearance of intra-erythrocytic parasites (Artavanis-Tsakonas *et al.*, 2003). The IFN-γ produced by $CD8^+$ T cells (in help of $CD4^+$) inhibit growth of, and kill intrahepatic parasites (Kinyanjui, 2012; Artavanis-Tsakonas *et al.*, 2003; Langhorne *et al.*, 2008). Moreover, antibodies and complement system that are ingested by mosquito during blood meal mediate the lysis of gametocytes and inhibit development of parasite in the mosquito (Langhorne *et al.*, 2008).

1.1.3 Antimalarial Drugs and Malaria Life Cycle

Pharmacotherapy is one of the the top three interventions to control and eliminate malaria, along with the use of insecticide-treated mosquito nets and indoor residual spraying (WHO, 2015). Antimalarials are categorized according to their pharmacodynamics and the stage in parasites life cycle they target. A tissue schizonticide is an antimalarial drug that destroys sporozoites or hepatic schizonts to prevent erythrocytic invasion, while the blood schizonticide is an antimalarial drug which acts on the asexual erythrocytic forms of parasites such as schizonts and merozoites to terminate the clinical attacks. A drug that destroys gametocytes in the bloodstream and prevents human-mosquito transmission is termed a gametocytocide. An antimalarial drug that inhibits sporogonic phase of malaria parasite within mosquito is called sporontocide. It either inhibits the formation of ookinete (fusion of gametes) and oocysts or kills sporozoites within a mosquito (Bullock and Manias, 2013).

A combination therapy is a treatment in which two or more classes of drugs with different biochemical properties and independent mechanism of actions are administered to a patient. Despite increasingly drug resistance by parasites , the use of antimalarial combination therapies is reported to be effective (Targett *et al.*, 2001; Price and Douglas, 2009; Eziefula *et al.*, 2014) as it reduces a likelihood of parasite to develop a drug resistance. However, this effectiveness is associated with the species of *plasmodium* and the stage of its life cycle that is targeted. For example, almost all blood schizonticides including artemisinin derivatives also serve as gametocytocides for immature gametocytes of *P.falciparum*, and mature gametocytes for other three remaining species (White, 2008; Boni *et al.*, 2008; Eziefula *et al.*, 2014). Primaque is the only existing gamocytocide for mature *P.falciparum* (Feachem and Sabot, 2008; White, 2013), that serves as tissue schizonticide for all species of *Plasmodium* (Sirimulla, 2007). Additionally, Primaque has a sporontocidal activity for all species with exception of *P. falciparum* (Kiszewski, 2010).

1.1.4 Mathematical Modelling on Malaria Dynamics

Mathematical models have been the useful tool to study the dynamics of infectious diseases because in most cases, real experiments are either impossible, unethical or expensive (Lutambi *et al.*, 2013). Understanding the complexity of *plasmodium's* life cycle, where parasite develops through various stages with unique shape and structure, suggests the use of mathematical models to increase insight on the disease dynamics and improve the likelihood of developing new safe and effective control strategies to rid us of malaria.

Over the past century, the use of mathematical models in examining the transmission dynamics of malaria has increasingly attracted researchers' interest (Mandal *et al.*, 2011). The earliest mathematical model for malaria transmission was formulated by Ross in 1911 (Cai *et al.*, 2013), which concluded that elimination of malaria can be achieved by reducing a mosquito population to be less than a certain threshold value, that depends on a number of mosquito bites and vectorial capacity. This was criticized by Tumwiine *et al.* (2014) that reducing mosquito population would have little effect on the epidemiology of malaria in areas with intense transmission.

As a consequence of the emergence and re-emergence of the disease, there have been a dramatic increase in mathematical modelling of both between-host and within-host dynamics of malaria. To date, various between-hosts models have been developed, which incorporate different features such as seasonality (Singh *et al.*, 2005), immunity (Tumwiine *et al.*, 2007a; Labadin *et al.*, 2009; Cai *et al.*, 2013), immigration (Singh *et al.*, 2005; Tumwiine *et al.*, 2010), age structure (Tumwiine *et al.*, 2008), vector contact rates (Lutambi *et al.*, 2014), and effects of heterogeneous transmission rates (Chitnis, Smith and Steketee, 2008) and the references therein.

On the other hand, a number of studies on mathematical modelling of *in vivo* (within-host) dynamics of malaria parasites have been done. Anderson *et al.* (1989) introduced the earliest model for *in vivo* dynamics of malaria, in which the interaction between uninfected RBCs, infected RBCs, and free merozoites was discussed. Extension of the model was done by many authors to incorporate the effect of immune effectors [See examples in Iggidr *et al.* (2006); Tumwiine *et al.* (2008); Dube *et al.* (2010); Li *et al.* (2011)], though some of these studies such as Li *et al.* (2011) ignored the absorption effect of parasites on human cells, where both populations (uninfected cells and parasites) decreases during the infection. However, the works of Tumwiine *et al.* (2008) and Chiyaka *et al.* (2008) are examples of studies in which the absorption effect was incorporated. In these studies, clearance of both free parasites and infected cells by immune responses were modelled either as a simple mass-action (Tumwiine *et al.*, 2008; Chiyaka *et al.*, 2008), an unbounded function or using the Michaelis-Menten-Monod function (MMMF) which is a nonlinear bounded function (Li *et al.*, 2011). In addition, Chiyaka *et al.* (2008) incorporated the effect of antibodies to inhibit parasites' production or block invasion of

host's cell by parasites using MMMF.

1.2 Rationale of the Study

Pharmacotherapy is among the best interventions against malaria (WHO, 2015). Antimalarial drugs are categorized according to their pharmacodynamics and the stage in *plasmodium's* life cycle they target. One advantage of combination therapies is to reduce the development of drug resistance, as pathogens may not be resistant to multiple drugs simultaneously. However, most of the currently used antimalarial drugs target mainly the erythrocytic stages of *plasmodium's* life cycle, but the eradication of malaria requires new drugs that will target various stages of the entire *plasmodium's* life cycle (Delves *et al.*, 2012). Thus, the in-human host and in-mosquito dynamics of *plasmodium* in relation to their interaction with combination therapy should be investigated to get insight on developing a new safe and effective drug to eradicate or control malaria.

1.3 Statement of the Problem

Evaluating the efficacy of control strategies through controlled experiments is practically infeasible, unethical or expensive (Lutambi *et al.*, 2013). Malaria parasite has a complex and multi-stage life cycle, in which parasite goes through distinct developmental stages as it moves from the mosquito to the human and back again. Understanding the complexity of this life cycle, suggests the use of mathematical models to increase insight on the disease dynamics and improve the likelihood of developing new effective control strategies. In this study, we formulated and analyzed the mathematical models which describe in-human host and in-mosquito dynamics of malaria parasite in entire life cycle of malaria parasites with effects of stage-specific immune responses and drug therapy.

1.4 Objectives

1.4.1 General objective

The general objective of this study was to formulate and analyze mathematical models for in-human host and in-mosquito dynamics of malaria parasite in the entire life cycle with effects of stage-specific immune responses and drug therapy.

1.4.2 Specific objectives

The specific objectives were:

(i) To formulate and analyze a basic mathematical model for the in-human host and in-mosquito dynamics of malaria parasites.

(ii) To formulate and analyze mathematical model for the in-human host and in-mosquito dynamics of malaria parasites with effect of immune responses.

(iii) To formulate and analyze a mathematical model for the in-human host and in-mosquito dynamics of malaria parasites with effect of treatment.

1.5 Research Questions

This study intended to answer the following research questions:

(i) How can the malaria infection of non-immune individual can be controlled?

(ii) Why does the malaria persist?

(iii) How can the immune system work during malaria infection?

(iv) How can malaria infection of individual with temporary immunity be controlled?

(v) What do current antimalarial drugs target?

(vi) What are the best antimalarial drugs to be used in controlling malaria?

1.6 Structure of the Dissertation

This work comprises of six chapters and the rest of the chapters are organized as follows:

Chapter 2: Mathematical description and formulation of a basic model for in-human host and in-mosquito dynamics of malaria parasites is presented. Analysis of the model including: determination of a positive invariant region, the existence of malaria-free equilibrium and computation of basic reproduction number, $\mathcal{R}_0$. Furthermore, the chapter covers discussion on the sensitivity analysis of $\mathcal{R}_0$ and some numerical simulations to assess impact of model parameters on $\mathcal{R}_0$.

Chapter 3: Stability analysis of equilibrium points of the model formulated in Chapter 2 is established, whereby conditions for their existence and stability are discussed. The chapter also presents numerical simulations to support and complement the theoretical findings.

Chapter 4: In this chapter, we extend the basic model presented in Chapters 1 and 2, by incorporating the effect of immune responses in all three phases of *plasmodium's* life cycle. An

extended model is analyzed. Numerical simulations and a detailed discussion of the results is presented.

Chapter 5: In this chapter, we extended the model presented in Chapter 4 by incorporating the effect of drugs in various stages of *plasmodium*'s life cycle. Analytical and numerical analysis of the extended model are presented.

Chapter 6: This chapter summarizes the results and concludes the study by giving recommendations on possible directions for extending this work.

1.7 List of Articles

The following articles were prepared for publications in the course of this study:

(i) Selemani, M. A, Luboobi, L. S, and Nkansah-Gyekye, Y. (2017a). Modelling the in-human host and in-mosquito dynamics of malaria parasites. *Journal of Mathematical and Computational Science*, **7**(3): 430-455.

(ii) Selemani, M. A, Luboobi, L. S, and Nkansah-Gyekye, Y. (2016). On Stability of the in-human host and in-mosquito dynamics of malaria parasites. *Asian Journal of Mathematics and Applications*. **2016**.

(iii) Selemani, M. A, Luboobi, L. S, and Nkansah-Gyekye, Y. (2017b). The in-human host and in-mosquito dynamics of malaria parasite with immune response. *New Trends in Mathematical Sciences*, **5**(3): 182-207.

(iv) Selemani, M. A, Luboobi, L. S, and Nkansah-Gyekye, Y. Modelling the in-human host and in-mosquito dynamics of malaria parasite with effect of immune responses and anti-malarial therapy. *Mathematical Biosciences* (In Review).

CHAPTER TWO

Modeling the in-human host and in-mosquito dynamics of Malaria Parasite[1]

Abstract

In this chapter, we proposed a basic mathematical model to describe in-human host and in-mosquito dynamics of malaria. The basic reproduction number, $\mathcal{R}_0$ of this model is established. Sensitivity analysis of $\mathcal{R}_0$ with respect to each of the parameters is carried out in model validation. Based on their sensitity indices, effects of these parameters were discussed to determine their implications in the control of malaria infection. Infection rate of red blood cells (RBCs) by merozoites, the death rate of merozoites, number of merozoites released per rupturing schizont were found to be crucial parameters in control strategies. Moreover, a number of merozoites released per rupturing schizont and the proportion of merozoites that proceed with asexual replication are the most sensitive parameters. However, numerical simulations show the latter is biologically impractical since a reduction in its magnitude reduces the number of merozoites and at the same time increases the number of gametocytes. Despite having lower sensitivity index compared to the death rate of merozoites, the death rate of schizonts has a greater impact on malaria control than that of merozoites.

2.1 Introduction

Despite being both preventable and curable, the impact of malaria on both public health and economic growth worldwide is still increasing (White *et al.*, 2014). Children under the age of five years and pregnant women are the most affected groups, and the incidence is highest in sub-Saharan Africa. For instance, in 2012, malaria killed almost one child below the age of five years in every minute worldwide (WHO, 2013) and global expenditure on malaria control increased from an estimated US$ 960 million to US$ 2.5 billion at annual rate of 4% between 2005 and 2014 (WHO, 2015).

In vertebrate hosts, malaria infection is caused by parasites of more than one hundred species of *Plasmodium*, but only four of these: *Plasmodium falciparum*, *Plasmodium vivax*, *Plasmodium ovale* and *Plasmodium malariae* infect humans. Among them, *P. falciparum* is the most pathogenic to humans, especially in Africa. The infection due to *P. falciparum* can develop quickly and produce several life-threatening complications such as miscarriage, fluid in the

[1]This chapter is based on the research paper: Mohamed A. Selemani, Livingstone S. Luboobi, Yaw Nkansah-Gyekye. Modelling the in-human host and in-mosquito Dynamics of Malaria Parasite (2017a). *Journal of Mathematical and Computational Science*, 7(3): 430-455.

lungs, kidney failure, abnormal liver function, anemia, low blood sugar. However, with immediate and effective treatement, it is always curable (Tumwiine *et al.*, 2008; WHO, 2015).

Between human hosts, malaria parasites are transmitted by bites of infected female mosquitoes. Malaria parasite has a complex and multi-stage life cycle in which parasite goes through over a dozen of discernible stages of development as it moves from the mosquito vector to the human host and back again (Oaks Jr *et al.*, 1991). A simple way to conceptualize this cycle is to consider it as a set of three sub-cycles: the *exo-erythrocytic* cycle [stage 1-3], the *erythrocytic* cycle [stage 4-5] and the *sporogonic* cycle [stage 6-9] (See Fig. 2). The first two cycles take place in human being and the latter occurs in mosquito. In mosquitoes, malaria parasites undergo sexual reproduction by merging the parasites sexual cells (macrogametes and microgametes) while in human, the parasite undergo asexual reproduction (by cell division), initially in hepatocyte liver cells (HLCs) and then, repeatedly, in red blood cells (RBCs).

The exo-erythrocytic cycle starts when the infected mosquito injects *sporozoites*, infectious form of parasites, into human host's skin during its blood meal. Within 15-30 minutes sporozoites travel to the liver through some defensive hepatic macrophages (Kupffer cells) which are impermeable to drugs (Dube *et al.*, 2010). The number of sporozoites injected is independent of sporozoites number within mosquito's salivary gland, and in most case less than twenty five sporozoites are injected per bite (Da *et al.*, 2015). In the liver, sporozoites infect the HLCs where they undergo asexual (mitotic) replication and mature to *schizonts*. After 5-16 days matured liver schizonts rupture and release thousands of *merozoites*, invasive form of malaria parasites, into the blood stream.

The erythrocytic cycle starts when the released merozoites recognize and invade RBCs. After 48 hours, merozoites starts another mitotic replication in RBCs which is quicker and less prolific compared to that in the liver (Chiyaka *et al.*, 2008). In RBCs they develop into matured schizonts through ring and trophozoite stages, which finally rupture and release an average of 16 new merozoites per infected RBCs (Garcia *et al.*, 2006) that re-invade other healthy RBCs. In each replication cycle, merozoites develop into one of two ways, either as *asexuals*, which go on to produce other new merozoites, or *sexually*, as gametocytes, which is form of parasite responsible for transmission to mosquito (Klein, 2013). Although, the reason some merozoites switch to gametocytes is not adequately researched, this occurs at or before the merozoites stage (Bannister and Sherman, 2009).

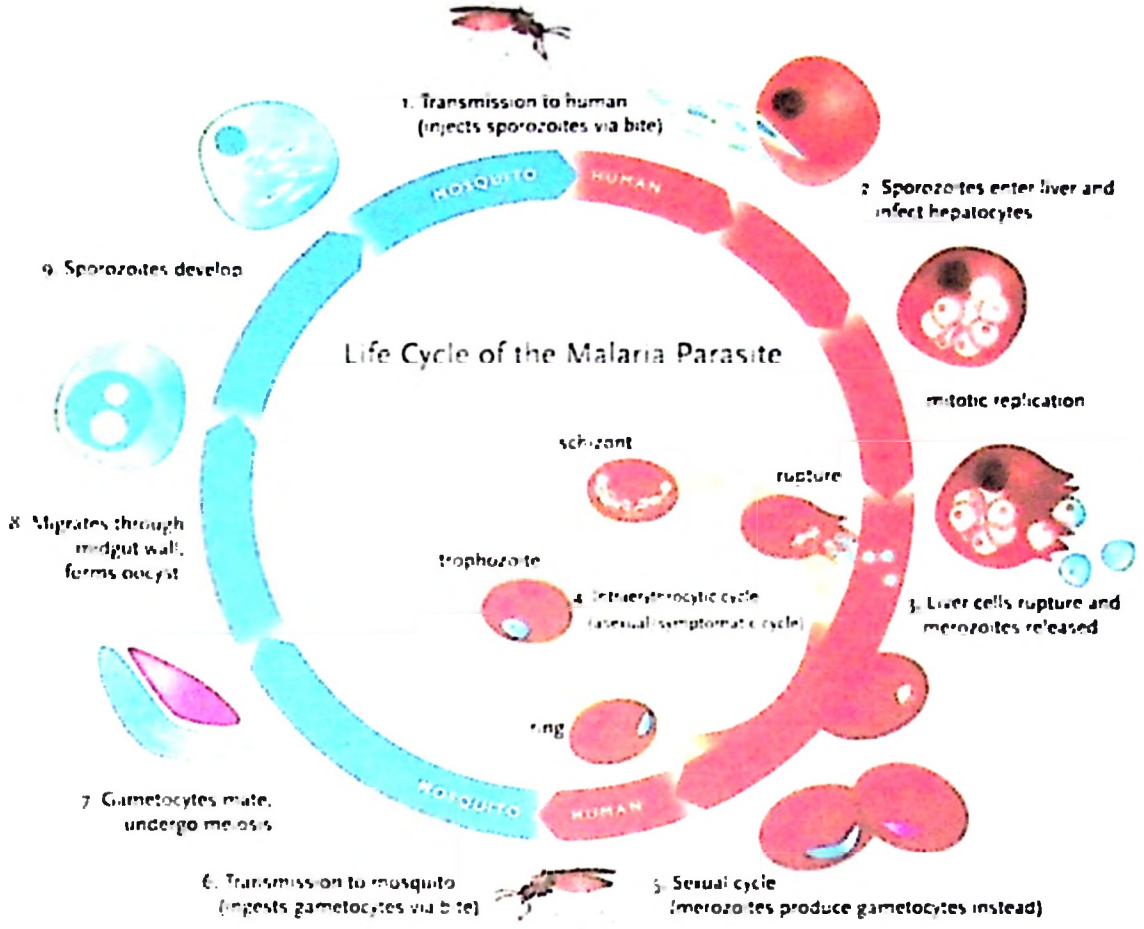

Figure 2: Malaria Life Cycle: (Klein, 2013)

The sporogonic cycle starts when a blood feeding-mosquito takes its meal and ingests gametocytes which then transformed into gametes within the mosquito's midgut. The number of gametocytes ingested by mosquito per bite depends on gametocytes load in bloodstream (Da *et al.*, 2015). The male and female gametes fuse and form a mobile fertilized zygote called ookinete that develops into oocyst. Finally, oocysts grow, rupture, and release sporozoites that migrate to the mosquito's salivary glands, ready for transmission to a new host.

Mathematical models have been a useful tool to study the dynamics of infectious diseases because in most cases real experiments are either impossible, unethical or expensive (Lutambi *et al.*, 2013). Undestanding the complexity of this life cycle, where parasite develops through various stages with unique shape and structure each, suggests the use of mathematical models to increase insight on the disease dynamics and improve the likelihood of developing new safe and effective control strategies to rid us of malaria (Haque and Engwerda, 2014; Cai *et al.*, 2013).

Several studies on mathematical modelling of *in vivo* dynamics of malaria parasites have been

done. Among the earliest models used to discuss *in vivo* dynamics of malaria was the one presented by Anderson and others in 1989 as described in Chiyaka *et al.* (2008) and Iggidr *et al.* (2006), where interaction between unifected RBCs, infected RBCs, and free merozoites was discussed. The extension of this model was done by many other authors to include immune effectors. [See Tumwiine *et al.* (2008); Chiyaka *et al.* (2008); Li *et al.* (2011) and the references therein]. Further extension of the model was done by Chiyaka *et al.* (2008) to include the antibodies and treatment.

All of these studies discussed the erythrocytic dynamics of malaria parasites. To the best knowledge of the authors, exo-erythrocytic and sprogonic dynamics have not adequately covered in the study of mathematical modelling for dynamics of malaria parasites. Moreover, Prudêncio *et al.* (2011) argued that liver stage has greatest and most under-exploited potential for intervention, despite being the most understudied stage of malaria parasite. In this chapter, we formulated and analyzed a basic mathematical model that includes all phases of malaria parasite's life cycle, in which the sporozoites-HLCs and merozoites-RBCs interaction assumed to be the mass action.

2.2 Model Formulation

2.2.1 In-human Host and in-mosquito Dynamics of Malaria Parasites

The model has two settings, within the human host and within the mosquito. Within the human host, the cells are divided into two sub-populations namely, the hepatocytes liver cells (HLCs) and the red blood cells (RBCs). HLCs are divided into uninfected HLCs, H; early infected HLCs, I_h; and matured infected HLCs (Liver-Schizonts), T_h. The RBCs are divided into uninfected RBCs, R; early infected RBCs, I_r; matured infected RBCs (Blood-Schizonts), T_r; which develop to either asexual form called merozoites, M; or sexual form called gametocytes, G_b.

Within the vector, when the mosquito bites the infected human it takes in gametocytes, which develops into mature sexual cells called gametes, G_m. The female and male gametes fuse and develop to Oocysts, C; and finally ruptures and form sporozoites, S_m. Table 1 shows the variables of the model.

Table 1 :List of state variables

Variable	Description
S_h :	number of sporozoites in human
H :	number of uninfected HLCs
I_h :	number of infected HLCs
T_h :	number of liver schizonts
T_r :	number of blood schizonts
M :	number of merozoites
R :	number of uninfected RBCs
I_r :	number of infected RBCs
G_h :	number of gametocytes
G_m :	number of gametes
C :	number of Oocysts
S_m :	number of sporozoites in mosquito

An infected mosquito bites an uninfected human host and injects the sporozoites, S_h; into the bloodstream at constant rate abv, where a is probability that a mosquito bite is infective to human, b is number of mosquito bites per individual, and v is number of sporozoites injected per bite. Within a short period of time (usually 15-30 minutes), sporozoites travel to the liver, where they attack the healthy HLCs, H at a rate $\beta_1 S_h H$; and multiply asexually in liver cells to generate infected HLCs I_h, which progress to liver-schizont, T_h at the rate, $\alpha_1 I_h$. Over time, T_h rupture to release merozoites, M at the rate $\delta_1 T_h$. Merozoites enter the bloodstream and attack uninfected RBCs, R; at the rate $\beta_2 RM$, and multiply again to generate infected RBCs, I_r. The I_r develop to blood-schizont, T_r at a rate $\alpha_2 I_r$. The T_r rupture to release r_2 new merozoites per cell at a rate, $\delta_2 T_r$. Some of these released merozoites continue with asexual multiplication to produce other merozoites, at $p\delta_2 T_r$ and invade new RBCs. Some of them switch to gametocytes, G_h (sexual form) at a rate $(1-p)\delta_2 T_2$.

An uninfected mosquito bites an infected human and ingests the gametocytes, G_b; which develop further into mature sexual cells called gametes, G_m; at the rate $\rho q \omega G_b$, where ρ is number of bites a mosquito made during its lifetime, ω is number of gametocytes ingested per bite and q is probability that a mosquito bite is infective to mosquito while G_b is number of gametocytes in blood stream. In the mosquito's midgut the microgametes fuse with macrogametes to form ookinetes that develop into oocysts C, at a rate, $\alpha_3 G_m$. Then, C; ruptures to release sporozoites S_m at a rate, $\delta_3 C$ which migrates to salivary glands ready for infection to the new host.

H and I_h die at rates, μ_h and μ_{ih} respectively, while T_h dies at a rate μ_{th}. Similary, R and I_r

die at rates μ_r and μ_{ir} respectively while T_r dies at a rate μ_{tr}. The death rates of S_h and S_m are μ_{sh} and μ_{sm} respectively, and that of M is, μ_m. The HLCs and RBCs are recruited from bone marrow at rates Λ_h and Λ_r respectively. The parameters used in this model are described in Table 2.

Table 2 : Parameters and their descriptions

Parameter	Description
a :	probability that a bite infects human
b :	number of mosquito bites per individual
c :	number of sporozoites injected per bite
β_1 :	infection rate of HLCs by sporozoites
r_1:	number of merozoites per liver schizont
α_1 :	progression rate of infected HLCs to schizonts
δ_1 :	rupture rate of liver schizonts
Λ_h :	the recruitmet rate of HLCs
μ_h :	natural death rate of uninfected HLCs
μ_{ih} :	death rate of infected HLCs
μ_{th} :	death rate of liver-schizonts
β_2 :	infection rate of RBCs by merozoites
δ_2 :	rupture rate of blood schizonts
α_2 :	progression rate of infected RBCs to schizonts
r_2 :	number of merozoites per blood schizont
q :	probability that a bite is infectious to mosquito
ω :	number of gametocytes ingested per bite
ρ :	number of bites made by mosquito in its lifetime
Λ_r :	the recruitmet rate of RBCs
μ_r :	natural death rate of uninfected RBCs
μ_{ir} :	total death rate of uninfected RBCs
μ_{tr} :	death rate of blood-schizonts
μ_m :	death rate of merozoites
μ_{gb} :	death rate of gametocytes in bloodstream
δ_3 :	rupture rate of Oocysts
r_3:	number of sporozoites per Oocyst
α_3 :	progresion rate of gametes to Oocysts
μ_{gm} :	death rate of gametes in mosquito's midgut
μ_c :	death rate of Oocysts
μ_{sm} :	death rate of sporozoites in mosqouito
μ_{sh} :	death rate of sporozoites in human liver
p:	proportion of asexual that differentiate to merozoites

2.2.2 Model Assumptions

In development of this model, we made the following assumptions:

(i) The HLCs are regenerated at constant rate from bone marrow stem cells and die naturally.

(ii) The RBCs are released from bone marrow at a constant rate and die naturally.

(iii) HLCs and RBCs are infected at a rate proportional to their density.

(iv) Mosquito-human infection is independent of sporozoites load in salivary gland, while human-mosquito infection depends on gametocytes load in blood stream (Da *et al.*, 2015).

(v) The infected cells die faster than uninfected ones.

(vi) The injected sporozoites and the released merozoites either die or successfully infect the HLCs and RBCs respectively.

(vii) The ingested gametocytes either die or macrogametes and microgametes successfully fuse.

(viii) Constant proportion of asexual parasites converts to gametocytes within each cycle.

(ix) The cycle starts when the infected mosquito bites the human.

(x) Bite of an infected mosquito onto an infected host is neglected.

(xi) Survival of mosquito depends on human blood for developing their eggs.

2.2.3 Compartmental diagram

Based on the dynamics described in Subsection 2.2.1 and the assumptions described in Subsection 2.2.2, the proposed model for the in-human host and in-mosquito dynamics of malaria parasites is shown in Fig. 3, the variables and parameters are described in Table 1 and Table 2 respectively.

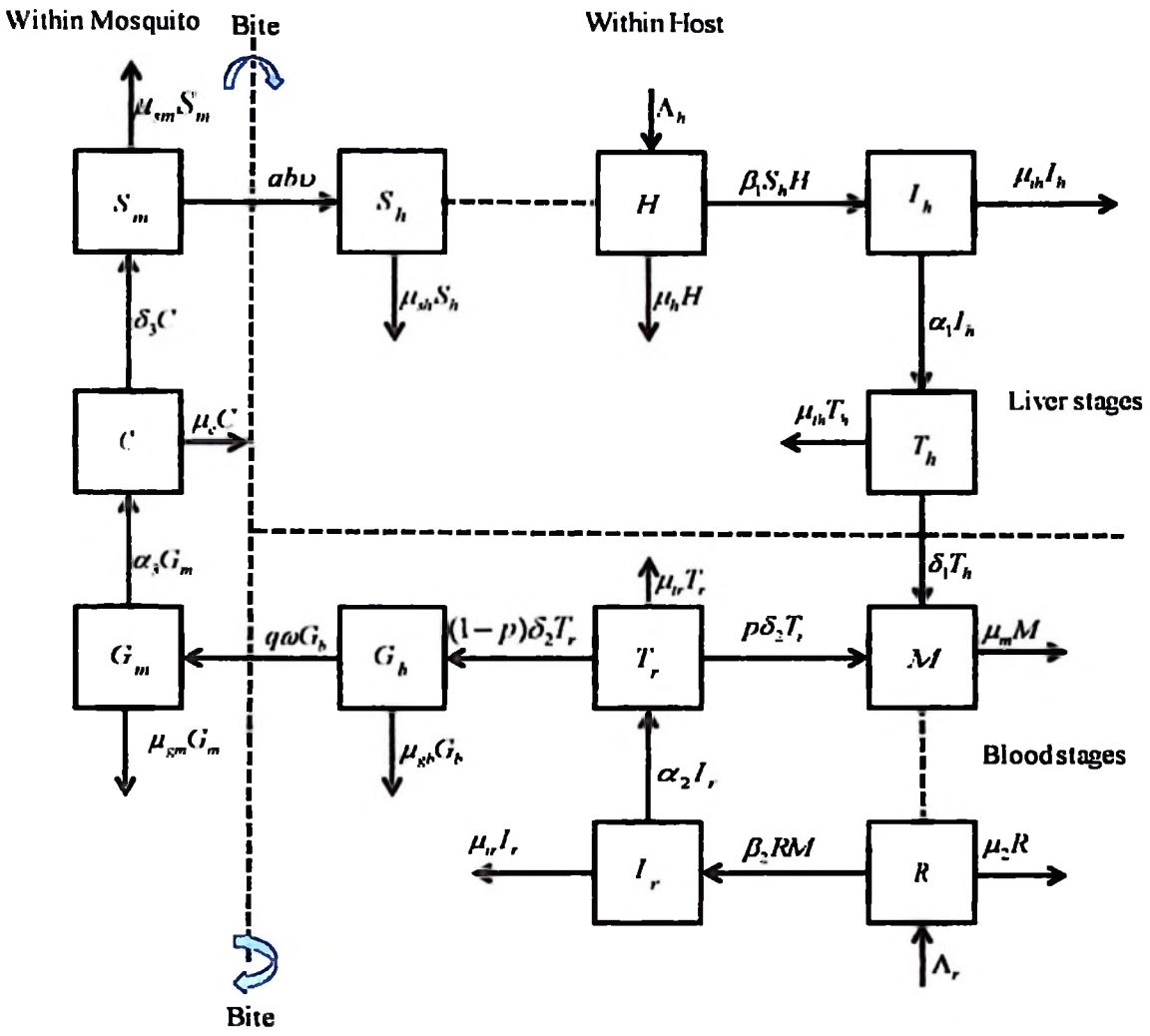

Figure 3: Model compartmental diagram for the in-human host and in-mosquito dynamics of malaria parasite

2.2.4 Model Equations

Based on the variables and parameters which are respectively described in Table 1 and Table 2, and the assumptions stated above, the in-human host and in-mosquito dynamics of malaria, captured in Fig. 3, are governed by the following system of ordinary differential equations.

$$\frac{dH}{dt} = \Lambda_h - \beta_1 S_h H - \mu_h H, \tag{2.1a}$$

$$\frac{dI_h}{dt} = \beta_1 S_h H - \alpha_1 I_h - \mu_{ih} I_h, \tag{2.1b}$$

$$\frac{dT_h}{dt} = \alpha_1 I_h - \delta_1 T_h - \mu_{th} T_h, \tag{2.1c}$$

$$\frac{dM}{dt} = r_1 \delta_1 T_h + p r_2 \delta_2 T_r - \beta_2 RM - \mu_m M, \tag{2.1d}$$

$$\frac{dR}{dt} = \Lambda_r - \beta_2 RM - \mu_r R, \tag{2.1e}$$

$$\frac{dI_r}{dt} = \beta_2 RM - \alpha_2 I_r - \mu_{ir} I_r, \tag{2.1f}$$

$$\frac{dT_r}{dt} = \alpha_2 I_r - \delta_2 T_r - \mu_{tr} T_r, \tag{2.1g}$$

$$\frac{dG_h}{dt} = (1-p) r_2 \delta_2 T_r - q\omega G_h - \mu_{gh} G_h, \tag{2.1h}$$

$$\frac{dG_m}{dt} = pq\omega G_h - \alpha_3 G_m - \mu_{gm} G_m, \tag{2.1i}$$

$$\frac{dC}{dt} = \alpha_3 G_m - \delta_3 C - \mu_c C, \tag{2.1j}$$

$$\frac{dS_m}{dt} = r_3 \delta_3 C - a\nu S_m - \mu_{sm} S_m, \tag{2.1k}$$

$$\frac{dS_h}{dt} = ab\nu - \beta_1 S_h H - \mu_{sh} S_h. \tag{2.1l}$$

2.3 Analysis of the Model

In this section, the invariant region, the positivity of solutions and existence of malaria free equilibrium of model system (2.1a)-(2.1l) are studied. The invariant region describes the region in which the solutions of the system are biologically feasible whereas positivity describes non negativity of the solutions of the system.

2.3.1 Invariant Region

Using equations (2.1a)-(2.1c) we define the function

$$N_h(t) = H(t) + I_h(t) + T_h(t)$$

to be the total population of liver cells which implies

$$\frac{dN_h(t)}{dt} = \frac{dH(t)}{dt} + \frac{dI_h(t)}{dt} + \frac{dT_h(t)}{dt}$$

Then,

$$\frac{dN_h}{dt} = \Lambda_h - \mu_h H - \mu_{ih} I_h - (\mu_{th} + \delta_1) T_h,$$

and hence,

$$\frac{dN_h}{dt} \leq \Lambda_h - \mu_1 N_h, \tag{2.2}$$

where,

$$\mu_1 = \min\{\mu_h,\ \mu_{th} + \delta_1\}$$

since we assumed that the infected cells die faster than uninfected one, which guarantees that $\mu_h < \mu_{th}$.

Using Birkhoff and Rota's theorem on differential inequalities, solving inequality (2.2) and applying initial conditions, we get

$$N_h(t) \leq \frac{\Lambda_h}{\mu_1} + \left(N_h(0) - \frac{\Lambda_h}{\mu_1}\right) e^{-\mu_1 t} \tag{2.3}$$

Here there are two cases to consider on $\left(N_h(0) - \frac{\Lambda_h}{\mu_1}\right)$

Case 1: When $N_h(0) - \frac{\Lambda_h}{\mu_1} > 0$,

The largest value of right-hand side (RHS) of inequality (2.3) occurs at $t = 0$, and that value is $N_h(0)$.

Hence,

$$N_h(t) \leq N_h(0), \quad \forall t. \tag{2.4}$$

Case 2: When $N_h(0) - \frac{\Lambda_h}{\mu_1} < 0$,

The value of $\left(N_h(0) - \frac{\Lambda_h}{\mu_1}\right) e^{-\mu_1 t}$ is negative and it approaches 0 as $t \to \infty$.

Therefore, the largest value that the RHS of inequality (2.3) takes is $\frac{\Lambda_h}{\mu_1}$, $\forall t$.

Thus,

$$N_h(t) \leq \frac{\Lambda_h}{\mu_1} \tag{2.5}$$

Hence from inequalities (2.4) and (2.5), we conclude that

$$N_h(t) = H(t) + I_h(t) + T_h(t) \leq \max\left\{N_h(0),\ \frac{\Lambda_h}{\mu_1}\right\}, \tag{2.6}$$

for all values of t and whatever value of $N_h(0)$.

In similar approach, from equations (2.1e)-(2.1g) we define the function

$$N_r = R + I_r + T_r$$

as the total population of RBCs which implies that

$$\frac{dN_r}{dt} = \Lambda_r - \mu_r R - \mu_{ir} I_r - (\mu_{tr} + \delta_2) T_r$$

hence

$$\frac{dN_r}{dt} \leq \Lambda_r - \mu_2 N_r \tag{2.7}$$

where $\mu_2 = \min\{\mu_r,\ \mu_{tr} + \delta_2\}$

Solving inequality (2.7), we obtain

$$N_r(t) \leq \frac{\Lambda_r}{\mu_2} + \left(N_r(0) - \frac{\Lambda_r}{\mu_2}\right) e^{-\mu_2 t} \tag{2.8}$$

Case 1: When $N_r(0) - \dfrac{\Lambda_r}{\mu_2} > 0$,

The RHS of inequality (2.8) assumes its largest value which is $N_r(0)$ at $t = 0$

Hence,

$$N_r(t) \leq N_r(0), \quad \forall t. \tag{2.9}$$

Case 2: When $N_r(0) - \dfrac{\Lambda_r}{\mu_2} < 0$,

The value of $\left(N_r(0) - \dfrac{\Lambda_r}{\mu_2}\right) e^{-\mu_2 t}$ is negative and it approaches 0 as $t \to \infty$.

Therefore, the largest value of the RHS of inequality (2.8) is $\dfrac{\Lambda_r}{\mu_2}$, $\quad \forall t$.

Thus,

$$N_r(t) \leq \frac{\Lambda_r}{\mu_2} \tag{2.10}$$

Hence from (2.9) and (2.10), we deduce that

$$N_r(t) = R(t) + I_r(t) + T_r(t) < \max\left\{N_r(0),\ \frac{\Lambda_r}{\mu_2}\right\}, \tag{2.11}$$

for all values of t and any value of $N_r(0)$.

From (2.1d), the population of merozoites in bloodstream, M is governed by

$$\frac{\mathrm{d}M}{dt} = r_1\delta_1 T_h + pr_2\delta_2 T_r - \beta_2 RM - \mu_m M \tag{2.12}$$

Using (2.6) and (2.11) we can respectively deduce that

$$T_h(t) \leq \frac{\Lambda_h}{\mu_1} \text{ and } T_r(t) \leq \frac{\Lambda_r}{\mu_2} \tag{2.13}$$

Substituting inequality (2.13) in the differential inequality (2.12), we get

$$\frac{\mathrm{d}M}{dt} \leq r_1\delta_1\frac{\Lambda_h}{\mu_1} + pr_2\delta_2\frac{\Lambda_r}{\mu_2} - \mu_m M \tag{2.14}$$

Solving this we get

$$M(t) \leq \frac{1}{\mu_m}\left[r_1\delta_1\frac{\Lambda_h}{\mu_1} + pr_2\delta_2\frac{\Lambda_r}{\mu_2}\right] + \left(M(0) - \frac{1}{\mu_m}\left[r_1\delta_1\frac{\Lambda_h}{\mu_1} + pr_2\delta_2\frac{\Lambda_r}{\mu_2}\right]\right) e^{-\mu_m t} \tag{2.15}$$

and by similar procedures we deduce that

$$M(t) \leq \max\left\{M(0),\ \frac{1}{\mu_m}\left[r_1\delta_1\frac{\Lambda_h}{\mu_1} + pr_2\delta_2\frac{\Lambda_r}{\mu_2}\right]\right\},$$

From equation (2.1h), the population of gametocytes in bloodstream, G_b is governed by

$$\frac{dG_b}{dt} = (1-p)r_2\delta_2 T_r - q\omega G_b - \mu_{gb}G_b \leq (1-p)r_2\delta_2 T_r - \mu_{gb}G_b$$

and so

$$\frac{dG_b}{dt} < (1 \quad p)r_2\delta_2 T_r \quad \mu_{gb}G_b \tag{2.16}$$

Using (2.13) in the inequality (2.16) we have

$$\frac{dG_b}{dt} \leq (1-p)r_2\delta_2 \frac{\Lambda_r}{\mu_2} - \mu_{gb}G_b \tag{2.17}$$

and whose solution is

$$G_b(t) \leq \frac{(1-p)r_2\delta_2}{\mu_{gb}}\frac{\Lambda_r}{\mu_2} + \left(G_b(0) - \frac{(1-p)r_2\delta_2}{\mu_{gb}}\frac{\Lambda_r}{\mu_2}\right)e^{-\mu_{gb}t} \tag{2.18}$$

We, then consider two case as follows:

Case 1: When $\left(G_b(0) - \frac{(1-p)r_2\delta_2}{\mu_{gb}}\frac{\Lambda_r}{\mu_2}\right)$ is positive,

the RHS of (2.18) takes its largest value at $t = 0$, and that value is $G_b(0)$. Thus,

$$G_b(t) \leq G_b(0), \ \forall t \tag{2.19}$$

Case 2: When $\left(G_b(0) - \frac{(1-p)r_2\delta_2}{\mu_{gb}}\frac{\Lambda_r}{\mu_2}\right)$ is negative,

Then $\left(G_b(0) - \frac{(1-p)r_2\delta_2}{\mu_{gb}}\frac{\Lambda_r}{\mu_2}\right)e^{-\mu_{gb}t}$ is always negative and it approaches 0 as $t \to \infty$.

Therefore, the largest value that the RHS of inequality (2.18) is $\frac{(1-p)r_2\delta_2}{\mu_{gb}}\frac{\Lambda_r}{\mu_2}$, $\forall t$.
Thus,

$$G_b(t) \leq \frac{(1-p)r_2\delta_2}{\mu_{gb}}\frac{\Lambda_r}{\mu_2}, \ \forall t \tag{2.20}$$

Hence from inequalities (2.19) and (2.20), we conclude that

$$G_b(t) \leq \max\left\{G_b(0), \ \frac{(1-p)r_2\delta_2}{\mu_{gb}}\frac{\Lambda_r}{\mu_2}\right\} \tag{2.21}$$

Using equations (2.1i) and (2.1j) we define

$$N_m(t) = G_m(t) + C(t)$$

as total the population of parasites in mosquito's midgut which implies that

$$\frac{dN_m}{dt} = q\rho\omega G_b - \mu_{gm}G_m - \mu_c C - \delta_3 C$$

$$\frac{dN_m}{dt} \leq qf\rho\omega G_h - \mu_3 N_m \tag{2.22}$$

where $\mu_3 = \min\{\mu_{gm}, \mu_c\}$.

Using (2.21), the inequality (2.22) becomes,

$$\frac{dN_m}{dt} \leq qf\rho\omega \frac{(1-p)r_2\delta_2}{\mu_{gb}} \frac{\Lambda_r}{\mu_2} - \mu_3 N_m \tag{2.23}$$

whose solution is

$$N_m(t) \leq \frac{qf\rho\omega}{\mu_3} \frac{(1-p)r_2\delta_2}{\mu_{gb}} \frac{\Lambda_r}{\mu_2} + \left(N_m(0) - \leq \frac{qf\rho\omega}{\mu_3} \frac{(1-p)r_2\delta_2}{\mu_{gb}} \frac{\Lambda_r}{\mu_2} \right) e^{-\mu_3 t} \tag{2.24}$$

Similarly, from (2.24) we deduce that

$$N_m(t) = G_m(t) + C(t) \leq \max\left\{ N_m(0), \frac{qf\rho\omega}{\mu_3} \left[\frac{(1-p)r_2\delta_2}{\mu_{gb}} \frac{\Lambda_r}{\mu_2} \right] \right\} \tag{2.25}$$

Lastly, from equations (2.1k) and (2.1l), the populations of sporozoites in mosquito's salivary glands, S_m and that in human liver, S_h are respectively governed by

$$\frac{dS_m}{dt} = r_3\delta_3 C - a\nu S_m - \mu_{sm} S_m \leq r_3\delta_3 C - \mu_{sm} S_m \tag{2.26}$$

and

$$\frac{dS_h}{dt} = ab\nu - \beta_1 S_h H - \mu_{sh} S_h \leq ab\nu - \mu_{sh} S_h \tag{2.27}$$

Using (2.25), the inequality (2.26) becomes

$$\frac{dS_m}{dt} \leq r_3\delta_3 \frac{qf\rho\omega}{\mu_3} \frac{(1-p)r_2\delta_2}{\mu_{gb}} \frac{\Lambda_r}{\mu_2} - \mu_{sm} S_m \tag{2.28}$$

and its solution is given by

$$S_m \leq \frac{r_3\delta_3}{\mu_{sm}} \frac{qf\rho\omega}{\mu_3} \left[\frac{(1-p)r_2\delta_2}{\mu_{gb}} \frac{\Lambda_r}{\mu_2} \right] + \left(S_m(0) - \frac{r_3\delta_3}{\mu_{sm}} \frac{qf\rho\omega}{\mu_3} \left[\frac{(1-p)r_2\delta_2}{\mu_{gb}} \frac{\Lambda_r}{\mu_2} \right] \right) e^{-\mu_{sm} t} \tag{2.29}$$

and hence we conclude that

$$S_m(t) \leq \max\left\{ S_m(0), \frac{r_3\delta_3}{\mu_{sm}} \frac{qf\rho\omega}{\mu_3} \left[\frac{(1-p)r_2\delta_2}{\mu_{gb}} \frac{\Lambda_r}{\mu_2} \right] \right\}$$

Solution of inequality (2.27) is given by

$$S_h \leq \frac{ab\nu}{\mu_{sh}} + \left(S_h(0) - \frac{ab\nu}{\mu_{sh}} \right) e^{-\mu_{sh} t} \tag{2.30}$$

which leads us to

$$S_h(t) \leq \max\left\{ S_h(0), \frac{ab\nu}{\mu_{sh}} \right\}$$

Therefore, the solution set for the model (2.1a)-(2.1l) is feasible and enters the region

$$\Omega = \left\{(H, I_h, T_h, M, R, I_r, T_r, G_b, G_m, C, S_m, S_h) \in \mathbb{R}_+^{12} : N_h(t) \leq \max\left\{N_h(0), \frac{\Lambda_h}{\mu_1}\right\},\right.$$
$$N_r(t) \leq \max\left\{N_r(0), \frac{\Lambda_r}{\mu_2}\right\}, \; M(t) \leq \max\left\{M(0), \frac{1}{\mu_m}\left[r_1\delta_1\frac{\Lambda_h}{\mu_1} + pr_2\delta_2\frac{\Lambda_r}{\mu_2}\right]\right\},$$
$$G_b(t) \leq \max\left\{G_b(0), \frac{(1-p)r_2\delta_2}{\mu_{gb}}\frac{\Lambda_r}{\mu_2}\right\}, \; N_m(t) \leq \max\left\{N_m(0), \frac{q\rho\omega}{\mu_3}\left[\frac{(1-p)r_2\delta_2}{\mu_{gb}}\frac{\Lambda_r}{\mu_2}\right]\right\},$$
$$\left.S_m \leq \max\left\{S_m(0), \frac{r_3\delta_3}{\mu_{sm}}\frac{q\rho\omega}{\mu_3}\left[\frac{(1-p)r_2\delta_2}{\mu_{gb}}\frac{\Lambda_r}{\mu_2}\right]\right\}, \; S_h(t) \leq \max\left\{S_h(0), \frac{ab\nu}{\mu_{sh}}\right\}\right\}$$

2.3.2 Positivity of the Solutions

Since the model (2.1a)-(2.1l) governs the population of cells and parasites within the human host and in-mosquito, then we need to show that solutions of the system (2.1a)-(2.1l) with positive initial conditions remain positive for all $t > 0$. That is, we need to prove that all the state variables are nonnegative. This is done by proving the following lemma.

Lemma 2.1

Let the initial conditions for the model (2.1a)-(2.1l) be

$$(H(0), I_h(0), T_h(0), M(0), R(0), I_r(0), T_r(0), G_b(0), G_m(0), C(0), S_m(0), S_h(0)) > 0,$$

then the solution

$$(H(t), I_h(t), T_h(t), M(t), R(t), I_r(t), T_r(t), G_b(t), G_m(t), C(t), S_m(t), S_h(t))$$

of the model (2.1a)-(2.1l) is non-negative for all values of $t > 0$.

Proof: From equation (2.1a), we have

$$\frac{dH}{dt} = \Lambda_h - \beta_1 S_h H - \mu_h H \geq -(\beta_1 S_h + \mu_h)H$$

which yields to

$$H(t) \geq H(0)\exp(-\int_0^t \beta_1 S(z)dz + \mu_h t) > 0$$

since $H(0) > 0$, and from equation (2.1b), we have

$$\frac{dI_h}{dt} = \beta_1 S_h H - \alpha_1 I_h - \mu_{ih} I_h \geq -(\alpha_1 + \mu_{ih})I_h$$

which gives

$$I_h(t) \geq I_h(0)\exp(-(\alpha_1 + \mu_{ih})t) > 0$$

since $I_h(0) > 0$.

Using similar approach for the equations (2.1c)-(2.1l), we obtain the following expressions.

$$\begin{aligned}
T_h(t) &\geq T_h(0)\exp(-(\delta_1 + \mu_{th})t) > 0, \text{ since } T_h(0) > 0 \\
M(t) &\geq M(0)\exp\left(-\int_0^t \beta_2 R(z)dz - \mu_m t\right) > 0, \text{ since } M(0) > 0 \\
R(t) &\geq R(0)\exp\left(-\int_0^t \beta_2 M(z)dz - \mu_r t\right) > 0, \text{ since } R(0) > 0 \\
I_r(t) &\geq I_r(0)\exp(-(\alpha_2 + \mu_{ir})t) > 0, \text{ since } I_r(0) > 0 \\
T_r(t) &\geq T_r(0)\exp(-(\delta_2 + \mu_{tr})t) > 0, \text{ since } T_r(0) > 0 \\
G_h(t) &\geq G_h(0)\exp(-(q\omega + \mu_{gh})t) > 0, \text{ since } G_h(0) > 0 \\
G_m(t) &\geq G_m(0)\exp(-(\alpha_3 + \mu_{gm})t) > 0, \text{ since } G_m(0) > 0 \\
C(t) &\geq C(0)\exp(-(\delta_3 + \mu_c)t) > 0, \text{ since } C(0) > 0 \\
S_m(t) &\geq S_m(0)\exp(-(\alpha\nu + \mu_{sm})t) > 0, \text{ since } S_m(0) > 0 \\
S_h(t) &\geq S_h(0)\exp\left(-\int_0^t \beta_1 H(z)dz - \mu_{sh}t\right) > 0, \text{ since } S_h(0) > 0
\end{aligned}$$

This completes the proof. Therefore the solution of the model (2.1a)-(2.1l) is non-negative for all values of $t > 0$

2.3.3 Existence of Malaria Free Equilibrium (MFE)

Malaria-free equilibrium (MFE) is the state where there is no infection. MFE of the system (2.1a)-(2.1l) is obtained by setting right hand side of the model equations to zero and solving for variables provided that all infectious state variables assume the value of zero.

Let

$$E^0 = (H^0, I_h^0, T_h^0, M^0, R^0, I_r^0, T_r^0, G_h^0, G_m^0, C^0, S_m^0, S_h^0)$$

be the MFE of the system (2.1a)-(2.1l), then in absence of infection,

$$I_h^0 = T_h^0 = M^0 = I_r^0 = T_r^0 = G_h^0 = G_m^0 = C^0 = S_m^0 = S_h^0 = 0.$$

Using equations (2.1a) and (2.1e), we obtain

$$H^0 = \frac{\Lambda_h}{\mu_h} \quad \text{and} \quad R^0 = \frac{\Lambda_r}{\mu_r}$$

Therefore the MFE is

$$E^0 = \left(\frac{\Lambda_h}{\mu_h}, 0, 0, 0, \frac{\Lambda_r}{\mu_r}, 0, 0, 0, 0, 0, 0, 0, 0\right)$$

2.3.4 Basic Reproduction Number, $\mathcal{R}_0$

For in-host dynamics models, Guardiola and Vecchio (2005) defined reproduction number as number of newly infected cells produced by a single infected cell during its infectious lifetime. In calculating the basic reproduction number for the model (2.1a)-(2.1l), we use the next generation matrix technique as described by Van den Driessche and Watmough (2002).

Re-arranging the model (2.1a)-(2.1l) so that the infection classes appeared first, we have

$$\frac{dI_h}{dt} = \beta_1 S_h I - \alpha_1 I_h - \mu_{ih} I_h, \tag{2.31a}$$

$$\frac{dT_h}{dt} = \alpha_1 I_h - \delta_1 T_h - \mu_{th} T_h, \tag{2.31b}$$

$$\frac{dM}{dt} = r_1 \delta_1 T_h + p r_2 \delta_2 T_r - \beta_2 R M - \mu_m M, \tag{2.31c}$$

$$\frac{dI_r}{dt} = \beta_2 R M - \alpha_2 I_r - \mu_{ir} I_r, \tag{2.31d}$$

$$\frac{dT_r}{dt} = \alpha_2 I_r - \delta_2 T_r - \mu_{tr} T_r, \tag{2.31e}$$

$$\frac{dG_b}{dt} = (1-p) r_2 \delta_2 T_r - q\omega G_b - \mu_{gb} G_b, \tag{2.31f}$$

$$\frac{dG_m}{dt} = pq\omega G_b - \alpha_3 G_m - \mu_{gm} G_m, \tag{2.31g}$$

$$\frac{dC}{dt} = \alpha_3 G_m - \delta_3 C - \mu_c C, \tag{2.31h}$$

$$\frac{dS_m}{dt} = r_3 \delta_3 C - a\nu S_m - \mu_{sm} S_m, \tag{2.31i}$$

$$\frac{dS_h}{dt} = ab\nu - \beta_1 S_h I - \mu_{sh} S_h, \tag{2.31j}$$

$$\frac{dH}{dt} = \Lambda_h - \beta_1 S_h H - \mu_h H, \tag{2.31k}$$

$$\frac{dR}{dt} = \Lambda_r - \beta_2 R M - \mu_r R, \tag{2.31l}$$

The first ten equations (2.31a)-(2.31j) represents infection classes.

Let x_i for $i = 1 \ldots 10$ be infection classes of variables for the model (2.1a)-(2.1l).

In this approach $\mathcal{R}_0$ is obtained by taking the dorminat eigenvalue of

$$\left[\frac{\partial \mathcal{F}_i}{\partial x_i}(E^0)\right]\left[\frac{\partial \mathcal{V}_i}{\partial x_i}(E^0)\right]^{-1}$$

where $\mathcal{F}_i$ be the rate of appearance of new infection in compartment i,

$\mathcal{V}_i^+$ be the rate of transfer of individuals into compartment i by all other means,

$\mathcal{V}_i^-$ be the rate of transfer of individuals out of compartment i by all other means and

$\mathcal{V}_i = \mathcal{V}_i^+ - \mathcal{V}_i^-$.

So from equations (2.31a)-(2.31j) we have

$$\mathcal{F}_i = \begin{pmatrix} \beta_1 S_h I \\ 0 \\ 0 \\ \beta_2 RM \\ 0 \\ 0 \\ \rho q \omega G_b \\ 0 \\ 0 \\ 0 \end{pmatrix} \tag{2.32}$$

and

$$\mathcal{V}_i = \begin{pmatrix} (\alpha_1 + \mu_{ih}) I_h \\ (\delta_1 + \mu_{th}) T_h - \alpha_1 I_h \\ (\beta_2 R + \mu_m) M - r_1 \delta_1 T_h - p r_2 \delta_2 T_r \\ (\alpha_2 + \mu_{ir}) I_r \\ (\delta_2 + \mu_{tr}) T_r - \alpha_2 I_r \\ (q\omega + \mu_{gb}) G_b - (1-p) r_2 \delta_2 T_r \\ (\alpha_3 + \mu_{gm}) G_m \\ (\delta_3 + \mu_c) C - \alpha_3 G_m \\ (a\nu + \mu_{sm}) S_{sm} - r_3 \delta_3 C \\ \beta_1 S_h I + \mu_{sh} S_h - a h \nu \end{pmatrix} \tag{2.33}$$

which implies from (2.32), we have

$$F = \left. \frac{\partial \mathcal{F}_i}{\partial x_j} \right|_{E^0} = \begin{pmatrix} 0 & 0 & 0 & 0 & 0 & 0 & 0 & 0 & 0 & \beta_1 \dfrac{\Lambda_h}{\mu_h} \\ 0 & 0 & 0 & 0 & 0 & 0 & 0 & 0 & 0 & 0 \\ 0 & 0 & 0 & 0 & 0 & 0 & 0 & 0 & 0 & 0 \\ 0 & 0 & \beta_2 \dfrac{\Lambda_r}{\mu_r} & 0 & 0 & 0 & 0 & 0 & 0 & 0 \\ 0 & 0 & 0 & 0 & 0 & 0 & 0 & 0 & 0 & 0 \\ 0 & 0 & 0 & 0 & 0 & 0 & 0 & 0 & 0 & 0 \\ 0 & 0 & 0 & 0 & 0 & \rho q \omega & 0 & 0 & 0 & 0 \\ 0 & 0 & 0 & 0 & 0 & 0 & 0 & 0 & 0 & 0 \\ 0 & 0 & 0 & 0 & 0 & 0 & 0 & 0 & 0 & 0 \\ 0 & 0 & 0 & 0 & 0 & 0 & 0 & 0 & 0 & 0 \end{pmatrix} \tag{2.34}$$

and from equation (2.33) we have

$$V = \left.\frac{\partial \mathcal{V}_i}{\partial x_j}\right|_{E^0} = \begin{pmatrix} v_1 & 0 & 0 & 0 & 0 & 0 & 0 & 0 & 0 & 0 \\ -\alpha_1 & v_2 & 0 & 0 & 0 & 0 & 0 & 0 & 0 & 0 \\ 0 & v_3 & v_4 & 0 & v_5 & 0 & 0 & 0 & 0 & 0 \\ 0 & 0 & 0 & v_6 & 0 & 0 & 0 & 0 & 0 & 0 \\ 0 & 0 & 0 & -\alpha_2 & v_7 & 0 & 0 & 0 & 0 & 0 \\ 0 & 0 & 0 & 0 & v_8 & v_9 & 0 & 0 & 0 & 0 \\ 0 & 0 & 0 & 0 & 0 & 0 & \alpha_3 & 0 & 0 & 0 \\ 0 & 0 & 0 & 0 & 0 & 0 & -\alpha_3 & v_{10} & 0 & 0 \\ 0 & 0 & 0 & 0 & 0 & 0 & 0 & v_{11} & v_{12} & 0 \\ 0 & 0 & 0 & 0 & 0 & 0 & 0 & 0 & 0 & v_{13} \end{pmatrix} \tag{2.35}$$

where

$$\begin{aligned} v_1 &= \alpha_1 + \mu_{ih}, \quad v_2 = \delta_1 + \mu_{ih}, v_3 = -r_1\delta_1, \quad v_4 = \beta_2\frac{\Lambda_r}{\mu_r} + \mu_m, \quad v_5 = -pr_2\delta_2, \\ v_6 &= \alpha_2 + \mu_{ir}, \quad v_7 = \delta_2 + \mu_{ir}, \quad v_8 = -(1-p)r_2\delta_2, \quad v_9 = q\omega + \mu_{gh}, \quad v_{10} = \delta_3 + \mu_c, \\ v_{11} &= -r_3\delta_3, \quad v_{12} = \alpha\nu + \mu_{sm}, \quad v_{13} = \beta_1\frac{\Lambda_h}{\mu_h} + \mu_{sh} \end{aligned} \tag{2.36}$$

Then we compute the inverse, V^{-1}, of V from (2.35), and we obtain

$$V^{-1} = \begin{pmatrix} \frac{1}{v_1} & 0 & 0 & 0 & 0 & 0 & 0 & 0 & 0 & 0 \\ \frac{\alpha_1}{v_2 v_1} & \frac{1}{v_2} & 0 & 0 & 0 & 0 & 0 & 0 & 0 & 0 \\ \frac{v_3\alpha_1}{v_4 v_2 v_1} & \frac{v_3}{v_4 v_2} & \frac{1}{v_4} & \frac{v_5\alpha_2}{v_7 v_6 v_4} & \frac{v_5}{v_7 v_4} & 0 & 0 & 0 & 0 & 0 \\ 0 & 0 & 0 & \frac{1}{v_6} & 0 & 0 & 0 & 0 & 0 & 0 \\ 0 & 0 & 0 & \frac{\alpha_2}{v_7 v_6} & \frac{1}{v_7} & 0 & 0 & 0 & 0 & 0 \\ 0 & 0 & 0 & \frac{\alpha_2 v_8}{v_9 v_7 v_6} & \frac{v_8}{v_9 v_7} & \frac{1}{v_9} & 0 & 0 & 0 & 0 \\ 0 & 0 & 0 & 0 & 0 & 0 & \frac{1}{\alpha_3} & 0 & 0 & 0 \\ 0 & 0 & 0 & 0 & 0 & 0 & \frac{1}{v_{10}} & \frac{1}{v_{10}} & 0 & 0 \\ 0 & 0 & 0 & 0 & 0 & 0 & \frac{v_{11}}{v_{10} v_{12}} & \frac{v_{11}}{v_{12} v_{10}} & \frac{1}{v_{12}} & 0 \\ 0 & 0 & 0 & 0 & 0 & 0 & 0 & 0 & 0 & \frac{1}{v_{13}} \end{pmatrix} \tag{2.37}$$

Hence, from (2.34) and (2.37), we have

$$FV^{-1} = \begin{pmatrix} 0 & 0 & 0 & 0 & 0 & 0 & 0 & 0 & 0 & A_1 \\ 0 & 0 & 0 & 0 & 0 & 0 & 0 & 0 & 0 & 0 \\ 0 & 0 & 0 & 0 & 0 & 0 & 0 & 0 & 0 & 0 \\ A_2 & A_3 & A_4 & A_5 & A_6 & 0 & 0 & 0 & 0 & 0 \\ 0 & 0 & 0 & 0 & 0 & 0 & 0 & 0 & 0 & 0 \\ 0 & 0 & 0 & 0 & 0 & 0 & 0 & 0 & 0 & 0 \\ 0 & 0 & 0 & 0 & 0 & 0 & 0 & 0 & 0 & 0 \\ 0 & 0 & 0 & A_7 & A_8 & A_9 & 0 & 0 & 0 & 0 \\ 0 & 0 & 0 & 0 & 0 & 0 & 0 & 0 & 0 & 0 \\ 0 & 0 & 0 & 0 & 0 & 0 & 0 & 0 & 0 & 0 \end{pmatrix} \tag{2.38}$$

where,

$$A_1 = \frac{\beta_1 \Lambda_h}{v_{13}\mu_h}, \quad A_2 = \frac{\beta_2 \alpha_1 v_3 \Lambda_r}{v_4 v_2 v_1 \mu_r}, \quad A_3 = \frac{\beta_2 v_3 \Lambda_r}{v_4 v_2 \mu_r}, \quad A_4 = \frac{\beta_2 \Lambda_r}{v_4 \mu_r}, \quad A_5 = \frac{\beta_2 \Lambda_r v_5 \alpha_2}{v_7 v_6 v_4 \mu_r}$$
$$A_6 = \frac{\beta_2 v_5 \Lambda_r}{v_7 v_4 \mu_r}, \quad A_6 = \frac{\beta_2 v_5 \Lambda_r}{v_7 v_4 \mu_r}, \quad A_7 = \frac{\rho q \omega v_8 \alpha_2}{v_9 v_7 v_6}, \quad A_8 = \frac{\rho q \omega v_8}{v_9 v_7}, \quad A_9 = \frac{\rho q \omega}{v_9} \tag{2.39}$$

We compute the eigenvalues of next generation matrix FV^{-1}, from $|FV^{-1} - I\lambda| = 0$ at E_0. The basic reproduction number $\mathcal{R}_0$ is obtained by taking the spectral radius (dorminant eigenvalue), $\rho(FV^{-1})$.

From (2.38), the only nonzero eigenvalue is A_5. Therefore the dominant eigenvalue is

$$\lambda = A_5 = \frac{\beta_2 \Lambda_r v_5 \alpha_2}{v_7 v_6 v_4 \mu_r}.$$

Hence, the basic reproduction number, $\mathcal{R}_0$ is given by

$$\mathcal{R}_0 = \frac{\beta_2 \Lambda_r v_5 \alpha_2}{v_7 v_6 v_4 \mu_r} \tag{2.40}$$

Substituting the values of v_4, v_5, v_6, and v_7 from equation (2.36) into equation (2.40) we get

$$\mathcal{R}_0 = \frac{\beta_2 \Lambda_r}{\beta_2 \Lambda_r + \mu_m \mu_r} \cdot \frac{\alpha_2}{(\alpha_2 + \mu_{ir})} \cdot \frac{pr_2 \delta_2}{(\delta_2 + \mu_{tr})}$$

which can be expressed as

$$\mathcal{R}_0 = \left[\frac{\beta_2 r_0}{(\beta_2 r_0 + \mu_m)}\right] \left[\frac{\alpha_2}{(\alpha_2 + \mu_{ir})}\right] \left[\frac{1}{(\delta_2 + \mu_{tr})}\right] pr_2 \delta_2 \tag{2.41}$$

where $r_0 = \dfrac{\Lambda_r}{\mu_r}$ is value of uninfected RBCs at E^0.

The term $\dfrac{\beta_2 r_0}{\beta_2 r_0 + \mu_m}$ in equation (2.41) is the proportion of RBCs that is infected by a merozite

introduced into entirely susceptile RBC population before it dies, while the term $\frac{\alpha_2}{\alpha_2+\mu_{ir}}$ represents the proportion of infected RBCs that progress to schizonts, the term $\frac{1}{\delta_2+\mu_{tr}}$ is the mean period spent by the blood-schizont before they rupture, and the term $pr_2\delta_2$ is number of released merozoites that proceeds to asexuals replication in each erythrocytic cycle.

2.4 Sensitivity Analysis of $\mathcal{R}_0$ and Numerical Simulations

Sensitivity analysis, also known as *what-if analysis*, is a technique used to determine how variations in input parameters affect the anticipated model outputs (Cariboni *et al.*, 2007). The main reason for why we need sensitivity analysis is that, it helps the modeller to identify parameters that need the most numerical attention and highlight which parameters should be targeted in planning and developing management strategies (Lutambi *et al.*, 2013).

In this study we computed the normalized sensitivity index $\Omega_{p_i}^{\mathcal{R}_0}$ of the basic reproduction number $\mathcal{R}_0$ using method described by Chitnis, Hyman and Cushing (2008) and Cariboni *et al.* (2007) , where partial derivatives of $\mathcal{R}_0$ with respect to each of its input parameter, p_i were obtained using the formula

$$\Omega_{p_i}^{\mathcal{R}_0} = \frac{\partial \mathcal{R}_0}{\partial p_i} \times \frac{p_i}{\mathcal{R}_0} \tag{2.42}$$

Substituting values of parameters given in Table 3 in equation (2.42) we obtained the sensitivity indices of $\mathcal{R}_0$ which are presented in Table 4.

Table 3 : Parameter estimates for the model (2.1a)-(2.1l)

Parameter	Description	Value	Reference
a :	probability that a bite infects human	0.75	(Tumwiine *et al.*, 2007 b)
b :	number of mosquito bites per individual	$15day^{-1}$	Estimated
ν :	number of sporozoites injected per bite	$10-20$	(Nelson and Williams, 2014)
β_1 :	infection rate of HLCs by sporozoites	$0.001\ \mu l cell^{-1} day^{-1}$	Estimated
r_1 :	number of merozoites per liver schizont	10000	(Tumwiine *et al.*, 2014)
α_1 :	progression rate of infected HLCs to schizonts	$0.125\ day^{-1}$	Estimated
δ_1 :	rupture rate of liver schizonts	$0.0975\ day^{-1}$	Estimated
Λ_h :	the recruitmet rate of HLCs	$3000\ cells day^{-1} \mu l^{-1}$	Estimated
μ_h :	natural death rate of uninfected HLCs	$0.04\ day^{-1}$	Estimated
μ_{ih} :	death rate of infected HLCs	$0.95\ day^{-1}$	Estimated
μ_{lh} :	death rate of liver-schizonts	$0.029\ day^{-1}$	Estimated
β_2 :	infection rate of RBCs by merozoites	$2 \times 10^{-6}\ \mu l cell^{-1} day^{-1}$	Estimated
δ_2 :	rupture rate of blood schizonts	$0.115\ day^{-1}$	Estimated
α_2 :	progression rate of infected RBCs to schizonts	$0.145\ day^{-1}$	Estimated
r_2 :	number of merozoites per blood schizont	16	(Dube *et al.*, 2010)
q :	probability that a bite is infectious to mosquito	0.09	(Agusto *et al.*, 2012)
ω :	number of gametocytes ingested per bite	10	Estimated
p :	number of bites made by mosquito in its lifetime	3	Estimated
Λ_r :	the recruitmet rate of RBCs	$4.15 \times 10^4\ cells\mu l^{-1} day^{-1}$	(Li *et al.*, 2011)
μ_r :	natural death rate of uninfected RBCs	$0.02\ day^{-1}$	(Dube *et al.*, 2010)
μ_{ir} :	total death rate of uninfected RBCs	$0.025\ day^{-1}$	(Diebner *et al.*, 2000)
μ_{lr} :	death rate of blood-schizonts	$0.185\ day^{-1}$	Estimated
μ_m :	death rate of merozoites	$48\ day^{-1}$	(Li *et al.*, 2011)
μ_{gb} :	death rate of gametocytes in bloodstream	$6.25 \times 10^{-5} day^{-1}$	Estimated
δ_3 :	rupture rate of Oocysts	$0.05\ day^{-1}$	Estimated
r_3 :	number of sporozoites per Oocyst	1000	(Nelson and Williams, 2014)
α_3 :	progresion rate of gametes to Oocysts	$0.07\ day^{-1}$	Estimated
μ_{gm} :	death rate of gametes in mosquito's midgut	$0.052\ day^{-1}$	Estimated
μ_o :	death rate of Oocysts	$0.024\ day^{-1}$	Estimated
μ_{sm} :	death rate of sporozoites in mosqouito	$40\ day^{-1}$	Estimated
μ_{sh} :	death rate of sporozoites in human liver	$1.2 \times 10^{-11}\ day^{-1}$	Estimated
p :	proportion of asexual that differentiate to merozoites	0.926	Estimated

Table 4 : Sensitivity indices of $\mathcal{R}_0$

Parameter, p_i	Sensitivity index, $\Omega_{p_i}^{\mathcal{R}_0}$
r_2	+1.00000
p	+0.99999
r_0	+0.97959
β_2	+0.97959
μ_m	−0.97959
μ_{ir}	−0.61667
δ_2	+0.61667
μ_{lr}	−0.14706
α_2	+0.14706

From Table 4, the number of merozoites released per rupturing schizont r_2, is the most sensitive parameter of the model ($\Omega_{r_2}^{\mathcal{R}_0} = 1.00000$), followed by proportion of released merozoites that proceed with asexual replication, p, with $\Omega_{p}^{\mathcal{R}_0} = +0.99999$, indicating that these parameters have a greatest effect on model outcomes. For example, an increase of 10% on r_2, will also cause the same effect (increase) of 10% on $\mathcal{R}_0$ and vice versa.

Parameters with next highest sensitivity index are initial suspectible population of RBCs, r_0, infection rate of RBCs by merozoites, β_2 and death rate of merozoites, μ_m. All these have the same of sensitivity indices, but r_0 and β_2 are positive while μ_m is negative. That is, an increase (a decrease) of 10% on r_0 or β_2 will results an increase (a decrease) of 9.7959% on $\mathcal{R}_0$, while with similar increase (decrease) on μ_m, $\mathcal{R}_0$ decreases (increases) by 9.7959%. These are followed by death rate of blood-schizonts, μ_{tr} and rupture rate of blood-schizonts to release merozoite, δ_2, with the same index in magnitude but different signs, implying that increasing μ_{tr} will cause a decrease on $\mathcal{R}_0$, though the increase in δ_2 will cause an increase in $\mathcal{R}_0$. The death rate of infected RBCs, μ_{ir} and progression rate of infected RBCs to schizonts α_2 are parameters having the least impact on $\mathcal{R}_0$.

$\mathcal{R}_0$ increases (decreases) as parameters with positives indices increases (decreases) and decreases (increases) as parameters with negative indices increases (decreases). In order for malaria infection to be eradicated, we need to reduce the value of $\mathcal{R}_0$ to be less than unity. Therefore, we can lower the value of $\mathcal{R}_0$ by reducing the values of r_2, p, r_0, β_2, δ_2 and α_2 or by increasing the values of μ_m, μ_{tr} and μ_{ir}. Fig. 4 illustrates the effect of variations of some parameters on reproduction numbers.

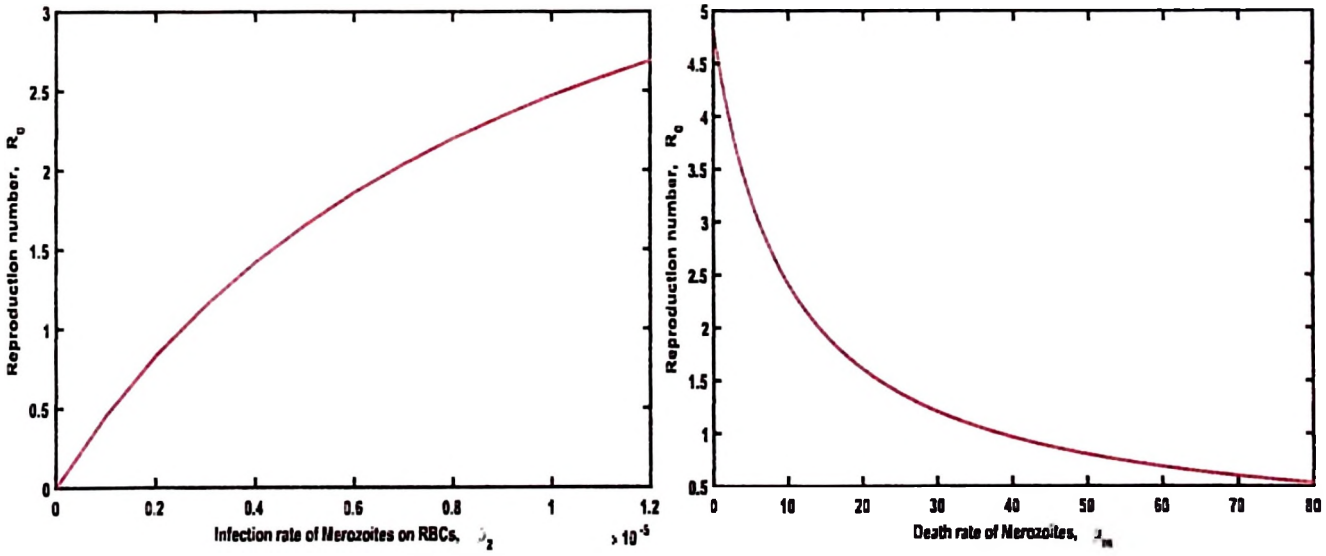

(a) Effect of β_2, on $\mathcal{R}_0$

(b) Effect of μ_m, on $\mathcal{R}_0$

Figure 4: Effect of infection rate of RBCs by merozoites, β_2 and death rate of merozoites μ_m, on basic reproduction number, $\mathcal{R}_0$

To control the malaria infection in nonimmune host, we need to have a stable malaria free equilibrium, which is achieved when $\mathcal{R}_0 < 1$. Now, we have to find out which parameters can lead us to this condition. Using information in the Table 4 and $\mathcal{R}_0$ in equation (2.41), we can infer the following: lessening the number of merozoites released, r_2, and infection rate of merozoites on RBCs, β_2 or raising the death rate of merozoites, μ_m will lessen $\mathcal{R}_0$. This conforms with the findings of Dube *et al.* (2010). A reduction of infection rate and rise in death rate of merozoites certainly reduce the number of succesful conctacts between merozoites and uninfected RBCs and hence reduces number of infected RBCs and increases number of uninfected RBCs, as indicated in Fig. 5 and Fig. 6.

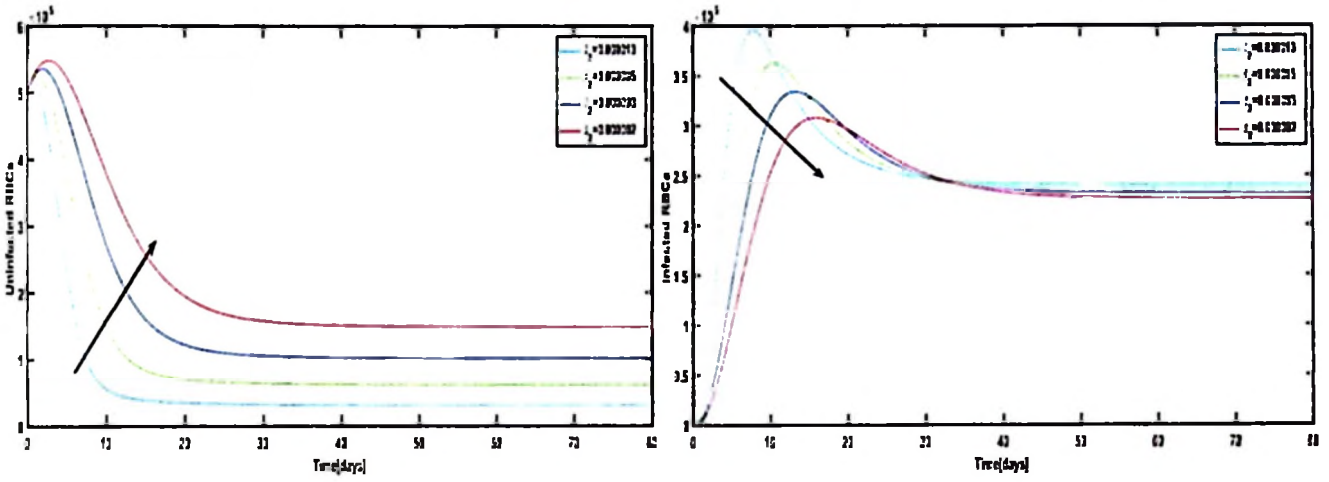

(a) Effect of decreasing β_2 on uninfected RBCs (b) Effect of decreasing β_2 on infected RBCs

Figure 5: Effect of decreasing infection rate of merozoites on number of uninfected RBCs and infected RBCs. Arrows are in direction of decreasing β_2

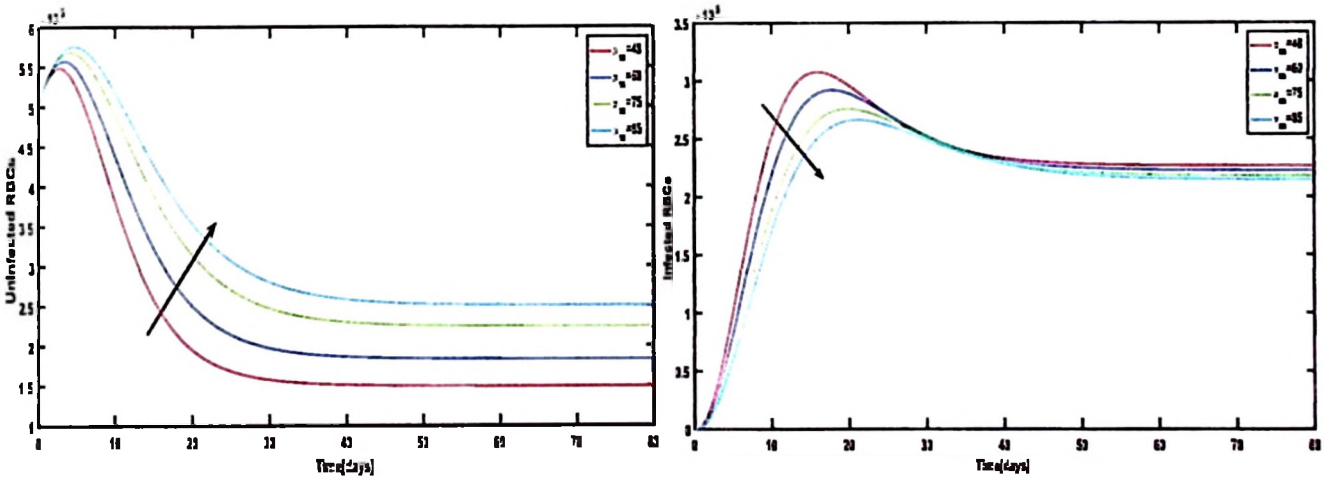

(a) Effect of increasing μ_m on uninfected RBCs (b) Effect of increasing μ_m on infected RBCs

Figure 6: Effect of increasing death rate of merozoites on densities of uninfected RBCs and infected RBCs. Arrows are in direction of increasing μ_m

With all other parameter values given in Table 3 are kept constant, we examine the effect of infection rate of RBCs by merozoites on the dynamics of malaria transmission using the following values of the infection rate: 0.000010, 0.000005, 0.000003, 0.000002. Their corresponding values of the reproduction number were 2.47, 1.66, 1.15, 0.84 respectively. These results are illustrated in Fig. 5, which confirm that, decreasing infection rate has the effect of reducing $\mathcal{R}_0$ (number of newly infected RBCs) and then reduce the infection of malaria parasites to RBCs.

Also, reducing the initial population of RBCs, r_0, reduces $\mathcal{R}_0$. This can either be done by reducing recruitment rate, Λ_r or increasing the death rate μ_r of uninfected RBCs. However, this is may be biologically impractical because it may cause catastrophic anemia (McQueen and McKenzie, 2004). This is indicated in Fig. 7, where Fig. 7a indicates that the decrease in r_0 reduces number of merozoites in bloodstream but also number of uninfected RBCs decreases as indicated in Fig. 7b.

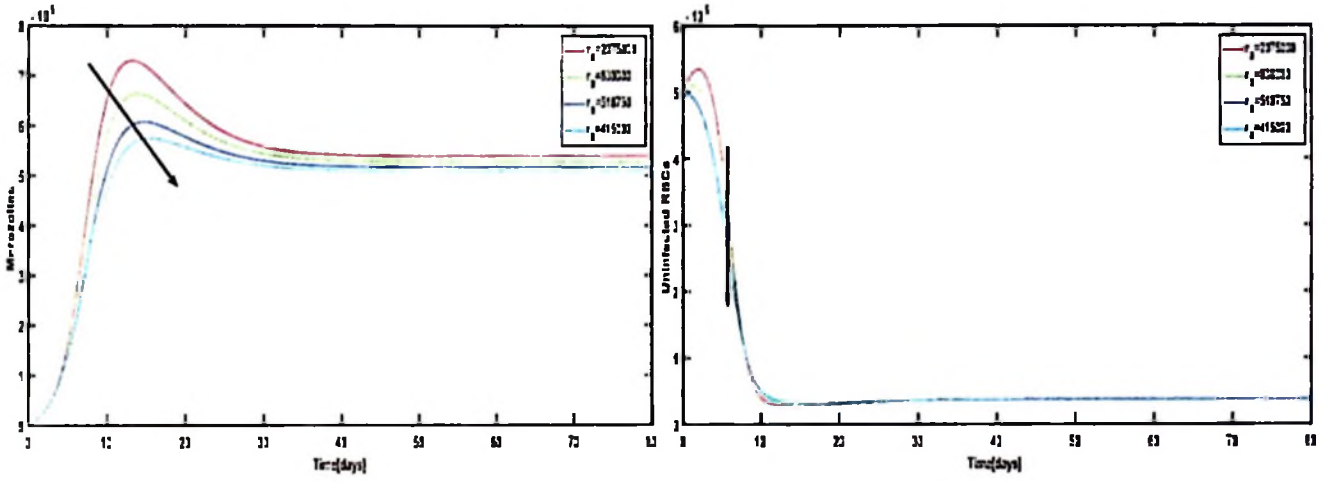

(a) Effect of decreasing r_0 on merozoites (b) Effect of decreasing r_0 on uninfected RBCs

Figure 7: Effect of decreasing r_0 on densities of uninfected merozoites and uninfected RBCs. Arrows are in direction of decreasing r_0. Values of r_0 are calculated using a fixed value of $\Lambda_r = 41500$, and different values of $\mu_r = 0.02,\ 0.05,\ 0.08$ and 0.10

Moreover, the same goal of reducing $\mathcal{R}_0$ can be achieved by a decrease in proportion of merozoites that proceeds with asexual replication, rupture rate of blood-schizonts, progression rate of infected RBCs to schizonts, and an increase in death rates of blood-schizonts and infected RBCs. Decreasing the proportion p, asexuals that differentiate to merozoites, despite its effect on decreasing number merozoites (see Fig. 8b) is still impractical because by doing so the number of gametocytes will increase as shown in Fig. 8a. Consequently, it will increase the probability of human-mosquito infection and persistence of disease.

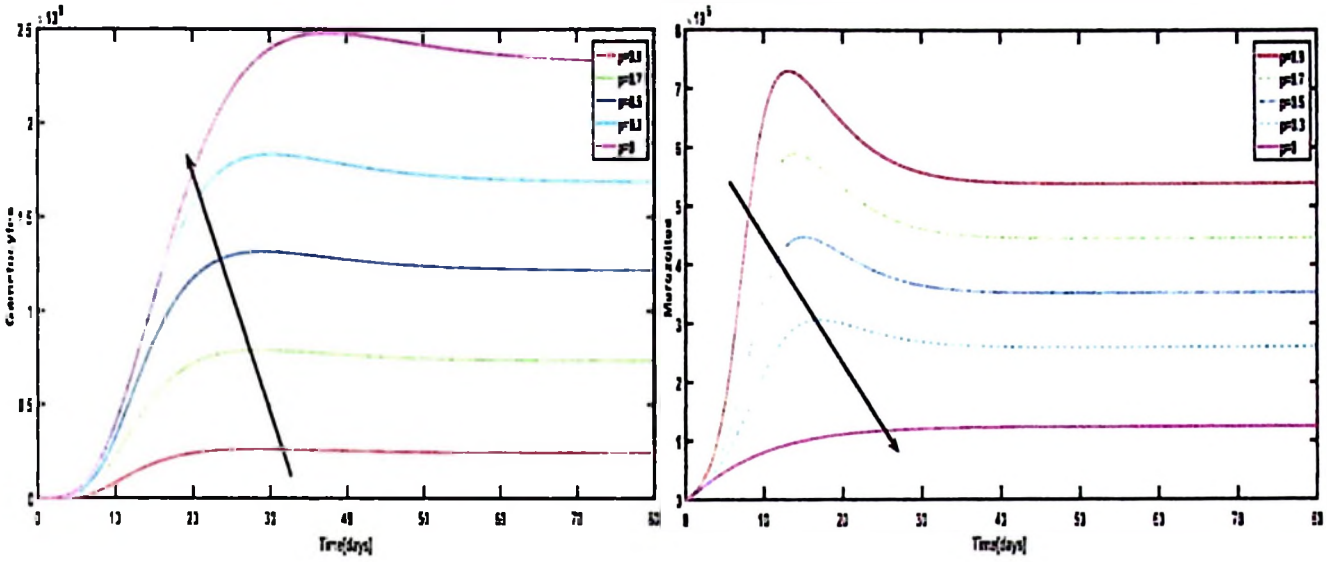

(a) Effect of p on gametocytes

(b) Effect of p on merozoites

Figure 8: Effect of reducing p on merozoites and gametocytes. Arrows are in direction of decreasing p. Values of p used are $p = 0.9,\ 0.7,\ 0.5,\ 0.3,\ 0.$

However, the impact of progression rate of infected RBCs to schizonts and death rate of infected RBCs is insignificant compared to others, because a change of 10% on these parameters will cause a change of about 1.4% on $\mathcal{R}_0$, while same change on the remaining paramenters will cause a change of at least 6.17% on $\mathcal{R}_0$.

Therefore, any biological means that will enhance the decrease of infection rate of RBCs by merozoites and number of merozoites per rupturing schizonts and/or increase the death rates of schizonts and merozoites will be of great importance on eradiction or control of malaria. These mechanism could be medication or vaccination to boost the immunity system.

2.5 Conclusion

A mathematical model for in-human host and in-mosquito dynamics of malaria parasites was developed and analyzed. The model involved three main phases in life cycle of malaria parasites. We considered four, five and three compartments in the liver, blood and mosquito stages respectively.

In analysis of the model, we included the determination of invariant region and positivity of the solutions which found to be mathematically and biologically well-posed. Malaria-free equilibrium (MFE) for the model was obtained. The threshold, $\mathcal{R}_0$, was obtained and found to a function that depends only on parameters in erythrocytic phase. This implies that the erythrocytic invasion may propagate without new infection from the liver (implying that even when

an individual is not bitten by the mosquitoes, s/he may maintain some level of malaria in the blood).

To complement the analytical solutions obtained on sensitivity indices, we carried some numerical simulations. The effects of varying the sensitive parameters on the basic reproduction number were examined, to determine their implications in the control of malaria infection (see Fig. 4, Fig. 5 and Fig. 8). The infection rate of RBCs by merozoites, death rate of merozoites, number of merozoites released are found be vital parameters in control of malaria infection. Despite having lower sensitivity index compared to death rate of merozoites, death rate of schizonts have greater impact on malaria control than that of merozoites. This is because each matured schizont bursts and releases an average of 8-32 merozoites (Tumwiine *et al.*, 2008). In addition to that, increasing the death rate of schizonts will automatically reduce the number of contact between RBCs and merozoites, hence reduces the number of infected RBCs. Therefore, the planned intervetions should aim at increasing the death of schizonts (liver or blood stage) to lower the total number of merozoites.

At this time where malaria eradication is on world agenda, this work may be used as starting point to examine how and which are new control strategies of malaria can be established to overcome the disease. Conditions for existence and stability of equilibria are discussed in the Chapter 3.

CHAPTER THREE

On Stability of the in-human host and in-mosquito Dynamics of Malaria Parasite[2]

Abstract

Stability analysis of a dynamical system is a basic requirement for its application in real-life settings. However, investigation of local stability is simpler than that for global stability, though the latter is more preferable. In this chapter, we perform a stability analysis of a mathematical model for in-human host and in-mosquito dynamics of malaria parasites and establish the existence of two types of equilibrium: malaria-free equilibrium (MFE) and malaria infection equilibrium (MIE). Using linearization of the system, MFE is proved to be locally asymptotically stable. By Metzler matrix theory, the MFE is reported to be globally asymptotically stable provided $\mathcal{R}_0 < 1$. By applying the Lyapunov functional method and LaSalle's invariance theory, we established that MIE is globally asymptotically stable, if $\mathcal{R}_0 > 1$. Numerical simulations are presented to confirm the analytical solutions.

3.1 Introduction

Mathematical models play an important role in undestanding the dynamics of infectious diseases and suggest control strategies. In the study of dynamical systems such as epidemiological models, the main focus is not on finding detailed solutions, but to investigate some characteristics of the system such as existence and stability of equilibrium points (Lungu *et al.*, 2007). A vector $\mathbf{x}^*$ is an *equilibrium point* of a dynamical system

$$\dot{\mathbf{x}} = f(\mathbf{x}, \mathbf{t})$$

if

$$f(\mathbf{x}^*, \mathbf{t}) = 0, \quad \forall t > 0.$$

An equilibrium $\mathbf{x}^*$ is said to be *stable* if an arbitrary point $\mathbf{x_0}$ of the system that starts near $\mathbf{x} = \mathbf{x}^*$ remains near it, and *unstable* if $\mathbf{x_0}$ moves away from $\mathbf{x}^*$. An equilibrium is said to be *locally stable* if for all initial values, $\mathbf{x_0}$; that are in a neighborhood $\mathcal{N}(\mathbf{x}^*)$ of $\mathbf{x}^*$, solution of the system remain near $\mathbf{x}^*$ for all values of t. The $\mathbf{x}^*$ is said to be *globally stable*, if it is stable for all initial values $\mathbf{x_0} \in \mathbb{R}^n$.

[2]This chapter is based on the research paper: Mohamed A. Selemani, Livingstone S. Luboobi, Yaw Nkansah-Gyekye. (2016). On Stability of the in-human host and in-mosquito Dynamics of Malaria Parasite. *Asian Journal of Mathematics and Applications*, article ID ama353, 23 pages

Moreover, $\mathbf{x}^*$ is *asymptotically stable* if it is stable and for an arbitrary initial value $\mathbf{x}_0$, the solution of the system converges to $\mathbf{x}^*$ as time tends to infinity. It is *locally asymptotically stable* if it is locally stable and all solutions that start in neighborhood of $\mathbf{x}^*$ converge to $\mathbf{x}^*$ as $t \to \infty$. The $\mathbf{x}^*$ is *globally asymptotically stable*, if it is globally stable and for all initial values $\mathbf{x}_0 \in \mathbb{R}^n$, the solution of the system tends to $\mathbf{x}^*$ as $t \to \infty$. Investigation of local stability is simpler than that of global stability, though the latter is more preferable (Cull, 1981). Stability of system is basic requirement for its applicability in real-life settings, since stability justify the convergence of solutions of system towards a particular equilibrium point of the system (Chen, 2004). This tells us how the system behaves if a solution started relatively near, but not exactly at equilibrium point.

A number of techniques have been proposed in investigation of stability of equilibrium points of epidemiological models (Mpeshe *et al.*, 2014b). Linearization (Mpeshe *et al.*, 2014b; Li *et al.*, 2011; Tumwiine *et al.*, 2007a) is used for proving local stability, and Metzler matrix theory is used for global stability of disease free equilibrium (Mpeshe *et al.*, 2014b; Wang and Liao, 2012; Dumont *et al.*, 2008; Kamgang and Sallet, 2008). Lyapunov fuctions have been useful tools to study of the global stability of endemic equilibrium (Kajiwara *et al.*, 2015; Korobeinikov and Maini, 2004). Morever, some models are complex such that existence and stability of equilibria cannot be investigated explicitly. Instead numerical simulations have been used to facilitate the purpose (Chiyaka *et al.*, 2008; Zhang *et al.*, 2014).

In this chapter, we investigated the existence and stability of equilibrium points of mathematical model for the in-human host and in-mosquito dynamics of malaria parasites developed in Chapter 2. We applied linearization technique to establish the local stability of MFE. We used Metzler theory to establish global stability of MFE. Global stability of MIE is established using Lyapunov function in combination with LaSalle's invariance principle. Moreover, we performed numerical simulations to prove the existence and stability of MIE.

3.2 Model Formulation

In the model formulated in Chapter 2, the in-human host and in-mosquito dynamics of malaria parasite are decribed based on interactions between twelve compartments: sporozoites injected into human, S_h; uninfected hepatic liver cells (uHLCs), H; infected hepatic liver cells (uHLCs), I_h; hepatic schizont, T_h; Merozoites, M; uninfected red blood cells (uRBCs), R; infected red blood cells (iRBCs), I_r; erythrocytic schizonts, T_r; gametocytes, G_b; oocysts, C; sporozoites in mosquito salivary gland, S_m. The detailed biological descriptions of parameters and their estimates are as presented in Table 3 (Chapter 2).

3.3 Stability Analysis of the Model

In this section, we discuss conditions for existence and stability of equilibra of the model (2.1a)-(2.1l). Conditions for their existence and asymptotic stability are established. Two nonnegative equilibria are obtained: malaria free equilibrium (MFE) and malaria infection equilibrium (MIE).

3.3.1 Local and Global Stability of MFE

In absence of infection, we obtain one equilibrium termed as malaria free equilibrium (MFE).

$$E^0 = \left(\frac{\Lambda_h}{\mu_h}, 0, 0, 0, \frac{\Lambda_r}{\mu_r}, 0, 0, 0, 0, 0, 0, 0, 0\right).$$

The stability of this equilibrium is discussed in next subsection.

We establish the local stability of E^0 by investigating the signs of the real parts of the eigenvalues of the Jacobian matrix of the system at E^0. Jacobian matrix of system (2.1a)-(2.1l) at E^0 is given by

$$J(E^0) = \begin{bmatrix}
-\mu_h & 0 & 0 & 0 & 0 & 0 & 0 & 0 & 0 & 0 & 0 & -z_1 \\
0 & -z_2 & 0 & 0 & 0 & 0 & 0 & 0 & 0 & 0 & 0 & z_1 \\
0 & \alpha_1 & -z_3 & 0 & 0 & 0 & 0 & 0 & 0 & 0 & 0 & 0 \\
0 & 0 & r_1\delta_1 & -z_4 & 0 & 0 & pr_2\delta_2 & 0 & 0 & 0 & 0 & 0 \\
0 & 0 & 0 & -z_5 & -\mu_r & 0 & 0 & 0 & 0 & 0 & 0 & 0 \\
0 & 0 & 0 & z_5 & 0 & -z_6 & 0 & 0 & 0 & 0 & 0 & 0 \\
0 & 0 & 0 & 0 & 0 & \alpha_2 & -z_7 & 0 & 0 & 0 & 0 & 0 \\
0 & 0 & 0 & 0 & 0 & 0 & z_8 & -z_9 & 0 & 0 & 0 & 0 \\
0 & 0 & 0 & 0 & 0 & 0 & 0 & q\omega & -z_{10} & 0 & 0 & 0 \\
0 & 0 & 0 & 0 & 0 & 0 & 0 & 0 & \alpha_3 & -z_{11} & 0 & 0 \\
0 & 0 & 0 & 0 & 0 & 0 & 0 & 0 & 0 & r_3\delta_3 & -z_{12} & 0 \\
0 & 0 & 0 & 0 & 0 & 0 & 0 & 0 & 0 & 0 & 0 & -z_{13}
\end{bmatrix},$$

where

$$\begin{aligned}
z_1 &= \beta_1\frac{\Lambda_h}{\mu_h}, \quad z_2 = \alpha_1 + \mu_{ih}, \quad z_3 = \delta_1 + \mu_{th}, \quad z_4 = \beta_2\frac{\Lambda_r}{\mu_r} + \mu_m, \quad z_5 = \beta_2\frac{\Lambda_r}{\mu_r}, \\
z_6 &= \alpha_2 + \mu_{ir}, \quad z_7 = \delta_2 + \mu_{tr}, \quad z_8 = (1-p)r_2\delta_2, \quad z_9 = q\omega + \mu_{gb}, \quad z_{10} = \alpha_3 + \mu_{gm}, \\
z_{11} &= \delta_3 + \mu_c, \quad z_{12} = a\nu + \mu_{sm}, \quad z_{13} = \beta_1\frac{\Lambda_h}{\mu_h} + \mu_{sh}
\end{aligned} \tag{3.1}$$

The MFE is locally asympotically stable if and only if trace of $J(E^0)$ is strictly negative and

determinat of $J(E_0)$ is strictly positive. We obtain the following results.

$$trace(J(E^0)) = [(\mu_h + \mu_r) + (\mu_{th} + \mu_{tr}) + (\mu_{ih} + \mu_{ir}) + (\alpha_1 + \alpha_2 + \alpha_3) + (\delta_1 + \delta_2 + \delta_3) + (\mu_m + \mu_{gb} + \mu_c + \mu_{sm} + mu_{sh}) + \beta_1 \frac{\Lambda_h}{\mu_h} + \beta_2 \frac{\Lambda_r}{\mu_r} + (q\omega + \mu_{gm} + +a\nu)] < 0 \tag{3.2}$$

and

$$\begin{aligned}
det(J(E^0)) =& -(\beta_1 \Lambda_h + \mu_{sh}\mu_h)(\delta_1 + \mu_{th})(\alpha_1 + \mu_{ih})(q\omega + \mu_{gb})(\alpha_3 + \mu_{gm})(\delta_3 + \mu_c)(a\nu + \mu_{sm}) \\
& (-\beta_2 \Lambda_r \alpha_2 \delta_2 - \beta_2 \Lambda_r \delta_2 \mu_{ir} - \beta_2 \Lambda_r \alpha_2 \mu_{tr} - \beta_2 \Lambda_r \mu_{tr} \mu_{ir} - \mu_m \mu_r \mu_{tr} \mu_{ir} - \mu_m \mu_r \mu_{tr} \alpha_2 \\
& - \mu_m \mu_r \delta_2 \alpha_2 - \mu_m \mu_r \delta_2 \mu_{ir} + \beta_2 \Lambda_r \alpha_2 pr_2 \delta_2) \\
=& (\beta_1 \Lambda_h + \mu_{sh}\mu_h)(\delta_1 + \mu_{th})(\alpha_1 + \mu_{ih})(q\omega + \mu_{gb})(\alpha_3 + \mu_{gm})(\delta_3 + \mu_c)(a\nu + \mu_{sm}) \\
& (\beta_2 \Lambda_r \delta_2 (\alpha_2 + \mu_{ir}) + \beta_2 \Lambda_r \mu_{tr} (\alpha_2 + \mu_{ir}) + \mu_m \mu_r \mu_{tr} (\alpha_2 + \mu_{ir}) \\
& + \mu_m \mu_r \delta_2 (\alpha_2 + \mu_{ir}) - \beta_2 \Lambda_r \alpha_2 pr_2 \delta_2)
\end{aligned}$$

$$\begin{aligned}
=& (\beta_1 \Lambda_h + \mu_{sh}\mu_h)(\delta_1 + \mu_{th})(\alpha_1 + \mu_{ih})(q\omega + \mu_{gb})(\alpha_3 + \mu_{gm})(\delta_3 + \mu_c)(a\nu + \mu_{sm}) \\
& [(\alpha_2 + \mu_{ir})(\beta_2 \Lambda_r \delta_2 + \beta_2 \Lambda_r \mu_{tr} + \mu_m \mu_r \mu_{tr} + \mu_m \mu_r \delta_2) - \beta_2 \Lambda_r \alpha_2 pr_2 \delta_2] \\
=& (\beta_1 \Lambda_h + \mu_{sh}\mu_h)(\delta_1 + \mu_{th})(\alpha_1 + \mu_{ih})(q\omega + \mu_{gb})(\alpha_3 + \mu_{gm})(\delta_3 + \mu_c)(a\nu + \mu_{sm}) \\
& [(\alpha_2 + \mu_{ir})(\beta_2 \Lambda_r (\delta_2 + \mu_{tr}) + \mu_m \mu_r (\mu_{tr} + \delta_2) - \beta_2 \Lambda_r \alpha_2 pr_2 \delta_2] \\
=& (\beta_1 \Lambda_h + \mu_{sh}\mu_h)(\delta_1 + \mu_{th})(\alpha_1 + \mu_{ih})(q\omega + \mu_{gb})(\alpha_3 + \mu_{gm})(\delta_3 + \mu_c)(a\nu + \mu_{sm}) \\
& [(\mu_{tr} + \delta_2)(\alpha_2 + \mu_{ir})(\beta_2 \Lambda_r + \mu_m \mu_r) - \beta_2 \Lambda_r \alpha_2 pr_2 \delta_2] \\
=& (\beta_1 \Lambda_h + \mu_{sh}\mu_h)(\delta_1 + \mu_{th})(\alpha_1 + \mu_{ih})(q\omega + \mu_{gb})(\alpha_3 + \mu_{gm})(\delta_3 + \mu_c)(a\nu + \mu_{sm}) \\
& (\mu_{tr} + \delta_2)(\alpha_2 + \mu_{ir})(\beta_2 \Lambda_r + \mu_m \mu_r) \left[1 - \frac{\beta_2 \Lambda_r p \alpha_2 r_2 \delta_2}{(\mu_{tr} + \delta_2)(\alpha_2 + \mu_{ir})(\beta_2 \Lambda_r + \mu_m \mu_r)}\right] \\
=& (\beta_1 \Lambda_h + \mu_{sh}\mu_h)(\delta_1 + \mu_{th})(\alpha_1 + \mu_{ih})(q\omega + \mu_{gb})(\alpha_3 + \mu_{gm})(\delta_3 + \mu_c)(a\nu + \mu_{sm}) \\
& (\mu_{tr} + \delta_2)(\alpha_2 + \mu_{ir})(\beta_2 \Lambda_r + \mu_m \mu_r)[1 - \mathcal{R}_0]
\end{aligned} \tag{3.3}$$

From (3.3) we deduce the following:

$$\begin{aligned}
det(J(E^0)) > 0 \Leftrightarrow & (\beta_1 \Lambda_h + \mu_{sh}\mu_h)(\delta_1 + \mu_{th})(\alpha_1 + \mu_{ih})(q\omega + \mu_{gb})(\alpha_3 + \mu_{gm})(\delta_3 + \mu_c)(a\nu + \mu_{sm}) \\
& (\mu_{tr} + \delta_2)(\alpha_2 + \mu_{ir})(\beta_2 \Lambda_r + \mu_m \mu_r)[1 - \mathcal{R}_0] > 0
\end{aligned} \tag{3.4}$$

where

$$\mathcal{R}_0 = \left[\frac{\beta_2 \Lambda_r}{\beta_2 \Lambda_r + \mu_m \mu_r}\right] \left[\frac{\alpha_2}{(\alpha_2 + \mu_{ir})}\right] \left[\frac{pr_2 \delta_2}{(\delta_2 + \mu_{tr})}\right]$$

as expressed in Equation 2.41 in Chapter 2.

Equation (3.4) holds only if $\mathcal{R}_0 < 1$; and because of this requirement $\mathcal{R}_0$ is interpreted as the basic reproduction number as computed in Chapter. This leads us to the following theorem.

Theorem 3.1

The malaria-free equilibrium, E^0 is locally asymptotically stable when $\mathcal{R}_0 < 1$ and unstable otherwise.

We establish the global stability of E^0 using the Metzler matrix theory technique used in Castillo-Chávez *et al.* (2002); Kamgang and Sallet (2008); Mpeshe *et al.* (2014b). In this approach, we re-write the model system in the form:

$$\begin{cases} \frac{dX_n}{dt} = A_1(x)(X_n - X_{E^0,n}) + A_{12}(x)X_c \\ \\ \frac{dX_c}{dt} = A_2(x)X_c \end{cases}$$

where X_n is the vector of uninfected classes and X_c is the vector of infected classes. For our case, we have

$$X_n = (H,\ R) \text{ and } X_c = (I_h, T_h, M, I_r, T_r, G_h, G_m, C, S_m, S_h) \tag{3.5}$$

$$X_{E^0,n} = \left(\frac{\Lambda_h}{\mu_h}, \frac{\Lambda_r}{\mu_r}\right) \tag{3.6}$$

and

$$A_1(x) = \begin{pmatrix} -\mu_h & 0 \\ 0 & -\mu_r \end{pmatrix}, \tag{3.7}$$

$$A_{12}(x) = \begin{pmatrix} 0 & 0 & 0 & 0 & 0 & 0 & 0 & 0 & 0 & -\beta_1 H \\ 0 & 0 & -\beta_2 R & 0 & 0 & 0 & 0 & 0 & 0 & 0 \end{pmatrix} \tag{3.8}$$

and

$$A_2(x) = \begin{pmatrix} -w_1 & 0 & 0 & 0 & 0 & 0 & 0 & 0 & 0 & \beta_1 H \\ \alpha_1 & -w_2 & 0 & 0 & 0 & 0 & 0 & 0 & 0 & 0 \\ 0 & r_1\delta_1 & -w_3 & 0 & pr_2\delta_2 & 0 & 0 & 0 & 0 & 0 \\ 0 & 0 & \beta_2 R & -w_4 & 0 & 0 & 0 & 0 & 0 & 0 \\ 0 & 0 & 0 & \alpha_2 & -w_5 & 0 & 0 & 0 & 0 & 0 \\ 0 & 0 & 0 & 0 & w_6 & -w_7 & 0 & 0 & 0 & 0 \\ 0 & 0 & 0 & 0 & 0 & pq\omega & -w_8 & 0 & 0 & 0 \\ 0 & 0 & 0 & 0 & 0 & 0 & \alpha_3 & -w_9 & 0 & 0 \\ 0 & 0 & 0 & 0 & 0 & 0 & 0 & r_3\delta_3 & -w_{10} & 0 \\ 0 & 0 & 0 & 0 & 0 & 0 & 0 & 0 & w_{11} & -w_{12} \end{pmatrix} \tag{3.9}$$

where

$$w_1 = \alpha_1 + \mu_{ih}, \quad w_2 = \delta_1 + \mu_{th}, \quad w_3 = \frac{\beta_2 \Lambda_r}{\mu_r} + \mu_m, \quad w_4 = \alpha_2 + \mu_{ir},$$
$$w_5 = \delta_1 + \mu_{tr}, \quad w_6 = (1-p) r_2 \delta_2, \quad w_7 = q\omega + \mu_{gb}, \quad w_8 = \alpha_3 + \mu_{gm},$$
$$w_9 = \delta_3 + \mu_c, \quad w_{10} = a\nu + \mu_{sm}, \quad w_{11} = \frac{ab\nu}{S_m}, \quad w_{12} = \beta_1 H + \mu_{sh} \tag{3.10}$$

It can easily be seen from (3.7) that, all eigenvalues of A_1 are real and negative.
So, the system

$$\frac{dX_n}{dt} = A_1(x)(X_n - X_{E^0,n}) + A_{12}(x) X_c$$

is globally asymptotically stable at X_{E^0}. From (3.9) and (3.10) it can be observed that all off diagonal elements of A_2 are non-negative. Therefore, A_2 is a Metzler matrix. To investigate the conditions under which MFE is the global asymptotically stability (GAS), we have to show that A_2 is Metzler stable matrix (all its diagonal elements are negative) by proving the following proposition.

Proposition 1. *(Kamgang and Sallet, 2008; Dumont* et al., *2008)*
Let M be a square block decomposed Metzler matrix: $M = \begin{pmatrix} A & B \\ C & D \end{pmatrix}$ with A and D square matrices. Then M is Metzler stable if and only if matrices A and $D - CA^{-1}B$ are Metzler stable.

For this case we have $M = A_2$, and $A = \begin{pmatrix} -w_1 & 0 & 0 & 0 & 0 \\ \alpha_1 & -w_2 & 0 & 0 & 0 \\ 0 & r_1\delta_1 & -w_3 & 0 & pr_2\delta_2 \\ 0 & 0 & \beta_2 R & -w_4 & 0 \\ 0 & 0 & 0 & \alpha_2 & -w_5 \end{pmatrix}$

$$B = \begin{pmatrix} 0 & 0 & 0 & 0 & \beta_1 H \\ 0 & 0 & 0 & 0 & 0 \\ 0 & 0 & 0 & 0 & 0 \\ 0 & 0 & 0 & 0 & 0 \\ 0 & 0 & 0 & 0 & 0 \end{pmatrix}, \quad C = \begin{pmatrix} 0 & 0 & 0 & 0 & w_6 \\ 0 & 0 & 0 & 0 & 0 \\ 0 & 0 & 0 & 0 & 0 \\ 0 & 0 & 0 & 0 & 0 \\ 0 & 0 & 0 & 0 & 0 \end{pmatrix}$$

and $D = \begin{pmatrix} -w_7 & 0 & 0 & 0 & 0 \\ \rho q\omega & -w_8 & 0 & 0 & 0 \\ 0 & \alpha_3 & -w_9 & 0 & 0 \\ 0 & 0 & r_3\alpha_3 & -w_{10} & 0 \\ 0 & 0 & 0 & w_{11} & -w_{12} \end{pmatrix}$

immediately we have

$$D - CA^{-1}B = \begin{pmatrix} -w_{11} & 0 & 0 & 0 & \frac{r_1\delta_1\alpha_1\alpha_2 w_6\Lambda_h\Lambda_r\beta_1\beta_2}{w_1w_2\mu_h(w_3w_4w_5\mu_r - \beta_2\Lambda_r pr_2\delta_2\alpha_2)} \\ w_{12} & -w_{13} & 0 & 0 & 0 \\ 0 & \alpha_3 & -w_{14} & 0 & 0 \\ 0 & 0 & w_{15} & w_{16} & 0 \\ 0 & 0 & 0 & w_{17} & -w_{18} \end{pmatrix}$$

Definition:

A Metzler matrix M is said to be stable if all of its diagonal elements are negative.

By that definition, A is Metzler stable matrix, and $D - CA^{-1}B$ is Metzler stable matrix if and only if

$$\frac{r_1\delta_1\alpha_1\alpha_2 w_6\Lambda_h\Lambda_r\beta_1\beta_2}{w_1w_2\mu_h(w_3w_4w_5\mu_r - \beta_2\Lambda_r pr_2\delta_2\alpha_2)} > 0 \tag{3.11}$$

It is observed that equation (3.11) holds only when

$$\frac{\beta_2\Lambda_r pr_2\delta_2\alpha_2}{w_3w_4w_5\mu_r} < 1 \tag{3.12}$$

Using w_3, w_4, and w_5 as given in equation (3.10), we get

$$\frac{\frac{\beta_2\Lambda_r}{\mu_r}\alpha_2 pr_2\delta_2}{\left(\frac{\beta_2\Lambda_r}{\mu_r} + \mu_m\right)(\alpha_2 + \mu_{ir})(\delta_2 + \mu_{tr})} < 1. \tag{3.13}$$

equivalently, $\mathcal{R}_0 < 1$. This leads us to the following theorem.

Theorem 3.2

The malaria-free equilibrium of the model system (2.1a)-(2.11) is *globally assymptotically stable* in Ω if $\mathcal{R}_0 < 1$ and unstable if $\mathcal{R}_0 > 1$.

3.3.2 Existence of Malaria Infection Equilibrium (MIE)

The model has one positive malaria infection equilibrium E^* which is given by

$$E^* = (H^*, I_h^*, T_h^*, M^*, R^*, I_r^*, T_r^*, G_b^*, G_m^*, C^*, S_m^*, S_h^*)$$

where

$$H^* = \frac{\Lambda_h}{\beta_1 S_h^* + \mu_h}, \quad I_h^* = \frac{\beta_1\Lambda_h S_h^*}{(\alpha_1 + \mu_{ih})(\beta_1 S_h^* + \mu_h)}, \quad T_h^* = \frac{\beta_1\Lambda_h\alpha_1 S_h^*}{(\delta_1 + \mu_{th})(\alpha_1 + \mu_{ih})(\beta_1 S_h^* + \mu_h)},$$

$$R^* = \frac{\Lambda_r}{\beta_2 M^* + \mu_r}, \quad I_r^* = \frac{\beta_2\Lambda_2 M^*}{(\alpha_2 + \mu_{ir})(\beta_2 M^* + \mu_r)}, \quad T_r^* = \frac{\mathcal{R}_0(\beta_2\Lambda_r + \mu_r\mu_m)M^*}{pr_2\delta_2(\beta_2 M^* + \mu_r)}$$

$$G_b^* = \frac{(1-p)\mathcal{R}_0}{p(q\omega+\mu_{gb})}\frac{(\beta_2\Lambda_r+\mu_r\mu_m)M^*}{(\beta_2 M^*+\mu_r)},\quad G_m = \left[\frac{pq\omega}{\alpha_3+\mu_{gm}}\right]\left[\frac{(1-p)\mathcal{R}_0}{p(q\omega+\mu_{gb})}\frac{(\beta_2\Lambda_r+\mu_r\mu_m)M^*}{(\beta_2 M^*+\mu_r)}\right],$$

$$C = \frac{\alpha_3}{\delta_3+\mu_c}\left[\frac{pq\omega}{\alpha_3+\mu_{gm}}\right]\left[\frac{(1-p)\mathcal{R}_0}{p(q\omega+\mu_{gb})}\frac{(\beta_2\Lambda_r+\mu_r\mu_m)M^*}{(\beta_2 M^*+\mu_r)}\right],$$

$$S_m^* = \frac{r_3\delta_3}{\alpha\nu+\mu_{sm}}\frac{\alpha_3}{\delta_3+\mu_c}\left[\frac{pq\omega}{\alpha_3+\mu_{gm}}\right]\left[\frac{(1-p)\mathcal{R}_0}{p(q\omega+\mu_{gb})}\frac{(\beta_2\Lambda_r+\mu_r\mu_m)M^*}{(\beta_2 M^*+\mu_r)}\right],$$

S_h^* and M^* are positive solutions of $F(S_h^*)=0$ and $G(M^*)=0$ respectively, where

$F(S_h^*) = A_3S_h^{*2} + A_2S_h^* + A_1$, $G(M^*) = B_3M^{*2} + B_2M^* + B_1$ and
$A_3 = \beta_1\mu_{sh}$, $A_2 = \beta_1(\Lambda_h - ab\nu) + \mu_{sh}\mu_h$, $A_1 = -ab\nu\mu_h$,
$B_3 = \beta_2\mu_m$, $B_2 = -[(\beta_2\Lambda_r + \mu_m\mu_r)(\mathcal{R}_0 - 1) + \beta_2\lambda^*]$, $B_1 = -\mu_r\lambda^*$ and

$$\lambda(S_h^*) = \frac{\theta S_h^*}{\beta_1 S_h^* + \mu_h}$$

Now we need to determine necessary and sufficient conditions for existence of malaria-infection equilibrium E^* by proving the following theorem

Theorem 3.3

The model system (2.1a)-(2.11) has a unique malaria infection equilibrium

$$E^* = (H^*, I_h^*, T_h^*, M^*, R^*, I_r^*, T_r^*, G_b^*, G_m^*, C^*, S_m^*, S_h^*)$$

if $\mathcal{R}_0 > 1$, $\Lambda_h > ab\nu$, $A_3S_h^{*2} + A_2S_h^* + A_1 = 0$ and $B_3M^{*2} + B_2M^* + B_1 = 0$ have roots $S_h^* > 0$ and $M^* > 0$ respectively.

Proof:

Let $E^* = (H^*, I_h^*, T_h^*, M^*, R^*, I_r^*, T_r^*, G_b^*, G_m^*, C^*, S_m^*, S_h^*)$ be malaria infection equilibrium of the system (2.1a)-(2.11). Substituting the expression for H^* into equation (2.11), we have

$$ab\nu - \frac{\beta_1 S_h^*\Lambda_h}{\beta_1 S_h^* + \mu_h} - \mu_{sh}S_h^* = 0$$

which yields

$$\beta_1\mu_{sh}S_h^{*2} + [\beta_1(\Lambda_h - ab\nu) + \mu_{sh}\mu_h]S_h^* - ab\nu\mu_h = 0 \tag{3.14}$$

Since $A_1 < 0$ and $A_3 > 0$, then the quadratic equation (3.14) has unique positive root S_h^* given by

$$S_h^* = \frac{-[\beta_1(\Lambda_h - ab\nu) + \mu_{sh}\mu_h] + \sqrt{\Delta_1}}{2\beta_1\mu_{sh}} \tag{3.15}$$

where

$$\Delta_1 = (\beta_1(\Lambda_h - ab\nu) + \mu_{sh}\mu_h)^2 + 4\beta_1 ab\nu\mu_{sh}\mu_h \tag{3.16}$$

only if $A_2 > 0$.

Hence, $A_2 = \beta_1(\Lambda_h - ab\nu) + \mu_{sh}\mu_h > 0$ only if $\Lambda_h > ab\nu$ (recruitment rate of uninfected HLCs is greater than recruitment of sporozoites into human liver).

Substituting expressions for T_h^*, T_r^* and R^* into equation (??) gives

$$\frac{\beta_1\Lambda_h\alpha_1 r_1\delta_1 S_h^*}{(\delta_1+\mu_{th})(\alpha_1+\mu_h+d_h)(\beta_1 S_h^*+\mu_h)} + \frac{\mathcal{R}_0(\beta_2\Lambda_r+\mu_m\mu_r)M^*}{(\beta_2 M^*+\mu_r)} - \frac{\beta_2\Lambda_r M^*}{\beta_2 M^*+\mu_r} - \mu_m M^* = 0 \tag{3.17}$$

Letting $\theta = \dfrac{\beta_1\Lambda_h\alpha_1 r_1\delta_1}{(\delta_1+\mu_{th})(\alpha_1+\mu_h+d_h)}$ equation (3.17) becomes

$$\frac{\theta S_h^*}{(\beta_1 S_h^*+\mu_h)} + \frac{\left[\mathcal{R}_0(\beta_2\Lambda_r+\mu_m\mu_r) - \beta_2\Lambda_r - \mu_m(\beta_2 M^*+\mu_r)\right]M^*}{(\beta_2 M^*+\mu_r)} = 0 \tag{3.18}$$

which can be further simplified to

$$\beta_2\mu_m M^{*2} - \left[(\beta_2\Lambda_r+\mu_m\mu_r)(\mathcal{R}_0-1)+\beta_2\lambda^*\right]M^* - \mu_r\lambda^* = 0 \tag{3.19}$$

where

$$\lambda^* = \frac{\theta S_h^*}{(\beta_1 S_h^*+\mu_h)}$$

Equation (3.19) has a unique positive real root M^* given by

$$M^* = \frac{\left[(\beta_2\Lambda_r+\mu_m\mu_r)(\mathcal{R}_0-1)+\beta_2\lambda^*\right]+\sqrt{\triangle_2}}{2\beta_2\mu_m\mu_r\lambda^*} \tag{3.20}$$

where

$$\triangle_2 = (\mathcal{R}_0-1)^2(\beta_2\Lambda_r+\mu_m\mu_r)^2 + 2\beta_2\lambda^*\left[\beta_2\Lambda_r+\mu_m\mu_r(\mathcal{R}_0-1)\right] + \beta_2^2\lambda^{*2} + 4\beta_2\mu_m\mu_r\lambda^*$$

only if $\mathcal{R}_0 > 1$. This is condition for the existence of malaria infection equilibrium.

Therefore, if $\mathcal{R}_0 > 1$, $\Lambda_h > ab\nu$ and quadratic equations $A_3 S_h^{*2} + A_2 S_h^* + A_1 = 0$ and $B_3 M^{*2} + B_2 M^* + B_1 = 0$ have respectively positive roots S_h^* and M^*, with

$$S_h^* = \frac{-\left[\beta_1(\Lambda_h - ab\nu)+\mu_{sh}\mu_h\right]+\sqrt{\triangle_1}}{2\beta_1\mu_{sh}} \text{ and } M^* = \frac{\left[(\beta_2\Lambda_r+\mu_m\mu_r)(\mathcal{R}_0-1)+\beta_2\lambda^*\right]+\sqrt{\triangle_2}}{2\beta_2\mu_m\mu_r\lambda^*}$$

then system (2.1a)-(2.1l) has malaria infection equilibrium E^*.

3.3.3 Global Stability of MIE

By theorem 3.1, MFE is locally asymptotically stable when $\mathcal{R}_0 < 1$. This suggests local stability of the MIE for the reverse condition (i.e. when $\mathcal{R}_0 > 1$) (Van den Driessche and Watmough, 2002). So we only investigate the global stability of the malaria infection equilibrium. We adopted the techiniques used by Pedro *et al.* (2014).

Theorem 3.4

if $\mathcal{R}_0 > 1$, the model described by equations (2.1a)-(2.1l) has unique positive MIE, E^*, such that

$$\frac{S_h^* H^*}{S_h H} \geq \frac{H^*}{H} \geq 1, \quad \text{for } 0 < S_h < S_h^* \text{ and } 0 < H < H^*,$$
$$\frac{S_h^* H^*}{S_h H} \geq \frac{S_h^*}{S_h} > 1 \quad \text{for } 0 < S_h < S_h^* \text{ and } 0 < H < H^*.$$
$$\frac{R^* M^*}{RM} \geq \frac{M^*}{M} \geq 1 \quad \text{for } 0 < M < M^* \text{ and } 0 < R < R^*,$$
$$\frac{R^* M^*}{RM} \geq \frac{R^*}{R} \geq 1 \quad \text{for } 0 < M < M^* \text{ and } 0 < R < R^*.$$

Then, E^* is globally asymptotic stable in $\Omega \subset \Omega$.

Proof: To estabilish the global stability of MIE, E^*, we define the Lyapunov function of the form

$$L(x) = \sum z_i (x_i - x_i^* \ln \frac{x}{x^*}), \text{ for } i = 1, 2, \ldots 12$$

as proposed by Castillo-Chávez *et al.* (2002) where x_i is a number of cells in the ith class, x_i^* are equilibrium values and z_i are constants. This approach has been found useful for more complex compartmental models of *in vivo* dynamics (Korobeinikov, 2004).

Now, we constructed the following lyapunov function

$$\begin{aligned} L =& z_1 \left(H - H^* \ln \frac{H}{H^*} \right) + z_2 \left(I_h - I_h^* \ln \frac{I_h}{I_h^*} \right) + z_3 \left(T_h - T_h^* \ln \frac{T_h}{T_h^*} \right) \\ &+ z_4 \left(M - M^* \ln \frac{M}{M^*} \right) + z_5 \left(R - R^* \ln \frac{R}{R^*} \right) + z_6 \left(I_r - I_r^* \ln \frac{I_r}{I_r^*} \right) \\ &+ z_7 \left(T_r - T_r^* \ln \frac{T_r}{T_r^*} \right) + z_8 \left(G_b - G_b^* \ln \frac{G_b}{G_b^*} \right) + z_9 \left(G_m - G_m^* \ln \frac{G_m}{G_m^*} \right) \\ &+ z_{10} \left(C - C^* \ln \frac{C}{C^*} \right) + z_{11} \left(S_m - S_m^* \ln \frac{S_m}{S_m^*} \right) + z_{12} \left(S_h - S_h^* \ln \frac{S_h}{S_h^*} \right) \end{aligned} \tag{3.21}$$

Differentiating equation (3.21) with respect to time, we get

$$\begin{aligned} \frac{dL}{dt} =& z_1 \left(1 - \frac{H^*}{H} \right) \frac{dH}{dt} + z_2 \left(1 - \frac{I_h^*}{I_h} \right) \frac{dI_h}{dt} + z_3 \left(1 - \frac{T_h^*}{T_h} \right) \frac{dT_h}{dt} + z_4 \left(1 - \frac{M^*}{M} \right) \frac{dM}{dt} \\ &+ z_5 \left(1 - \frac{R^*}{R} \right) \frac{dR}{dt} + z_6 \left(1 - \frac{I_r^*}{I_r} \right) \frac{dI_r}{dt} + z_7 \left(1 - \frac{T_r^*}{T_r} \right) \frac{dT_r}{dt} + z_8 \left(1 - \frac{G_b^*}{G_b} \right) \frac{dG_b}{dt} \\ &+ z_9 \left(1 - \frac{G_m^*}{G_m} \right) \frac{dG_m}{dt} + z_{10} \left(1 - \frac{C^*}{C} \right) \frac{dC}{dt} + z_{11} \left(1 - \frac{S_m^*}{S_m} \right) \frac{dS_m}{dt} + z_{12} \left(1 - \frac{S_h^*}{S_h} \right) \frac{dS_h}{dt} \end{aligned} \tag{3.22}$$

and using (2.1a)-(2.1l) in (3.22), we get

$$\begin{aligned}\frac{dL}{dt} =& z_1\left(1-\frac{H^*}{H}\right)(\Lambda_h-\beta_1 S_h H-\mu_h H)+z_2\left(1-\frac{I_h^*}{I_h}\right)(\beta_1 S_h H-\alpha_1 I_h-\mu_{ih} I_h)\\ &+z_3\left(1-\frac{T_h^*}{T_h}\right)(\alpha_1 I_h-\delta_1 T_h-\mu_{th} T_h)+z_4\left(1-\frac{M^*}{M}\right)(r_1\delta_1 T_h+pr_2\delta_2 T_r-\beta_2 RM-\mu_m M)\\ &+z_5\left(1-\frac{R^*}{R}\right)(\Lambda_r-\beta_2 RM-\mu_r R)+z_6\left(1-\frac{I_r^*}{I_r}\right)(\beta_2 RM-\alpha_2 I_r-\mu_{ir} I_r)\\ &+z_7\left(1-\frac{T_r^*}{T_r}\right)(\alpha_2 I_r-\delta_2 T_r-\mu_{tr} T_r)+z_8\left(1-\frac{G_b^*}{G_b}\right)((1-p)r_2\delta_2 T_r-q\omega G_b-\mu_{gb} G_b)\\ &+z_9\left(1-\frac{G_m^*}{G_m}\right)(pq\omega G_b-\alpha_3 G_m-\mu_{gm} G_m)+z_{10}\left(1-\frac{C^*}{C}\right)(\alpha_3 G_m-\delta_3 C-\mu_c C)\\ &+z_{11}\left(1-\frac{S_m^*}{S_m}\right)(r_3\delta_3 C-a\nu S_m-\mu_{sm} S_m)+z_{12}\left(1-\frac{S_h^*}{S_h}\right)(a b\nu-\beta_1 S_{sh} H-\mu_{sh} S_h)\end{aligned} \tag{3.23}$$

At malaria-infection equilibrium, we have

$$\begin{aligned}\Lambda_h =&\beta_1 S_h^* H^*+\mu_h H^*,\quad \beta_1 S_h^* H^*=(\alpha_1+\mu_{ih})I_h^*,\quad a b\nu=\beta_1 S_h^* H^*+\mu_{sh} S_h,\\ r_1\delta_1 T_h^*+pr_2\delta_2 T_r^* =&\beta_2 R^* M^*+\mu_m M^*,\quad \Lambda_r=\beta_2 R^* M^*+\mu_r R^*,\quad \beta_2 R^* M^*=(\alpha_2+\mu_{ir})I_r^*,\\ pq\omega G_b^* =&(\alpha_3+\mu_{gm})G_m^*,\quad (1-p)r_2\delta_2 T_r^*=(q\omega+\mu_{gb})G_b^*,\quad \alpha_3 G_m^*=(\delta_3+\mu_c)C^*,\\ r_3\delta_3 C^* =&(a\nu+\mu_{sm})S_m^*\end{aligned} \tag{3.24}$$

Substuting expressions at MIE given in (3.24) into equation (3.23), we obtain

$$\begin{aligned}
\frac{dL}{dt} &= z_1\left(1-\frac{H^*}{H}\right)[\beta_1 S_h^* H^* + \mu_h H^* - \beta_1 S_h H - \mu_h H] \\
&+ z_2\left(1-\frac{I_h^*}{I_h}\right)[(\alpha_1+\mu_{ih})I_h^* - (\alpha_1+\mu_{ih})I_h] \\
&+ z_3\left(1-\frac{T_h^*}{T_h}\right)[(\delta_1+\mu_{th})T_1^* - (\delta_1+\mu_{th})T_h] \\
&+ z_4\left(1-\frac{M^*}{M}\right)[\beta_2 R^* M^* + \mu_m M^* - \beta_2 RM - \mu_m M] \\
&+ z_5\left(1-\frac{R^*}{R}\right)[\beta_2 R^* M^* + \mu_r R^* - \beta_2 RM - \mu_r R] \\
&+ z_6\left(1-\frac{I_r^*}{I_r}\right)[(\alpha_2+\mu_{ir})I_r^* - (\alpha_2+\mu_{ir})I_r] \\
&+ z_7\left(1-\frac{T_r^*}{T_r}\right)[(\delta_2+\mu_{tr})T_r^* - (\delta_2+\mu_{tr})T_r] \\
&+ z_8\left(1-\frac{G_b^*}{G_b}\right)[q\omega+\mu_{gb})G_b^* - q\omega+\mu_{gb})G_b] \\
&+ z_9\left(1-\frac{G_m^*}{G_m}\right)[(\alpha_3+\mu_{gm})G_m^* - (\alpha_3+\mu_{gm})G_m] \\
&+ z_{10}\left(1-\frac{C^*}{C}\right)[(\delta_3+\mu_c)C^* - (\delta_3+\mu_c)C] \\
&+ z_{11}\left(1-\frac{S_m^*}{S_m}\right)[(a\nu+\mu_{sm})S_m^* - (a\nu+\mu_{sm})S_m^*] \\
&+ z_{12}\left(1-\frac{S_h^*}{S_h}\right)[\beta_1 S_h^* H^* + \mu_{sh}S_h^* - \beta_1 S_h H - \mu_{sh}S_h]
\end{aligned}$$

Further algebraic manupulations leads us to

$$\begin{aligned}
\frac{dL}{dt} &= -z_1\mu_h H\left[1-\frac{H^*}{H}\right]^2 + z_1\beta_1 S_h H\left[1-\frac{H^*}{H}\right]\left[\frac{S_h^* H^*}{S_h H}-1\right] \\
&- z_2(\alpha_1+\mu_h+d_h)I_h\left[1-\frac{I_h^*}{I_h}\right]^2 - z_3(\delta_1+\mu_{th})T_h\left[1-\frac{T_h^*}{T_h}\right]^2 \\
&- z_4\mu_m M\left[1-\frac{M^*}{M}\right]^2 + z_4\beta_2 RM\left[1-\frac{M^*}{M}\right]\left[\frac{R^*M^*}{RM}-1\right] \\
&- z_5\mu_r R\left[1-\frac{R^*}{R}\right]^2 + z_5\beta_2 RM\left[1-\frac{R^*}{R}\right]\left[\frac{R^*M^*}{RM}-1\right] \\
&- z_6(\alpha_2+\mu_r+d_r)I_r\left[1-\frac{I_r^*}{I_r}\right]^2 - z_7(\delta_2+\mu_{tr})T_r\left[1-\frac{T_r^*}{T_r}\right]^2 \\
&- z_8(q\omega+\mu_{gb})G_b\left[1-\frac{G_b^*}{G_b}\right]^2 - z_9(\alpha_3+\mu_{gm})G_m\left[1-\frac{G_m^*}{G_m}\right]^2 \\
&- z_{10}(\delta_3+\mu_c)C\left[1-\frac{C^*}{C}\right]^2 - z_{11}(a\nu+\mu_{sm})S_m\left[1-\frac{S_m^*}{S_m}\right]^2
\end{aligned}$$

$$- z_{12}\mu_{sh}S_h\left[1-\frac{S_h^*}{S_h}\right]^2 + z_{12}\beta_1 S_h H\left[1-\frac{S_h^*}{S_h}\right]\left[\frac{S_h^* H^*}{S_h H}-1\right]$$

This leads to

$$\begin{aligned}\frac{dL}{dt} = &- z_1\mu_h H\left[1-\frac{H^*}{H}\right]^2 - z_2(\alpha_1+\mu_{ih})I_h\left[1-\frac{I_h^*}{I_h}\right]^2 - z_3(\delta_1+\mu_{th})T_h\left[1-\frac{T_h^*}{T_h}\right]^2\\ &- z_4\mu_m M\left[1-\frac{M^*}{M}\right]^2 - z_5\mu_r R\left[1-\frac{R^*}{R}\right]^2 - z_6(\alpha_2+\mu_{ir})I_r\left[1-\frac{I_r^*}{I_r}\right]^2\\ &z_7(\delta_2+\mu_{tr})T_r\left[1-\frac{T_r^*}{T_r}\right]^2 - z_8(q\omega+\mu_{gb})G_b\left[1-\frac{G_b^*}{G_b}\right]^2 - z_9(\alpha_3+\mu_{gm})G_m\left[1-\frac{G_m^*}{G_m}\right]^2\\ &- z_{10}(\delta_3+\mu_c)C\left[1-\frac{C^*}{C}\right]^2 - z_{11}(a\nu+\mu_{sm})S_m\left[1-\frac{S_m^*}{S_m}\right]^2 - z_{12}\mu_{sh}S_h\left[1-\frac{S_h^*}{S_h}\right]^2 + f(\Omega)\end{aligned}$$

where

$$\begin{aligned}f(\Omega) =& z_1\beta_1 S_h H\left[1-\frac{H^*}{H}\right]\left[\frac{S_h^* H^*}{S_h H}-1\right] + z_4\beta_2 RM\left[1-\frac{M^*}{M}\right]\left[\frac{R^* M^*}{RM}-1\right]\\ &+ z_5\beta_2 RM\left[1-\frac{R^*}{R}\right]\left[\frac{R^* M^*}{RM}-1\right] + z_{12}\beta_1 S_h H\left[1-\frac{S_h^*}{S_h}\right]\left[\frac{S_h^* H^*}{S_h H}-1\right]\end{aligned}$$

and $\Omega = \{(H, I_h, T_h, M, R, I_r, T_r, G_b, G_m, C, S_m, S_h) > 0\}$

By hypothesis of Theorem 3.4, we have

$$z_1\beta_1 S_h H\left[1-\frac{H^*}{H}\right]\left[\frac{S_h^* H^*}{S_h H}-1\right] \le 0, \quad z_4\beta_2 RM\left[1-\frac{M^*}{M}\right]\left[\frac{R^* M^*}{RM}-1\right] \le 0$$

$$z_5\beta_2 RM\left[1-\frac{R^*}{R}\right]\left[\frac{R^* M^*}{RM}-1\right] \le 0, \quad z_{12}\beta_1 S_h H\left[1-\frac{S_h^*}{S_h}\right]\left[\frac{S_h^* H^*}{S_h H}-1\right] \le 0$$

where equality applies only when $H = H^*$, $S_h = S_h^*$, $M = M^*$, $R = R^*$.

Therefore $f(\Omega) \le 0$ for all $H = H^*$, $S_h = S_h^*$, $M = M^*$, $R = R^*$.

Hence, $\frac{dL}{dt} \le 0$ for all $(H, I_h, T_h, M, R, I_r, T_r, G_b, G_m, C, S_m, S_h) > 0$ and $\frac{dL}{dt} = 0$ only when $H = H^*$, $I_h = I_h^*$, $T_h = T_h^*$, $M = M^*$, $R = R^*$, $I_r = I_r^*$, $T_r = T_r^*$, $G_b = G_b^*$, $G_m = G_m^*$, $C = C^*$, $S_m = S_m^*$, $S_h = S_h^*$, and E^* is the only equilibrium state of the system on this plane.

Therefore, the largest compact invariant set in Ω such that $\frac{dL}{dt} = 0$ is the singleton $\{E^*\}$ which is the MIE. LaSalles invariant principle (LaSalle, 1976) guarantees that E^* is globally asymptotically stable (GAS) in the interior $\dot{\Omega}$ of Ω.

3.4 Numerical simulations

In this section, we perform some numerical simulations of the model (2.1a)-(2.1l), to illustrate the dynamics of the model using MATLAB symbolic package run in intel (R) Pentium (R) CPU

B980 2.40GHz, 2.40GHz, 4.00GB machine. The initial values used in simulation of this model are largely assummed to allow computer executions, and their values are listed in Table 5.

Table 5 : Initial values of variables of the model (2.1a)-(2.1l)

Variable	H	I_h	T_h	M	R	I_r	T_r	G_h	G_m	C	S_m	S_h
Initial values	3000	0	0	2000	500000	0	1000	3000	1500	1000	2000	2000

Although the decision on values of parameters for the in vivo dynamincs is challenging (Chiyaka *et al.*, 2008), the numerical values of parameters used in the numerical simulation of this model are presented in Table 3. These values are either estimated or taken from various articles among existing literature. The reason why some parameters values have been estimated is that modelling of liver and mosquito stages of malaria parasite have not been done or the parameter values found in existing literature are not suitable in our model. Even those that have been taken from other related studies may not be as accurate as we need for our mathematical forecasts. However, the main issue here is the effect of these parameters on the basic reproduction number, which gives clues on how to eradicate or control the disease (Chiyaka *et al.*, 2008).

It is observed from Fig. 9a that population density for sporozoites, uninfected HLCs, and infected HLCs vary with time and attain constant values (malaria infection point). However, sporozoites injected into human start by falling within very short time before they begin to rise. This fall is probably due the fact that when sporozoites injected into the human, they migrate to the liver through bloodstream where they ingested by phagocytes (Smyth and Wakelin, 1994) or they probably die due to change of environment from mosquito's salivary gland to human bloodstream. Then its population increases after they succefully reach the liver and start the asexual replication (exo-erythrocytic schizogony) within HLCs. In contrast to the population of sporozoites, population of uninfected HLCs decreases with time until it reaches its equilibrium value. This population decreases because of infection of HLCs by sporozoites, which on other hand cause rise in population of infected HLCs and liver schizonts.

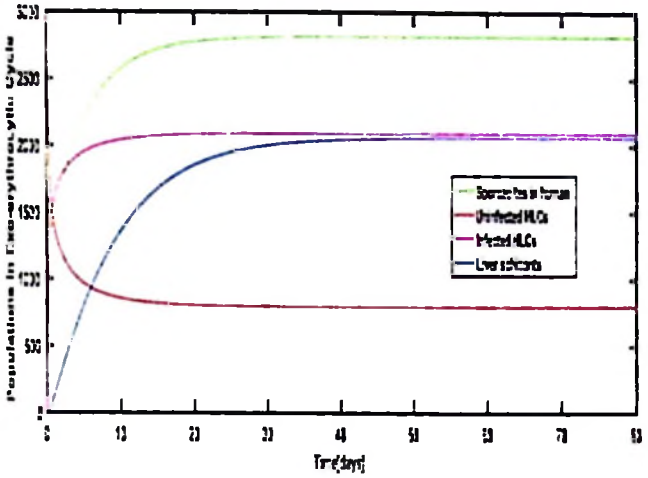

(a) Erythrocytic cycle

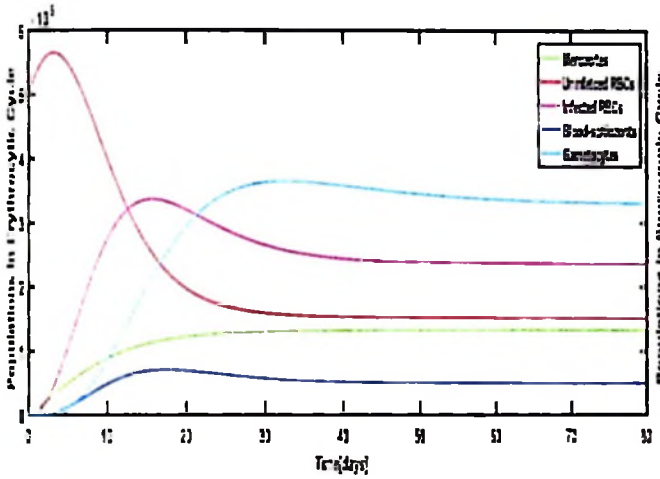

(b) Erythrocytic cycle

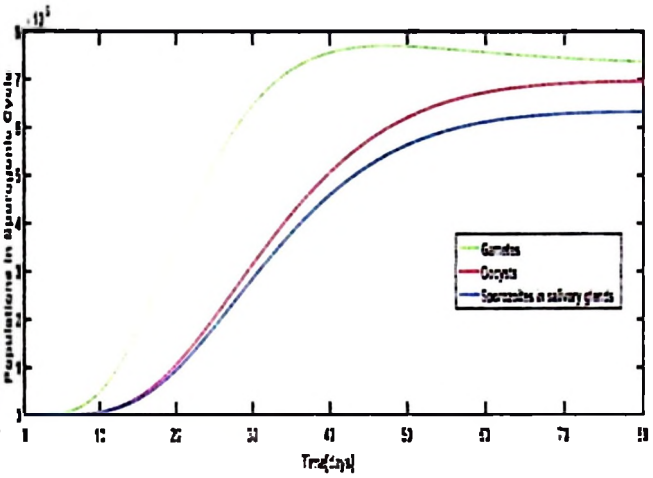

(c) Sporogonic cycle

Figure 9: Time variation of variables at liver, blood and mosquito stages of malaria parasite

Fig. 9b indicates the behavior of model sub system for variables at blood stage as the time increase. In this graph, it has been observed that as time increases, populations of merozoites, uninfected RBCs, infected RBCs, schizonts and gametocytes attain certain constant values which are values of malaria infection point. It is observed that the density of uninfected RBCs increases initially before starts to decrease with time until it reaches that constant value. This increase of RBCs density is caused by its rapid recruitment which is catalyzed by the released merozoites into blood stream (Wickramasinghe and Abdalla, 2000), and they decrease after being infected by merozoites.

Similarly, the density of infected RBCs increases before it starts to decrease with time to constant value. They increase due to infection of RBCs by merozoites, while their decrease is probably caused by clearance done by immune system. Density of blood-schizonts seems to behave in a similar manner as infected RBCs do, by rising before starting to drop and stabilize at a constant value. Its rise is caused by the increase in infected RBCs which eventually progress

to schizonts. While the densities of merozoites and gamotocytes increase with time until they reach their maximum constant values.

Fig. 9c shows that the density of gametes rises to its maximum value before falling to its equilibrium value, while those of oocysts and in-mosquito sporozoites increase with time until they attain constant values (values at malaria infection equilibrium). The decrease of gametes may be it is due to the formation of ookinetes. Therefore from the Fig. 9, we conclude that the malaria-infection equilibrium, E^* for this model exists. Now let us assess for stability of E^*.

Using the parameter values given in Table 3, we obtained $\mathcal{R}_0 = 1.590\ 25 > 1$. Thus, by Theorem 3.4 implies that the malaria infection equilibrium E^* is globally asymptotically stable as depicted in Fig. 10, Fig. 11 and Fig. 12. It has observed from these figures. that with different initial values, solutions trajectories for all state variables converge to malaria infection equilibrium.

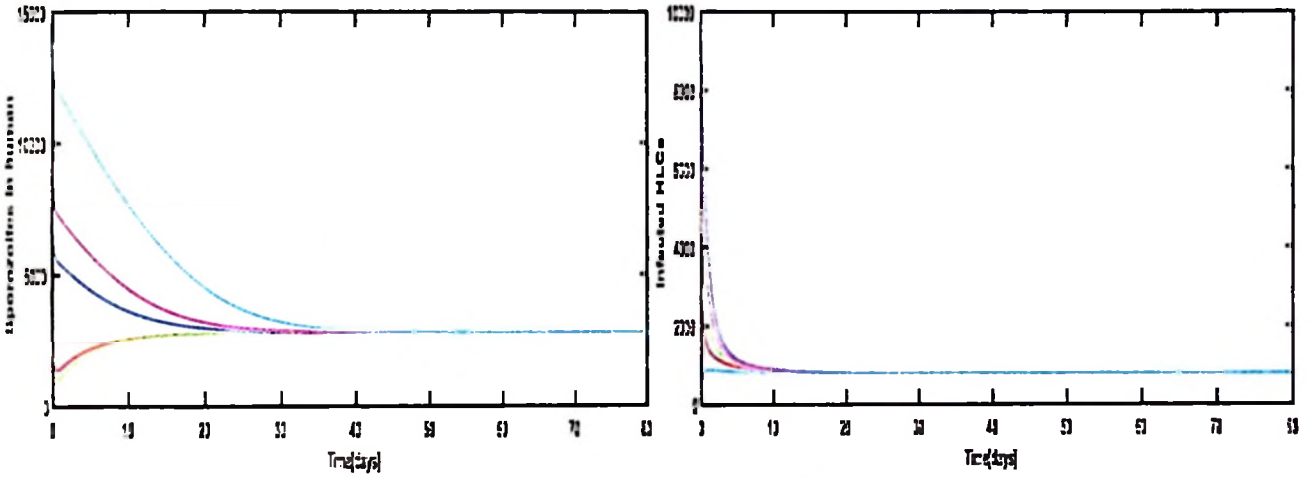

(a) $S_h^0 = 1\ 000, 2\ 000, 8\ 000, 10\ 000, 15\ 000$

(b) $H^0 = 500, 3\ 000, 5\ 000, 7\ 500, 10\ 000$

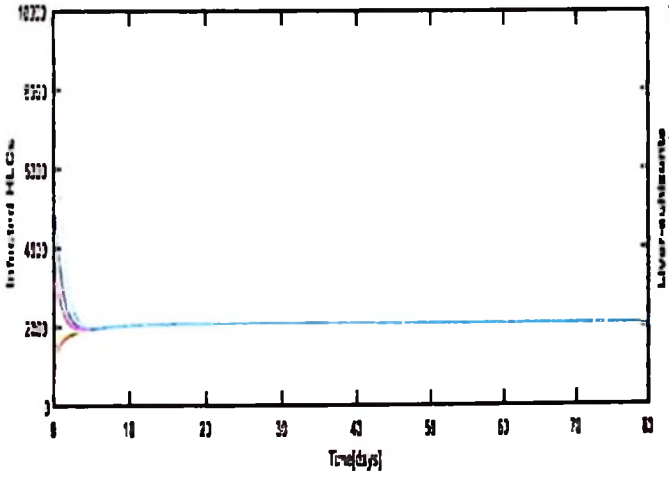

(c) $I_h^0 = 0, 500, 3\ 000, 5\ 000, 10\ 000$

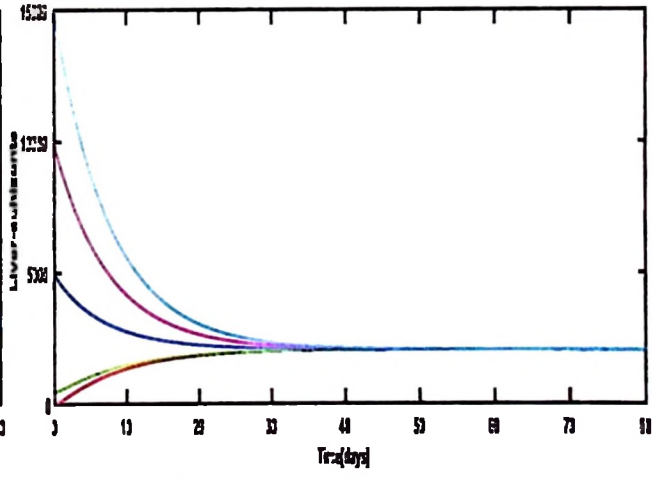

(d) $T_h^0 = 0, 500, 5\ 000, 10\ 000, 15\ 000$

Figure 10: Numerical Simulations to show a global asymptotic stability of MIE for exo-erythrocytic variables

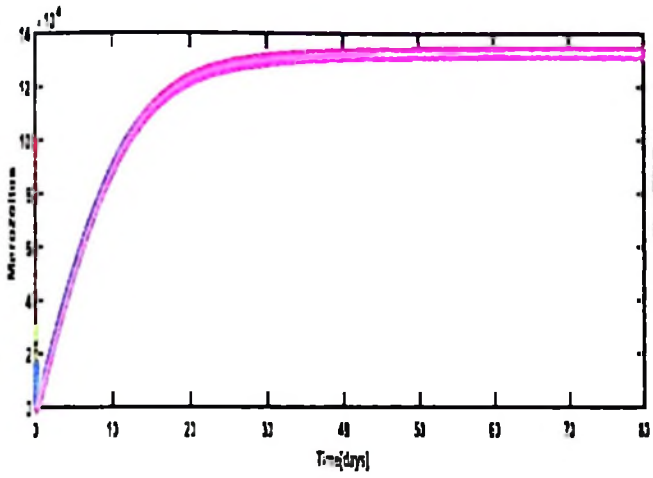

(a) $M^0 = 0, 2\,000, 15\,000, 30\,000, 100\,000$

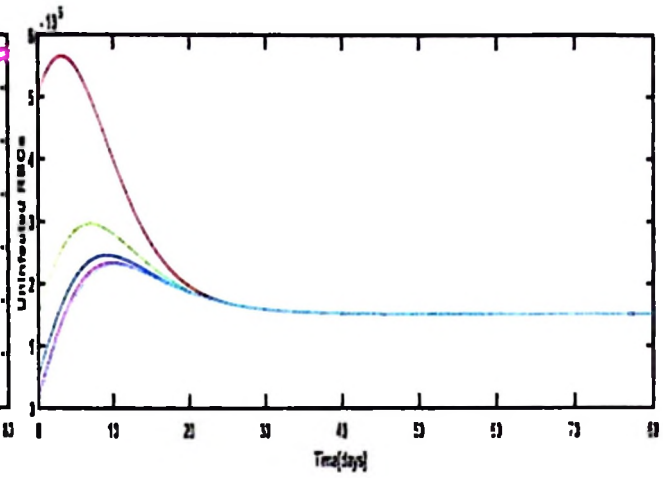

(b) $R^0 = 10\,000, 20\,000, 50\,000, 150\,000, 500\,000$

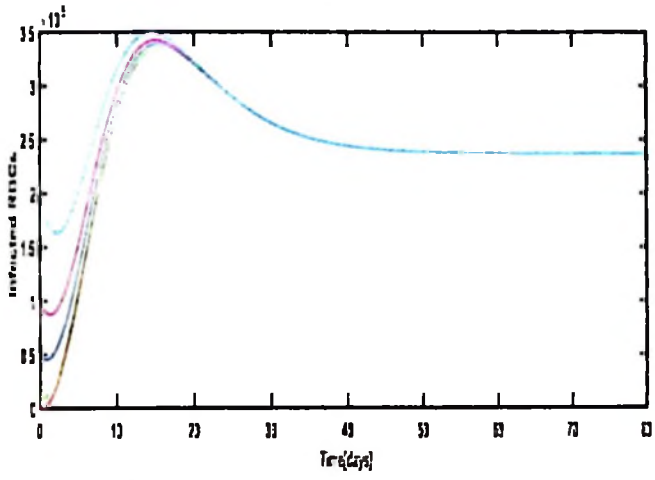

(c) $I_r^0 = 0, 10\,000, 50\,000, 100\,000, 200\,000$

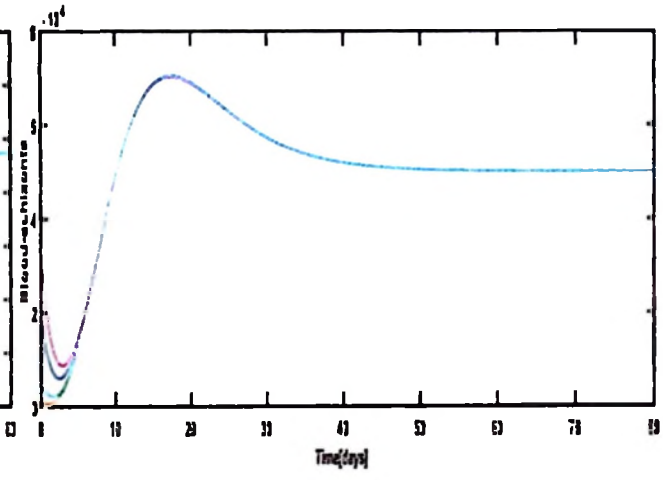

(d) $T_r^0 = 0, 1\,000, 5\,000, 20\,000, 35\,000$

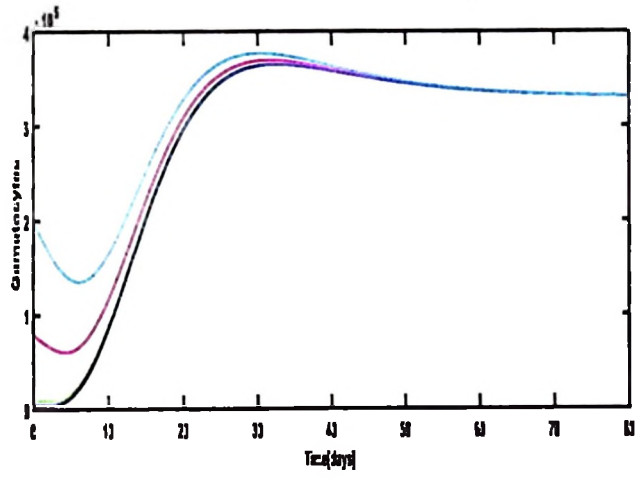

(e) $G_b^0 = 3\,000, 5\,000, 10\,000, 80\,000, 200\,000$

Figure 11: Numerical Simulations to show global asymptotic stability of MIE for erythrocytic variables

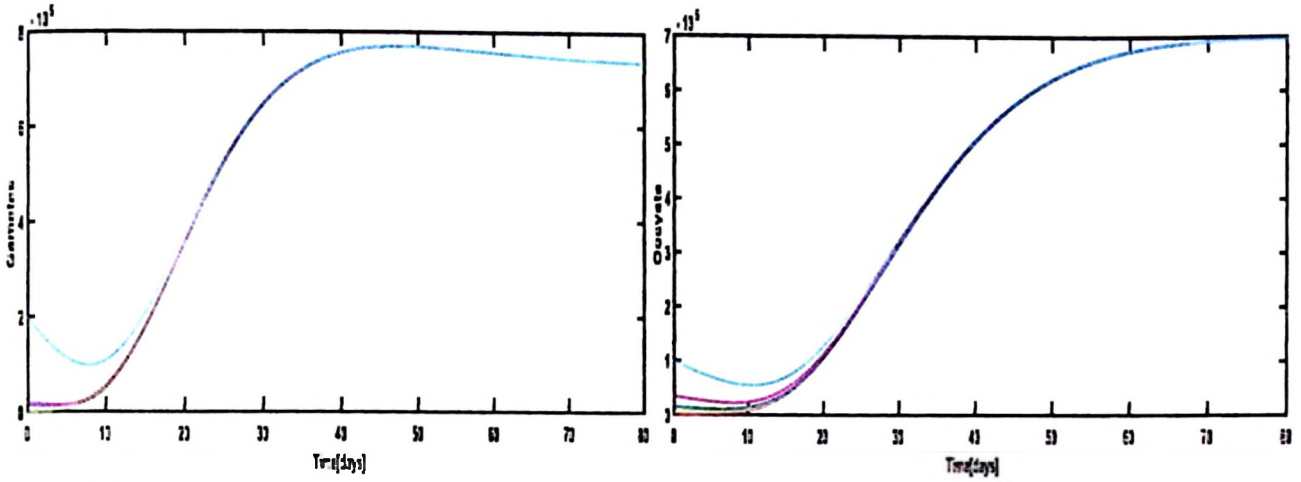

(a) $G_m^0 = 500, 1\,500, 3\,000, 15\,000, 20\,000$ (b) $C^0 = 1\,000, 8\,000, 15\,000, 35\,000, 100\,000$

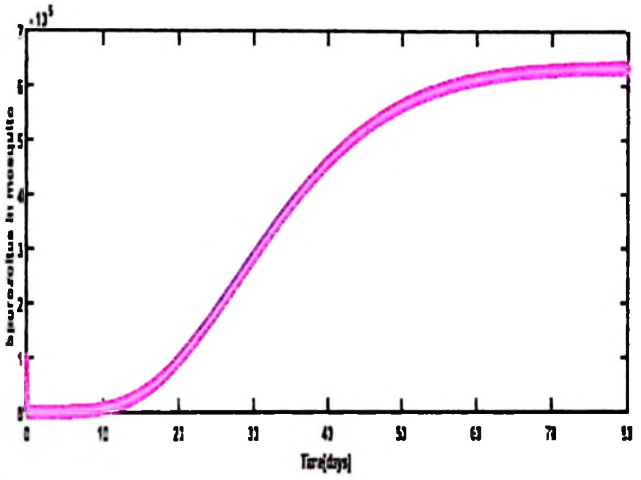

(c) $S_m^0 = 2\,000, 15\,000, 50\,000, 7\,000, 100\,000$

Figure 12: Numerical simulations to show global asymptotic stability of MIE for sporogonic variables

3.5 Discussions and Conclusion

Stability analysis of the model developed in Chapter 2 was done, where two steady states, malaria-free equilibrium (MFE) and malaria-infection equilibrium (MIE) were determined. Stability (in terms of reproduction number $\mathcal{R}_0$) of equilibrium points was established.

The necessary conditions for stability of MFE are established using trace-determinant of jacobian matrix of the model evaluated at this point showed that, MFE is locally asymptotically stable provided $\mathcal{R}_0 < 1$ and unstable otherwise. The global stability of MFE was investigated using Metzler matrix technique, and shown that MFE is globally asymptotically stable when $\mathcal{R}_0 < 1$. MIE exists only if the recruitnent rate of sporozoites into human host less than recruitment of hepatocytes liver cells (HLCs) and $\mathcal{R}_0 > 1$. Global stability of this was investigated using Lyaponuv function.

An insight of dynamics of malaria parasites within human host and within mosquito is signifi-

cant in development and assessment of transmission blocking interventions (TBIs). Merozoites play an important role in propagation of malaria infection in human, and they initially produced in the HLCs after invasion of sporozoites. This may suggest that blocking this invasion to be one of the best targets for TBIs as it will significantly inhibits the infection of HLCs, and eventually the production of merozoites from the liver schizonts. Therefore, it reduces the possibility for infection of RBCs by merozites from the liver.

However, as it has been stated earlier (in Chapter 2) that infection of RBCs by merozoites may propagate without a new infection from the liver, but this would occur only when initial invasion of RBCs by merozoites from the liver was successful. Therefore, implementing the TBIs at liver stage will probably reduce possibility of having erythrocyte invasion of merozoites and finally the human-mosquito transmission may be stopped.

This work provides a basic model for studying the in-human host and in-mosquito vector dynamics of malaria parasite, that will set a benchmark for other studies. In the next chapter, the extension of this model to incorporate the effect of immune responses is presented.

CHAPTER FOUR

Mathematical Model for the in-human host and in-mosquito Dynamics of Malaria Parasite and Effect of Immune Responses [3]

Abstract

In this chapter, a mathematical model for the in-human host and in-mosquito dynamics of malaria parasite with immune responses was formulated and analyzed. A positive invariant region of the model was established, and a basic reproduction number $\mathcal{R}_{01}$, of the model was computed. Existence and stability of two non-negative equilibrium points: malaria free equilibrium (MFE) and malaria infection equilibrium (MIE) were established. We, also proved that MFE is locally asymptotically stable if $\mathcal{R}_{01} < 1$ and globally asymptotically stable (GAS) if $\mathcal{R}_{01} < 1$. Numerical simulations prove that MIE exists and is GAS. Moreover, our results revealed that immunity has significant influence on lowering malaria infection at blood and mosquito stages. However, an insignificant effect of immunity on both cells and parasites at liver stage infection was observed. Furthermore, the model depicts that infection decreases as lifespan of immune cells increases. The impact of immune cells in suppressing the production of merozoites is noted to be higher than that of antibodies to block invasion of sporozoites and merozoites.

4.1 Introduction

In human, malaria infection is initiated by a bite from a parasite-carrying mosquito which seeks for blood to facilitate egg development, where sporozoites are injected into the bloodstream through the dermis. Sporozoites quickly migrate to the liver and penetrate hepatic liver cells (HLCs) where they develop to schizonts that give rise to thousands of merozoites (Corradin and Levitskaya, 2014). Then merozoites enter the bloodstream and invade red blood cells (RBCs), that develop into erythrocytic schizonts which finally burst and release an average of 16 merozoites (Tumwiine *et al.*, 2008) which either re-invade new RBCs or switch to sexual form termed gametocytes. Human-mosquito infection of malaria begins through ingestion of gametocytes into parasite-free mosquito during its blood-meal. Ingested gametocytes (microgametes and macrogametes) then fuse and develop into oocysts through ookinetes stage. Then each oocyst ruptures and releases an average of 1000 sporozoites (Nelson and Williams, 2014) that are responsible for infection of a new susceptible human host.

[3]This chapter is based on the research paper: Mohamed A. Selemani, Livingstone S. Luboobi, Yaw Nkansah-Gyekye. The in-Human Host and in-Mosquito Dynamics of Malaria Parasites With Immune Responses. *New Trends in Mathematical Sciences* (2017b), 5(3):182-207.

In human, malaria infection is initiated by a bite from a parasite-carrying mosquito which seeks for blood to facilitate egg development, where sporozoites are injected into bloodstream through the dermis. Sporozoites quickly migrate to the liver and penetrate hepatic liver cells (HLCs) where they develop to schizonts that give rise to thousands of merozoites (Corradin and Levitskaya, 2014). Then merozoites enter the bloodstream and invade red blood cells (RBCs), that develop into erythrocytic schizonts which finally burst and release an average of 16 merozoites (Tumwiine *et al.*, 2008) which either re-invade new RBCs or switch to sexual form termed gametocytes. Human-mosquito infection of malaria begins through ingestion of gametocytes into parasite-free mosquito during its blood-meal. Ingested gametocytes (microgametes and macrogametes) then fuse and develop into oocysts through ookinetes stage. Then each oocyst ruptures and releases an average of 1000 sporozoites (Nelson and Williams, 2014) that are responsible for infection of a new suspectible human host.

A major role of the human immune system is to defend a body against the infection-causing organisms, called pathogens like bacteria, virus, fungi and parasites. Human immune system has two main components termed as: innate (non-specific) immunity and adaptive (specific) immunity. Innate immune responses defend the body against any pathogenic invasion, while adaptive immune responses provide protection against a specific pathogen, and usually comes into action after the infections outrun the innate immunity. Innate immune responses include macrophages, interferon and natural killer (NK) cells, while T-lymphocyte (cytotoxic T and helper T) and B-lymphocyte (B-cells) are some elements of adaptive immune responses. Cellular-mediated responses involves cell effectors such as cytotoxic T ($CD8^+$ T) and NK cells to kill intracellular pathogens while humoral responses involve effector molecules such as antibodies (secreted by B-cells) to clear free pathogens in body's fluid such as blood.

In malaria infection, both innate and adaptive immune responses are stimulated (Li *et al.*, 2011; Langhorne *et al.*, 2008) to obstruct parasites by either preventing the re-invasion of parasite or increasing the death rate of infected cells (Good, 2001; Stevenson and Riley, 2004; Li *et al.*, 2011), and both humoral and cell-mediated immune effector mechanisms are involved in immunology of malaria (Langhorne *et al.*, 2008; Kinyanjui, 2012). Antibodies neutralize the sporozoites and merozoites and inhibit sporozoites' invasion to HLCs (Kinyanjui, 2012; Langhorne *et al.*, 2008) and merozoites' invasion to RBCs (Tumwiine *et al.*, 2008; Kinyanjui, 2012). They are also restrain the parasite growth (Chiyaka *et al.*, 2008; Kinyanjui, 2012; Dent *et al.*, 2008). Macrophages are activated by NK cells to intensify phagocytosis and clearance of intra-erythrocytic parasites (Artavanis-Tsakonas *et al.*, 2003). The IFN-γ produced by $CD8^+$ T cells (in help of $CD4^+$) inhibit growth of, and kill intrahepatic parasites (Kinyanjui, 2012; Artavanis-Tsakonas *et al.*, 2003; Langhorne *et al.*, 2008). Moreover, antibodies and complement system that are ingested by mosquito during blood meal mediate the lysis of gametocytes

and inhibit development of parasite in the mosquito (Langhorne *et al.*, 2008).

In recent years, there has been increasing interest in mathematical models of in vivo dynamics (especially intra-host) of malaria with immune responses (Li *et al.*, 2011; Tumwiine *et al.*, 2008; Chiyaka *et al.*, 2008) and references therein. Some of these studies ignored the absorption effect of merozoites into RBC (Li *et al.*, 2011). However, some authors incorporate this effect since during malaria infection parasite penetrates into healthy cells. Therefore, in this case both populations (parasites and uninfected cells) decrease (Anderson *et al.*, 1989; Tumwiine *et al.*, 2008; Chiyaka *et al.*, 2008). Moreover, the clearance of free parasites or infected cells by immune responses has been modelled either as simple mass-action (Tumwiine *et al.*, 2008; Chiyaka *et al.*, 2008) which is unbounded function or using the Michaelis-Menten-Monod function (MMMF) which is nonlinear-bounded (Li *et al.*, 2011). Furthermore, Chiyaka *et al.* (2008) incorporate the effects of antibodies to inhibit parasite's growth or block invasion of host's cells by parasites using MMMF.

However, none of these studies discussed the liver stage dynamics of malaria parasites. As it has been stated in the previous paragraph, some studies did not incorporate the absorption effect of parasites into uninfected cells. Moreover, some of these models ignored either the saturation effect on cell proliferation and/or suppression of parasites replication. In this chapter, we formulate a mathematical model for the in-human host and in-mosquito dynamics of malaria parasite with immune responses, where the MMMF is used to describe the effect of immune responses on clearance of both, infected cells and free parasites. The effect of antibodies on suppressing the replication of parasites at liver and blood stages of malaria infection is included. Lastly, we incorporate the effect of antibodies picked-up by mosquito in mediating the lysis of gametocytes and preventing parasites development in the mosquito.

4.2 Model Formulation

4.2.1 Model Description

In development of this model, we extend the model presented by Selemani *et al.* (2016) which has been discussed in Chapters 1 and 2, by incorporating the effect of immune system. The dynamics of interactions of malaria parasites in-mosquito vector and in-human host with immune responses are described using a system of nonlinear ordinary differential equations. Variables involved in this model are: the uninfected hepatic liver cells (uHLCs), H; infected hepatic liver cells (iHLCs), I_h; hepatic schizonts, T_h; merozoites, M; uninfected red blood cells (uRBCs), R; infected red blood cells (iRBCs), I_r; erythrocytic schizonts, T_r; gametocytes, G_b; gametes, G_m; and oocysts, C. Others are sporozoites in mosquito's salivary gland, S_m; sporozoites in human, S_h; immune cells against liver stage and blood stage infections , Z_1 and Z_2 respectively;

and antibodies, B.

Sporozoites, S_h are injected into uninfected human host at a constant rate $ab\nu$, during a blood meal of infected mosquito, where a is probability that a mosquito bite is infective to human, b is number of mosquito bites per individual, and ν is number of sporozoites injected per bite. Once the sporozoites reach the liver, they attack the uHLCs at the rate $\beta_1 S_h H/(1+k_1 B)$, where β_1 is infection rate of uHLCs by sporozoites and k_1 is efficiency of antibodies to block invasion of uHLCs. They die naturally at $\mu_{sh} S_h$ and are killed by immune cells (macrophages) at a rate $\sigma_{sh} Z_1 S_h/(1+\pi_{sh} S_h)$, where σ_{sh} is a rate of successful removal of intra-human sporozoites by immune cells and $1/\pi_{sh}$ is a half-saturation constant of intra-human sporozoites. The uHLCs are constantly recruited at rate Λ_h, from the bone marrow stem cells. They die naturally at rate $\mu_h H$ and reduced at rate $\beta_1 S_h H/(1+k_1 B)$ due to infection by sporozoites.

The iHLCs increase at a rate $\beta_1 S_h H(1+k_1 B)$ due to infection of uHLCs by sporozoites and die at a rate $\mu_{ih} I_h$. Some of them progress to schizonts at a rate $\alpha_1 I_h$. They also killed by immune cells (IFN-γ, $CD8^+$, NK) at a rate $\sigma_{ih} Z_1 I_h/(1+\pi_{ih} I_h)$, where σ_{ih} is rate of successful removal of iHLCs by immune cells and $1/\pi_{ih}$ is a half saturation constant of I_h. The hepatic schizonts die naturally at a rate $\mu_{th} T_h$ or rupture to release an average of r_1 merozoites per rupturing schizont at a rate $\delta_1 T_h$, and cleared by immune cells (IFN-γ, $CD8^+$, NK) at a rate $\sigma_{th} Z_1 T_h/(1+\pi_{th} T_h)$, where σ_{th} is rate of successful removal of hepatic schizonts by immune cells and $1/\pi_{th}$ is a half saturation constant of hepatic schizonts.

Merozoites are released from the hepatic schizonts at a rate $r_1 \delta_1 T_h/(1+c_1 Z_1)$, where c_1 is efficiency of immune cells (IFN-γ and $CD8^+$) to inhibit the production of merozoites. Merozoites invade uRBCs at a rate $\beta_2 RM/(1+k_2 B)$ and they die naturally at $\mu_m M$. The parameter β_2 is infection rate of uRBCs by merozoites and k_2 is efficiency of antibodies to inhibit or reduce the infection of uRBCs by merozoites. They are cleared by immune cells (macrophages activated by IFN-γ) at a rate $\sigma_m Z_2 M/(1+\pi_m M)$, where σ_m is rate of successful removal of merozoites by immune cells and $1/\pi_m$ is a half saturation constant of merozoites.

The uRBCs are constantly recruited at a rate Λ_r from the bone marrow. Their density is reduced by natural death at a rate $\mu_r R$ and due to the infection by merozoites at a rate $\beta_2 RM/(1+k_2 B)$. The iRBCs increases at a rate $\beta_2 RM/(1+k_2 B)$ and decreases due to death at a rate $\mu_{ir} I_r$ and due to progression to erythrocytic schizonts at a rate $\alpha_2 T_r$. The immune cells (macrophages activated by IFN-γ) phagocytize the iRBCs at a rate $\sigma_{ir} Z_2 I_r/(1+\pi_{ir} I_r)$, where σ_{ir} is rate of successful removal of iRBCs by immune cells and $1/\pi_{ir}$ is a half saturation constant of iRBCs.

The erythrocytic schizonts die at rate $\mu_{tr} T_r$ and rupture at rate $\delta_2 T_r$ and release new r_2 merozoites which starts a series of repetitive cycles to infect other uRBCs. Proportion p, of these

newly released merozoites proceeds with asexual replication cycle at a rate $pr_2\delta_2 T_r/(1+c_2Z_2)$, while the other proportion $1-p$ switch to sexual form of parasites called gametocytes at a rate $(1-p)(r_2\delta_2 T_r)/(1+c_2Z_2)$. The parameter c_2 is efficiency of immune cells to inhibit the production of intra-erythrocytic merozoites or gametocytes. They also killed by immune cells (macrophages) at a rate $\sigma_{tr}Z_2T_r/(1+\pi_{tr}T_r)$. The parameter σ_{tr} is rate of successful removal of erythrocytic schizonts by immune cells and $1/\pi_{tr}$ is a half saturation constant of erythrocytic schizonts.

The gametocytes in blood stream increases at a rate $(1-p)(r_2\delta_2 T_r)/(1+c_2Z_2)$ and decrease by natural death at a rate $\mu_{gb}G_b$, for being ingested by mosquito at a rate $q\omega G_b$ and being cleared by immune cells at a rate $\sigma_{gb}Z_2G_b/(1+\pi_{gb}G_b)$. The parameters σ_{gb} and $1/\pi_{gb}$ are respectively, the rate of successful removal of gametocytes by immune cells and the half saturation constant of gametocytes.

The gametes in mosquitoes are recruited at a rate $\rho q\omega G_b/(1+k_3B)$, where ρ is number of bites a mosquito can make during its lifetime, ω is number of gametocytes ingested per bite and q is probability that a mosquito bite is infective to mosquito, while k_3 is efficiency of antibodies picked up by mosquito during its blood meal to mediate lysis of gametocytes and prevent parasite's development in mosquito (Langhorne *et al.*, 2008). Gametes decrease by natural death at rate $\mu_{gm}G_m$ and progression to oocysts at a rate, $\alpha_3 G_m$. The oocysts rupture to release an average of r_3 sporozoites per rupturing oocyst at a rate, $\delta_3 C$ and die at a rate $\mu_c C$. The released sporozoites, S_m migrate to salivary glands where they either naturally die at a rate $\mu_{sm}S_m$ or injected into a new host at rate $ab\nu$. Table 6 below summarizes the variables of the model and their biological descriptions.

Table 6 : Variables and their descriptions

Variable	Description
S_h :	number of sporozoites injected to the liver
H :	number of uninfected HLCs
I_h :	number of infected HLCs
T_h :	number of schizonts developed from infected HLCs
T_r :	number of schizonts developed from infected RBCs
M :	number of merozoites in bloodstream
R :	number of uninfected RBCs
I_r :	number of infected RBCs
G_b :	number of gametocytes in the bloodstream
G_m :	number of gametes in the mosquito
O :	number of oocysts
S_m :	number of sporozoites in mosqouito's salivary gland
Z_1 :	number of immune cells that fight against malaria infection at the liver stage
Z_2 :	number of immune cells that fight against malaria infection at the blood stage
B :	number of antibodies

4.2.2 Model Assumptions

In addition to the assumptions made during the formulation of the basic model in Chapter 1, in the development of this model we made the following assumptions:

(i) For simplicity, all immune cells that fight against malaria infection in human are grouped into two compartments: immune cells against liver-stage infection and immune cells against blood-stage infection. All malaria-specific antibodies are considered as single compartment.

(ii) Production of immune cells is due constant recruitement from hematopoietic stem cell in the bone marrow, and stimulation by presence of sprozoites, schizonts, infected HLCs and RBCs, merozoites and gametocytes. They naturally die at constant rate.

(iii) Proliferation of antibodies that inhibit invasion of HLCs and RBCs depends only presence of sporozoites and merozoites. They die constantly.

(iv) Antibodies ingested with gametocytes during the blood meal prevent the fusion of gametocytes (macro- and micro-gametes) and other developmental stages of parasites within mosquito.

Table 7 : Model parameters and their descriptions

Parameter	Description
a :	the proportion of mosquito bites that are infectious to human
b :	average number of mosquito bites per individual per unit time
ν :	average number of sporozoites injected in the liver per bite
β_1 :	infection rate of HLCs by sporozoites
β_2 :	infection rate of RBCs by merozoites
δ_1 :	rupture rate of liver-stage schizonts to release merozoites
δ_2 :	rupture rate of blood-stage schizonts to release merozoites or gametocytes
δ_3 :	rupture rate of Oocysts to liberate sporozoites
r_1 :	number of released merozoites per each of ruptured liver-stage schizont
r_2 :	number of released merozoites per each of ruptured blood-stage schizont
r_3 :	number of released sporozoites per each of ruptured Oocyst
α_1 :	progression rate of infected HCLs to liver-Schizonts
α_2 :	progression rate of infected RBCs to blood-schizonts
α_3 :	progresion rate of gametes in mosquito's stomach to Oocysts
q :	the proportion of mosquito bites that are infectious to mosquito
ρ :	average number of bites made by mosquito during its lifetime
ω :	average number of gametocytes ingested into mosquito per bite
Λ_h :	the recruitmet rate of HLCs from bone marrow stem cells
Λ_r :	the recruitmet rate of RBCs from bone marrow
μ_h :	natural death rate of HLCs
μ_{ih} :	total death rate of infected HLCs
μ_{th} :	death rate of liver-schizonts
μ_r :	natural death rate of RBCs
μ_{ir} :	total death rate of infected RBCs
μ_{tr} :	death rate of blood-schizonts
μ_m :	death rate of merozoites
μ_{gb} :	death rate of gametocytes in bloodstream
μ_{gm} :	death rate of gametes in mosquito's midgut
μ_c :	death rate of Oocysts
μ_{sm} :	death rate of Sporozoites in mosqouito's salivary gland
μ_{sh} :	death rate of Sporozoites in human liver
p :	proportion of relesead merozoites continues with asexual multiplication cycle
$1-p$:	proportion of relesead merozoites that switch to sexual form (gametocytes)
c_1 :	efficiency of immune cells to suppress the production of M from liver-schizonts
c_2 :	efficiency of immune cells to suppress the production of M from blood-schizonts
k_1 :	efficiency of antibodies to inhibit invasion of HLCs by sporozoites
k_2 :	efficiency of antibodies to inhibit invasion of RBCs by merozoites
k_3 :	efficiency of antibodies to mediate lysis of gametocytes and inhibit fertilization
σ_{sh} :	rate at which sporozoites are cleared by immune cells
σ_{ih} :	rate at which infected HLCs are cleared by immune cells
σ_{th} :	rate at which liver schizonts are cleared by immune cells

Continued on next page

Table 7 -- *Continued from previous page*

Parameter	Description
σ_m :	rate at which merozoites are cleared by immune cells
σ_{ir} :	rate at which infected RBCs are cleared by immune cells
σ_{tr} :	rate at which blood schizonts are cleared by immune cells
σ_{gh} :	rate at which gametocytes are cleared by immune cells
ϵ_{sh} :	proliferation rate of immune cells due to contact with sporozoites
ϵ_{ih} :	proliferation rate of immune cells due to contact with infected HLCs
ϵ_{th} :	proliferation rate of immune cells due to contact with liver schizonts
ϵ_m :	proliferation rate of immune cells due to contact with merozoites
ϵ_{ir} :	proliferation rate of immune cells due to contact with infected RBCs
ϵ_{tr} :	proliferation rate of immune cells due to contact with blood schizonts
ϵ_{gh} :	proliferation rate of immune cells due to contact with gametocytes
π_{sh} :	$1/\pi_{sh}$ half saturation constant of sporozoites
π_{ih} :	$1/\pi_{ih}$ half saturation constant of infected HLCs
π_{th} :	$1/\pi_{th}$ half saturation constant of liver schizonts
π_m :	$1/\pi_m$ half saturation constant of merozoites
π_{ir} :	$1/\pi_{ir}$ half saturation constant of infected RBCs
π_{tr} :	$1/\pi_{tr}$ half saturation constant of blood schizonts
π_{gh} :	$1/\pi_{gh}$ half saturation constant of gametocytes
η_1 :	maximum rate of increase of antibodies due to presence of sporozoites
η_2 :	maximum rate of increase of antibodies due to presence of merozoites

4.2.3 Compartmental Diagram

Based on the dynamics described in Section 4.2.1 and the assumptions described in Section 4.2.2, the proposed model for the in-human host and in-mosquito dynamics of entire life cycle of malaria parasites with immune responses is shown in Fig. 13, in which the variables and parameters are described in Table 6 and Table 4.2 respectively.

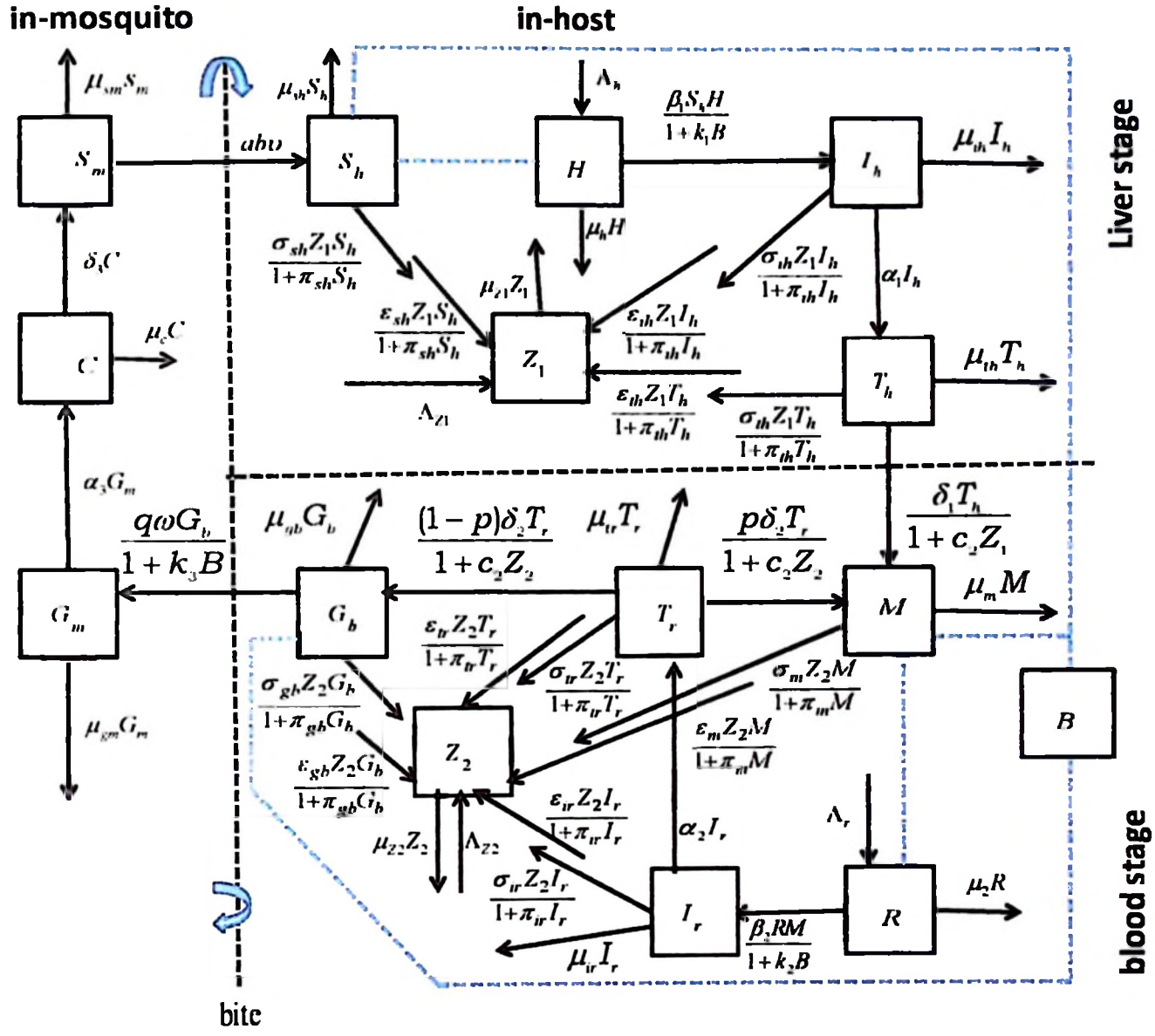

Figure 13: Compartmental model diagram for the in-human host and in-mosquito dynamics of malaria parasites with immune responses

4.2.4 Model Equations

Based on the compartmental diagram illustrated in Fig. 13 above, the in-human host and in-mosquito dynamics for the entire life cycle of malaria parasite with immune responses are governed by the following system of ordinary differential equations.

$$\frac{dH}{dt} = \Lambda_h - \frac{\beta_1 S_h H}{1 + k_1 B} - \mu_h H, \tag{4.1a}$$

$$\frac{dI_h}{dt} = \frac{\beta_1 S_h H}{1 + k_1 B} - (\alpha_1 + \mu_{ih}) I_h - \frac{\sigma_{ih} Z_1 I_h}{1 + \pi_{ih} I_h}, \tag{4.1b}$$

$$\frac{dT_h}{dt} = \alpha_1 I_h - (\delta_1 + \mu_{th}) T_h - \frac{\sigma_{th} Z_1 T_h}{1 + \pi_{th} T_h}, \tag{4.1c}$$

$$\frac{dM}{dt} = \frac{r_1 \delta_1 T_h}{1 + c_1 Z_1} + \frac{p r_2 \delta_2 T_r}{1 + c_2 Z_2} - \frac{\beta_2 R M}{1 + k_2 B} - \frac{\sigma_m Z_2 M}{1 + \pi_m M} - \mu_m M, \tag{4.1d}$$

$$\frac{dR}{dt} = \Lambda_r - \frac{\beta_2 R M}{1 + k_2 B} - \mu_r R, \tag{4.1e}$$

$$\frac{dI_r}{dt} = \frac{\beta_2 R M}{1 + k_2 B} - (\alpha_2 + \mu_{ir}) I_r - \frac{\sigma_{ir} Z_2 I_r}{1 + \pi_{ir} I_r}, \tag{4.1f}$$

$$\frac{dT_r}{dt} = \alpha_2 I_r - (\delta_2 + \mu_{tr}) T_r - \frac{\sigma_{tr} Z_2 T_r}{1 + \pi_{tr} T_r}, \tag{4.1g}$$

$$\frac{dG_b}{dt} = (1 - p) \frac{r_2 \delta_2 T_r}{1 + c_2 Z_2} - (q\omega + \mu_{gb}) G_b - \frac{\sigma_{gb} Z_2 G_b}{1 + \pi_{gb} G_b}, \tag{4.1h}$$

$$\frac{dG_m}{dt} = \frac{p q \omega G_b}{1 + k_3 B} - \alpha_3 G_m - \mu_{gm} G_m, \tag{4.1i}$$

$$\frac{dC}{dt} = \alpha_3 G_m - \delta_3 C - \mu_c C, \tag{4.1j}$$

$$\frac{dS_m}{dt} = r_3 \delta_3 C - a\nu S_m - \mu_{sm} S_m, \tag{4.1k}$$

$$\frac{dS_h}{dt} = ab\nu - \frac{\beta_1 S_h H}{1 + k_1 B} - \mu_{sh} S_h - \frac{\sigma_{sh} Z_1 S_h}{1 + \pi_{sh} S_h}, \tag{4.1l}$$

$$\frac{dZ_1}{dt} = \Lambda_{z_1} + \left(\frac{\epsilon_{sh} S_h}{1 + \pi_{sh} S_h} + \frac{\epsilon_{ih} I_h}{1 + \pi_{ih} I_h} + \frac{\epsilon_{th} T_h}{1 + \pi_{th} T_h} \right) Z_1 - \mu_{z_1} Z_1, \tag{4.1m}$$

$$\frac{dZ_2}{dt} = \Lambda_{z_2} + \left(\frac{\epsilon_m M}{1 + \pi_m M} + \frac{\epsilon_{ir} I_r}{1 + \pi_{ir} I_r} + \frac{\epsilon_{tr} T_r}{1 + \pi_{tr} T_r} + \frac{\epsilon_{gb} G_b}{1 + \pi_{gb} G_b} \right) Z_2 - \mu_{z_2} Z_2, \tag{4.1n}$$

$$\frac{dB}{dt} = \eta_1 \frac{S_h}{1 + \pi_{sh} S_h} Z_1 + \eta_2 \frac{M}{1 + \pi_m M} Z_2 - \mu_b B. \tag{4.1o}$$

4.3 Analysis of the Model

4.3.1 Wellposedness of the model

In this section, we assess the wellposedness of the model by investigating the existence and feasibility of its solution. That is, to test whether the solutions are epidemiologically (variables have biological interpretation) and mathematically (a unique bounded solution exists for all the time) well-posed. The model system (4.1a)-(4.1o) can be expressed in the compact form (Dumont *et al.*, 2008; Mpeshe *et al.*, 2014a) as follows

$$\frac{\mathrm{d}X}{dt} = A(x)X + F$$

where

$$X = (H, I_h, T_h, M, R, I_r, T_r, G_b, G_m, C, S_m, S_h, Z_1, Z_2, B)^T,$$

$$A(x) = \begin{bmatrix}
-a_1 & 0 & 0 & 0 & 0 & 0 & 0 & 0 & 0 & 0 & 0 & 0 & 0 & 0 & 0 \\
a_2 & -a_3 & 0 & 0 & 0 & 0 & 0 & 0 & 0 & 0 & 0 & 0 & 0 & 0 & 0 \\
0 & a_1 & -a_4 & 0 & 0 & 0 & 0 & 0 & 0 & 0 & 0 & 0 & 0 & 0 & 0 \\
0 & 0 & a_5 & -a_6 & 0 & 0 & a_7 & 0 & 0 & 0 & 0 & 0 & 0 & 0 & 0 \\
0 & 0 & 0 & 0 & -a_8 & 0 & 0 & 0 & 0 & 0 & 0 & 0 & 0 & 0 & 0 \\
0 & 0 & 0 & 0 & a_9 & -a_{10} & 0 & 0 & 0 & 0 & 0 & 0 & 0 & 0 & 0 \\
0 & 0 & 0 & 0 & 0 & a_2 & -a_{11} & 0 & 0 & 0 & 0 & 0 & 0 & 0 & 0 \\
0 & 0 & 0 & 0 & 0 & 0 & a_{12} & -a_{13} & 0 & 0 & 0 & 0 & 0 & 0 & 0 \\
0 & 0 & 0 & 0 & 0 & 0 & 0 & a_{14} & -a_{15} & 0 & 0 & 0 & 0 & 0 & 0 \\
0 & 0 & 0 & 0 & 0 & 0 & 0 & 0 & a_3 & -a_{16} & 0 & 0 & 0 & 0 & 0 \\
0 & 0 & 0 & 0 & 0 & 0 & 0 & 0 & 0 & r_3\delta_3 & -a_{17} & 0 & 0 & 0 & 0 \\
0 & 0 & 0 & 0 & 0 & 0 & 0 & 0 & 0 & 0 & 0 & -a_{18} & 0 & 0 & 0 \\
0 & a_{19} & a_{20} & 0 & 0 & 0 & 0 & 0 & 0 & 0 & 0 & a_{21} & -\mu_{z_1} & 0 & 0 \\
0 & 0 & 0 & a_{22} & 0 & a_{23} & a_{24} & a_{25} & 0 & 0 & 0 & 0 & 0 & -\mu_{z_2} & 0 \\
0 & 0 & 0 & a_{26} & 0 & 0 & 0 & 0 & 0 & 0 & 0 & a_{27} & 0 & 0 & -\mu_b
\end{bmatrix}$$

where

$$\begin{aligned}
a_1 &= \frac{\beta_1 S_h}{1+k_1 B} + \mu_h, \quad a_2 = \frac{\beta_1 S_h}{1+k_1 B}, \quad a_3 = \alpha_1 + \mu_{ih} + \frac{\sigma_{ih} Z_1}{1+\pi_{ih} I_h}, \quad a_4 = \delta_1 + \mu_{th} + \frac{\sigma_{th} Z_1}{1+\pi_{th} T_h}, \\
a_5 &= \frac{r_1 \delta_1}{1+c_1 Z_1}, \quad a_6 = \mu_m + \frac{\beta_2 R}{1+k_2 B} + \frac{\sigma_m Z_2}{1+\pi_m M}, \quad a_7 = \frac{p r_2 \delta_2}{1+c_2 Z_2}, \quad a_8 = \frac{\beta_2 M}{1+k_2 B} + \mu_r, \\
a_9 &= \frac{\beta_2 M}{1+k_2 B}, \quad a_{10} = \alpha_2 + \mu_{ir} + \frac{\sigma_{ir} Z_2}{1+\pi_{ir} I_r}, \quad a_{11} = \delta_2 + \mu_{tr} + \frac{\sigma_{tr} Z_2}{1+\pi_{tr} T_r}, \quad a_{12} = \frac{(1-p) r_2 \delta_2}{1+c_2 Z_2}, \\
a_{13} &= q\omega + \mu_{gb} + \frac{\sigma_{gb} Z_2}{1+\pi_{gb} G_b}, \quad a_{14} = \frac{\rho q \omega}{1+k_3 B}, \quad a_{15} = \alpha_3 + \mu_{gm}, \quad a_{16} = \delta_3 + \mu_c, \quad a_{17} = a\nu + \mu_{sm}, \\
a_{18} &= \frac{\beta_1 H}{1+k_1 B} + \mu_{sh} + \frac{\sigma_{sh} Z_1}{1+\pi_{sh} S_h}, \quad a_{19} = \frac{\epsilon_{ih} Z_1}{1+\pi_{ih} I_h}, \quad a_{20} = \frac{\epsilon_{th} Z_1}{1+\pi_{th} T_h}, \quad a_{21} = \frac{\epsilon_{sh} Z_1}{1+\pi_{sh} S_h}, \\
a_{22} &= \frac{\epsilon_m Z_2}{1+\pi_m M}, \quad a_{23} = \frac{\epsilon_{ir} Z_2}{1+\pi_{ir} I_r}, a_{24} = \frac{\epsilon_{tr} Z_2}{1+\pi_{tr} T_r}, \quad a_{25} = \frac{\epsilon_{gb} Z_2}{1+\pi_{gb} G_b}, \quad a_{26} = \frac{\eta_2 M Z_2}{1+\pi_m M}, \\
a_{27} &= \frac{\eta_1 S_h Z_1}{1+\pi_{sh} S_h}
\end{aligned} \tag{4.2}$$

and F is a column vector given by

$$F = (\Lambda_h, 0, 0, 0, \Lambda_r, 0, 0, 0, 0, 0, 0, ab\nu, \Lambda_{z_1}, \Lambda_{z_2}, 0)^T$$

4.3 Analysis of the Model

4.3.1 Wellposedness of the model

In this section, we assess the wellposedness of the model by investigating the existence and feasibility of its solution. That is, to test whether the solutions are epidemiologically (variables have biological interpretation) and mathematically (a unique bounded solution exists for all the time) well-posed. The model system (4.1a)-(4.1o) can be expressed in the compact form (Dumont *et al.*, 2008; Mpeshe *et al.*, 2014a) as follows

$$\frac{\mathrm{d}X}{dt} = A(x)X + F$$

where

$$X = (H, I_h, T_h, M, R, I_r, T_r, G_b, G_m, C, S_m, S_h, Z_1, Z_2, B)^T,$$

$$A(x) = \begin{bmatrix}
a_1 & 0 & 0 & 0 & 0 & 0 & 0 & 0 & 0 & 0 & 0 & 0 & 0 & 0 & 0 \\
a_2 & -a_3 & 0 & 0 & 0 & 0 & 0 & 0 & 0 & 0 & 0 & 0 & 0 & 0 & 0 \\
0 & a_1 & -a_4 & 0 & 0 & 0 & 0 & 0 & 0 & 0 & 0 & 0 & 0 & 0 & 0 \\
0 & 0 & a_5 & -a_6 & 0 & 0 & a_7 & 0 & 0 & 0 & 0 & 0 & 0 & 0 & 0 \\
0 & 0 & 0 & 0 & -a_8 & 0 & 0 & 0 & 0 & 0 & 0 & 0 & 0 & 0 & 0 \\
0 & 0 & 0 & 0 & a_9 & -a_{10} & 0 & 0 & 0 & 0 & 0 & 0 & 0 & 0 & 0 \\
0 & 0 & 0 & 0 & 0 & a_2 & -a_{11} & 0 & 0 & 0 & 0 & 0 & 0 & 0 & 0 \\
0 & 0 & 0 & 0 & 0 & 0 & a_{12} & -a_{13} & 0 & 0 & 0 & 0 & 0 & 0 & 0 \\
0 & 0 & 0 & 0 & 0 & 0 & 0 & a_{14} & -a_{15} & 0 & 0 & 0 & 0 & 0 & 0 \\
0 & 0 & 0 & 0 & 0 & 0 & 0 & 0 & a_3 & a_{16} & 0 & 0 & 0 & 0 & 0 \\
0 & 0 & 0 & 0 & 0 & 0 & 0 & 0 & 0 & r_3\delta_3 & -a_{17} & 0 & 0 & 0 & 0 \\
0 & 0 & 0 & 0 & 0 & 0 & 0 & 0 & 0 & 0 & 0 & -a_{18} & 0 & 0 & 0 \\
0 & a_{19} & a_{20} & 0 & 0 & 0 & 0 & 0 & 0 & 0 & 0 & a_{21} & -\mu_{z_1} & 0 & 0 \\
0 & 0 & 0 & a_{22} & 0 & a_{23} & a_{24} & a_{25} & 0 & 0 & 0 & 0 & 0 & -\mu_{z_2} & 0 \\
0 & 0 & 0 & a_{26} & 0 & 0 & 0 & 0 & 0 & 0 & 0 & a_{27} & 0 & 0 & -\mu_b
\end{bmatrix}$$

where

$$a_1 = \frac{\beta_1 S_h}{1+k_1 B} + \mu_h, \quad a_2 = \frac{\beta_1 S_h}{1+k_1 B}, \quad a_3 = \alpha_1 + \mu_{ih} + \frac{\sigma_{ih} Z_1}{1+\pi_{ih} I_h}, \quad a_4 = \delta_1 + \mu_{th} + \frac{\sigma_{th} Z_1}{1+\pi_{th} T_h},$$

$$a_5 = \frac{r_1 \delta_1}{1+c_1 Z_1}, \quad a_6 = \mu_m + \frac{\beta_2 R}{1+k_2 B} + \frac{\sigma_m Z_2}{1+\pi_m M}, \quad a_7 = \frac{p r_2 \delta_2}{1+c_2 Z_2}, \quad a_8 = \frac{\beta_2 M}{1+k_2 B} + \mu_r,$$

$$a_9 = \frac{\beta_2 M}{1+k_2 B}, \quad a_{10} = \alpha_2 + \mu_{ir} + \frac{\sigma_{ir} Z_2}{1+\pi_{ir} I_r}, \quad a_{11} = \delta_2 + \mu_{tr} + \frac{\sigma_{tr} Z_2}{1+\pi_{tr} T_r}, \quad a_{12} = \frac{(1-p) r_2 \delta_2}{1+c_2 Z_2},$$

$$a_{13} = q\omega + \mu_{gb} + \frac{\sigma_{gb} Z_2}{1+\pi_{gb} G_b}, \quad a_{14} = \frac{\rho q \omega}{1+k_3 B}, \quad a_{15} = \alpha_3 + \mu_{gm}, \quad a_{16} = \delta_3 + \mu_c, \quad a_{17} = a\nu + \mu_{sm},$$

$$a_{18} = \frac{\beta_1 H}{1+k_1 B} + \mu_{sh} + \frac{\sigma_{sh} Z_1}{1+\pi_{sh} S_h}, \quad a_{19} = \frac{\epsilon_{ih} Z_1}{1+\pi_{ih} I_h}, \quad a_{20} = \frac{\epsilon_{th} Z_1}{1+\pi_{th} T_h}, \quad a_{21} = \frac{\epsilon_{sh} Z_1}{1+\pi_{sh} S_h},$$

$$a_{22} = \frac{\epsilon_m Z_2}{1+\pi_m M}, \quad a_{23} = \frac{\epsilon_{ir} Z_2}{1+\pi_{ir} I_r}, a_{24} = \frac{\epsilon_{tr} Z_2}{1+\pi_{tr} T_r}, \quad a_{25} = \frac{\epsilon_{gb} Z_2}{1+\pi_{gb} G_b}, \quad a_{26} = \frac{\eta_2 M Z_2}{1+\pi_m M},$$

$$a_{27} = \frac{\eta_1 S_h Z_1}{1+\pi_{sh} S_h} \tag{4.2}$$

and F is a column vector given by

$$F = (\Lambda_h, 0, 0, 0, \Lambda_r, 0, 0, 0, 0, 0, 0, a b \nu, \Lambda_{z_1}, \Lambda_{z_2}, 0)^T$$

4.3 Analysis of the Model

4.3.1 Wellposedness of the model

In this section, we assess the wellposedness of the model by investigating the existence and feasibility of its solution. That is, to test whether the solutions are epidemiologically (variables have biological interpretation) and mathematically (a unique bounded solution exists for all the time) well-posed. The model system (4.1a)-(4.1o) can be expressed in the compact form (Dumont *et al.*, 2008; Mpeshe *et al.*, 2014a) as follows

$$\frac{\mathrm{d}X}{dt} = A(x)X + F$$

where

$$X = (H, I_h, T_h, M, R, I_r, T_r, G_b, G_m, C, S_m, S_h, Z_1, Z_2, B)^T,$$

$$A(x) = \begin{bmatrix}
a_1 & 0 & 0 & 0 & 0 & 0 & 0 & 0 & 0 & 0 & 0 & 0 & 0 & 0 & 0 \\
a_2 & -a_3 & 0 & 0 & 0 & 0 & 0 & 0 & 0 & 0 & 0 & 0 & 0 & 0 & 0 \\
0 & a_4 & -a_4 & 0 & 0 & 0 & 0 & 0 & 0 & 0 & 0 & 0 & 0 & 0 & 0 \\
0 & 0 & a_5 & -a_6 & 0 & 0 & a_7 & 0 & 0 & 0 & 0 & 0 & 0 & 0 & 0 \\
0 & 0 & 0 & 0 & -a_8 & 0 & 0 & 0 & 0 & 0 & 0 & 0 & 0 & 0 & 0 \\
0 & 0 & 0 & 0 & a_9 & -a_{10} & 0 & 0 & 0 & 0 & 0 & 0 & 0 & 0 & 0 \\
0 & 0 & 0 & 0 & 0 & a_2 & -a_{11} & 0 & 0 & 0 & 0 & 0 & 0 & 0 & 0 \\
0 & 0 & 0 & 0 & 0 & 0 & a_{12} & -a_{13} & 0 & 0 & 0 & 0 & 0 & 0 & 0 \\
0 & 0 & 0 & 0 & 0 & 0 & 0 & a_{14} & -a_{15} & 0 & 0 & 0 & 0 & 0 & 0 \\
0 & 0 & 0 & 0 & 0 & 0 & 0 & 0 & a_3 & -a_{16} & 0 & 0 & 0 & 0 & 0 \\
0 & 0 & 0 & 0 & 0 & 0 & 0 & 0 & 0 & r_3\delta_3 & -a_{17} & 0 & 0 & 0 & 0 \\
0 & 0 & 0 & 0 & 0 & 0 & 0 & 0 & 0 & 0 & 0 & -a_{18} & 0 & 0 & 0 \\
0 & a_{19} & a_{20} & 0 & 0 & 0 & 0 & 0 & 0 & 0 & 0 & a_{21} & -\mu_{z_1} & 0 & 0 \\
0 & 0 & 0 & a_{22} & 0 & a_{23} & a_{24} & a_{25} & 0 & 0 & 0 & 0 & 0 & -\mu_{z_2} & 0 \\
0 & 0 & 0 & a_{26} & 0 & 0 & 0 & 0 & 0 & 0 & 0 & a_{27} & 0 & 0 & -\mu_b
\end{bmatrix}$$

where

$$a_1 = \frac{\beta_1 S_h}{1 + k_1 B} + \mu_h, \quad a_2 = \frac{\beta_1 S_h}{1 + k_1 B}, \quad a_3 = \alpha_1 + \mu_{ih} + \frac{\sigma_{ih} Z_1}{1 + \pi_{ih} I_h}, \quad a_4 = \delta_1 + \mu_{th} + \frac{\sigma_{th} Z_1}{1 + \pi_{th} T_h},$$

$$a_5 = \frac{r_1 \delta_1}{1 + c_1 Z_1}, \quad a_6 = \mu_m + \frac{\beta_2 R}{1 + k_2 B} + \frac{\sigma_m Z_2}{1 + \pi_m M}, \quad a_7 = \frac{p r_2 \delta_2}{1 + c_2 Z_2}, \quad a_8 = \frac{\beta_2 M}{1 + k_2 B} + \mu_r,$$

$$a_9 = \frac{\beta_2 M}{1 + k_2 B}, \quad a_{10} = \alpha_2 + \mu_{ir} + \frac{\sigma_{ir} Z_2}{1 + \pi_{ir} I_r}, \quad a_{11} = \delta_2 + \mu_{tr} + \frac{\sigma_{tr} Z_2}{1 + \pi_{tr} T_r}, \quad a_{12} = \frac{(1-p) r_2 \delta_2}{1 + c_2 Z_2},$$

$$a_{13} = q\omega + \mu_{gb} + \frac{\sigma_{gb} Z_2}{1 + \pi_{gb} G_b}, \quad a_{14} = \frac{\rho q \omega}{1 + k_3 B}, \quad a_{15} = \alpha_3 + \mu_{gm}, \quad a_{16} = \delta_3 + \mu_c, \quad a_{17} = a\nu + \mu_{sm},$$

$$a_{18} = \frac{\beta_1 H}{1 + k_1 B} + \mu_{sh} + \frac{\sigma_{sh} Z_1}{1 + \pi_{sh} S_h}, \quad a_{19} = \frac{\epsilon_{ih} Z_1}{1 + \pi_{ih} I_h}, \quad a_{20} = \frac{\epsilon_{th} Z_1}{1 + \pi_{th} T_h}, \quad a_{21} = \frac{\epsilon_{sh} Z_1}{1 + \pi_{sh} S_h},$$

$$a_{22} = \frac{\epsilon_m Z_2}{1 + \pi_m M}, \quad a_{23} = \frac{\epsilon_{ir} Z_2}{1 + \pi_{ir} I_r}, a_{24} = \frac{\epsilon_{tr} Z_2}{1 + \pi_{tr} T_r}, \quad a_{25} = \frac{\epsilon_{gb} Z_2}{1 + \pi_{gb} G_b}, \quad a_{26} = \frac{\eta_2 M Z_2}{1 + \pi_m M},$$

$$a_{27} = \frac{\eta_1 S_h Z_1}{1 + \pi_{sh} S_h} \tag{4.2}$$

and F is a column vector given by

$$F = (\Lambda_h, 0, 0, 0, \Lambda_r, 0, 0, 0, 0, 0, 0, ab\nu, \Lambda_{z_1}, \Lambda_{z_2}, 0)^T$$

It is observed that $A(x)$ is Meltzer matrix since all its off diagonal elements are non negative, for $x \in \mathbb{R}^{15}_+$ and $F \geq 0$. Therefore, the system (4.1a)-(4.1o) is positively invariant in $\mathbb{R}^{15}_+$, meaning that an arbitrary trajectory of the sytstem started in $\mathbb{R}^{15}_+$ remains there forever. Also F is Lipschitz continous. Hence, a unique maximal solution exists and so

$$\mathcal{D} = \{(H, I_h, T_h, M, R, I_r, T_r, G_b, G_m, C, S_m, S_h, Z_1, Z_2, B) \geq 0 \in \mathbb{R}^{15}_+\}$$

is the feasible region for the model. Thus, the model (4.1a)-(4.1o) is epidemilogically and mathematically wellposed in the region $\mathcal{D}$.

4.3.2 Malaria Free Equilibrium (MEF)

Let $E^{01} = (H^{01}, I_h^{01}, T_h^{01}, M^{01}, R^{01}, I_r^{01}, T_r^{01}, G_b^{01}, G_m^{01}, C^{01}, S_m^{01}, S_h^{01}, Z_1^{01}, Z_2^{01}, B^{01})$ be the MFE of the system (4.1a)-(4.1o). We obtained equilibrium points of the system by setting right hand side of model equations equal to zero and solve for variables.

In absence of malaria infection,

$$I_h^{01} = T_h^{01} = M^{01} = I_r^{01} = T_r^{01} = G_b^{01} = G_m^{01} = C^{01} = S_m^{01} = S_h^{01} = B^{01} = 0.$$

From equations (4.1a) , (4.1e), (4.1m) and (4.1n), we respectively obtain

$$H^{01} = \frac{\Lambda_h}{\mu_h}, \qquad R^{01} = \frac{\Lambda_r}{\mu_r}, \qquad Z_1^{01} = \frac{\Lambda_{z_1}}{\mu_{z_1}} \quad \text{and } Z_2^{01} = \frac{\Lambda_{z_2}}{\mu_{z_2}}$$

Thus the MFE is

$$E^{01} = \left(\frac{\Lambda_h}{\mu_h}, 0, 0, \frac{\Lambda_r}{\mu_r}, 0, 0, 0, 0, 0, 0, 0, \frac{\Lambda_{z_1}}{\mu_{z_1}}, \frac{\Lambda_{z_2}}{\mu_{z_2}}, 0\right)$$

4.3.3 Basic Reproduction Number, $\mathcal{R}_{01}$

In this context of in vivo dynamics, Guardiola and Vecchio (2005) defined reproduction number as a number of newly infected cells that single infected cell can produce during its infectious period. We calculate basic reproduction number for the model (4.1a)-(4.1o) using the next generation matrix method (Van den Driessche and Watmough, 2002). The equations for model

(4.1a)-(4.1o) are re-arranged so that the infection classes appeared first. Thus we have,

$$\frac{dI_h}{dt} = \frac{\beta_1 S_h H}{1+k_1 B} - (\alpha_1 + \mu_{ih})I_h - \frac{\sigma_{ih} Z_1 I_h}{1+\pi_{ih}} \tag{4.3a}$$

$$\frac{dT_h}{dt} = \alpha_1 I_h - (\delta_1 + \mu_{th})T_h - \frac{\sigma_{th} Z_1 T_h}{1+\pi_{th} T_h} \tag{4.3b}$$

$$\frac{dM}{dt} = \frac{r_1 \delta_1 T_h}{1+c_1 Z_1} + \frac{p r_2 \delta_2 T_r}{1+c_2 Z_2} - \frac{\beta_2 R M}{1+k_2 B} - \frac{\sigma_m Z_2 M}{1+\pi_m M} - \mu_m M \tag{4.3c}$$

$$\frac{dI_r}{dt} = \frac{\beta_2 R M}{1+k_2 B} - (\alpha_2 + \mu_{ir})I_r - \frac{\sigma_{ir} Z_1 I_r}{1+\pi_{ir} I_r} \tag{4.3d}$$

$$\frac{dT_r}{dt} = \alpha_2 I_r - (\delta_2 + \mu_{tr})T_r - \frac{\sigma_{ir} Z_2 T_r}{1+\pi_{tr} T_r} \tag{4.3e}$$

$$\frac{dG_b}{dt} = (1-p)\frac{r_2 \delta_2 T_r}{1+c_2 Z_2} - (q\omega + \mu_{gb})G_b - \frac{\sigma_{ir} Z_2 G_b}{1+\pi_{gb} G_b} \tag{4.3f}$$

$$\frac{dG_m}{dt} = \frac{p q \omega G_b}{1+k_3 B} - \alpha_3 G_m - \mu_{gm} G_m \tag{4.3g}$$

$$\frac{dC}{dt} = \alpha_3 G_m - \delta_3 C - \mu_c C \tag{4.3h}$$

$$\frac{dS_m}{dt} = r_3 \delta_3 C - a\nu S_m - \mu_{sm} S_m \tag{4.3i}$$

$$\frac{dS_h}{dt} = a b \nu - \frac{\beta_1 S_h H}{1+k_1 B} - \mu_{sh} S_h - \frac{\sigma_{sh} Z_1 S_h}{1+\pi_{sh} S_h} \tag{4.3j}$$

$$\frac{dR}{dt} = \Lambda_r - \frac{\beta_2 R M}{1+k_2 B} - \mu_r R \tag{4.3k}$$

$$\frac{dH}{dt} = \Lambda_h - \frac{\beta_1 S_h H}{1+k_1 B} - \mu_h H \tag{4.3l}$$

$$\frac{dZ_1}{dt} = \Lambda_{z_1} + \left(\frac{\epsilon_{sh} S_h}{1+\pi_{sh} S_h} + \frac{\epsilon_{ih} I_h}{1+\pi_{ih} I_h} + \frac{\epsilon_{th} T_h}{1+\pi_{th} T_h}\right) Z_1 - \mu_{z_1} Z_1 \tag{4.3m}$$

$$\frac{dZ_2}{dt} = \Lambda_{z_2} + \left(\frac{\epsilon_m M}{1+\pi_m M} + \frac{\epsilon_{ir} I_r}{1+\pi_{ir} I_r} + \frac{\epsilon_{tr} T_r}{1+\pi_{tr} T_r} + \frac{\epsilon_{gb} G_b}{1+\pi_{gb} G_{gb}}\right) Z_2 - \mu_{z_2} Z_2 \tag{4.3n}$$

$$\frac{dB}{dt} = \eta_1 \frac{S_h Z_1}{1+\pi_{sh} S_h} + \eta_2 \frac{M Z_2}{1+\pi_m M} - \mu_b B \tag{4.3o}$$

Reproduction number, $\mathcal{R}_{01}$, is the spectral radius $\rho(F_1 V_1^{-1})$, of next generation matrix $F_1 V_1^{-1}$. where $F_1 = \frac{\partial \mathcal{F}_{1i}}{\partial x_i}(E^{01})$ is transmission matrix and $V_1 = \frac{\partial \mathcal{V}_{1i}}{\partial x_i}(E^{01})$ is transition matrix.

$\mathcal{F}_{1i}$ be the rate of appearance of new infection in compartment i,

$\mathcal{V}_{1i}^{+}$ be the rate of transfer of individuals into compartment i by all other means,

$\mathcal{V}_{1i}^{-}$ be the rate of transfer of individuals out of compartment i by all other means and $\mathcal{V}_{1i} =$

$\mathcal{V}_{1i}^{+} - \mathcal{V}_{1i}^{-}$. Hence, using equations (4.3a)-(4.3j) we have

$$\mathcal{F}_{1i} = \begin{pmatrix} \dfrac{\beta_1 S_h H}{1+c_1 S_h} \\ 0 \\ 0 \\ \dfrac{\beta_2 R M}{1+c_2 M} \\ 0 \\ 0 \\ \dfrac{p q \omega G_b}{1+k_3 B} \\ 0 \\ 0 \\ 0 \end{pmatrix} \tag{4.4}$$

and

$$\mathcal{V}_{1i} = \begin{pmatrix} \left(\alpha_1 + \mu_{ih} + \dfrac{\sigma_{ih} Z_1}{1+\pi_{ih} I_h}\right) I_h \\ \left(\delta_1 + \mu_{th} + \dfrac{\sigma_{th} Z_1}{1+\pi_{th} T_h}\right) T_h - \alpha_1 I_h \\ \left(\dfrac{\beta_2 R}{1+k_2 B} + \dfrac{\sigma_m Z_2}{1+\pi_m M} + \mu_m\right) M - \left(\dfrac{r_1 \delta_1}{1+c_1 Z_1}\right) T_h - \left(\dfrac{p r_2 \delta_2}{1+c_2 Z_2}\right) T_r \\ \left(\alpha_2 + \mu_{ir} + \dfrac{\sigma_{ir} Z_2}{1+\pi_{ir} I_r}\right) I_r \\ \left(\delta_2 + \mu_{tr} + \dfrac{\sigma_{tr} Z_2}{1+\pi_{tr} T_r}\right) T_r - \alpha_2 I_r \\ \left(q\omega + \mu_{gb} + \dfrac{\sigma_{gb} Z_2}{1+\pi_{gb} G_b}\right) G_b - \left((1-p)\dfrac{r_2 \delta_2}{1+c_2 Z_2}\right) T_r \\ (\alpha_3 + \mu_{gm}) G_m \\ (\delta_3 + \mu_c) C - \alpha_3 G_m \\ (a\nu + \mu_{sm}) S_{sm} - r_3 \delta_3 C \\ \left(\dfrac{\beta_1 H}{1+k_1 B} + \dfrac{\sigma_{sh} Z_1}{1+\pi_{sh} S_h} + \mu_{sh}\right) S_h - ab\nu \end{pmatrix} \tag{4.5}$$

From matrices in (4.4) and (4.5) we obtain

$$F_1 = \begin{pmatrix} 0 & 0 & 0 & 0 & 0 & 0 & 0 & 0 & 0 & \beta_1\frac{\Lambda_h}{\mu_h} \\ 0 & 0 & 0 & 0 & 0 & 0 & 0 & 0 & 0 & 0 \\ 0 & 0 & 0 & 0 & 0 & 0 & 0 & 0 & 0 & 0 \\ 0 & 0 & \beta_2\frac{\Lambda_r}{\mu_r} & 0 & 0 & 0 & 0 & 0 & 0 & 0 \\ 0 & 0 & 0 & 0 & 0 & 0 & 0 & 0 & 0 & 0 \\ 0 & 0 & 0 & 0 & 0 & 0 & 0 & 0 & 0 & 0 \\ 0 & 0 & 0 & 0 & 0 & p\eta\omega & 0 & 0 & 0 & 0 \\ 0 & 0 & 0 & 0 & 0 & 0 & 0 & 0 & 0 & 0 \\ 0 & 0 & 0 & 0 & 0 & 0 & 0 & 0 & 0 & 0 \\ 0 & 0 & 0 & 0 & 0 & 0 & 0 & 0 & 0 & 0 \end{pmatrix} \tag{4.6}$$

and

$$V_1 = \begin{pmatrix} v_1 & 0 & 0 & 0 & 0 & 0 & 0 & 0 & 0 & 0 \\ -\alpha_1 & v_2 & 0 & 0 & 0 & 0 & 0 & 0 & 0 & 0 \\ 0 & -v_3 & v_4 & 0 & -v_5 & 0 & 0 & 0 & 0 & 0 \\ 0 & 0 & 0 & v_6 & 0 & 0 & 0 & 0 & 0 & 0 \\ 0 & 0 & 0 & -\alpha_2 & v_7 & 0 & 0 & 0 & 0 & 0 \\ 0 & 0 & 0 & 0 & -v_8 & v_9 & 0 & 0 & 0 & 0 \\ 0 & 0 & 0 & 0 & 0 & 0 & v_{10} & 0 & 0 & 0 \\ 0 & 0 & 0 & 0 & 0 & 0 & -\alpha_3 & v_{11} & 0 & 0 \\ 0 & 0 & 0 & 0 & 0 & 0 & 0 & -v_{12} & v_{13} & 0 \\ 0 & 0 & 0 & 0 & 0 & 0 & 0 & 0 & 0 & v_{14} \end{pmatrix} \tag{4.7}$$

respectively, where

$$\begin{aligned} v_1 &= \alpha_1 + \mu_{ih} + \frac{\sigma_{ih}\Lambda_{z_1}}{\mu_{z_1}}, \quad v_2 = \delta_1 + \mu_{th} + \frac{\sigma_{th}\Lambda_{z_1}}{\mu_{z_1}}, \quad v_3 = \frac{r_1\delta_1\mu_{z_1}}{\mu_{z_1} + c_1\Lambda_{z_1}}, \quad v_4 = \beta_2\frac{\Lambda_r}{\mu_r} + \frac{\sigma_m\Lambda_{z_2}}{\mu_{z_2}} + \mu_m \\ v_5 &= \frac{pr_2\delta_2\mu_{z_2}}{\mu_{z_2} + c_2\Lambda_{z_2}}, \quad v_6 = \alpha_2 + \mu_{ir} + \frac{\sigma_{ir}\Lambda_{z_2}}{\mu_{z_2}}, \quad v_7 = \delta_2 + \frac{\sigma_{tr}\Lambda_{z_2}}{\mu_{z_2}} + \mu_{tr}, \quad v_8 = \frac{(1-p)r_2\delta_2\mu_{z_2}}{\mu_{z_2} + c_2Z_2}, \\ v_9 &= q\omega + \mu_{gb} + \frac{\sigma_{gb}\Lambda_{z_2}}{\mu_{z_2}}, \quad v_{10} = \alpha_3 + \mu_{gm}, \quad v_{11} = \delta_3 + \mu_c, \quad v_{12} = r_3\delta_3, \quad v_{13} = a\nu + \mu_{sm}, \\ v_{14} &= \beta_1\frac{\Lambda_h}{\mu_h} + \frac{\sigma_{sh}\Lambda_{z_1}}{\mu_{z_1}} + \mu_{sh} \end{aligned} \tag{4.8}$$

From (4.7) we obtained the inverse, V_1^{-1}, of V_1 given by

$$V_1^{-1} = \begin{pmatrix} \frac{1}{v_1} & 0 & 0 & 0 & 0 & 0 & 0 & 0 & 0 & 0 \\ \frac{\alpha_1}{v_2 v_1} & \frac{1}{v_2} & 0 & 0 & 0 & 0 & 0 & 0 & 0 & 0 \\ \frac{v_3\alpha_1}{v_4 v_2 v_1} & \frac{v_3}{v_4 v_2} & \frac{1}{v_4} & \frac{v_5\alpha_2}{v_7 v_6 v_4} & \frac{v_5}{v_7 v_4} & 0 & 0 & 0 & 0 & 0 \\ 0 & 0 & 0 & \frac{1}{v_6} & 0 & 0 & 0 & 0 & 0 & 0 \\ 0 & 0 & 0 & \frac{\alpha_2}{v_7 v_6} & \frac{1}{v_7} & 0 & 0 & 0 & 0 & 0 \\ 0 & 0 & 0 & \frac{\alpha_2 v_8}{v_9 v_7 v_6} & \frac{v_8}{v_9 v_7} & \frac{1}{v_9} & 0 & 0 & 0 & 0 \\ 0 & 0 & 0 & 0 & 0 & 0 & \frac{1}{v_{10}} & 0 & 0 & 0 \\ 0 & 0 & 0 & 0 & 0 & 0 & \frac{\alpha_3}{v_{11} v_{10}} & \frac{1}{v_{11}} & 0 & 0 \\ 0 & 0 & 0 & 0 & 0 & 0 & \frac{v_{12}\alpha_3}{v_{13} v_{11} v_{10}} & \frac{v_{12}}{v_{113} v_{11}} & \frac{1}{v_{13}} & 0 \\ 0 & 0 & 0 & 0 & 0 & 0 & 0 & 0 & 0 & \frac{1}{v_{14}} \end{pmatrix} \tag{4.9}$$

Hence, from (4.6) and (4.9), we have

$$F_1 V_1^{-1} = \begin{pmatrix} 0 & 0 & 0 & 0 & 0 & 0 & 0 & 0 & 0 & A_1 \\ 0 & 0 & 0 & 0 & 0 & 0 & 0 & 0 & 0 & 0 \\ 0 & 0 & 0 & 0 & 0 & 0 & 0 & 0 & 0 & 0 \\ A_2 & A_3 & A_4 & A_5 & A_6 & 0 & 0 & 0 & 0 & 0 \\ 0 & 0 & 0 & 0 & 0 & 0 & 0 & 0 & 0 & 0 \\ 0 & 0 & 0 & 0 & 0 & 0 & 0 & 0 & 0 & 0 \\ 0 & 0 & 0 & 0 & 0 & 0 & 0 & 0 & 0 & 0 \\ 0 & 0 & 0 & A_7 & A_8 & A_9 & 0 & 0 & 0 & 0 \\ 0 & 0 & 0 & 0 & 0 & 0 & 0 & 0 & 0 & 0 \\ 0 & 0 & 0 & 0 & 0 & 0 & 0 & 0 & 0 & 0 \end{pmatrix} \tag{4.10}$$

$$\begin{aligned} A_1 &= \frac{\beta_1 \Lambda_h}{v_{14}\mu_h}, \quad A_2 = \frac{\beta_2 \alpha_1 v_3 \Lambda_r}{v_4 v_2 v_1 \mu_r}, \quad A_3 = \frac{\beta_2 v_3 \Lambda_r}{v_4 v_2 \mu_r}, \quad A_4 = \frac{\beta_2 \Lambda_r}{v_4 \mu_r}, \quad A_5 = \frac{\beta_2 \Lambda_r v_5 \alpha_2}{v_7 v_6 v_4 \mu_r}, \\ A_6 &= \frac{\beta_2 v_5 \Lambda_r}{v_7 v_4 \mu_r}, \quad A_7 = \frac{\rho q \omega v_8 \alpha_2}{v_9 v_7 v_6}, \quad A_8 = \frac{\rho q \omega v_8}{v_9 v_7}, \quad A_9 = \frac{\rho q \omega}{v_9} \end{aligned} \tag{4.11}$$

The eigenvalues of next generation matrix, $F_1 V_1^{-1}$ are obtained from

$$|F_1 V_1^{-1} - I\lambda| = 0$$

The basic reproduction number, $\mathcal{R}_{01}$, is the dorminant eigenvalue of $F_1 V_1^{-1}$. From (4.10), we obtain only one nonzero eigenvalue

$$\lambda = A_5 = \frac{\beta_2 \Lambda_r v_5 \alpha_2}{v_7 v_6 v_4 \mu_r}.$$

Therefore, the dorminant eigenvalue is

$$\lambda = \frac{\beta_2 \Lambda_r v_5 \alpha_2}{v_7 v_6 v_4 \mu_r}$$

.

and hence, the basic reproduction number, $\mathcal{R}_{01}$ is

$$\mathcal{R}_{01} = \frac{\beta_2 \Lambda_r v_5 \alpha_2}{v_7 v_6 v_4 \mu_r} \tag{4.12}$$

Substituting the values of v_4, v_5, v_6, and v_7 from equation (4.8) into equation (4.12) we get

$$\mathcal{R}_{01} = \frac{\beta_2 \frac{\Lambda_r}{\mu_r} \alpha_2 \frac{p r_2 \delta_2 \mu_{z_2}}{\mu_{z_2} + c_2 \Lambda_{z_2}}}{\left(\delta_2 + \mu_{tr} + \sigma_{tr} \frac{\Lambda_{z_2}}{\mu_{z_2}}\right)\left(\alpha_2 + \mu_{ir} + \sigma_{ir} \frac{\Lambda_{z_2}}{\mu_{z_2}}\right)\left(\mu_m + \beta_2 \frac{\Lambda_r}{\mu_r} + \sigma_m \frac{\Lambda_{z_2}}{\mu_{z_2}}\right)}$$

which can be expressed as

$$\mathcal{R}_{01} = \left[\frac{\beta_2 r_0}{\beta_2 r_0 + \sigma_m z_0 + \mu_m}\right]\left[\frac{\alpha_2}{\alpha_2 + \mu_{ir} + \sigma_{ir} z_0}\right]\left[\frac{1}{\delta_2 + \mu_{tr} + \sigma_{tr} z_0}\right]\left[\frac{p r_2 \delta_2}{1 + c_2 z_0}\right] \tag{4.13}$$

$r_0 = \frac{\Lambda_r}{\mu_r}$ and $z_0 = \frac{\Lambda_{z_2}}{\mu_{z_2}}$ respectively represent the values of uninfected RBCs and immune cells that fight against blood stage malaria at malaria-free equilibrium. From equation (4.13), $\left(\frac{\beta_2 r_0}{\beta_2 r_0 + \sigma_m z_0 + \mu_m}\right)$ is the proportion of RBCs that can be infected by a merozite introduced into entirely susceptile RBCs population before it dies (either naturally or cleared by immune cells), $\left(\frac{\alpha_2}{\alpha_2 + \mu_{ir} + \sigma_{ir} z_0}\right)$ represents the proportion of infected RBCs that progress to schizonts before dying, $\left(\frac{1}{\delta_2 + \mu_{tr} + \sigma_{tr} z_0}\right)$ is an average duration a schizont spends before it burst or cleared by immune cells and $\left(\frac{p r_2 \delta_2}{1 + c_2 z_0}\right)$ is number of merozoites produced by a schizont when it bursts.

4.3.4 Local and Global Stability of MFE

The Jacobian matrix of the system (4.1a)-(4.1o) evaluated at malaria-free equilibrium, E^{01}, is

$$J(E^{01}) = \begin{bmatrix}
-\mu_h & 0 & 0 & 0 & 0 & 0 & 0 & 0 & 0 & 0 & 0 & -u_1 & 0 & 0 & 0 \\
0 & -u_2 & 0 & 0 & 0 & 0 & 0 & 0 & 0 & 0 & 0 & u_1 & 0 & 0 & 0 \\
0 & \alpha_1 & -u_3 & 0 & 0 & 0 & 0 & 0 & 0 & 0 & 0 & 0 & 0 & 0 & 0 \\
0 & 0 & u_4 & -u_5 & 0 & 0 & u_6 & 0 & 0 & 0 & 0 & 0 & 0 & 0 & 0 \\
0 & 0 & 0 & -u_7 & -\mu_r & 0 & 0 & 0 & 0 & 0 & 0 & 0 & 0 & 0 & 0 \\
0 & 0 & 0 & u_7 & 0 & -u_8 & 0 & 0 & 0 & 0 & 0 & 0 & 0 & 0 & 0 \\
0 & 0 & 0 & 0 & 0 & \alpha_2 & -u_9 & 0 & 0 & 0 & 0 & 0 & 0 & 0 & 0 \\
0 & 0 & 0 & 0 & 0 & 0 & u_{10} & -u_{11} & 0 & 0 & 0 & 0 & 0 & 0 & 0 \\
0 & 0 & 0 & 0 & 0 & 0 & 0 & pq\omega & -u_{12} & 0 & 0 & 0 & 0 & 0 & 0 \\
0 & 0 & 0 & 0 & 0 & 0 & 0 & 0 & \alpha_3 & -u_{13} & 0 & 0 & 0 & 0 & 0 \\
0 & 0 & 0 & 0 & 0 & 0 & 0 & 0 & 0 & r_3\delta_3 & -u_{14} & 0 & 0 & 0 & 0 \\
0 & 0 & 0 & 0 & 0 & 0 & 0 & 0 & 0 & 0 & 0 & -u_{15} & 0 & 0 & 0 \\
0 & u_{16} & u_{17} & 0 & 0 & 0 & 0 & 0 & 0 & 0 & 0 & u_{18} & -\mu_{z_1} & 0 & 0 \\
0 & 0 & 0 & u_{19} & 0 & u_{20} & u_{21} & u_{22} & 0 & 0 & 0 & 0 & 0 & -\mu_{z_2} & 0 \\
0 & 0 & 0 & u_{23} & 0 & 0 & 0 & 0 & 0 & 0 & 0 & u_{24} & 0 & 0 & -\mu_b
\end{bmatrix}$$

where

$$\begin{aligned}
u_1 &= \beta_1 \frac{\Lambda_h}{\mu_h}, \quad u_2 = \alpha_1 + \mu_{ih} + \sigma_{ih}\frac{\Lambda_{z_1}}{\mu_{z_1}}, \quad u_3 = \delta_1 + \mu_{th} + \sigma_{th}\frac{\Lambda_{z_1}}{\mu_{z_1}}, \quad u_4 = \frac{r_1\delta_1\mu_{z_1}}{\mu_{z_1} + c_1\Lambda_{z_1}}, \\
u_5 &= \beta_2\frac{\Lambda_r}{\mu_r} + \sigma_m\frac{\Lambda_{z_2}}{\mu_{z_2}} + \mu_m, \quad u_6 = \frac{pr_2\delta_2\mu_{z_2}}{\mu_{z_2} + c_2\Lambda_{z_2}}, \quad u_7 = \beta_2\frac{\Lambda_r}{\mu_r}, \quad u_8 = \mu_{ir} + \alpha_2 + \sigma_{ir}\frac{\Lambda_{z_2}}{\mu_{z_2}} \\
u_9 &= \delta_2 + \mu_{tr} + \sigma_{tr}\frac{\Lambda_{z_2}}{\mu_{z_2}}, \quad u_{10} = \frac{(1-p)r_2\delta_2\mu_{z_2}}{\mu_{z_2} + c_2\Lambda_{z_2}}, \quad u_{11} = q\omega + \mu_{gb} + \sigma_{gb}\frac{\Lambda_{z_2}}{\mu_{z_2}}, \quad u_{12} = \alpha_3 + \mu_{gm}, \\
u_{13} &= \delta_3 + \mu_c, \quad u_{14} = \alpha\nu + \mu_{sm}, \quad u_{15} = \beta_1\frac{\Lambda_h}{\mu_h} + \sigma_{sh}\frac{\Lambda_{z_1}}{\mu_{z_1}} + \mu_{sh}, \quad u_{16} = c_{ih}\frac{\Lambda_{z_1}}{\mu_{z_1}}, \quad u_{17} = c_{th}\frac{\Lambda_{z_1}}{\mu_{z_1}}, \\
u_{18} &= c_{sh}\frac{\Lambda_{z_1}}{\mu_{z_1}}, \quad u_{19} = c_m\frac{\Lambda_{z_2}}{\mu_{z_2}}, \quad u_{20} = c_{ir}\frac{\Lambda_{z_2}}{\mu_{z_2}}, \quad u_{21} = c_{tr}\frac{\Lambda_{z_2}}{\mu_{z_2}}, \quad u_{22} = c_{gb}\frac{\Lambda_{z_2}}{\mu_{z_2}}, \quad u_{22} = c_{sh}\frac{\Lambda_{z_1}}{\mu_{z_1}}, \\
u_{23} &= \eta_2\frac{\Lambda_{z_2}}{\pi_m\mu_{z_2}}, \quad u_{24} = \eta_1\frac{\Lambda_{z_1}}{\pi_{sh}\mu_{z_1}}
\end{aligned} \tag{4.14}$$

Local stability of a MFE, E^{01}, is determined by using the signs of real part of eigenvalues of the Jacobian matrix of the system evaluated at E^{01}. We denote the Jacobian matrix of model system (4.1a)-(4.1o) evaluated at the MFE by $J(E^{01})$. The MFE is locally assympotically stable if and only if all eigenvalues of $J(E^{01})$ have negative real parts.

Clearly, six eigenvalues $-\mu_h$, $-\mu_r$, $-u_{14}$, $-\mu_{z_1}$, $-\mu_{z_2}$ and $-\mu_b$ are negative. The other nine eigenvalues are obtained from remaining 9 × 9 submatrix, $J_1(E^{01})$, given by

$$J_1(E^{01}) = \begin{bmatrix} -u_2 & 0 & 0 & 0 & 0 & 0 & 0 & 0 & u_1 \\ \alpha_1 & -u_3 & 0 & 0 & 0 & 0 & 0 & 0 & 0 \\ 0 & u_4 & -u_5 & 0 & u_6 & 0 & 0 & 0 & 0 \\ 0 & 0 & u_7 & -u_8 & 0 & 0 & 0 & 0 & 0 \\ 0 & 0 & 0 & \alpha_2 & -u_9 & 0 & 0 & 0 & 0 \\ 0 & 0 & 0 & 0 & u_{10} & -u_{11} & 0 & 0 & 0 \\ 0 & 0 & 0 & 0 & 0 & \rho q \omega & -u_{12} & 0 & 0 \\ 0 & 0 & 0 & 0 & 0 & 0 & \alpha_3 & -u_{13} & 0 \\ 0 & 0 & 0 & 0 & 0 & 0 & 0 & 0 & -u_{15} \end{bmatrix}$$

From eighth column of $J_1(E^{01})$ we observe that other eigenvalue is $-u_{13}$ which is also negative. Further reduction of this, leads us to 8×8 submatrix given by

$$J_2(E^{01}) = \begin{bmatrix} -u_2 & 0 & 0 & 0 & 0 & 0 & 0 & u_1 \\ \alpha_1 & -u_3 & 0 & 0 & 0 & 0 & 0 & 0 \\ 0 & u_4 & -u_5 & 0 & u_6 & 0 & 0 & 0 \\ 0 & 0 & u_7 & -u_8 & 0 & 0 & 0 & 0 \\ 0 & 0 & 0 & \alpha_2 & -u_9 & 0 & 0 & 0 \\ 0 & 0 & 0 & 0 & u_{10} & -u_{11} & 0 & 0 \\ 0 & 0 & 0 & 0 & 0 & \rho q \omega & -u_{12} & 0 \\ 0 & 0 & 0 & 0 & 0 & 0 & 0 & -u_{15} \end{bmatrix}$$

from which another eigenvalue $-u_{12}$ is obtained. Another reduction leads a 7×7 submatrix given by

$$J_3(E^{01}) = \begin{bmatrix} -u_2 & 0 & 0 & 0 & 0 & 0 & u_1 \\ \alpha_1 & -u_3 & 0 & 0 & 0 & 0 & 0 \\ 0 & u_4 & -u_5 & 0 & u_6 & 0 & 0 \\ 0 & 0 & u_7 & -u_8 & 0 & 0 & 0 \\ 0 & 0 & 0 & \alpha_2 & -u_9 & 0 & 0 \\ 0 & 0 & 0 & 0 & u_{10} & -u_{11} & 0 \\ 0 & 0 & 0 & 0 & 0 & 0 & -u_{15} \end{bmatrix}$$

And from $J_3(E^{01})$ above we obtained another eigenvalue $-u_{11}$, and a new reduced matrix is

$$J_4(E^{01}) = \begin{bmatrix} -u_2 & 0 & 0 & 0 & 0 & u_1 \\ \alpha_1 & -u_3 & 0 & 0 & 0 & 0 \\ 0 & u_4 & -u_5 & 0 & u_6 & 0 \\ 0 & 0 & u_7 & -u_8 & 0 & 0 \\ 0 & 0 & 0 & \alpha_2 & -u_9 & 0 \\ 0 & 0 & 0 & 0 & 0 & -u_{15} \end{bmatrix}$$

We investigate the signs of other remaining six eigenvalues using the trace-determinant technique. If the trace and determinat of $J_4(E^{01})$ are strictly negative and positive respectively, then all eigenvalues of $J_4(E^{01})$ have negative real parts. The following results were obtained using MAPLE 12,

$$tr(J_4(E^{01})) = -\left[u_2 + u_3 + u_5 + u_8 + u_9 + u_{15}\right] < 0 \tag{4.15}$$

and

$$det(J_4(E^{01})) = (u_2u_3u_{15})(u_5u_8u_9 - \alpha_2u_6u_7) > 0 \tag{4.16}$$

since the values of $u's$ given in equation (5.13) are all positive, then equation (5.15) is true only if

$$u_5u_8u_9 > \alpha_2u_6u_7$$

equivalently

$$\frac{\alpha_2u_6u_7}{u_5u_8u_9} < 1 \tag{4.17}$$

Substituting the values of u_5, u_6, u_7, u_8, and u_9 as given in equation (4.14) into equation (4.17), we obtain

$$\frac{\beta_2\frac{\Lambda_r}{\mu_r}\alpha_2\frac{pr_2\delta_2\mu_{z_2}}{\mu_{z_2}+c_2\Lambda_{z_2}}}{\left(\mu_{tr}+\delta_2+\sigma_{tr}\frac{\Lambda_{z_2}}{\mu_{z_2}}\right)\left(\mu_{ir}+\alpha_2+\sigma_{ir}\frac{\Lambda_{z_2}}{\mu_{z_2}}\right)\left(\mu_m+\beta_2\frac{\Lambda_r}{\mu_r}+\sigma_m\frac{\Lambda_{z_2}}{\mu_{z_2}}\right)} < 1$$

which is the same as

$$\mathcal{R}_{01} < 1 \tag{4.18}$$

Thus, all eigenvalues of $J(E^{01})$ have negative real parts only if $\mathcal{R}_{01} < 1$. Hence, MFE is locally assymptotically stable provided $\mathcal{R}_{01} < 1$, which leads us to the following theorem.

Theorem 4.5

The malaria-free equilibrium, E^{01}, of the model (4.1a)-(4.1o), is locally asymptotically stable when $\mathcal{R}_{01} < 1$ and unstable otherwise.

We applied the Metzler matrix theory to establish the global stability of MFE as used in Castillo-Chávez *et al.* (2002) and Mpeshe *et al.* (2014b) by expressing the model (4.1a)-(4.1o) in the form

$$\begin{cases} \frac{dX_n}{dt} = A_1(x)(X_n - X_{E^0,n}) + A_{12}(x)X_c \\ \\ \frac{dX_c}{dt} = A_2(x)X_c \end{cases}$$

where X_n is the vector of non-transmitting classes and X_c is the vector of transmitting classes. For our model, we have

$$X_n = (H,\ R,\ Z_1,\ Z_2,\ B) \text{ and } X_c = (I_h,\ T_h,\ M,\ I_r,\ T_r,\ G_b,\ G_m,\ C,\ S_m,\ S_h) \tag{4.19}$$

$$X_{E^0,n} = \left(\frac{\Lambda_h}{\mu_h}, \frac{\Lambda_r}{\mu_r}, \frac{\Lambda_{z_1}}{\mu_{z_1}}, \frac{\Lambda_{z_2}}{\mu_{z_2}}, 0\right) \tag{4.20}$$

and

$$A_1(x) = \begin{pmatrix} -\mu_h & 0 & 0 & 0 & 0 \\ 0 & -\mu_r & 0 & 0 & 0 \\ 0 & 0 & -\mu_{z_1} & 0 & 0 \\ 0 & 0 & 0 & -\mu_{z_2} & 0 \\ 0 & 0 & 0 & 0 & -\mu_b \end{pmatrix}, \tag{4.21}$$

$$A_{12}(x) = \begin{pmatrix} 0 & 0 & 0 & 0 & 0 & 0 & 0 & 0 & 0 & -d_1 \\ 0 & 0 & -d_2 & 0 & 0 & 0 & 0 & 0 & 0 & 0 \\ d_3 & d_4 & 0 & 0 & 0 & 0 & 0 & 0 & 0 & d_5 \\ 0 & 0 & d_6 & d_7 & d_8 & d_9 & 0 & 0 & 0 & 0 \\ 0 & 0 & d_{10} & 0 & 0 & 0 & 0 & 0 & 0 & d_{11} \end{pmatrix} \tag{4.22}$$

where

$$\begin{aligned} d_1 &= \frac{\beta_1 H}{1 + k_1 B}, \quad d_2 = \frac{\beta_2 R}{1 + k_2 B}, \quad d_3 = \frac{\epsilon_{ih} Z_1}{1 + \pi_{ih} I_h}, \quad d_4 = \frac{\epsilon_{th} Z_1}{1 + \pi_{th} T_h}, \quad d_5 = \frac{\epsilon_{sh} Z_1}{1 + \pi_{sh} S_h}, \\ d_6 &= \frac{\epsilon_m Z_2}{1 + \pi_m M}, \quad d_7 = \frac{\epsilon_{ir} Z_2}{1 + \pi_{ir} I_r}, \quad d_8 = \frac{\epsilon_{ir} Z_2}{1 + \pi_{tr} T_r}, d_9 = \frac{\epsilon_{gb} Z_2}{1 + \pi_{gb} G_b}, \quad d_{10} = \frac{\eta_2 Z_2}{1 + \pi_m M}, \\ d_{11} &= \frac{\eta_1 Z_1}{1 + \pi_{sh} S_h} \end{aligned} \tag{4.23}$$

and

$$A_2(x) = \begin{pmatrix} -w_1 & 0 & 0 & 0 & 0 & 0 & 0 & 0 & 0 & w_2 \\ \alpha_1 & -w_3 & 0 & 0 & 0 & 0 & 0 & 0 & 0 & 0 \\ 0 & w_4 & -w_5 & 0 & w_6 & 0 & 0 & 0 & 0 & 0 \\ 0 & 0 & w_7 & -w_8 & 0 & 0 & 0 & 0 & 0 & 0 \\ 0 & 0 & 0 & \alpha_2 & -w_9 & 0 & 0 & 0 & 0 & 0 \\ 0 & 0 & 0 & 0 & w_{10} & -w_{11} & 0 & 0 & 0 & 0 \\ 0 & 0 & 0 & 0 & 0 & w_{12} & -w_{13} & 0 & 0 & 0 \\ 0 & 0 & 0 & 0 & 0 & 0 & \alpha_3 & -w_{14} & 0 & 0 \\ 0 & 0 & 0 & 0 & 0 & 0 & 0 & w_{15} & -w_{16} & 0 \\ 0 & 0 & 0 & 0 & 0 & 0 & 0 & 0 & w_{17} & -w_{18} \end{pmatrix} \tag{4.24}$$

where

$$\begin{aligned} w_1 &= \alpha_1 + \mu_{ih} + \frac{\sigma_{ih} Z_1}{1 + \pi_{ih} I_h}, \quad w_2 = \frac{\beta_1 H}{1 + k_1 B}, \quad w_3 = \delta_1 + \mu_{th} + \frac{\sigma_{th} Z_1}{1 + \pi_{th} T_h}, \quad w_4 = \frac{r_1 \delta_1}{1 + c_1 Z_1}, \\ w_5 &= \frac{\beta_2 R}{1 + k_2 B} + \mu_m + \frac{\sigma_m Z_2}{1 + \pi_m M}, \quad w_6 = \frac{p r_2 \delta_2}{1 + c_2 Z_2}, \quad w_7 = \frac{\beta_2 R}{1 + k_2 B}, \quad w_8 = \alpha_2 + \mu_{ir} + \frac{\sigma_{ir} Z_2}{1 + \pi_{ir} I_r}, \\ w_9 &= \delta_2 + \mu_{tr} + \frac{\sigma_{tr} Z}{1 + \pi_{tr} T_r}, \quad w_{10} = \frac{(1-p) r_2 \delta_2}{1 + c_2 Z_2}, \quad w_{11} = q\omega + \mu_{gb} + \frac{\sigma_{gb} Z_2}{1 + \pi_{gb} G_b}, \quad w_{12} = \frac{\rho q \omega}{1 + k_3 B}, \\ w_{13} &= \alpha_3 + \mu_{gm}, \quad w_{14} = \delta_3 + \mu_c, \quad w_{15} = r_3 \delta_3, \quad w_{16} = a\nu + \mu_{sm}, \quad w_{17} = \frac{a b \nu}{S_m}, \\ w_{18} &= \frac{\beta_1 H}{1 + k_1 B} + \frac{\sigma_{sh} Z_1}{1 + \pi_{sh} S_h} + \mu_{sh} \end{aligned} \tag{4.25}$$

It can easily be observed from (4.21) that, all eigenvalues of A_1 are real and negative.
So, the system

$$\frac{dX_n}{dt} = A_1(x)(X_n - X_{E^{01},n}) + A_{12}(x) X_c$$

is globally assymptotically stable at E^{01}. It can be observed from (4.24) and (4.25) that all off diagonal elements of A_2 are non-negative. Therefore, A_2 is a Metzler matrix. To establish the global asymptotic stability of MFE, we have to show that A_2 is Metzler stable matrix (all its diagonal elements are negative) by proving the following lemma as described in Dumont *et al.* (2008) and Kamgang and Sallet (2008).

Lemma 4.2

Let M be a square Metzler matrix written in block form $M = \begin{pmatrix} M_{11} & M_{12} \\ M_{21} & M_{22} \end{pmatrix}$ with M_{11} and M_{22} square matrices. M is Metzler stable if and only if matrices M_{11} and $M_{22} - M_{21} M_{11}^{-1} M_{12}$ are Metzler stable.

From equation (4.24) we have $M = A_2$ and $M_{11} = \begin{pmatrix} -w_1 & 0 & 0 & 0 & 0 \\ \alpha_1 & -w_3 & 0 & 0 & 0 \\ 0 & w_4 & -w_5 & 0 & w_6 \\ 0 & 0 & w_7 & -w_8 & 0 \\ 0 & 0 & 0 & \alpha_2 & -w_9 \end{pmatrix}$

$M_{12} = \begin{pmatrix} 0 & 0 & 0 & 0 & w_2 \\ 0 & 0 & 0 & 0 & 0 \\ 0 & 0 & 0 & 0 & 0 \\ 0 & 0 & 0 & 0 & 0 \\ 0 & 0 & 0 & 0 & 0 \end{pmatrix}$, $M_{21} = \begin{pmatrix} 0 & 0 & 0 & 0 & w_2 \\ 0 & 0 & 0 & 0 & 0 \\ 0 & 0 & 0 & 0 & 0 \\ 0 & 0 & 0 & 0 & 0 \\ 0 & 0 & 0 & 0 & 0 \end{pmatrix}$

and $M_{22} = \begin{pmatrix} -w_{11} & 0 & 0 & 0 & 0 \\ w_{12} & -w_{13} & 0 & 0 & 0 \\ 0 & \alpha_3 & -w_{14} & 0 & 0 \\ 0 & 0 & w_{15} & -w_{16} & 0 \\ 0 & 0 & 0 & w_{17} & -w_{18} \end{pmatrix}$

Hence $M_{22} - M_{21}M_{11}^{-1}M_{12} = \begin{pmatrix} -w_{11} & 0 & 0 & 0 & \frac{\alpha_1\alpha_2 w_{10}w_7w_4w_2}{w_1w_3(w_5w_8w_9 - \alpha_2w_6w_7)} \\ w_{12} & -w_{13} & 0 & 0 & 0 \\ 0 & \alpha_3 & -w_{14} & 0 & 0 \\ 0 & 0 & w_{15} & -w_{16} & 0 \\ 0 & 0 & 0 & w_{17} & -w_{18} \end{pmatrix}$

Clearly, M_{11} is Metzler stable matrix. But, $M_{22} - M_{21}M_{11}^{-1}M_{12}$ is Metzler stable matrix only if

$$\frac{\alpha_1\alpha_2 w_{10}w_7w_4w_2}{w_1w_3(w_5w_8w_9 - \alpha_2w_6w_7)} \geq 0 \tag{4.26}$$

It is observed that equation (4.26) holds only when

$$\frac{\alpha_2 w_6 w_7}{w_5w_8w_9} < 1 \tag{4.27}$$

When the expressions for w_5, w_6, w_7, w_8 and w_9 given in equation (4.25) are evaluated at MFE, obtain the following expressions

$$\begin{aligned} w_5 &= \frac{\beta_2\Lambda_r}{\mu_r} + \mu_m + \frac{\sigma_m\Lambda_z}{\mu_z}, \quad w_6 = \frac{pr_2\delta_2\mu_z}{\mu_z + c_2\Lambda_z}, \quad w_7 = \frac{\beta_2\Lambda_r}{\mu_r}, \\ w_8 &= \alpha_2 + \mu_{ir} + \frac{\sigma_{ir}\Lambda_z}{\mu_z}, \quad w_9 = \delta_2 + \mu_{tr} + \frac{\sigma_{tr}\Lambda_z}{\mu_z} \end{aligned} \tag{4.28}$$

Now substituting equation (4.28) in equation (4.27), we obtain

$$\frac{\frac{\beta_2\Lambda_r}{\mu_r}(v_2\frac{pr_2\delta_2\mu_z}{\mu_z+v_2\Lambda_z}}{\left(\frac{\beta_2\Lambda_r}{\mu_r}+\mu_m+\frac{\sigma_m\Lambda_z}{\mu_z}\right)\left(v_2+\mu_{ir}+\frac{\sigma_{ir}\Lambda_z}{\mu_z}\right)\left(\delta_2+\mu_{tr}+\frac{\sigma_{tr}\Lambda_z}{\mu_z}\right)}<1 \tag{4.29}$$

equivalently

$$\mathcal{R}_{01}<1 \tag{4.30}$$

which leads us to the following theorem.

Theorem 4.6

A MFE, E^{01} of the model (4.1a)-(4.1o) is globally assymptotically stable in $\mathcal{D}$ if $\mathcal{R}_{01}<1$ and unstable if $\mathcal{R}_{01}>1$.

4.3.5 Existence and Stability of Malaria Infection Equilibrium

If $\mathcal{R}_{01}>1$, then Theorem 4.6 suggests the existence of malaria-infection equilibrium (MIE), which is given by

$$E^*=(H^*,I_h^*,T_h^*,M^*,R^*,I_r^*,T_r^*,G_b^*,G_m^*,C^*,S_m^*,S_h^*,Z_1^*,Z_2^*,B^*)$$

Due to the complexity of the model system (4.1a)-(4.1o), it is found awkward to express MIE explicitly. Therefore, the existence and stability are established numerically in the next section.

4.4 Numerical Simulations and Discussions

In this section, we perform numerical simulations of the model (4.1a)-(4.1o), to illustrate the dynamics of model using MATLAB symbolic package. In the simulation of this model, initial values are assummed to allow computer executions, and their values are as listed in Table 8.

Table 8 :Initial values of variables of the model (4.1a)-(4.1o)

Variable	H	I_h	T_h	M	R	I_r	T_r	G_b	G_m	C	S_m	S_h	Z_1	Z_2	B
Initial values	3 000	0	0	2 000	500 000	0	1 000	3 000	1 500	1 000	2 000	2 000	10	10	0

Estimation of parameter values of in vivo models is challenging work (Chiyaka *et al.*, 2008). The numerical values of parameters used for simulation of our model are listed in Table 9. These values are either assumed or taken from some related studies among existing literature.

The reason as to why some parameters values are assumed is that, mathematical modelling on liver and/or mosquito stage dynamics of malaria infection have not yet been done or the values found on existing literatures are not suitable for this model. However, our main concern is

not on accuracy of these parameter values, rather is on the effect of these parameters on basic reproduction number, which alerts on how and where to target to eradicate or control the disease (Chiyaka *et al.*, 2008).

Table 9 : Parameters estimates of the model 4.1a-4.1o

Par	Description	Value	References
a :	probability that a bite infects human	0.75	(Tumwiine *et al.*, 2007 b)
b :	number of mosquito bites per individual	$15d^{-1}$	(Selemani *et al.*, 2016)
ν :	number of sporozoites injected per bite	$10-20$	(Nelson and Williams, 2014)
β_1 :	infection rate of HLCs by sporozoites	$0.001\ \mu lc^{-1}d^{-1}$	(Selemani *et al.*, 2016)
r_1 :	number of merozoites per liver schizont	10 000	(Tumwiine *et al.*, 2014)
α_1 :	progression rate of infected HCLs		
	to schizonts	$0.125\ d^{-1}$	(Selemani *et al.*, 2016)
δ_1 :	rupture rate of liver schizonts	$0.0975\ d^{-1}$	(Selemani *et al.*, 2016)
Λ_h :	the recruitmet rate of HLCs	$3\ 000\ c\mu l^{-1}d^{-1}$	(Selemani *et al.*, 2016)
μ_h :	natural death rate of uninfected HLCs	$0.94\ d^{-1}$	(Selemani *et al.*, 2016)
μ_{ih} :	death rate of infected HLCs	$0.95\ d^{-1}$	(Selemani *et al.*, 2016)
μ_{th} :	death rate of liver-schizonts	$0.029\ d^{-1}$	(Selemani *et al.*, 2016)
β_2 :	infection rate of RBCs by merozoites	$2\times10^{-6}\ \mu lc^{-1}d^{-1}$	(Selemani *et al.*, 2016)
δ_2 :	rupture rate of blood schizonts	$0.115\ d^{-1}$	(Selemani *et al.*, 2016)
α_2 :	progression rate of infected RBCs		
	to schizonts	$0.145\ d^{-1}$	(Selemani *et al.*, 2016)
r_2 :	number of merozoites per blood schizont	16	(Dube *et al.*, 2010)
q :	probability that a bite is infectious		
	to mosquito	0.09	(Agusto *et al.*, 2012)
ω :	number of gametocytes ingested per bite	10	(Selemani *et al.*, 2016)
ρ :	number of bites made by mosquito		
	in its lifetime	3	(Selemani *et al.*, 2016)
Λ_r :	the recruitmet rate of RBCs	$41\ 500\ c\mu l^{-1}d^{-1}$	(Li *et al.*, 2011)
μ_r :	death rate of uninfected RBCs	$0.02\ d^{-1}$	(Dube *et al.*, 2010)
μ_{ir} :	total death rate of uninfected RBCs	$0.025\ d^{-1}$	(Diebner *et al.*, 2000)
μ_{tr} :	death rate of blood-schizonts	0.185	(Selemani *et al.*, 2016)
μ_m :	death rate of merozoites	$48\ d^{-1}$	(Li *et al.*, 2011)
μ_{gb} :	death rate of gametocytes	$6.25\times10^{-5}d^{-1}$	(Selemani *et al.*, 2016)
δ_3 :	rupture rate of Oocysts	$0.05\ d^{-1}$	(Selemani *et al.*, 2016)
r_3 :	number of sporozoites per Oocyst	1 000	(Nelson and Williams, 2014)
α_3 :	progresion rate of gametes to Oocysts	$0.07\ d^{-1}$	(Selemani *et al.*, 2016)
μ_{gm} :	death rate of gametes	$0.052\ d^{-1}$	(Selemani *et al.*, 2016)
μ_c :	death rate of Oocysts	$0.024\ d^{-1}$	(Selemani *et al.*, 2016)
μ_{sm} :	death rate of sporozoites in mosqouito	$40\ d^{-1}$	(Selemani *et al.*, 2016)
μ_{sh} :	death rate of sporozoites in human liver	$1.2\times10^{-11}\ d^{-1}$	(Selemani *et al.*, 2016)
p :	proportion of asexual that differentiate		
	to merozoites	0.926	(Selemani *et al.*, 2016)
Λ_{z_1} :	the recruitmet rate of immune cells in the liver	$30\ c\mu l^{-1}d^{-1}$	Estimated

Continued on next page

not on accuracy of these parameter values, rather is on the effect of these parameters on basic reproduction number, which alerts on how and where to target to eradicate or control the disease (Chiyaka *et al.*, 2008).

Table 9 : Parameters estimates of the model 4.1a-4.1o

Par	Description	Value	References
a :	probability that a bite infects human	0.75	(Tumwiine *et al.*, 2007 b)
b :	number of mosquito bites per individual	$15d^{-1}$	(Selemani *et al.*, 2016)
ν :	number of sporozoites injected per bite	10 – 20	(Nelson and Williams, 2014)
β_1 :	infection rate of HLCs by sporozoites	0.001 $\mu lc^{-1}d^{-1}$	(Selemani *et al.*, 2016)
r_1 :	number of merozoites per liver schizont	10 000	(Tumwiine *et al.*, 2014)
α_1 :	progression rate of infected HCLs to schizonts	0.125 d^{-1}	(Selemani *et al.*, 2016)
δ_1 :	rupture rate of liver schizonts	0.0975 d^{-1}	(Selemani *et al.*, 2016)
Λ_h :	the recruitmet rate of HLCs	3 000 $c\mu l^{-1}d^{-1}$	(Selemani *et al.*, 2016)
μ_h :	natural death rate of uninfected HLCs	0.94 d^{-1}	(Selemani *et al.*, 2016)
μ_{ih} :	death rate of infected HLCs	0.95 d^{-1}	(Selemani *et al.*, 2016)
μ_{th} :	death rate of liver-schizonts	0.029 d^{-1}	(Selemani *et al.*, 2016)
β_2 :	infection rate of RBCs by merozoites	2×10^{-6} $\mu lc^{-1}d^{-1}$	(Selemani *et al.*, 2016)
δ_2 :	rupture rate of blood schizonts	0.115 d^{-1}	(Selemani *et al.*, 2016)
α_2 :	progression rate of infected RBCs to schizonts	0.145 d^{-1}	(Selemani *et al.*, 2016)
r_2 :	number of merozoites per blood schizont	16	(Dube *et al.*, 2010)
q :	probability that a bite is infectious to mosquito	0.09	(Agusto *et al.*, 2012)
ω :	number of gametocytes ingested per bite	10	(Selemani *et al.*, 2016)
ρ :	number of bites made by mosquito in its lifetime	3	(Selemani *et al.*, 2016)
Λ_r :	the recruitmet rate of RBCs	41 500 $c\mu l^{-1}d^{-1}$	(Li *et al.*, 2011)
μ_r :	death rate of uninfected RBCs	0.02 d^{-1}	(Dube *et al.*, 2010)
μ_{ir} :	total death rate of uninfected RBCs	0.025 d^{-1}	(Diebner *et al.*, 2000)
μ_{tr} :	death rate of blood-schizonts	0.185	(Selemani *et al.*, 2016)
μ_m :	death rate of merozoites	48 d^{-1}	(Li *et al.*, 2011)
μ_{gb} :	death rate of gametocytes	$6.25 \times 10^{-5}d^{-1}$	(Selemani *et al.*, 2016)
δ_3 :	rupture rate of Oocysts	0.05 d^{-1}	(Selemani *et al.*, 2016)
r_3 :	number of sporozoites per Oocyst	1 000	(Nelson and Williams, 2014)
α_3 :	progresion rate of gametes to Oocysts	0.07 d^{-1}	(Selemani *et al.*, 2016)
μ_{gm} :	death rate of gametes	0.052 d^{-1}	(Selemani *et al.*, 2016)
μ_c :	death rate of Oocysts	0.024 d^{-1}	(Selemani *et al.*, 2016)
μ_{sm} :	death rate of sporozoites in mosqouito	40 d^{-1}	(Selemani *et al.*, 2016)
μ_{sh} :	death rate of sporozoites in human liver	1.2×10^{-11} d^{-1}	(Selemani *et al.*, 2016)
p :	proportion of asexual that differentiate to merozoites	0.926	(Selemani *et al.*, 2016)
Λ_{z_1} :	the recruitmet rate of immune cells in the liver	30 $c\mu l^{-1}d^{-1}$	Estimated

Continued on next page

Table 9 – *Continued from previous page*

Par	Description	Value	References
Λ_{z_2} :	the recruitmet rate of immune cells in the blood	30 $c\mu l^{-1}d^{-1}$	(Chiyaka *et al.*, 2008)
μ_{z_1} :	death rate of immune cells	1.5	Estimated
μ_{z_2} :	death rate of immune cells	1.53	(Chiyaka *et al.*, 2008)
μ_h :	deterioration rate of antibodies	0.4	(Chiyaka *et al.*, 2008)
c_1 :	efficiency of immune cells to suppress the production of M from liver-schizonts	10^{-5}	Estimated
c_2 :	efficiency of immune cells to suppress the production of M from blood-schizonts	3×10^{-5}	Estimated
k_1 :	efficiency of immune cells to inhibit invasion of HLCs by sporozoites	0.035	Estimated
k_2 :	efficiency of immune cells to inhibit invasion of RBCs by merozoites	0.0015	Estimated
k_3 :	efficiency of immune cells to mediate lysis of gametocytes and inhibit fertilization	0.03	Estimated
σ_{sh} :	rate at which sporozoites are cleared by immune cells	9×10^{-9}	Estimated
σ_{ih} :	rate at which infected HLCs are cleared by immune cells	9×10^{-9}	Estimated
σ_{th} :	rate at which liver schizonts are cleared by immune cells	1×10^{-8}	Estimated
σ_m :	rate at which merozoites are cleared by immune cells	1×10^{-8}	(Li *et al.*, 2011)
σ_{ir} :	rate at which infected RBCs are cleared by immune cells	1×10^{-8}	(Li *et al.*, 2011)
σ_{tr} :	rate at which blood schizonts are cleared by immune cells	1×10^{-8}	Estimated
σ_{gh} :	rate at which gametocytes are cleared by immune cells	1×10^{-8}	(Austin *et al.*, 1998)
ϵ_{sh} :	proliferation rate of immune cells due to contact with sporozoites	5×10^{-5}	Estimated
ϵ_{ih} :	proliferation rate of immune cells due to contact with infected HLCs	4.6×10^{-5}	Estimated
ϵ_{th} :	proliferation rate of immune cells due to contact with liver schizonts	4.63×10^{-5}	Estimated
ϵ_m :	proliferation rate of immune cells due to contact with merozoites	4.69×10^{-5}	(Li *et al.*, 2011)
ϵ_{ir} :	proliferation rate of immune cells due to contact with infected RBCs	2.5×10^{-5}	(Li *et al.*, 2011)
ϵ_{tr} :	proliferation rate of immune cells due to contact with blood schizonts	2.5×10^{-5}	Estimated
ϵ_{gh} :	proliferation rate of immune cells due to contact with gametocytes	2.5×10^{-5}	Estimated

Continued on next page

Table 9 – *Continued from previous page*

Par	Description	Value	References
π_{sh} :	$1/\pi_{sh}$ saturation constant of sporozoites	5×10^{-4}	Estimated
π_{ih} :	$1/\pi_{ih}$ saturation constant of infected HLCs	5×10^{-4}	Estimated
π_{th} :	$1/\pi_{th}$ saturation constant of liver schizonts	5×10^{-4}	Estimated
π_m :	$1/\pi_m$ saturation constant of merozoites	7×10^{-4}	(Li *et al.*, 2011)
π_{ir} :	$1/\pi_{ir}$ saturation constant of infected RBCs	5×10^{-4}	(Li *et al.*, 2011)
π_{tr} :	$1/\pi_{tr}$ saturation constant of blood schizonts	5×10^{-4}	Estimated
η_1 :	maximum rate of increase of antibodies due to presence of sporozoites	1×10^{-4}	Estimated
η_2 :	maximum rate of increase of antibodies due to presence of merozoites	4×10^{-4}	Estimated

We performed numerical simulations to establish the existence of malaria infection equilibrium (MIE) as stated earlier. Fig. 14a , Fig. 14b, Fig. 14c and Fig. 14d indicate that each variable varies with time and reaches a constant value (i.e., a value at MIE). In Fig. 14a we show how number of injected sporozoites, healthy liver hepatic cells, parasitized hepatic liver cells and schizont vary with time. Fig. 14b shows the variations of uninfected RBCs, infected RBCs, merozoites, blood-schizonts and gametocytes. Fig. 14c illustrates the time variation of variables in sporogonic cycle while Fig. 14d indicates the variation of immune responses with time. Therefore, Fig. 14 depicts the existence of malaria-infection equilibrium, E^* for the model (4.1a) -(4.1o).

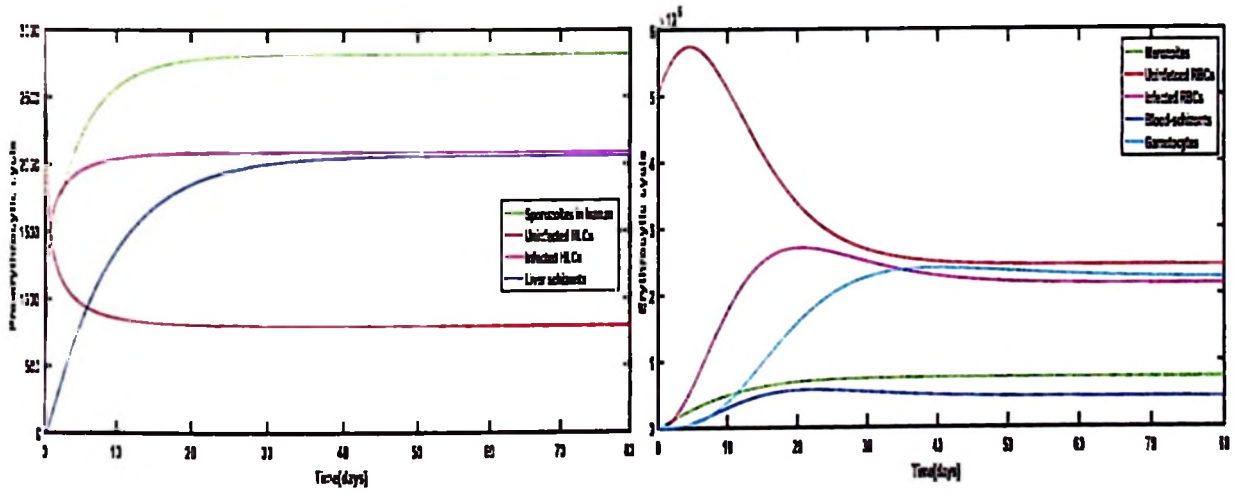

(a) Exo-erythrocytic cycle

(b) Erythrocytic cycle

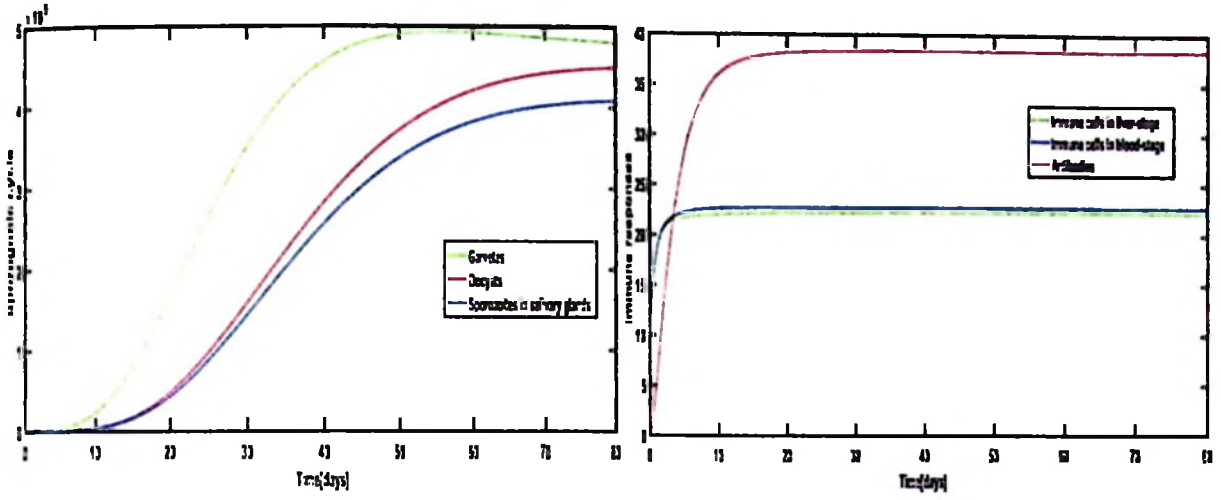

(c) Sporogonic cycle (d) immune responses

Figure 14: Time variation of variables at exo-erythrocytic, erythrocytic, sporogonic cycles and immune responses with time to verify the existence of MIE

Now, let us assess for stability of E^*. Fig. 15 depicts that with different initial values, each model variable converges to certain value (value at MIE).

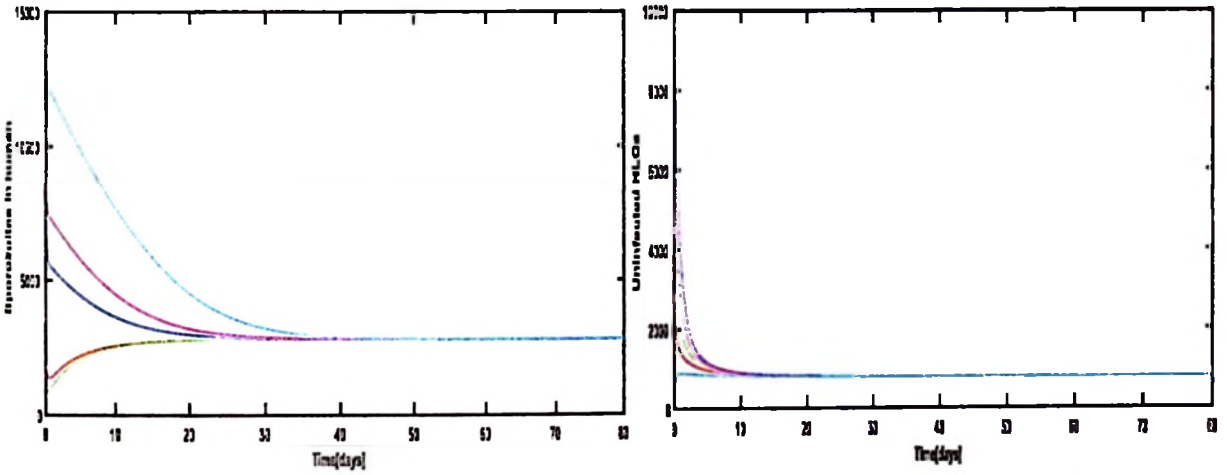

(a) $S_h^0 = 1\,000, 2\,000, 8\,000, 10\,000, 15\,000$ (b) $H^0 = 500, 3\,000, 5\,000, 7\,500, 10\,000$

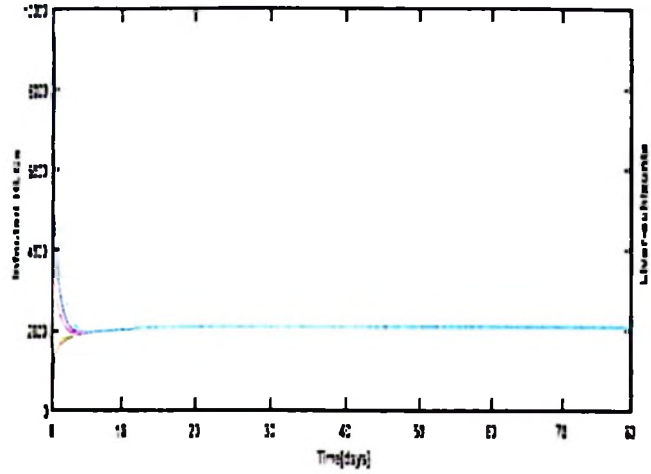

(c) $I_h^0 = 0, 500, 3\,000, 5\,000, 10\,000$

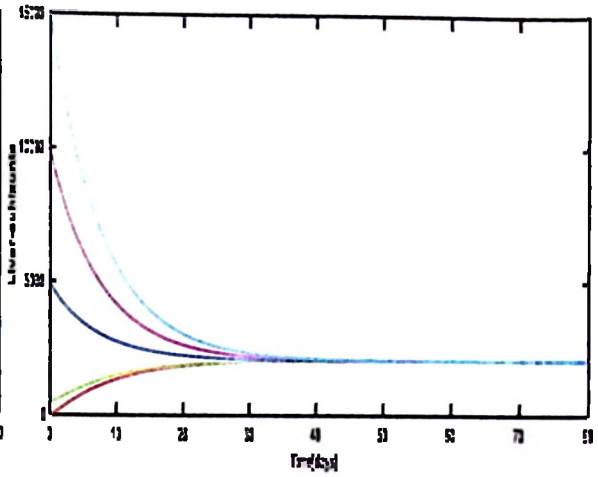

(d) $T_h^0 = 0, 500, 5\,000, 10\,000, 15\,000$

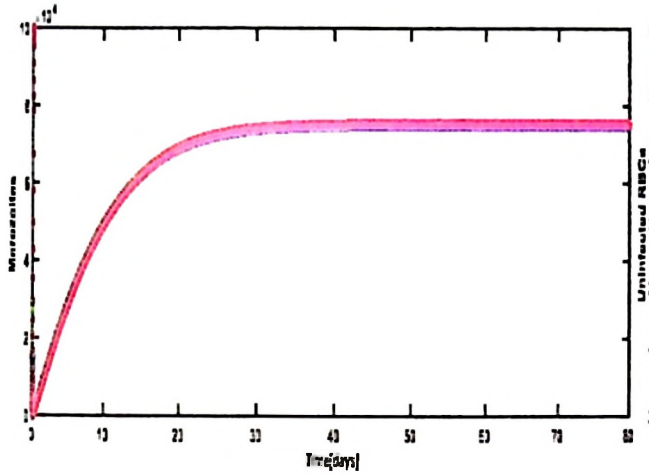

(e) $M^0 = 0, 2\,000, 15\,000, 30\,000, 100\,000$

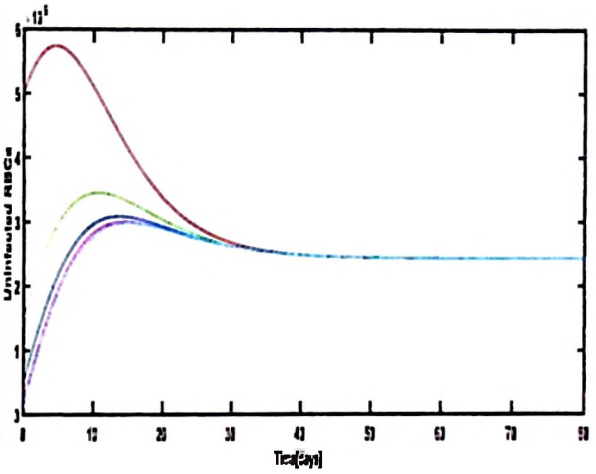

(f) $R^0 = 10\,000, 20\,000, 50\,000, 150\,000, 500\,000$

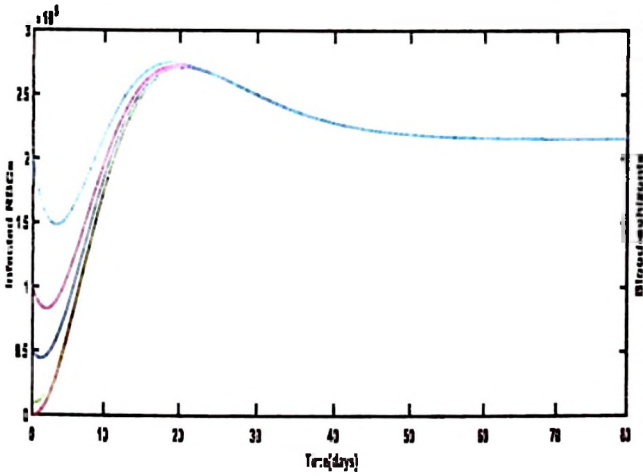

(g) $I_r^0 = 0, 10\,000, 50\,000, 100\,000, 200\,000$

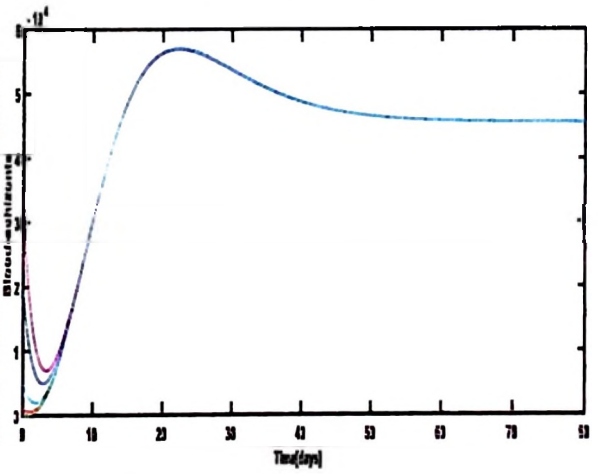

(h) $T_r^0 = 0, 1\,000, 5\,000, 20\,000, 35\,000$

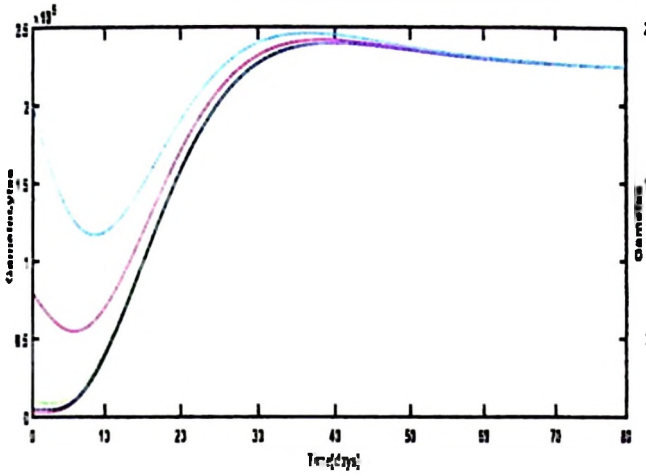

(i) $G_h^0 = 3\,000, 5\,000, 10\,000, 80\,000, 200\,000$

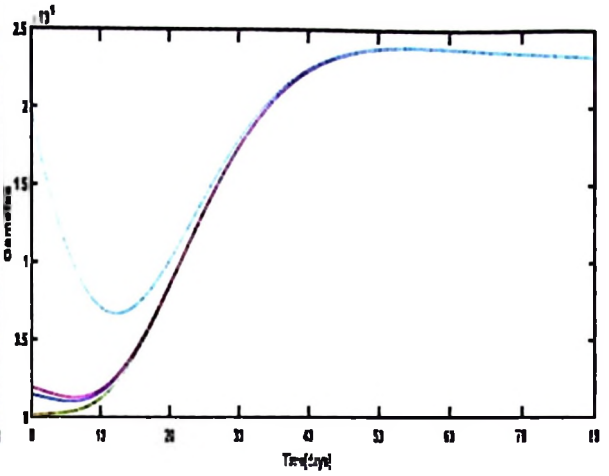

(j) $G_{TH}^0 = 500, 1\,500, 3\,000, 15\,000, 20\,000$

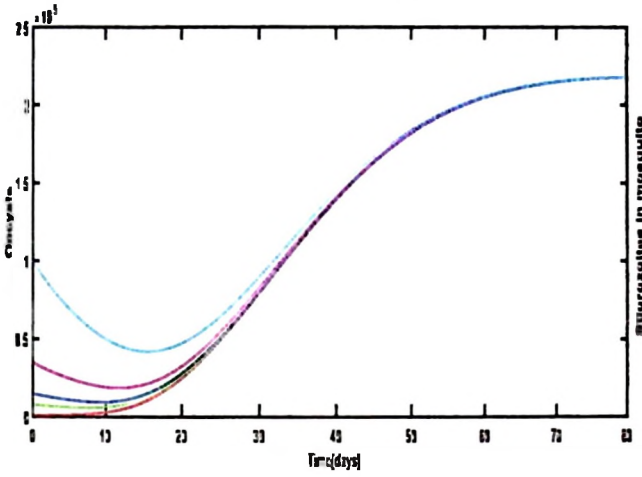

(k) $C^0 = 1\,000, 8\,000, 15\,000, 35\,000, 100\,000$

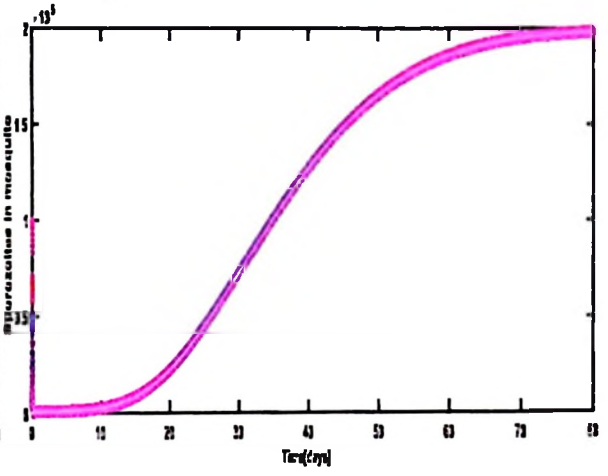

(l) $S_{TH}^0 = 2\,000, 15\,000, 50\,000, 7\,000, 100\,000$

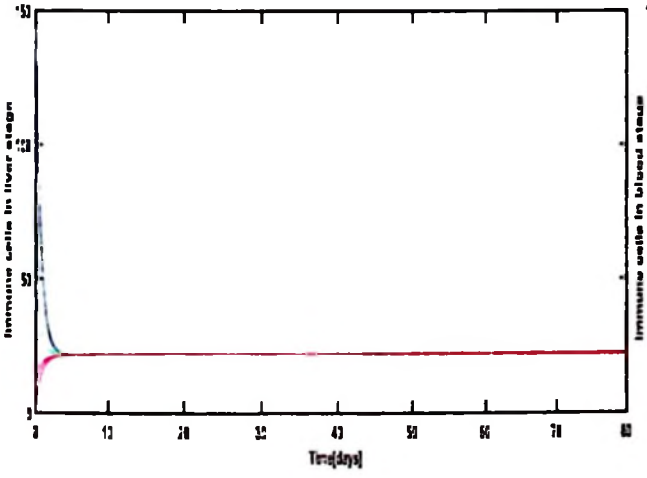

(m) $Z_1^0 = 0, 10, 50, 80, 150$

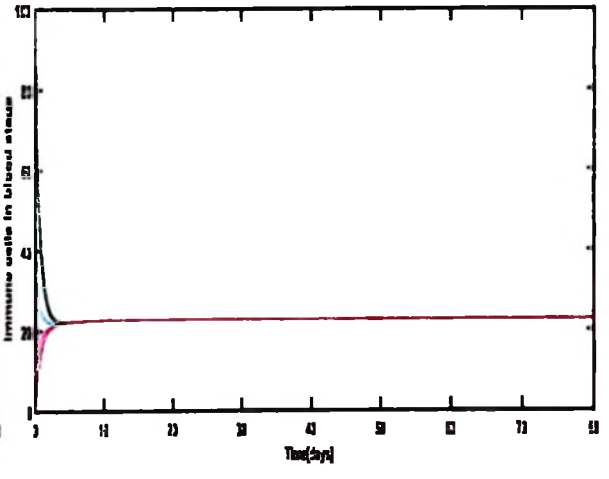

(n) $Z_2^0 = 0, 10, 35, 80, 100$

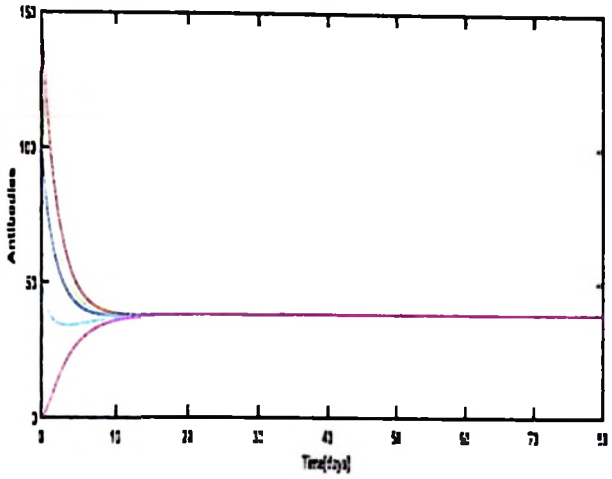

(o) $B^0 = 0, 50, 100, 120, 150$

Figure 15: Numerical simulation to show global stability of MIE for model (4.1a)-(4.1o)

Therefore, with reference to Fig. 15, we suspect that, malaria infection equilibrium, E^*, is globally asymptotically stable.

Moreover, this model indicates promising results on the control of malaria infection at the erythrocytic stages. From Fig. 16 it is observed that inclusion of immune responses in the model has impact on increasing the number of uRBCs and reducing the number of iRBCs, merozoites and gametocytes. The minimum number of uRBCs to basic model (nonimmune) is below 2×10^{-5} cells per microlitre, while in this model where effects of immune responses are included, the minimal number of uRBCs is found to be above 2×10^{-5} cells per microlitre as indicated in Fig. 16a. On the other hand, maximal number of iRBCs in a nonimmune model and in a model with immune effect are approximately to 3.4×10^{-5} and 2.7×10^{-5} cells per microlitre respectively as illustrated in Fig. 16b. In addition to that, there is noticable decrease in number of merozoites and gametocytes (See Fig. 16c and Fig. 16d respectively).

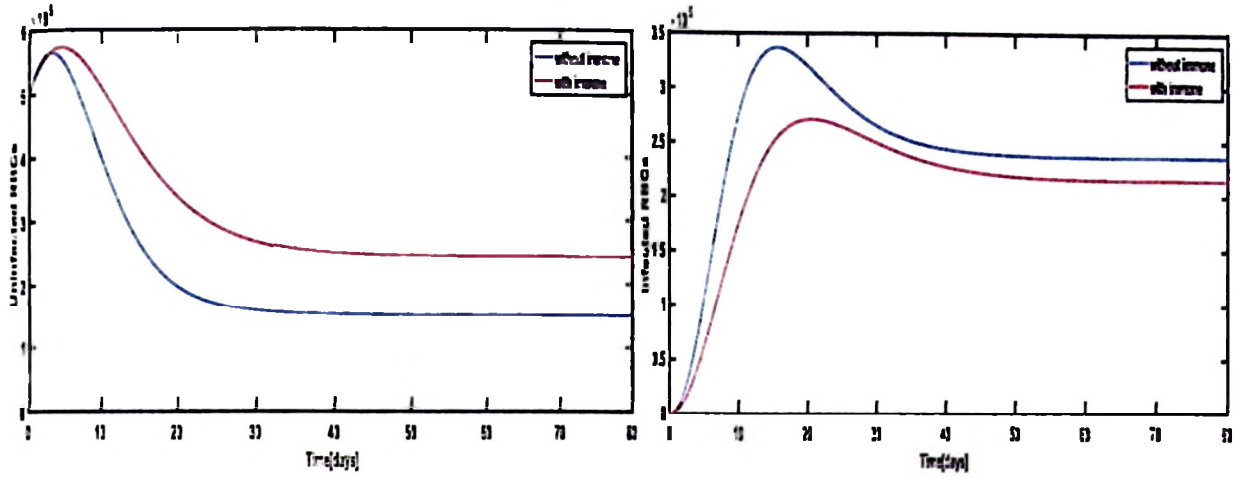

(a) Uninfected RBCs

(b) Infected RBCs

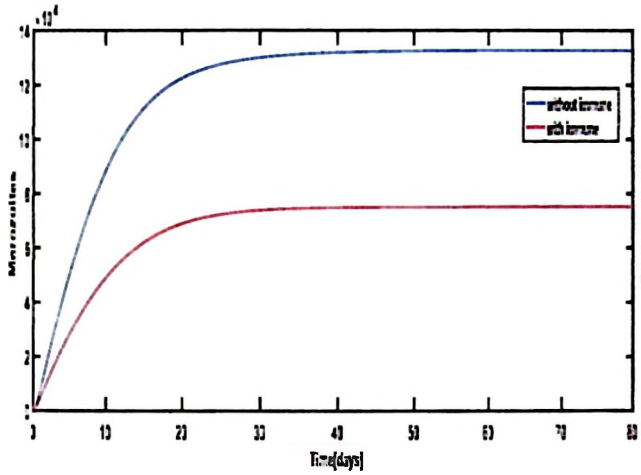

(c) Merozoites

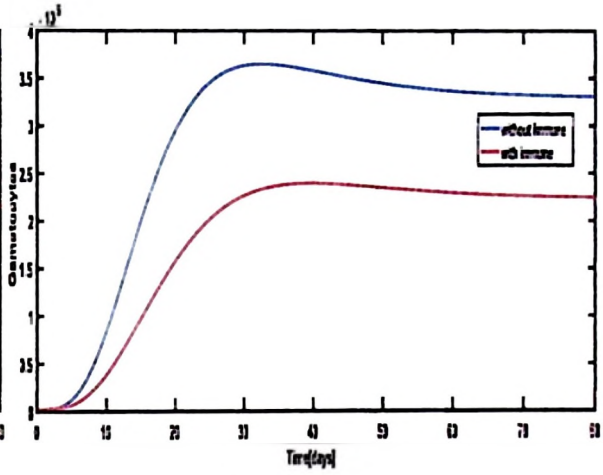

(d) Gametocytes

Figure 16: Effects of immune responses on uRBCs, iRBCs, merozoites and gametocytes

However, the immune responses are shown to have little or almost no effect on attacking liver stage malaria infection. This is because there is unnoticable change in number of uHLCs and iHLCs even after immune system being included the model as indicated in Fig. 17. It can be observed that despite of the big change in value of k_1 (efficiency of antibodies to block invasion of hepatocytes by sporozoites) from $0.075/day$ to $0.9/day$, but still the change on number of uHLCs and iHLCs is almost negligible. The case is the same to sporozoites injected and hepatic schizonts. These results suggest that at the liver stage is not a good target for intervetion using immune responses.

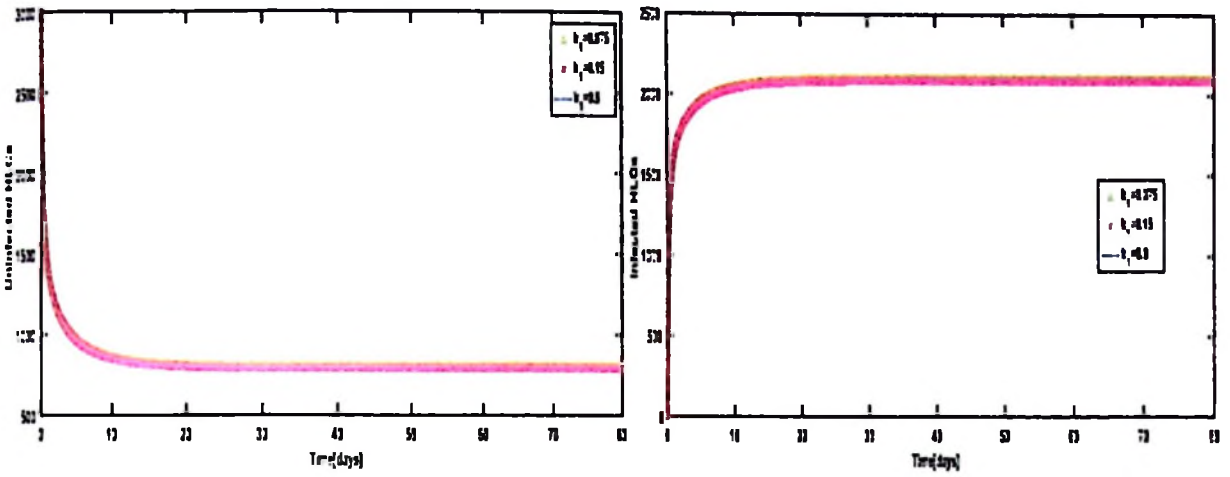

(a) Unifected HLCs (b) Infected HLCs

Figure 17: Graphs of liver-stage dynamics showing effect of immune responses

This finding supports the Langhorne *et al.* (2008)'s argument that the effect of antibodies to sporozoites is thought to be insignificant. However, it contradicts the argument of Prudêncio *et al.* (2011) that the exo-erythrocytic stage has greatest potential for intervention.

Furthermore, the immune responses has shown positive results on the sporogonic stages of malaria parasites as shown in Fig. 18. This implies that, the antibodies taken up by mosquito during the blood meal results on lysis of gametocytes and prevent the development of parasites within mosquito. Consequently, it can lead us to a population of non-infectious mosquitoes, and reduce further mosquito-human malaria transmission.

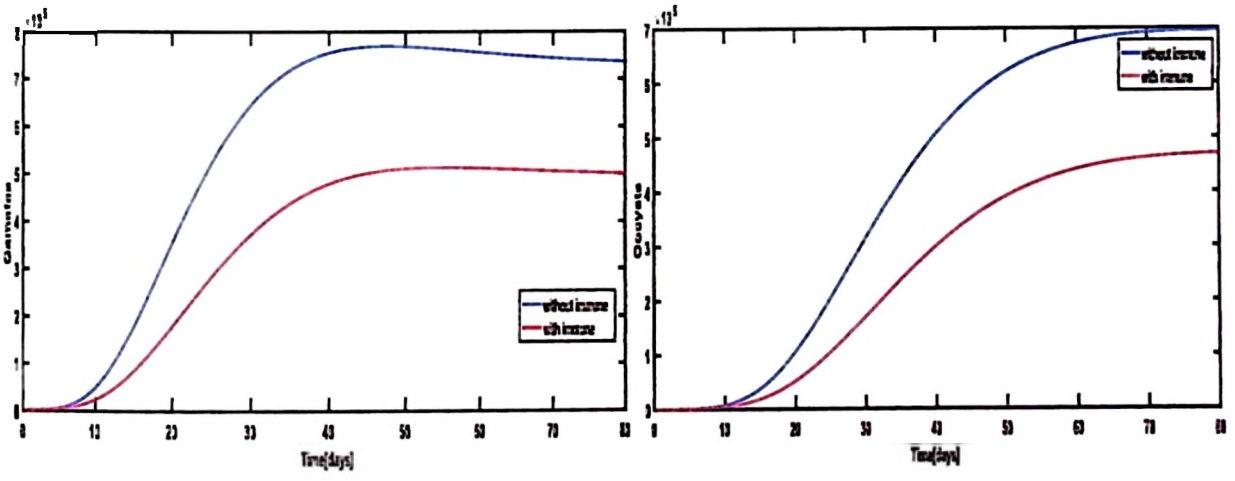

(a) Gametes (b) Oocysts

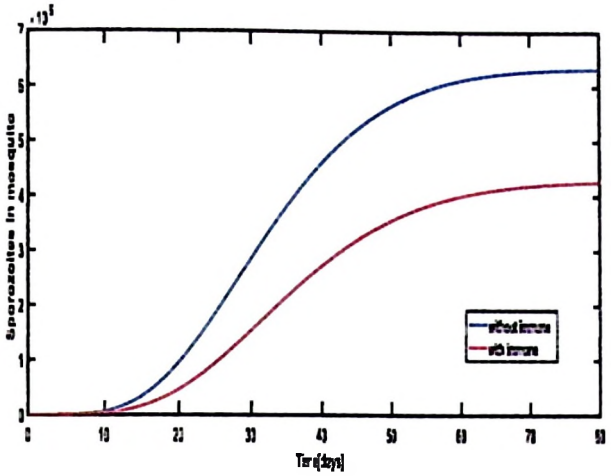

(c) Sporozoites in mosquito

Figure 18: Effects of antibodies taken up by mosquito during the blood meal on gametes, oocysts and sporozoites

Since the immune responses are mostly stimulated by infection and in most cases they last within a short period of time, we have assessed the impact of lifespan of immune cells on the elimination (reduction) of malaria infection. The results show that the lifespan varies inversely with number of infected RBCs, merozoites and gametocytes as depicted in Fig. 19b, 19c and 19d respectively. On the other hand, from Fig. 19a we observed that the lifespan of immune cells has great influence on the number of uninfected RBCs. It shows that the number of uRBCs increases with immune cells' lifespan. Hence, using Fig. 19 we argue that introducing a long-term immunity may significantly reduce the infection.

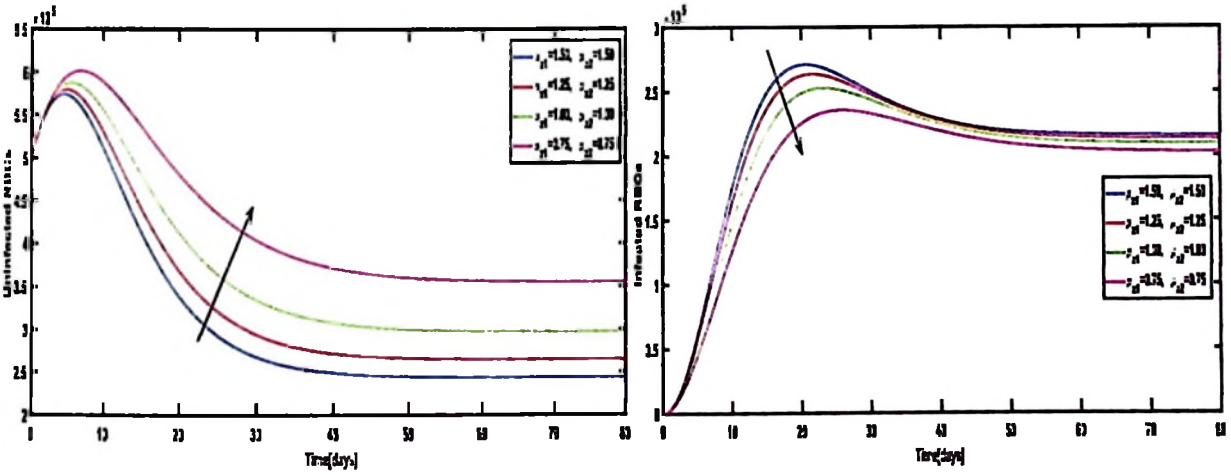

(a) Uninfected RBCs

(b) Infected RBCs

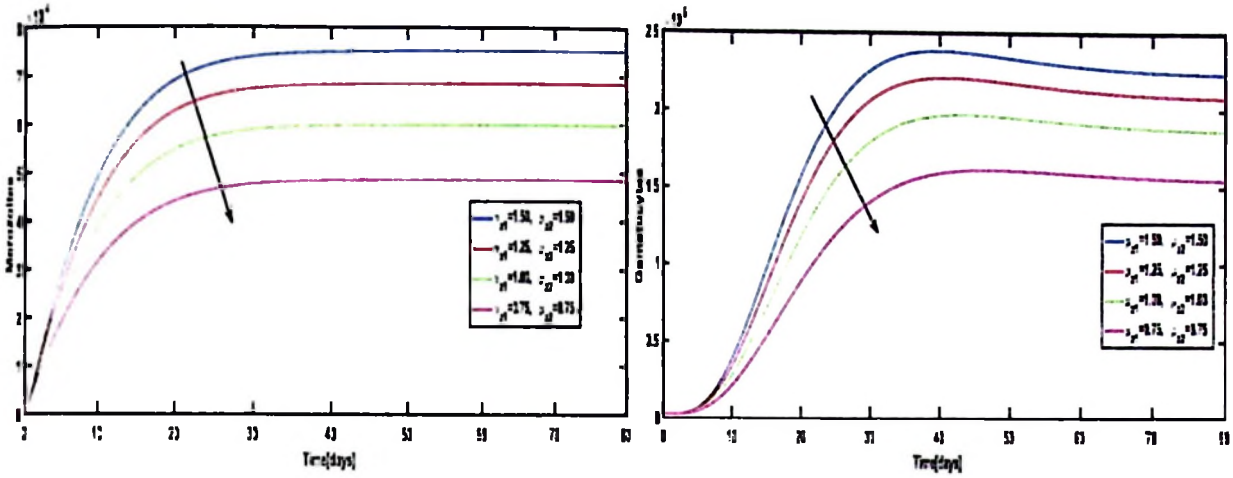

(c) Merozoites (d) Gametocytes

Figure 19: Effects of life span of immune responses on uRBCs, iRBCs, merozoites and gametocytes. Arrows are in direction of increasing life span ($1/\mu_{z_2}$) of immune responses against blood stage infection

With reference to basic reproduction number, $\mathcal{R}_0$; as expressed in equation (4.13) it is noted that $\mathcal{R}_0$ can be made less than or equal to unity by: decreasing the infection rate, β_2 of uRBCs by merozoites; increasing death rates of iRBCs, blood-schizonts and merozoites; increasing the rates at which iRBCs, blood-schizonts and merozoites are cleared by immune cells; and increasing the rate at which immune cells suppress the production of merozoites from blood-schizonts. Therefore, any biological means that can be implemented to facilitate these may have impact on development of control strategies.

4.5 Conclusion

In this work, we have formulated and analyzed a mathematical model for the in-human host and in-human dynamics of malaria parasite with effect of immune responses. In this model, we included the effect of immune responses to block invasion of sporozoites and merozoites on hepatic liver cells and red blood cells respectively. The effect of immune responses to inhibit the production of merozoites from both liver and blood cells was included. Additionally, the model includes terms for influence of immune responses on clearance of both parasites and infected cells. Finally, we include the term for antibodies on gametocytes picked-up during the blood meal. In all cases immune response are described using the nonlinear-bounded Michaelis-Menten-Monod function.

A positive invariant region, where the model is epidemiologically (variables biological interpretation meaningful) and mathematically (always a bounded solution exists) well-posed was

established. Using the next generation method, basic reproduction number $\mathcal{R}_{01}$, of the model was computed. Also, existence and stability of two non-negative equilibrium points: malaria free equilibrium (MFE) and malaria infection equlibrium (MIE) were established. Furthermore, we proved that MFE is locally asymptotically stable if $\mathcal{R}_{01} < 1$ and globally asymptotically stable (GAS) if $\mathcal{R}_{01} \leq 1$.

In addition, we noted that the impact of immune cells in suppressing the production of merozoites is higher than that of antibodies to block invasion of sporozoites and merozoites into liver and blood cells respectively. This is because none of $k's$, efficiency of antibodies to inhibit invasion appeared into the expression of $\mathcal{R}_{01}$, while one of the $c's$ (c_2), efficiency of immune cells to suppress production of merozoites does appear.

Numerical simulations guarantee the existence of MIE, which is GAS irrespective of the initial values do state variables have. Moreover, in comparison with the results of Selemani *et al.* (2016) presented in Chapter 3, our results revealed that including immunity has significant influence on lowering infection at blood and mosquito stages only. An increase on number of uninfected cells, and a decrease on number of infected cells and free parasite were noted. Also, antibodies picked-up by mosquito seems to have an effect on reducing the number of parasites within mosquito.

However, an insignificant effect of immunity on both cells (uninfected and infected) and parasites at liver stage infection was observed. This reveals that it is difficult to control liver infection with immune system. Furthermore, this model depicts that longevity of immunity reduces number of parasites and infected cells in erythrocytic infection. Meaning that, as lifespan of immune cells increases the infection decreases.

Based on the results, this study proposes that the immune system should be boosted so as to improve their ability to suppress parasite's production in bloodstream. Also, causing lysis to gametocytes is of great importance in preventing parasite' development in mosquito as it may lead us to a population of non-infectious mosquito. Hence, reduce mosquito-human infection.

Our work serves an example on how mathematical models can be used to get insight of complex systems like malaria life cycle. In next chapter, we extend this model by incorporating the effect of anti-malaria drugs.

CHAPTER FIVE

Modelling the in-human host and in-mosquito Dynamics of Malaria Parasite with Effect of Immune Response and Antimalarial Therapy [4]

Abstract

One advantage of combination therapies (CTs) is to reduce the development of drug resistance, as pathogens may not be resistant to multiple drugs simultaneously. Therapeutic classification of antimalarial drugs depends on the stage in parasite's life cycle they target. In this chapter, a mathematical model for the in-human host and in-mosquito dynamics of malaria parasite with the effect of immune responses and drug therapy is proposed and analyzed, in which four therapeutic classes of antimalarial drugs are incorporated. We establish the conditions for existence and stability of two equilibria: malaria free equilibrium and malaria infection equilibrium. Although its components do not appear in the expression of reproduction number, tissue schizonticides manifest a remarkable effect on reducing the infection at each stage of malaria life cycle, while sporontocides ingested by a mosquito during its blood meal shows an effect on reducing the number of parasites within the mosquito. An artemisinin derivatives-primaquine combination therapy is proposed, as it contains components of all four classes of antimalarial drugs.

5.1 Introduction

Despite numerous efforts taken worldwide to combat malaria, it is estimated that 3.2 billion people are still at risk of malaria and approximately 80% of deaths associated with malaria occur in Africa (WHO, 2015). Malaria is caused by *Plasmodium* parasite through a bite by an infected female Anopheles mosquito. More than a hundred species of *Plasmodium* parasites can infect vertebrate hosts, however, only four of them: *Plasmodium falciparum*, *Plasmodium vivax*, *Plasmodium ovale* and *Plasmodium malariae* can infect human (U. S. National Institute of Allergy and Infectious Diseases, 2007). All of these species develop through the same complex and multistage life cyle as illustrated in Fig. 20. Moreover, *P.falciparum* and *P. vivax* are the most common, and *P.falciparum* is the most dangerous species (Cravo *et al.*, 2001; Tumwiine *et al.*, 2007a; Li *et al.*, 2011).

[4]This chapter is based on the research paper: Mohamed A. Selemani, Livingstone S. Luboobi, Yaw Nkansah-Gyekye. Modelling the in-human host and in-mosquito Dynamics of Malaria Parasite with Effect of Immune Response and Antimalarial Therapy. *Mathematical Biosciences*(In Review)

During its blood meal, an infected female mosquito injects sporozoites into bloodstream that quickly travel to the liver and initiate an *exo-erythrocytic* stage of parasite's life cycle by attacking hepatocytes. Within hepatocytes, parasites replicate asexually and develop into schizonts which eventually rupture and release merozoites into bloodstream marking the beginning of *erythrocytic* stage. Merozoites attack red blood cells (RBCs) and asexually replicate within. Then, they develop into erythrocytic schizonts and burst to release a new generation of merozoites that initiate infection to other RBCs. For still unknown reasons, some of the merozoites (about 1%) switch into sexual form of parasites called gametocytes (Kiszewski, 2010; Delves *et al.*, 2012), which are responsible for human-mosquito transmission. A *sporogonic* stage of parasite's life cycle begins when a parasite-free mosquito ingests the mature gametocytes, which are sexually dimorphic (microgametocytes and macrogametocytes) during its blood-meal. Ingested gametocytes generate male and female gametes within the mosquito, which then fuse and further develop into oocysts. Then oocysts rupture and release sporozoites that migrate to salivary glands ready for new mosquito-human transmission.

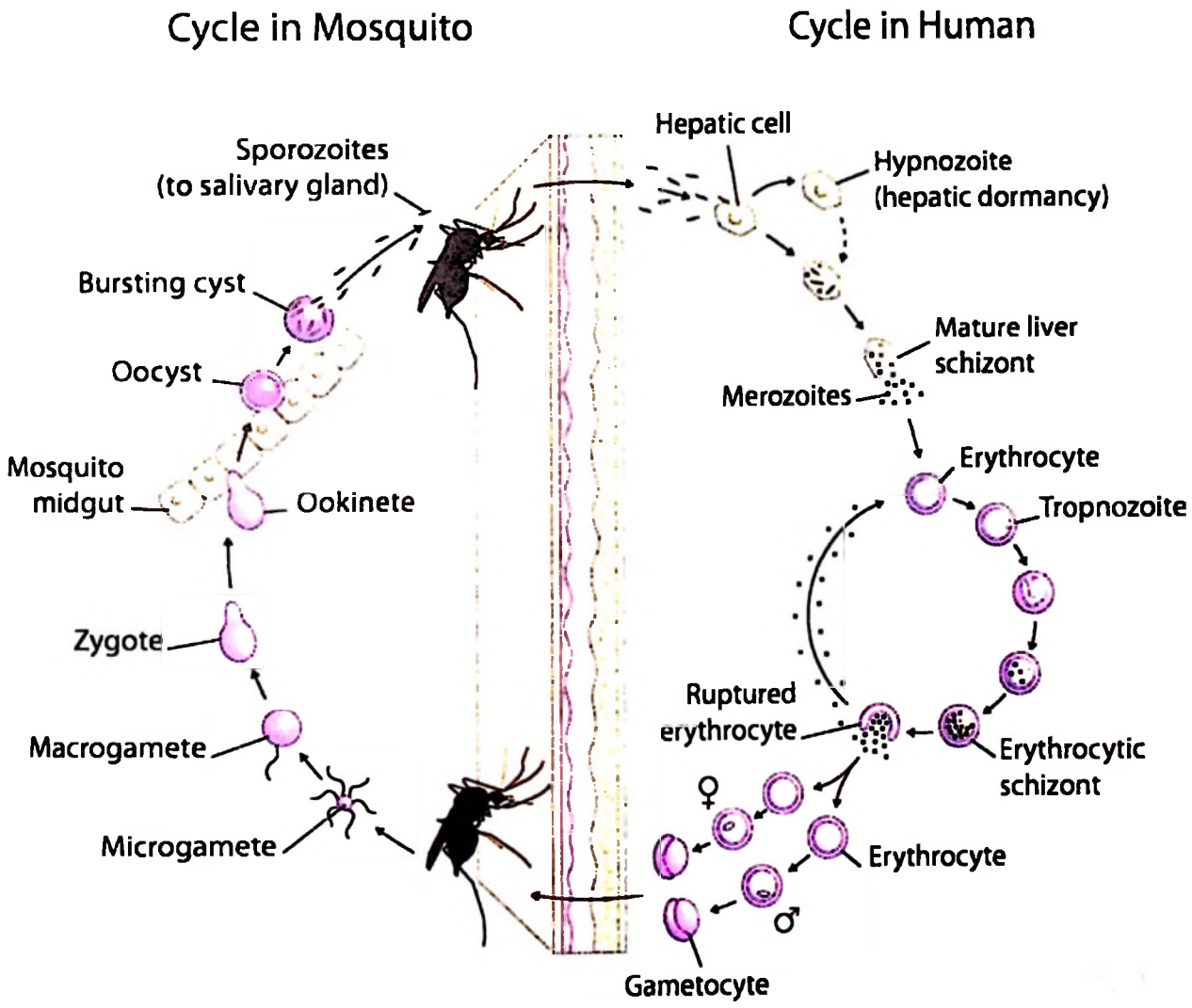

Figure 20: Malaria Life Cycle [Source: (Life cycle, 2015)]

The pharmacotherapy is one among the top three interventions to control and eliminate malaria, along with the use of insecticide-treated mosquito nets and indoor residual spraying (WHO, 2015). Efficaciousness of drugs is a indispensible component of malaria prevention and elimination strategies as it reduces not only morbidity of the disease but also transmission (Feachem and Sabot, 2008). Antimalarials are categorized according to their pharmacodynamics and the stage in parasite's life cycle they target. A *tissue schizonticide* is an antimalarial drug that destroy sporozoites or hepatic schizonts to prevent erythrocytic invasion, while the *blood schizonticide* is an antimalarial drug which act on the asexual erythrocytic forms of parasites such as schizonts and merozoites to terminate the clinical attacks. A drug that destroy gametocytes in the bloodstream and prevent human-mosquito transmission is termed as a *gametocytocide*. An antimalarial drug that inhibits sporogonic phase of malaria parasite within mosquito is called *sporontocide*. It either inhibits formation of ookinete (fusion of gametes) and oocysts or kills sporozoites within mosquito. (Bullock and Manias, 2013).

A combination therapy (CT) is treament in which two or more classes of drugs with different biochemical properties and independent mechanism of actions are administered to a patient. Despite of increasingly drug resistance developed by parasites, the use of antimalarial CTs is reported to be more effective (Targett *et al.*, 2001; Price and Douglas, 2009; Eziefula *et al.*, 2014) as it reduces a likelihood of parasite to develop a drug resistance. However, this effectiveness is associated to the species of *plasmodium* and the stage of its life cycle that is targeted. For example, almost all *blood schizonticides* including artemisinin derivatives also serve as gametocytocides for immature gametocytes of *P.falciparum*, and mature gametocytes for other three remaining species (White, 2008; Boni *et al.*, 2008; Eziefula *et al.*, 2014). Primaquine is the only existing gametocytocide for mature *P.falciparum* (Feachem and Sabot, 2008; White, 2013), which also serves as tissue schizonticide for all species of *Plasmodium* (Sirimulla, 2007). In addition, Primaque has a sporontocidal activity for all species with exceptional of *P. falciparum* (Kiszewski, 2010).

Antimalarial drugs therapy works better to an individual with background immunity (Mayxay *et al.*, 2001), however the use of antimalarial drugs modulates the way immune responses work (Gurarie and McKenzie, 2006). The explicit interaction for antimalarial drugs and immune immune system is not adequately researched (Boni *et al.*, 2008). Therefore, understanding the interaction between immune responses, drugs and malaria parasites suggests the use of mathematical models so as to get new insight on how to control and eradicate malaria. A number of mathematical models on intra host dynamics of *plasmodium* have been done (Gurarie and McKenzie, 2006; Chiyaka *et al.*, 2008; Li *et al.*, 2011; Selemani *et al.*, 2016), and references therein. Though most of them focus on effect of immune responses on dynamics of *plasmodium* (Gurarie and McKenzie, 2006; Tumwiine *et al.*, 2008; Li *et al.*, 2011; Selemani *et al.*, 2017).

The early mathematical model that explicitly incorporate effect of both immunity and drug therapy was done by Chiyaka *et al.* (2008), where erythrocytic dynamics of *plasmodium* in relation to immune responses and antimalarial drug therapy was discussed. Apart from the exceptional work by Selemani *et al.* (2017) which incorporated the effect of immunity on the in-human host and in-mosquito dynamics of *plasmodium*, the rest of these studies were based on erythrocytic dynamics of parasites.

In this chapter, the work of Selemani *et al.* (2017) which describes the effect of immune responses in the in-human host and in-mosquito dynamics of *plasmodium* was extended, by incorporating effect of antimalarials therapy. Most of the currently used antimalarials target on the erythrocytic stages of *plasmodium's* life cycle, while the eradication of malaria requires new drugs that will target on various stages of the entire parasites life cycle (Delves *et al.*, 2012). We, therefore, incorporate the effect of antimalarial CT that contains tissue schizonticidal, blood schizonticidal, gametocytocidal and sporontocidal activities.

5.2 Model Formulation

5.2.1 Model Description

The model formulated in this study is based on an extension of the model developed by Selemani *et al.* (2017) by incorporating the effect of drug therapy. Here, we describe the interaction between hepatic liver cells (HLCs), red blood cells (RBCs), malaria parasites with immune responses and antimalarial drugs using a set of ordinary nonlinear differential equations. In this model, the following set of state variables are used: the uninfected hepatocytic liver cells (uHLCs), H; infected hepatocytic liver cells (iHLCs), I_h; hepatic schizonts, T_h; merozoites, M; uninfected red blood cells (uRBCs), R; infected red blood cells (iRBCs), I_r; erythrocytic schizonts, T_r; gametocytes, G_h; gametes, G_m; and oocysts, C. Others are sporozoites in mosquito's salivary gland, S_m; sporozoites in human, S_h; immune cells against liver stage and blood stage infections , Z_1 and Z_2 respectively; and antibodies, B.

During its blood meal, an infected female mosquito injects sporozoites, S_h; into uninfected human host at a constant rate $ab\nu$, where a is probability that a mosquito bite is infective to human, b is number of mosquito bites per individual, and ν is number of sporozoites injected per bite. The sporozoites attack the uHLCs at the rate $\beta_1 S_h H/(1+k_1 B)$. A parameter β_1 is infection rate of sporozoites to uHLCs while k_1 is efficiency of antibodies to block invasion of uHLCs. They die naturally at a rate $\mu_{sh} S_h$ or cleared by macrophages at a rate $\sigma_{sh} Z_1 S_h/(\pi_{sh}+S_h)$. The uHLCs are recruited at a constant rate Λ_h, from the bone marrow stem cells, and die naturally at rate $\mu_h H$, and also reduced at rate $\beta_1 S_h H/(1+k_1 B)$ due to infection by sporozoites. A parameter σ_{sh} represents a rate of successful removal of intra-human sporozoites

by macrophages and π_{sh} is a half saturation constant of intra-human sporozoites (i.e a number of S_h at which the rate of immune cells to clear sporozoites is halved).

Due to infection of uHLCs by sporozoites, the number of the iHLCs increases at a rate $(1-\tau_1)(\beta_1 S_h H)/(1+k_1 B)$, where τ_1 is the drug (tissue schizonticide) efficacy on inhibiting sporozoites to attack hepatocytes. The iHLCs die at a rate $\mu_{ih} I_h$ or progress to hepatic schizonts at a rate $\alpha_1 I_h$. Immune cells and antimalarial drugs clear the iHLCs at the rates $\sigma_{ih} Z_1 I_h/(\pi_{ih}+I_h)$ and $\tau_2 I_h$ respectively, σ_{ih} is rate of successful removal of iHLCs by immune cells and π_{ih} is a half saturation constant of I_h. The hepatic schizonts die naturally at a rate $\mu_{th} T_h$ or rupture to release merozoites at a rate $\delta_1 T_h$. They also cleared by immune cells at a rate $\sigma_{th} Z_1 T_h/(\pi_{th}+T_h)$, or destroyed by antimalarial drug (*tissue schizonticide*) at a rate $\tau_2 T_h$. A parameter σ_{th} represent a rate of successful removal of hepatic schizonts by immune cells and π_{th} is a half saturation constant of hepatic schizonts. While τ_2 is efficacy of *tissue schizonticide* on destroying iHLCs or hepatic schizonts.

Hepatic schizonts release merozoites at a rate $(1-\tau_3)(r_1\delta_1 T_h)/(1+c_1 Z_1)$, where c_1 and τ_3 are respectively the efficiency of immune cells and efficacy of *tissue schizonticide* to inhibit (suppress) merozoites' production from hepatic schizonts. Merozoites invade uRBCs at a rate $\beta_2 RM/(1+k_2 B)$ and they die naturally at a rate $\mu_m M$. A parameter β_2 is infection rate of uRBCs by merozoites and k_2 is efficiency of antibodies to prevent and reduce the infection of uRBCs by merozoites. They are killed by immune cells at a rate $\sigma_m Z_2 M/(\pi_m+M)$ or by antimalarial drug (blood schizonticides) at a rate $\tau_5 M$, where σ_m is rate of successful removal of merozoites by immune cells, π_m is a half saturation constant of merozoites and τ_5 is efficacy of a drug to clear free merozoites.

The uRBCs are recruited at a constant rate Λ_r from the bone marrow. Their density is reduced by natural death at a rate $\mu_r R$ and due to the infection by merozoites at a rate $\beta_2 RM/(1+k_2 B)$. The number of iRBCs increases at a rate $\beta_2 RM/(1+k_2 B)$ and decreases due to death at a rate $\mu_{ir} I_r$ and due to progression to erythrocytic schizonts at a rate $\alpha_2 T_r$. The immune cells phagocytize the iRBCs at a rate $\sigma_{ir} Z_2 I_r/(\pi_{ir}+I_r)$, while blood schizonticide destroys iRBCs at a rate $\tau_6 I_r$. A parameter σ_{ir} is rate of successful removal of iRBCs by immune cells and π_{ir} is a half saturation constant of iRBCs.

The erythrocytic schizonts die at rate $\mu_{tr} T_r$ and rupture at rate $\delta_2 T_r$ and release new r_2 merozoites which starts a series of repetitive cycles to infect other uRBCs. A proportion p, of these daughter merozoites proceeds with asexual replication cycle at a rate $(1-\tau_4)(pr_2\delta_2 T_r)/(1+c_2 Z_2)$. A parameter c_2 is efficiency of immune cells to suppress the production of intra-erythrocytic merozoites or gametocytes, while τ_4 is efficacy of drug (blood schizonticide) to suppress merozoites' production from erythrocytic schizonts. The erythrocytic schizonts are

cleared by immune cells and drugs (blood schizonticide) at the rates $\sigma_{tr}Z_2T_r/(\pi_{tr}+T_r)$ and τ_6T_r respectively. A parameter σ_{tr} represents a rate of successful removal of erythrocytic schizonts by immune cells, while a π_{tr} is a half saturation constant of erythrocytic schizonts, and a τ_6 is efficacy of drug to destroy iRBCs or erythrocytic schizonts.

The proportion $1-p$, of newly released merozoites differentiate into gametocytes. The number of gametocytes increases at a rate $(1-\tau_7)(1-p)(r_2\delta_2T_r)/(1+c_2Z_2)$, where τ_7 is efficacy of a drug (*gametocytocide*) to suppress gametocytes' production. They decrease by natural death at a rate $\mu_{gb}G_b$, for being ingested by mosquito at a rate $q\omega G_b$ and being cleared by immune cells at a rate $\sigma_{gb}Z_2G_b/(\pi_{gb}+G_b)$. They are also cleared by antimalarial drug (gametocytocides) at a rate τ_8G_b. A parameter σ_{gb} is the rate of successful removal of gametocytes by immune cells, while a π_{gb} is the half saturation constant of gametocytes and a τ_8 is efficacy of drug to clear gametocytes.

The gametes in mosquitoes are recruited at a rate $(1-\tau_9)(\rho q\omega G_b)/(1+k_3B)$, where ρ is number of bites a mosquito can make during its lifetime, ω is number of gametocytes ingested per bite and q is probability that a mosquito bite is infective to mosquito. A parameter k_3 is efficiency of antibodies picked up by mosquito during its blood meal to mediate lysis of gametocytes and inhibit parasite's growth in mosquito (Langhorne *et al.*, 2008) and τ_9 is efficacy of antimalarial drug (sporonticide) sucked with gametocytes to inhibit a formation of oocysts and sporozoites within the mosquito by suppressing a fusion of gametes. The gametes die naturally at rate $\mu_{gm}G_m$ and progress to oocysts at a rate, α_3G_m. The oocysts rupture to release sporozoites at a rate, δ_3C and die at a rate μ_cC. The released sporozoites, S_m migrate to salivary glands where they either naturally die at a rate $\mu_{sm}S_m$ or injected into a new host at rate $ab\nu$. The variables used in this model have been represented and described in previous chapter (See Table 6).

5.2.2 Model Assumptions

In the development of this model, besides the assumptions used in Chapter 4, we assume the following:

(i) Antimalarial drugs ingested with gametocytes during the blood meal prevent the fusion of gametocytes (macro- and micro-gametes) and other developmental stages of parasites within mosquito.

(ii) All gametocytes are cleared after taking gametocyticidal drug regardless of age.

Table 10 : Additional parameters (to those used in Chapter 4) and their descriptions

Parameter	Description
σ_{gb} :	rate at which gametocytes are cleared by immune cells
ϵ_{sh} :	proliferation rate of immune cells due to contact with sporozoites
ϵ_{ih} :	proliferation rate of immune cells due to contact with infected HLCs
ϵ_{th} :	proliferation rate of immune cells due to contact with liver schizonts
ϵ_m :	proliferation rate of immune cells due to contact with merozoites
ϵ_{ir} :	proliferation rate of immune cells due to contact with infected RBCs
ϵ_{tr} :	proliferation rate of immune cells due to contact with blood schizonts
ϵ_{gb} :	proliferation rate of immune cells due to contact with gametocytes
π_{sh} :	half saturation constant of sporozoites
π_{ih} :	half saturation constant of infected HLCs
π_{th} :	half saturation constant of liver schizonts
π_m :	half saturation constant of merozoites
π_{ir} :	half saturation constant of infected RBCs
π_{tr} :	half saturation constant of blood schizonts
π_{gb} :	half saturation constant of gametocytes
η_1 :	maximum rate of increase of antibodies due to presence of sporozoites
η_2 :	maximum rate of increase of antibodies due to presence of merozoites
τ_1 :	efficacy of a drug to inhibit sporozoites from infecting hepatocytes
τ_2 :	efficacy of a drug to destroy infected HLCs or hepatic schizonts
τ_3 :	efficacy of a drug to suppress the merozoites' production from hepatic schizonts
τ_4 :	efficacy of a drug to suppress the merozoites' production from erythrocytic schizonts
τ_5 :	efficacy of a drug to destroy merozoites
τ_6 :	efficacy of a drug to destroy infected RBCs or erythrocytic schizonts
τ_7 :	efficacy of a drug to suppress gametocytes' production
τ_8 :	efficacy of a drug to clear the gametocytes
τ_9 :	efficacy of a drug to inhibit parasites' development (fertilization) within the mosquito

5.2.3 Compartmental diagram

Based on the dynamics described in Section 5.2.1 and the assumptions described in Section 5.2.2, the proposed model for the in-human host and in-mosquito dynamics of entire life cycle of malaria parasites with the effect of immune responses and drug therapy is shown in Fig. 21. The additional parameters, used formulation of this model are described in Table Table 10 respectively.

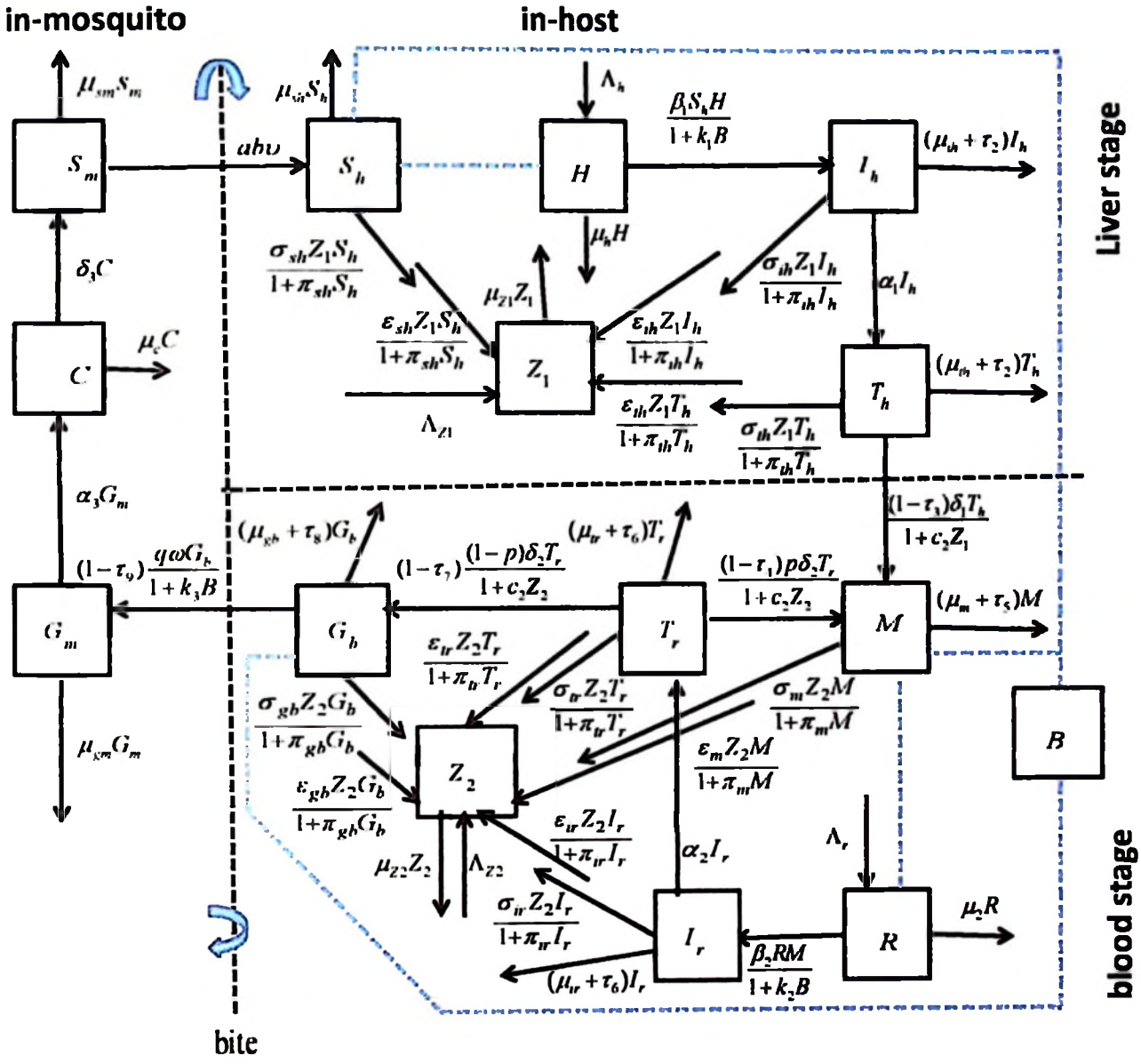

Figure 21: Compartmental model diagram for the in-human host and in-mosquito dynamics of malaria parasites with immune responses and drug therapy

5.2.4 Model Equations

Basing on the compartmental diagram illustrated in Fig. 21, thus the in-human host and in-mosquito dynamics for the entire life cycle of malaria parasite with immune responses and drug therapy is governed by the following system of ordinary differential equations:

$$\frac{dH}{dt} = \Lambda_h - \frac{\beta_1 S_h H}{1 + k_1 B} - \mu_h H, \tag{5.1a}$$

$$\frac{dI_h}{dt} = (1 - \tau_1)\frac{\beta_1 S_h H}{1 + k_1 B} - (\alpha_1 + \mu_{ih} + \tau_2) I_h - \frac{\sigma_{ih} Z_1 I_h}{\pi_{ih} + I_h}, \tag{5.1b}$$

$$\frac{dT_h}{dt} = \alpha_1 I_h - (\delta_1 + \mu_{th} + \tau_2) T_h - \frac{\sigma_{th} Z_1 T_h}{\pi_{th} + T_h}, \tag{5.1c}$$

$$\frac{dM}{dt} = (1 - \tau_3)\frac{r_1 \delta_1 T_h}{1 + c_1 Z_1} + (1 - \tau_4)\frac{p r_2 \delta_2 T_r}{1 + c_2 Z_2} - \frac{\beta_2 R M}{1 + k_2 B} - \frac{\sigma_m Z_2 M}{\pi_m + M} - (\mu_m + \tau_5) M, \tag{5.1d}$$

$$\frac{dR}{dt} = \Lambda_r - \frac{\beta_2 R M}{1 + k_2 B} - \mu_r R, \tag{5.1e}$$

$$\frac{dI_r}{dt} = \frac{\beta_2 R M}{1 + k_2 B} - (\alpha_2 + \mu_{ir} + \tau_6) I_r - \frac{\sigma_{ir} Z_2 I_r}{\pi_{ir} + I_r}, \tag{5.1f}$$

$$\frac{dT_r}{dt} = \alpha_2 I_r - (\delta_2 + \mu_{tr} + \tau_6) T_r - \frac{\sigma_{tr} Z_2 T_r}{\pi_{tr} + T_r}, \tag{5.1g}$$

$$\frac{dG_b}{dt} = (1 - \tau_7)\frac{(1 - p) r_2 \delta_2 T_r}{1 + c_2 Z} - (q\omega + \mu_{gb} + \tau_8) G_b - \frac{\sigma_{gb} Z_{gb} G_b}{\pi_{gb} + G_b}, \tag{5.1h}$$

$$\frac{dG_m}{dt} = (1 - \tau_9)\frac{pq\omega G_b}{1 + k_3 B} - \alpha_3 G_m - \mu_{gm} G_m, \tag{5.1i}$$

$$\frac{dC}{dt} = \alpha_3 G_m - \delta_3 C - \mu_c C, \tag{5.1j}$$

$$\frac{dS_m}{dt} = r_3 \delta_3 C - a\nu S_m - \mu_{sm} S_m, \tag{5.1k}$$

$$\frac{dS_h}{dt} = ab\nu - \frac{\beta_1 S_h H}{1 + k_1 B} - \mu_{sh} S_h - \frac{\sigma_{sh} Z_1 S_h}{\pi_{sh} + S_h}, \tag{5.1l}$$

$$\frac{dZ_1}{dt} = \Lambda_{z_1} + \left(\frac{\epsilon_{sh} S_h}{\pi_{sh} + S_h} + \frac{\epsilon_{ih} I_h}{\pi_{ih} + I_h} + \frac{\epsilon_{th} T_h}{\pi_{th} + T_h} \right) Z_1 - \mu_{z_1} Z_1, \tag{5.1m}$$

$$\frac{dZ_2}{dt} = \Lambda_{z_2} + \left(\frac{\epsilon_m M}{\pi_m + M} + \frac{\epsilon_{ir} I_r}{\pi_{ir} + I_r} + \frac{\epsilon_{tr} T_r}{\pi_{tr} + T_r} + \frac{\epsilon_{gb} G_b}{\pi_{gb} + G_b} \right) Z_2 - \mu_{z_2} Z_2, \tag{5.1n}$$

$$\frac{dB}{dt} = \frac{\eta_1 S_h Z_1}{\pi_{sh} + S_h} + \frac{\eta_2 M Z_2}{\pi_m + M} - \mu_b B. \tag{5.1o}$$

5.3 Analysis of the Model

5.3.1 Wellposedness of the model

In this section, the wellposedness of the model is determined by investigating the existence and feasibility of its solution. That is, to test whether a bounded and biologically meaningful solution exists at anytime.

The model system (5.1a)-(5.1o) can be expressed in the compact form (Mpeshe *et al.*, 2014b; Selemani *et al.*, 2016)

$$\frac{\mathrm{d}X}{dt} = C(x)X + F$$

where

$$X = (H, I_h, T_h, M, R, I_r, T_r, G_b, G_m, C, S_m, S_h, Z_1, Z_2, B)^T,$$

$$C(x) = \begin{bmatrix}
-c_1 & 0 & 0 & 0 & 0 & 0 & 0 & 0 & 0 & 0 & 0 & 0 & 0 & 0 & 0 \\
c_2 & -c_3 & 0 & 0 & 0 & 0 & 0 & 0 & 0 & 0 & 0 & 0 & 0 & 0 & 0 \\
0 & \alpha_1 & -c_4 & 0 & 0 & 0 & 0 & 0 & 0 & 0 & 0 & 0 & 0 & 0 & 0 \\
0 & 0 & c_5 & -c_6 & 0 & 0 & c_7 & 0 & 0 & 0 & 0 & 0 & 0 & 0 & 0 \\
0 & 0 & 0 & 0 & -c_8 & 0 & 0 & 0 & 0 & 0 & 0 & 0 & 0 & 0 & 0 \\
0 & 0 & 0 & 0 & c_9 & -c_{10} & 0 & 0 & 0 & 0 & 0 & 0 & 0 & 0 & 0 \\
0 & 0 & 0 & 0 & 0 & \alpha_2 & -c_{11} & 0 & 0 & 0 & 0 & 0 & 0 & 0 & 0 \\
0 & 0 & 0 & 0 & 0 & 0 & c_{12} & -c_{13} & 0 & 0 & 0 & 0 & 0 & 0 & 0 \\
0 & 0 & 0 & 0 & 0 & 0 & 0 & c_{14} & -c_{15} & 0 & 0 & 0 & 0 & 0 & 0 \\
0 & 0 & 0 & 0 & 0 & 0 & 0 & 0 & \alpha_3 & -c_{16} & 0 & 0 & 0 & 0 & 0 \\
0 & 0 & 0 & 0 & 0 & 0 & 0 & 0 & 0 & r_3\delta_3 & -c_{17} & 0 & 0 & 0 & 0 \\
0 & 0 & 0 & 0 & 0 & 0 & 0 & 0 & 0 & 0 & 0 & -c_{18} & 0 & 0 & 0 \\
0 & c_{19} & c_{20} & 0 & 0 & 0 & 0 & 0 & 0 & 0 & 0 & c_{21} & -\mu_{z_1} & 0 & 0 \\
0 & 0 & 0 & c_{22} & 0 & c_{23} & c_{24} & c_{25} & 0 & 0 & 0 & 0 & 0 & -\mu_{z_2} & 0 \\
0 & 0 & 0 & c_{26} & 0 & 0 & 0 & 0 & 0 & 0 & 0 & c_{27} & 0 & 0 & -\mu_b
\end{bmatrix}$$

where

$$\begin{aligned}
c_1 &= \frac{\beta_1 S_h}{1+k_1 B} + \mu_h, \quad c_2 = (1-\tau_1)\frac{\beta_1 S_h}{1+k_1 B}, \quad c_3 = \alpha_1 + \mu_{ih} + \tau_2 + \frac{\sigma_{ih} Z_1}{1+\pi_{ih} I_h}, \\
c_4 &= \delta_1 + \mu_{th} + \tau_2 + \frac{\sigma_{th} Z_1}{1+\pi_{th} T_h}, \quad c_5 = (1-\tau_3)\frac{r_1\delta_1}{1+c_1 Z_1}, \quad c_6 = \mu_m + \tau_5 + \frac{\beta_2 R}{1+k_2 B} + \frac{\sigma_m Z_2}{1+\pi_m M}, \\
c_7 &= (1-\tau_4)\frac{pr_2\delta_2}{1+c_2 Z_2}, \quad c_8 = \frac{\beta_2 M}{1+k_2 B} + \mu_r, \quad c_9 = \frac{\beta_2 M}{1+k_2 B}, \quad c_{10} = \alpha_2 + \mu_{ir} + \tau_6 + \frac{\sigma_{ir} Z_2}{\pi_{ir} + I_r} \\
c_{11} &= \delta_2 + \mu_{tr} + \tau_6 + \frac{\sigma_{tr} Z_2}{1+\pi_{tr} T_r}, \quad c_{12} = (1-\tau_7)\frac{(1-p)r_2\delta_2}{1+c_2 Z_2}, \quad c_{13} = q\omega + \mu_{gb} + \tau_8 + \frac{\sigma_{gb} Z_2}{\pi_{gb} + G_b}, \\
c_{14} &= (1-\tau_9)\frac{pq\omega}{1+k_3 B}, \quad c_{15} = \alpha_3 + \mu_{gm}, \quad c_{16} = \delta_3 + \mu_c, \quad c_{17} = a\nu + \mu_{sm}, \\
c_{18} &= \frac{\beta_1 H}{1+k_1 B} + \mu_{sh} + \frac{\sigma_{sh} Z_1}{\pi_{sh} + S_h}, \quad c_{19} = \frac{\epsilon_{ih} Z_1}{\pi_{ih} + I_h}, \quad c_{20} = \frac{\epsilon_{th} Z_1}{\pi_{th} + T_h}, \quad c_{21} = \frac{\epsilon_{sh} Z_1}{\pi_{sh} + S_h}, \\
c_{22} &= \frac{\epsilon_m Z_2}{\pi_m + M}, \quad c_{23} = \frac{\epsilon_{ir} Z_2}{\pi_{ir} + I_r}, c_{24} = \frac{\epsilon_{tr} Z_2}{\pi_{tr} + T_r}, \quad c_{25} = \frac{\epsilon_{gb} Z_2}{\pi_{gb} + G_b}, \quad c_{26} = \frac{\eta_2 M Z_2}{\pi_m + M}, \\
c_{27} &= \frac{\eta_1 S_h Z_1}{\pi_{sh} + S_h}
\end{aligned} \tag{5.2}$$

and F is a column vector given by

$$F = (\Lambda_h, 0, 0, 0, \Lambda_r, 0, 0, 0, 0, 0, 0, ab\nu, \Lambda_{z_1}, \Lambda_{z_2}, 0)^T$$

. Clearly $C(x)$ is Metzler matrix since all its off diagonal elements are non negative, for all $x \in \mathbb{R}^{15}_+$ and $F \geq 0$. Therefore, the system (5.1a)-(5.1o) is positively invariant in $\mathbb{R}^{15}_+$, implying

that any trajectory of the system initiated in $\mathbb{R}^{15}_{+}$ will always remains there, and F is Lipschitz continuous. Hence, a maximal (unique) solution exists and so

$$\mathcal{D} = \{(H, I_h, T_h, M, R, I_r, T_r, G_b, G_m, C, S_m, S_h, Z_1, Z_2, B) \geq 0 \in \mathbb{R}^{15}_{+}\}$$

is the positively invariant set for the model. Thus, the model (5.1a)-(5.1o) is epidemilogically and mathematically wellposed in the region $\mathcal{D}$.

5.3.2 Malaria Free Equilibrium (MEF)

Let $E^{02} = (H^{02}, I_h^{02}, T_h^{02}, M^{02}, R^{02}, I_r^{02}, T_r^{02}, G_b^{02}, G_m^{02}, C^{02}, S_m^{02}, S_h^{02}, Z_1^{02}, Z_2^{02}, B^{02})$ be the malaria free equilibrium of the system (5.1a)-(5.1o). We obtained equilibrium points of the system by setting right hand side of model equations equal to zero and solve for variables.

When there is no malaria infection,

$$I_h^{02} = T_h^{02} = M^{02} = I_r^{02} = T_r^{02} = G_b^{02} = G_m^{02} = C^{02} = S_m^{02} = S_h^{02} = B^{02} = 0$$

From equations (5.1a) , (5.1e), (5.1m) and (5.1n), we respectively obtain

$$H^{02} = \frac{\Lambda_h}{\mu_h}, \qquad R^{02} = \frac{\Lambda_r}{\mu_r}, \qquad Z_1^{02} = \frac{\Lambda_{z_1}}{\mu_{z_1}} \quad \text{and } Z_2^{02} = \frac{\Lambda_{z_2}}{\mu_{z_2}}$$

Thus the MFE is

$$E^{02} = \left(\frac{\Lambda_h}{\mu_h}, 0, 0, \frac{\Lambda_r}{\mu_r}, 0, 0, 0, 0, 0, 0, 0, \frac{\Lambda_{z_1}}{\mu_{z_1}}, \frac{\Lambda_{z_2}}{\mu_{z_2}}, 0\right)$$

5.3.3 Effective Reproduction Number, $\mathcal{R}_e$

Guardiola and Vecchio (2005) defined intra-host reproduction number as a number of newly infected cells that single infected cell can produce during its infectious period. An effective reproduction number for the model (5.1a)-(5.1o) was computed using the next generation matrix method introduced by Van den Driessche and Watmough (2002). In this approach a reproduction number, $\mathcal{R}_e$, is given by the spectral radius $\rho(F_2 V_2^{-1})$, of next generation matrix $F_2 V_2^{-1}$. where $F_2 = \dfrac{\partial \mathcal{F}_{2i}}{\partial x_i}(E^{02})$ is called a transmission matrix and $V_2 = \dfrac{\partial \mathcal{V}_{2i}}{\partial x_i}(E^{02})$ is called a transition matrix.

$\mathcal{F}_{2i}$ be the rate of appearance of new infection in compartment i,
$\mathcal{V}_{2i}^{+}$ be the rate of transfer of individuals into compartment i by all other means,
$\mathcal{V}_{2i}^{-}$ be the rate of transfer of individuals out of compartment i by all other means and

$\mathcal{V}_{2i} = \mathcal{V}_{2i}^{+} - \mathcal{V}_{2i}^{-}$. Hence, we have

$$\mathcal{F}_{2i} = \begin{pmatrix} (1-\tau_1)\dfrac{\beta_1 S_h I}{1+c_1 S_h} \\ 0 \\ 0 \\ \dfrac{\beta_2 RM}{1+c_2 M} \\ 0 \\ 0 \\ (1-\tau_9)\dfrac{\rho\eta\omega G_b}{1+k_3 B} \\ 0 \\ 0 \\ 0 \end{pmatrix} \tag{5.3}$$

and

$$\mathcal{V}_{2i} = \begin{pmatrix} \left(\alpha_1 + \mu_{ih} + \tau_2 + \dfrac{\sigma_{ih} Z_1}{1+\pi_{ih} I_h}\right) I_h \\ \left(\delta_1 + \mu_{th} + \tau_2 + \dfrac{\sigma_{th} Z_1}{1+\pi_{th} T_h}\right) T_h - \alpha_1 I_h \\ \left(\dfrac{\beta_2 R}{1+k_2 B} + \dfrac{\sigma_m Z_2}{1+\pi_m M} + \mu_m + \tau_5\right) M - \left(\dfrac{(1-\tau_3) r_1 \delta_1}{1+c_1 Z_1}\right) T_h - \left(\dfrac{(1-\tau_4) p r_2 \delta_2}{1+c_2 Z_2}\right) T_r \\ \left(\alpha_2 + \mu_{ir} + \tau_6 + \dfrac{\sigma_{ir} Z_2}{1+\pi_{ir} I_r}\right) I_r \\ \left(\delta_2 + \mu_{tr} + \tau_6 + \dfrac{\sigma_{tr} Z_2}{1+\pi_{tr} T_r}\right) T_r - \alpha_2 I_r \\ \left(q\omega + \mu_{gb} + \tau_8 + \dfrac{\sigma_{gb} Z_2}{1+\pi_{gb} G_b}\right) G_b - \left(\dfrac{(1-\tau_7)(1-p) r_2 \delta_2}{1+c_2 Z_2}\right) T_r \\ (\alpha_3 + \mu_{gm}) G_m \\ (\delta_3 + \mu_c) C - \alpha_3 G_m \\ (a\nu + \mu_{sm}) S_{sm} - r_3 \delta_3 C \\ \left(\dfrac{\beta_1 H}{1+k_1 B} + \dfrac{\sigma_{sh} Z_1}{1+\pi_{sh} S_h} + \mu_{sh}\right) S_h - ab\nu \end{pmatrix} \tag{5.4}$$

From matrices in (5.3) and (5.4) we obtain

$$F_2 = \begin{pmatrix} 0 & 0 & 0 & 0 & 0 & 0 & 0 & 0 & 0 & (1-\tau_1)\beta_1\frac{\Lambda_h}{\mu_h} \\ 0 & 0 & 0 & 0 & 0 & 0 & 0 & 0 & 0 & 0 \\ 0 & 0 & 0 & 0 & 0 & 0 & 0 & 0 & 0 & 0 \\ 0 & 0 & \beta_2\frac{\Lambda_r}{\mu_r} & 0 & 0 & 0 & 0 & 0 & 0 & 0 \\ 0 & 0 & 0 & 0 & 0 & 0 & 0 & 0 & 0 & 0 \\ 0 & 0 & 0 & 0 & 0 & 0 & 0 & 0 & 0 & 0 \\ 0 & 0 & 0 & 0 & 0 & (1-\tau_9)p\alpha\omega & 0 & 0 & 0 & 0 \\ 0 & 0 & 0 & 0 & 0 & 0 & 0 & 0 & 0 & 0 \\ 0 & 0 & 0 & 0 & 0 & 0 & 0 & 0 & 0 & 0 \\ 0 & 0 & 0 & 0 & 0 & 0 & 0 & 0 & 0 & 0 \end{pmatrix} \tag{5.5}$$

and

$$V_2 = \begin{pmatrix} v_1 & 0 & 0 & 0 & 0 & 0 & 0 & 0 & 0 & 0 \\ -\alpha_1 & v_2 & 0 & 0 & 0 & 0 & 0 & 0 & 0 & 0 \\ 0 & -v_3 & v_4 & 0 & -v_5 & 0 & 0 & 0 & 0 & 0 \\ 0 & 0 & 0 & v_6 & 0 & 0 & 0 & 0 & 0 & 0 \\ 0 & 0 & 0 & -\alpha_2 & v_7 & 0 & 0 & 0 & 0 & 0 \\ 0 & 0 & 0 & 0 & -v_8 & v_9 & 0 & 0 & 0 & 0 \\ 0 & 0 & 0 & 0 & 0 & 0 & v_{10} & 0 & 0 & 0 \\ 0 & 0 & 0 & 0 & 0 & 0 & -\alpha_3 & v_{11} & 0 & 0 \\ 0 & 0 & 0 & 0 & 0 & 0 & 0 & -v_{12} & v_{13} & 0 \\ 0 & 0 & 0 & 0 & 0 & 0 & 0 & 0 & 0 & v_{14} \end{pmatrix} \tag{5.6}$$

respectively, where

$$\begin{aligned} v_1 &= \alpha_1 + \mu_{ih} + \tau_2 + \frac{\sigma_{ih}\Lambda_{z_1}}{\mu_{z_1}}, \quad v_2 = \delta_1 + \mu_{th} + \tau_2 + \frac{\sigma_{th}\Lambda_{z_1}}{\mu_{z_1}}, \quad v_3 = (1-\tau_3)\frac{r_1\delta_1\mu_{z_1}}{\mu_{z_1} + c_1\Lambda_{z_1}} \\ v_4 &= \beta_2\frac{\Lambda_r}{\mu_r} + \frac{\sigma_{rh}\Lambda_{z_2}}{\mu_{z_2}} + \mu_{rh} + \tau_5, \quad v_5 = (1-\tau_4)\frac{pr_2\delta_2\mu_{z_2}}{\mu_{z_2} + c_2\Lambda_{z_2}}, \quad v_6 = \alpha_2 + \mu_{ir} + \tau_6 + \frac{\sigma_{ir}\Lambda_{z_2}}{\mu_{z_2}}, \\ v_7 &= \delta_2 + \mu_{tr} + \tau_6 + \frac{\sigma_{tr}\Lambda_{z_2}}{\mu_{z_2}}, \quad v_8 = (1-\tau_7)\frac{(1-p)r_2\delta_2\mu_{z_2}}{\mu_{z_2} + c_2Z_2}, \quad v_9 = q\omega + \mu_{gb} + \tau_8 + \frac{\sigma_{gb}\Lambda_{z_2}}{\mu_{z_2}}, \\ v_{10} &= \alpha_3 + \mu_{gm}, \quad v_{11} = \delta_3 + \mu_c, \quad v_{12} = r_3\delta_3, \quad v_{13} = a\nu + \mu_{sm}, \quad v_{14} = \beta_1\frac{\Lambda_h}{\mu_h} + \frac{\sigma_{sh}\Lambda_{z_1}}{\mu_{z_1}} + \mu_{sh} \end{aligned} \tag{5.7}$$

Using equation (5.6), we obtained the inverse, V_2^{-1}, of V_2 given by

$$V_2^{-1} = \begin{pmatrix} \frac{1}{v_1} & 0 & 0 & 0 & 0 & 0 & 0 & 0 & 0 & 0 \\ \frac{\alpha_1}{v_2 v_1} & \frac{1}{v_2} & 0 & 0 & 0 & 0 & 0 & 0 & 0 & 0 \\ \frac{v_3\alpha_1}{v_4 v_2 v_1} & \frac{v_3}{v_4 v_2} & \frac{1}{v_4} & \frac{v_5\alpha_2}{v_7 v_6 v_4} & \frac{v_5}{v_7 v_4} & 0 & 0 & 0 & 0 & 0 \\ 0 & 0 & 0 & \frac{1}{v_6} & 0 & 0 & 0 & 0 & 0 & 0 \\ 0 & 0 & 0 & \frac{\alpha_2}{v_7 v_6} & \frac{1}{v_7} & 0 & 0 & 0 & 0 & 0 \\ 0 & 0 & 0 & \frac{\alpha_2 v_8}{v_9 v_7 v_6} & \frac{v_8}{v_9 v_7} & \frac{1}{v_9} & 0 & 0 & 0 & 0 \\ 0 & 0 & 0 & 0 & 0 & 0 & \frac{1}{v_{10}} & 0 & 0 & 0 \\ 0 & 0 & 0 & 0 & 0 & 0 & \frac{\alpha_3}{v_{11} v_{10}} & \frac{1}{v_{11}} & 0 & 0 \\ 0 & 0 & 0 & 0 & 0 & 0 & \frac{v_{12}\alpha_3}{v_{13} v_{11} v_{10}} & \frac{v_{12}}{v_{113} v_{11}} & \frac{1}{v_{13}} & 0 \\ 0 & 0 & 0 & 0 & 0 & 0 & 0 & 0 & 0 & \frac{1}{v_{14}} \end{pmatrix} \tag{5.8}$$

Hence, from (5.5) and (5.8), we have

$$F_2V_2^{-1} = \begin{pmatrix} 0 & 0 & 0 & 0 & 0 & 0 & 0 & 0 & 0 & A_1 \\ 0 & 0 & 0 & 0 & 0 & 0 & 0 & 0 & 0 & 0 \\ 0 & 0 & 0 & 0 & 0 & 0 & 0 & 0 & 0 & 0 \\ A_2 & A_3 & A_4 & A_5 & A_6 & 0 & 0 & 0 & 0 & 0 \\ 0 & 0 & 0 & 0 & 0 & 0 & 0 & 0 & 0 & 0 \\ 0 & 0 & 0 & 0 & 0 & 0 & 0 & 0 & 0 & 0 \\ 0 & 0 & 0 & 0 & 0 & 0 & 0 & 0 & 0 & 0 \\ 0 & 0 & 0 & A_7 & A_8 & A_9 & 0 & 0 & 0 & 0 \\ 0 & 0 & 0 & 0 & 0 & 0 & 0 & 0 & 0 & 0 \\ 0 & 0 & 0 & 0 & 0 & 0 & 0 & 0 & 0 & 0 \end{pmatrix} \tag{5.9}$$

$$\begin{aligned} A_1 &= \frac{\beta_1\Lambda_h}{v_{14}\mu_h}, \quad A_2 = \frac{\beta_2\alpha_1 v_3\Lambda_r}{v_4 v_2 v_1\mu_r}, \quad A_3 = \frac{\beta_2 v_3\Lambda_r}{v_4 v_2\mu_r}, \quad A_4 = \frac{\beta_2\Lambda_r}{v_4\mu_r}, \quad A_5 = \frac{\beta_2\Lambda_r v_5\alpha_2}{v_7 v_6 v_4\mu_r}, \\ A_6 &= \frac{\beta_2 v_5\Lambda_r}{v_7 v_4\mu_r}, \quad A_7 = \frac{\rho q\omega v_8\alpha_2}{v_9 v_7 v_6}, \quad A_8 = \frac{\rho q\omega v_8}{v_9 v_7}, \quad A_9 = \frac{\rho q\omega}{v_9} \end{aligned} \tag{5.10}$$

The eigenvalues of next generation matrix, $F_2V_2^{-1}$ are obtained from

$$|F_2V_2^{-1} - I\lambda| = 0$$

The effective reproduction number, $\mathcal{R}_e$, is the dominant eigenvalue of $F_2V_2^{-1}$. From (5.9), the only nonzero eigenvalue is

$$\lambda = A_5 = \frac{\beta_2\Lambda_r v_5\alpha_2}{v_7 v_6 v_4\mu_r}.$$

Therefore, the dominant eigenvalue is

$$\lambda = \frac{\beta_2 \Lambda_r v_5 \alpha_2}{v_7 v_6 v_4 \mu_r}$$

.

Hence, the effective reproduction number, $\mathcal{R}_e$ is given by

$$\mathcal{R}_e = \frac{\beta_2 \Lambda_r v_5 \alpha_2}{v_7 v_6 v_4 \mu_r} \tag{5.11}$$

After substitution expressions of v_4, v_5, v_6, and v_7 given in equation (5.7) into equation (5.11) we obtain

$$\mathcal{R}_e = \left[\frac{\beta_2 \frac{\Lambda_r}{\mu_r}}{\beta_2 \frac{\Lambda_r}{\mu_r} + \sigma_m \frac{\Lambda_{z_2}}{\mu_{z_2}} + \mu_m + \tau_5}\right]\left[\frac{\alpha_2}{\alpha_2 + \mu_{ir} + \tau_6 + \sigma_{ir}\frac{\Lambda_{z_2}}{\mu_{z_2}}}\right]\left[\frac{1}{\delta_2 + \mu_{tr} + \tau_6 + \sigma_{tr}\frac{\Lambda_{z_2}}{\mu_{z_2}}}\right]\left[\frac{(1-\tau_4)p r_2 \delta_2}{1 + c_2 \frac{\Lambda_{z_2}}{\mu_{z_2}}}\right]$$

which can be simplified to

$$\mathcal{R}_e = \left[\frac{\beta_2 r_0}{\beta_2 r_0 + \sigma_m z_0 + \mu_m + \tau_5}\right]\left[\frac{\alpha_2}{\alpha_2 + \mu_{ir} + \tau_6 + \sigma_{ir} z_0}\right]\left[\frac{1}{\delta_2 + \mu_{tr} + \tau_6 + \sigma_{tr} z_0}\right]\left[\frac{(1-\tau_4)p r_2 \delta_2}{1 + c_2 z_0}\right] \tag{5.12}$$

where $r_0 = \frac{\Lambda_r}{\mu_r}$ and $z_0 = \frac{\Lambda_{z_2}}{\mu_{z_2}}$ respectively represent the values of uninfected RBCs and immune

cells that fight against blood stage malaria at malaria-free equilibrium. The terms in equation (5.12) can defined as follows:

$\left[\frac{\beta_2 r_0}{\beta_2 r_0 + \sigma_m z_0 + \mu_m + \tau_5}\right]$ represents the probability that a merozoite introduced into an completely susceptible RBC population will infect a RBC before it dies (either naturally, or killed by immune cells or destroyed by drug); $\left[\frac{\alpha_2}{\alpha_2 + \mu_{ir} + \tau_6 + \sigma_{ir} z_0}\right]$ is the proportion of infected RBCs that progress to schizonts before dying (natural death, killed by immune cells or antimalarial drugs); $\left[\frac{1}{\delta_2 + \mu_{tr} + \tau_6 + \sigma_{tr} z_0}\right]$ represents an average time a schizont spends before it burst, cleared by immune cells or destroyed by antimalarial drugs; and $\left[\frac{(1-\tau_4)p r_2 \delta_2}{1 + c_2 z_0}\right]$ is number of merozoites produced by a schizont when it bursts.

5.3.4 Local and Global Stability of MFE

At malaria-free equilibrium, E^{02}, the Jacobian matrix of the system (5.1a)-(5.1o) is given by

$$J(E^{02}) = \begin{bmatrix}
-\mu_h & 0 & 0 & 0 & 0 & 0 & 0 & 0 & 0 & 0 & 0 & -u_1 & 0 & 0 & 0 \\
0 & -u_2 & 0 & 0 & 0 & 0 & 0 & 0 & 0 & 0 & 0 & u_1 & 0 & 0 & 0 \\
0 & \alpha_1 & -u_3 & 0 & 0 & 0 & 0 & 0 & 0 & 0 & 0 & 0 & 0 & 0 & 0 \\
0 & 0 & u_4 & -u_5 & 0 & 0 & u_6 & 0 & 0 & 0 & 0 & 0 & 0 & 0 & 0 \\
0 & 0 & 0 & -u_7 & -\mu_r & 0 & 0 & 0 & 0 & 0 & 0 & 0 & 0 & 0 & 0 \\
0 & 0 & 0 & u_7 & 0 & -u_8 & 0 & 0 & 0 & 0 & 0 & 0 & 0 & 0 & 0 \\
0 & 0 & 0 & 0 & 0 & \alpha_2 & -u_9 & 0 & 0 & 0 & 0 & 0 & 0 & 0 & 0 \\
0 & 0 & 0 & 0 & 0 & 0 & u_{10} & -u_{11} & 0 & 0 & 0 & 0 & 0 & 0 & 0 \\
0 & 0 & 0 & 0 & 0 & 0 & 0 & u_{12} & -u_{13} & 0 & 0 & 0 & 0 & 0 & 0 \\
0 & 0 & 0 & 0 & 0 & 0 & 0 & 0 & \alpha_3 & -u_{14} & 0 & 0 & 0 & 0 & 0 \\
0 & 0 & 0 & 0 & 0 & 0 & 0 & 0 & 0 & r_3\delta_3 & u_{15} & 0 & 0 & 0 & 0 \\
0 & 0 & 0 & 0 & 0 & 0 & 0 & 0 & 0 & 0 & 0 & -u_{16} & 0 & 0 & 0 \\
0 & u_{17} & u_{18} & 0 & 0 & 0 & 0 & 0 & 0 & 0 & 0 & u_{19} & -\mu_{z_1} & 0 & 0 \\
0 & 0 & 0 & u_{20} & 0 & u_{21} & u_{22} & u_{23} & 0 & 0 & 0 & 0 & 0 & -\mu_{z_2} & 0 \\
0 & 0 & 0 & u_{24} & 0 & 0 & 0 & 0 & 0 & 0 & 0 & u_{25} & 0 & 0 & -\mu_b
\end{bmatrix}$$

where

$$\begin{aligned}
u_1 &= \beta_1 \frac{\Lambda_h}{\mu_h}, \quad u_2 = \alpha_1 + \mu_{ih} + \tau_2 + \sigma_{ih}\frac{\Lambda_{z_1}}{\mu_{z_1}}, \quad u_3 = \delta_1 + \mu_{th} + \tau_2 + \sigma_{th}\frac{\Lambda_{z_1}}{\mu_{z_1}}, \\
u_4 &= (1-\tau_3)\frac{r_1\delta_1\mu_{z_1}}{\mu_{z_1} + c_1\Lambda_{z_1}}, \quad u_5 = \beta_2\frac{\Lambda_r}{\mu_r} + \sigma_{in}\frac{\Lambda_{z_2}}{\mu_{z_2}} + \mu_m + \tau_5, \quad u_6 = (1-\tau_4)\frac{pr_2\delta_2\mu_{z_2}}{\mu_{z_2} + c_2\Lambda_{z_2}}, \\
u_7 &= \beta_2\frac{\Lambda_r}{\mu_r}, \quad u_8 = \mu_{ir} + \alpha_2 + \tau_6 + \sigma_{ir}\frac{\Lambda_{z_2}}{\mu_{z_2}}, \quad u_9 = \delta_2 + \mu_{tr} + \tau_6 + \sigma_{tr}\frac{\Lambda_{z_2}}{\mu_{z_2}}, \\
u_{10} &= (1-\tau_7)\frac{(1-p)r_2\delta_2\mu_{z_2}}{\mu_{z_2} + c_2\Lambda_{z_2}}, \quad u_{11} = q\omega + \mu_{gb} + \tau_8 + \sigma_{gb}\frac{\Lambda_{z_2}}{\mu_{z_2}}, \quad u_{12} = (1-\tau_9)\rho\omega, \\
u_{13} &= \alpha_3 + \mu_{gm}, \quad u_{14} = \delta_3 + \mu_c, \quad u_{15} = a\nu + \mu_{sm}, \quad u_{16} = \beta_1\frac{\Lambda_h}{\mu_h} + \sigma_{sh}\frac{\Lambda_{z_1}}{\mu_{z_1}} + \mu_{sh}, \\
u_{17} &= c_{ih}\frac{\Lambda_{z_1}}{\mu_{z_1}}, \quad u_{18} = c_{th}\frac{\Lambda_{z_1}}{\mu_{z_1}}, \quad u_{19} = c_{sh}\frac{\Lambda_{z_1}}{\mu_{z_1}}, \quad u_{20} = c_m\frac{\Lambda_{z_2}}{\mu_{z_2}}, \quad u_{21} = c_{ir}\frac{\Lambda_{z_2}}{\mu_{z_2}}, \quad u_{22} = c_{tr}\frac{\Lambda_{z_2}}{\mu_{z_2}}, \\
u_{23} &= c_{gb}\frac{\Lambda_{z_2}}{\mu_{z_2}}, \quad u_{24} = \eta_1\frac{\Lambda_{z_1}}{\pi_{sh}\mu_{z_1}}, \quad u_{25} = \eta_2\frac{\Lambda_{z_2}}{\pi_m\mu_{z_2}}
\end{aligned} \tag{5.13}$$

Local stability of a MFE, E^{02}, is examined by using the signs of real part of eigenvalues of the Jacobian matrix of the system evaluated at E^{02}. The Jacobian matrix of the system (5.1a)-(5.1o) at the MFE is denoted by $J(E^{02})$. The MFE is locally assympotically stable if and only if all eigenvalues of $J(E^{02})$ have negative real parts. Evidently, $-\mu_h$, $-\mu_r$, $-u_{15}$, $-\mu_{z_1}$, $-\mu_{z_2}$ and $-\mu_b$ are negative eigenvalues of $J(E^{02})$. The other remaining eigenvalues are obtained from a 9×9 submatrix, $J_1(E^{02})$, given by

$$J_1(E^{02}) = \begin{bmatrix}
-u_2 & 0 & 0 & 0 & 0 & 0 & 0 & 0 & u_1 \\
\alpha_1 & -u_3 & 0 & 0 & 0 & 0 & 0 & 0 & 0 \\
0 & u_4 & -u_5 & 0 & u_6 & 0 & 0 & 0 & 0 \\
0 & 0 & u_7 & -u_8 & 0 & 0 & 0 & 0 & 0 \\
0 & 0 & 0 & \alpha_2 & -u_9 & 0 & 0 & 0 & 0 \\
0 & 0 & 0 & 0 & u_{10} & -u_{11} & 0 & 0 & 0 \\
0 & 0 & 0 & 0 & 0 & u_{12} & -u_{13} & 0 & 0 \\
0 & 0 & 0 & 0 & 0 & 0 & \alpha_3 & -u_{14} & 0 \\
0 & 0 & 0 & 0 & 0 & 0 & 0 & 0 & -u_{16}
\end{bmatrix}$$

Clearly. it is observed from eighth column of $J_1(E^{02})$ that $-u_{14}$ is another negative eigenvalue. Further reduction on $J_1(E^{02})$, gives us an 8×8 submatrix given by

$$J_2(E^{02}) = \begin{bmatrix} -u_2 & 0 & 0 & 0 & 0 & 0 & 0 & u_1 \\ \alpha_1 & -u_3 & 0 & 0 & 0 & 0 & 0 & 0 \\ 0 & u_4 & -u_5 & 0 & u_6 & 0 & 0 & 0 \\ 0 & 0 & u_7 & -u_8 & 0 & 0 & 0 & 0 \\ 0 & 0 & 0 & \alpha_2 & -u_9 & 0 & 0 & 0 \\ 0 & 0 & 0 & 0 & u_{10} & -u_{11} & 0 & 0 \\ 0 & 0 & 0 & 0 & 0 & u_{12} & -u_{13} & 0 \\ 0 & 0 & 0 & 0 & 0 & 0 & 0 & -u_{16} \end{bmatrix}$$

where another eigenvalue $-u_{13}$ is obtained. A reduction of $J_2(E^{02})$ leads us to a 7×7 submatrix given

$$J_3(E^{02}) = \begin{bmatrix} -u_2 & 0 & 0 & 0 & 0 & 0 & u_1 \\ \alpha_1 & -u_3 & 0 & 0 & 0 & 0 & 0 \\ 0 & u_4 & -u_5 & 0 & u_6 & 0 & 0 \\ 0 & 0 & u_7 & -u_8 & 0 & 0 & 0 \\ 0 & 0 & 0 & \alpha_2 & -u_9 & 0 & 0 \\ 0 & 0 & 0 & 0 & u_{10} & -u_{11} & 0 \\ 0 & 0 & 0 & 0 & 0 & 0 & -u_{16} \end{bmatrix}$$

From sixth column of $J_3(E^{01})$ we obtained another negative eigenvalue which is $-u_{11}$, and a new submatrix obtained after reduction is

$$J_4(E^{02}) = \begin{bmatrix} -u_2 & 0 & 0 & 0 & 0 & u_1 \\ \alpha_1 & -u_3 & 0 & 0 & 0 & 0 \\ 0 & u_4 & -u_5 & 0 & u_6 & 0 \\ 0 & 0 & u_7 & -u_8 & 0 & 0 \\ 0 & 0 & 0 & \alpha_2 & -u_9 & 0 \\ 0 & 0 & 0 & 0 & 0 & -u_{16} \end{bmatrix}$$

Signs for other remaining six eigenvalues are investigated using the trace-determinant technique. If the traceof $J_4(E^{02})$ is strictly negative and determinat of $J_4(E^{02})$ is strictly positive, then all eigenvalues of $J_4(E^{02})$ have negative real parts. Using MAPLE 12 we obtained the following results:

$$tr(J_4(E^{02})) = -\left[u_2 + u_3 + u_5 + u_8 + u_9 + u_{16}\right] < 0 \tag{5.14}$$

and

$$det(J_4(E^{02})) = (u_2u_3u_{16})(u_5u_8u_9 - \alpha_2u_6u_7) > 0 \tag{5.15}$$

Equation (5.15) holds only if

$$\frac{\alpha_2u_6u_7}{u_5u_8u_9} < 1 \tag{5.16}$$

since all $u's$ given in equation (5.13) are positive.

Substituting the values of u_5, u_6, u_7, u_8, and u_9 as given in equation (5.13) into equation (5.16), we obtain

$$\left[\frac{\beta_2\frac{\Lambda_r}{\mu_r}}{\beta_2\frac{\Lambda_r}{\mu_r} + \sigma_m\frac{\Lambda_z}{\mu_{z2}} + \mu_m + \tau_5}\right]\left[\frac{\alpha_2}{\alpha_2 + \mu_{ir} + \tau_6 + \sigma_{ir}\frac{\Lambda_z}{\mu_{z2}}}\right]\left[\frac{1}{\delta_2 + \mu_{tr} + \tau_6 + \sigma_{tr}\frac{\Lambda_z}{\mu_{z2}}}\right]\left[\frac{(1-\tau_4)pr_2\delta_2}{1 + c_2\frac{\Lambda_z}{\mu_{z2}}}\right] < 1$$

which implies that

$$\mathcal{R}_c < 1 \tag{5.17}$$

Therefore, all eigenvalues of $J(E^{02})$ have negative real parts only if $\mathcal{R}_c < 1$. Consequently, MFE is locally asymptotically stable only if $\mathcal{R}_c < 1$. Hence, we deduce the following theorem.

Theorem 5.7

The malaria-free equilibrium, E^{02}, of the model (5.1a)-(5.1o), is locally asymptotically stable only if $\mathcal{R}_c < 1$ and unstable otherwise.

To establish the global stability of the of MFE, we employed the Metzler matrix theory as described in Castillo-Chávez *et al.* (2002), Mpeshe *et al.* (2014b) and Selemani *et al.* (2016). In this approach we re-write the model (5.1a)-(5.1o) in the form

$$\begin{cases} \frac{dX_n}{dt} = A_1(x)(X_n - X_{E^{02},n}) + A_{12}(x)X_c \\ \frac{dX_c}{dt} = A_2(x)X_c \end{cases}$$

where X_n is the vector of non-transmitting classes and X_c is the vector of transmitting classes. For our model, we have

$$X_n = (H,\ R,\ Z_1,\ Z_2, B) \text{ and } X_c = (I_h,\ T_h,\ M,\ I_r,\ T_r,\ G_b,\ G_m,\ C,\ S_m,\ S_h) \tag{5.18}$$

$$X_{E^{01},n} = \left(\frac{\Lambda_h}{\mu_h}, \frac{\Lambda_r}{\mu_r}, \frac{\Lambda_{z_1}}{\mu_{z_1}}, \frac{\Lambda_{z_2}}{\mu_{z_2}}, 0\right) \tag{5.19}$$

and

$$A_1(x) = \begin{pmatrix} -\mu_h & 0 & 0 & 0 & 0 \\ 0 & -\mu_r & 0 & 0 & 0 \\ 0 & 0 & -\mu_{z_1} & 0 & 0 \\ 0 & 0 & 0 & -\mu_{z_2} & 0 \\ 0 & 0 & 0 & 0 & -\mu_b \end{pmatrix}, \tag{5.20}$$

$$A_{12}(x) = \begin{pmatrix} 0 & 0 & 0 & 0 & 0 & 0 & 0 & 0 & 0 & -d_1 \\ 0 & 0 & -d_2 & 0 & 0 & 0 & 0 & 0 & 0 & 0 \\ d_3 & d_4 & 0 & 0 & 0 & 0 & 0 & 0 & 0 & d_5 \\ 0 & 0 & d_6 & d_7 & d_8 & d_9 & 0 & 0 & 0 & 0 \\ 0 & 0 & d_{10} & 0 & 0 & 0 & 0 & 0 & 0 & d_{11} \end{pmatrix} \tag{5.21}$$

where

$$\begin{aligned} d_1 &= \frac{\beta_1 H}{1+k_1 B}, \quad d_2 = \frac{\beta_2 R}{1+k_2 B}, \quad d_3 = \frac{\epsilon_{ih} Z_1}{1+\pi_{ih} I_h}, \quad d_4 = \frac{\epsilon_{th} Z_1}{1+\pi_{th} T_h}, \quad d_5 = \frac{\epsilon_{sh} Z_1}{1+\pi_{sh} S_h}, \\ d_6 &= \frac{\epsilon_m Z_2}{1+\pi_m M}, \quad d_7 = \frac{\epsilon_{ir} Z_2}{1+\pi_{ir} I_r}, \quad d_8 = \frac{\epsilon_{ir} Z_2}{1+\pi_{tr} T_r}, d_9 = \frac{\epsilon_{gb} Z_2}{1+\pi_{gb} G_b}, \quad d_{10} = \frac{\eta_2 Z_2}{1+\pi_m M}, \\ d_{11} &= \frac{\eta_1 Z_1}{1+\pi_{sh} S_h} \end{aligned} \tag{5.22}$$

and

$$A_2(x) = \begin{pmatrix} -w_1 & 0 & 0 & 0 & 0 & 0 & 0 & 0 & 0 & w_2 \\ \alpha_1 & -w_3 & 0 & 0 & 0 & 0 & 0 & 0 & 0 & 0 \\ 0 & w_4 & -w_5 & 0 & w_6 & 0 & 0 & 0 & 0 & 0 \\ 0 & 0 & w_7 & -w_8 & 0 & 0 & 0 & 0 & 0 & 0 \\ 0 & 0 & 0 & \alpha_2 & -w_9 & 0 & 0 & 0 & 0 & 0 \\ 0 & 0 & 0 & 0 & w_{10} & -w_{11} & 0 & 0 & 0 & 0 \\ 0 & 0 & 0 & 0 & 0 & w_{12} & -w_{13} & 0 & 0 & 0 \\ 0 & 0 & 0 & 0 & 0 & 0 & \alpha_3 & -w_{14} & 0 & 0 \\ 0 & 0 & 0 & 0 & 0 & 0 & 0 & w_{15} & -w_{16} & 0 \\ 0 & 0 & 0 & 0 & 0 & 0 & 0 & 0 & w_{17} & -w_{18} \end{pmatrix} \tag{5.23}$$

where

$$\begin{aligned} w_1 &= \alpha_1 + \mu_{ih} + \tau_2 + \frac{\sigma_{ih} Z_1}{1+\pi_{ih} I_h}, \quad w_2 = (1-\tau_1)\frac{\beta_1 H}{1+k_1 B}, \quad w_3 = \delta_1 + \mu_{th} + \tau_2 + \frac{\sigma_{th} Z_1}{1+\pi_{th} T_h}, \\ w_4 &= (1-\tau_3)\frac{r_1 \delta_1}{1+c_1 Z_1}, \quad w_5 = \mu_m + \tau_5 + \frac{\beta_2 R}{1+k_2 B} + \frac{\sigma_m Z_2}{1+\pi_m M}, \quad w_6 = (1-\tau_4)\frac{p r_2 \delta_2}{1+c_2 Z_2}, \\ w_7 &= \frac{\beta_2 R}{1+k_2 B}, \quad w_8 = \alpha_2 + \mu_{ir} + \tau_6 + \frac{\sigma_{ir} Z_2}{1+\pi_{ir} I_r}, \quad w_9 = \delta_2 + \mu_{tr} + \tau_6 + \frac{\sigma_{tr} Z}{1+\pi_{tr} T_r}, \\ w_{10} &= ((1-\tau_7))\frac{(1-p) r_2 \delta_2}{1+c_2 Z_2}, \quad w_{11} = q\omega + \mu_{gb} + \tau_8 + \frac{\sigma_{gb} Z_2}{1+\pi_{gb} G_b}, \quad w_{12} = (1-\tau_9)\frac{\rho q \omega}{1+k_3 B}, \\ w_{13} &= \alpha_3 + \mu_{gm}, \quad w_{14} = \delta_3 + \mu_c, \quad w_{15} = r_3 \delta_3, \quad w_{16} = a\nu + \mu_{sm}, \quad w_{17} = \frac{abv}{S_m}, \\ w_{18} &= \frac{\beta_1 H}{1+k_1 B} + \frac{\sigma_{sh} Z_1}{1+\pi_{sh} S_h} + \mu_{sh} \end{aligned} \tag{5.24}$$

It can easily be observed from (5.20) that, all eigenvalues of A_1 are real and negative.

So, the system

$$\frac{dX_n}{dt} = A_1(x)(X_n - X_{E^{02}{}_n}) + A_{12}(x) X_e$$

is globally asymptotically stable at E^{02}. It can be observed from (5.23) and (5.24) that all off diagonal elements of A_2 are non-negative. Therefore, A_2 is a Metzler matrix. To establish the global asymptotic stability of MFE, we have to show that A_2 is Metzler stable matrix (all its diagonal elements are negative) by proving the following lemma as described in Dumont *et al.* (2008) and Kamgang and Sallet (2008).

Lemma 5.3

Let M be a square Metzler matrix written in block form $M = \begin{pmatrix} M_{11} & M_{12} \\ M_{21} & M_{22} \end{pmatrix}$ with M_{11} and M_{22} square matrices. M is Metzler stable if and only if matrices M_{11} and $M_{22} - M_{21}M_{11}^{-1}M_{12}$ are Metzler stable.

From equation (5.23) we have $M = A_2$ and $M_{11} = \begin{pmatrix} -w_1 & 0 & 0 & 0 & 0 \\ \alpha_1 & -w_3 & 0 & 0 & 0 \\ 0 & w_4 & -w_5 & 0 & w_6 \\ 0 & 0 & w_7 & -w_8 & 0 \\ 0 & 0 & 0 & \alpha_2 & -w_9 \end{pmatrix}$

$$M_{12} = \begin{pmatrix} 0 & 0 & 0 & 0 & w_2 \\ 0 & 0 & 0 & 0 & 0 \\ 0 & 0 & 0 & 0 & 0 \\ 0 & 0 & 0 & 0 & 0 \\ 0 & 0 & 0 & 0 & 0 \end{pmatrix}, \quad M_{21} = \begin{pmatrix} 0 & 0 & 0 & 0 & w_2 \\ 0 & 0 & 0 & 0 & 0 \\ 0 & 0 & 0 & 0 & 0 \\ 0 & 0 & 0 & 0 & 0 \\ 0 & 0 & 0 & 0 & 0 \end{pmatrix}$$

and $M_{22} = \begin{pmatrix} -w_{11} & 0 & 0 & 0 & 0 \\ w_{12} & -w_{13} & 0 & 0 & 0 \\ 0 & \alpha_3 & -w_{14} & 0 & 0 \\ 0 & 0 & w_{15} & -w_{16} & 0 \\ 0 & 0 & 0 & w_{17} & -w_{18} \end{pmatrix}$

Hence

$$M_{22} - M_{21}M_{11}^{-1}M_{12} = \begin{pmatrix} -w_{11} & 0 & 0 & 0 & \frac{\alpha_1\alpha_2 w_{10}w_7w_4w_2}{w_1w_3(w_5w_8w_9 - \alpha_2 w_6w_7)} \\ w_{12} & -w_{13} & 0 & 0 & 0 \\ 0 & \alpha_3 & -w_{14} & 0 & 0 \\ 0 & 0 & w_{15} & -w_{16} & 0 \\ 0 & 0 & 0 & w_{17} & -w_{18} \end{pmatrix}$$

Clearly, M_{11} is Metzler stable matrix. But, $M_{22} - M_{21}M_{11}^{-1}M_{12}$ is Metzler stable matrix only if

$$\frac{\alpha_1\alpha_2 w_{10}w_7w_4w_2}{w_1w_3(w_5w_8w_9 - \alpha_2w_6w_7)} \geq 0 \tag{5.25}$$

It is observed that equation (5.25) holds only when

$$\frac{\alpha_2 w_6 w_7}{w_5 w_8 w_9} < 1 \tag{5.26}$$

When the expressions for w_5, w_6, w_7, w_8 and w_9 given in equation (5.24) are evaluated at MFE, obtain the following expressions

$$\begin{aligned} w_5 &= \mu_m + \tau_5 + \frac{\beta_2\Lambda_r}{\mu_r} + \frac{\sigma_{mz}\Lambda_z}{\mu_z}, \quad w_6 = \frac{(1-\tau_4)pr_2\delta_2\mu_z}{\mu_z + c_2\Lambda_z}, \quad w_7 = \frac{\beta_2\Lambda_r}{\mu_r}, \\ w_8 &= \alpha_2 + \mu_{ir} + \tau_6 + \frac{\sigma_{ir}\Lambda_z}{\mu_z}, \quad w_9 = \delta_2 + \mu_{tr} + \tau_6 + \frac{\sigma_{tr}\Lambda_z}{\mu_z} \end{aligned} \tag{5.27}$$

Now substituting equation (5.27) in equation (5.26), we obtain

$$\frac{\alpha_2 \frac{(1-\tau_4)pr_2\delta_2\mu_z}{\mu_z + c_2\Lambda_z}\frac{\beta_2\Lambda_r}{\mu_r}}{\left(\mu_m + \tau_5 + \frac{\beta_2\Lambda_r}{\mu_r} + \frac{\sigma_{mz}\Lambda_z}{\mu_z}\right)\left(\alpha_2 + \mu_{ir} + \tau_6 + \frac{\sigma_{ir}\Lambda_z}{\mu_z}\right)\left(\delta_2 + \mu_{tr} + \tau_6 + \frac{\sigma_{tr}\Lambda_z}{\mu_z}\right)} < 1 \tag{5.28}$$

equivalently

$$\mathcal{R}_e < 1 \tag{5.29}$$

which leads us to the following theorem.

Theorem 5.8

A MFE, E^{02} of the model (5.1a)-(5.1o) is globally asymptotically stable in $\mathcal{D}$ if $\mathcal{R}_e < 1$ and unstable if $\mathcal{R}_e > 1$

5.3.5 Existence and Stability of Malaria Infection Equilibrium

Theorem 5.8 suggests the existence of malaria-infection equilibrium (MIE), E_2^*, given by

$$E_2^* = (H^*, I_h^*, T_h^*, M^*, R^*, I_r^*, T_r^*, G_b^*, G_m^*, C^*, S_m^*, S_h^*, Z_1^*, Z_2^*, B^*)$$

only if $\mathcal{R}_e > 1$.

Owing to the complexity of the model system (5.1a)-(5.1o). it found to be difficult to express MIE explicitly. Therefore, the existence and stability are established numerically in the next section.

5.4 Numerical Simulations and Discussions

In this section, we performed numerical simulations of the model (5.1a)-(5.1o) to investigate the dynamics of model using MATLAB symbolic package. In the simulation of this model, initial values are assummed to allow computer executions, and their values are as listed in Table 11

Table 11 :Initial values of variables of the model (5.1a)-(5.1o)

Variable	H	I_h	T_h	M	R	I_r	T_r	G_b	G_m	C	S_m	S_h	Z_1	Z_2	B
Initial values	3 000	0	0	2 000	50 0000	0	1 000	3 000	1 500	1 000	2 000	2 000	10	10	0

One of the demanding work in the study of *in vivo* models is estimation of parameter values (Chiyaka *et al.*, 2008). The values of parameters used in simulations of this model are presented in Table 12. Most of these values are taken from some of related works among the existing literature, while some values are assumed.

The reason as to why some parameters values are assumed is that, mathematical modelling on the entire life cycle of *plasmodium* is just on start up or the values found on existing literatures are not suitable for this model. However, the accuracy of parameter values is not of the great importance, rather their impact on reproduction number, a key parameter that gives clues on how and where to target to eradicate or control infection (Chiyaka *et al.*, 2008).

Table 12 :Parameters estimates for the model (5.1a)-(5.1o)

Par	Description	Value	References
a :	probability that a bite infects human	0.75	(Laxminarayan, 2004)
b :	number of mosquito bites per individual	$15day^{-1}$	(Selemani *et al.*, 2016)
ν :	number of sporozoites injected per bite	10 – 20	(Nelson and Williams, 2014)
β_1 :	infection rate of HLCs by sporozoites	0.001 $\mu lc^{-1}d^{-1}$	(Selemani *et al.*, 2016)
r_1 :	number of merozoites per liver schizont	10 000	(Tumwiine *et al.*, 2014)
α_1 :	progression rate of infected HCLs		
	to schizonts	0.125 day^{-1}	(Selemani *et al.*, 2016)
δ_1 :	rupture rate of liver schizonts	0.097 5 day^{-1}	(Selemani *et al.*, 2016)
Λ_h :	the recruitmet rate of HLCs	3 000 $c\mu l^{-1}d^{-1}$	(Selemani *et al.*, 2016)
μ_h :	natural death rate of uninfected HLCs	0.94 day^{-1}	(Selemani *et al.*, 2016)
μ_{ih} :	death rate of infected HLCs	0.95 day^{-1}	(Selemani *et al.*, 2016)
μ_{th} :	death rate of liver-schizonts	0.029 day^{-1}	(Selemani *et al.*, 2016)
β_2 :	infection rate of RBCs by merozoites	2×10^{-6} $\mu lc^{-1}d^{-1}$	(Selemani *et al.*, 2016)
δ_2 :	rupture rate of blood schizonts	0.115 d^{-1}	(Selemani *et al.*, 2016)
α_2 :	progression rate of infected RBCs		
	to schizonts	0.145 d^{-1}	(Selemani *et al.*, 2016)
r_2 :	number of merozoites per blood schizont	16	(Dube *et al.*, 2010)
q :	probability that a bite is infectious		
	to mosquito	0.09	(Agusto *et al.*, 2012)
ω :	number of gametocytes ingested per bite	10	(Selemani *et al.*, 2016)
ρ :	number of bites made by mosquito		
	in its lifetime	3	(Selemani *et al.*, 2016)
Λ_r :	the recruitmet rate of RBCs	41 500 $c\mu l^{-1}d^{-1}$	(Li *et al.*, 2011)
μ_r :	death rate of uninfected RBCs	0.02 d^{-1}	(Dube *et al.*, 2010)
μ_{ir} :	total death rate of uninfected RBCs	0.025 d^{-1}	(Diebner *et al.*, 2000)
μ_{tr} :	death rate of blood-schizonts	0.185	(Selemani *et al.*, 2016)
μ_m :	death rate of merozoites	48 d^{-1}	(Li *et al.*, 2011)
μ_{gh} :	death rate of gametocytes	$6.25 \times 10^{-5}d^{-1}$	(Selemani *et al.*, 2016)
δ_3 :	rupture rate of Oocysts	0.05 day^{-1}	(Selemani *et al.*, 2016)
r_3 :	number of sporozoites per Oocyst	10 00	(Nelson and Williams, 2014)
α_3 :	progresion rate of gametes to Oocysts	0.07 d^{-1}	(Selemani *et al.*, 2016)
μ_{gm} :	death rate of gametes	0.052 d^{-1}	(Selemani *et al.*, 2016)
μ_c :	death rate of Oocysts	0.024 d^{-1}	(Selemani *et al.*, 2016)
μ_{sm} :	death rate of sporozoites in mosqouito	40 d^{-1}	(Selemani *et al.*, 2016)
μ_{sh} :	death rate of sporozoites in human liver	1.2×10^{-11} d^{-1}	(Selemani *et al.*, 2016)
p :	proportion of asexual that differentiate		
	to merozoites	0.926	(Selemani *et al.*, 2016)
Λ_{z_1} :	the recruitmet rate of immune cells in the liver	30 $c\mu l^{-1}d^{-1}$	(Selemani *et al.*, 2017)
Λ_{z_2} :	the recruitmet rate of immune cells in the blood	30 $c\mu l^{-1}d^{-1}$	(Chiyaka *et al.*, 2008)
μ_{z_1} :	death rate of immune cells	1.5	(Selemani *et al.*, 2017)
μ_{z_2} :	death rate of immune cells	1.53	(Chiyaka *et al.*, 2008)

Continued on next page

Table 12 – *Continued from previous page*

Par	Description	Value	References
μ_b :	deterioration rate of antibodies	0.4	(Chiyaka *et al.*, 2008)
c_1 :	efficiency of immune cells to suppress the production of M from liver-schizonts	10^{-5}	(Selemani *et al.*, 2017)
c_2 :	efficiency of immune cells to suppress the production of M from blood-schizonts	3×10^{-5}	(Selemani *et al.*, 2017)
k_1 :	efficiency of immune cells to inhibit invasion of HLCs by sporozoites	0.035	(Selemani *et al.*, 2017)
k_2 :	efficiency of immune cells to inhibit invasion of RBCs by merozoites	0.001 5	(Selemani *et al.*, 2017)
k_3 :	efficiency of immune cells to mediate lysis of gametocytes and inhibit fertilization	0.03	(Selemani *et al.*, 2017)
σ_{sh} :	rate at which sporozoites are cleared by immune cells	9×10^{-9}	(Selemani *et al.*, 2017)
σ_{ih} :	rate at which infected HLCs are cleared by immune cells	9×10^{-9}	(Selemani *et al.*, 2017)
σ_{th} :	rate at which liver schizonts are cleared by immune cells	1×10^{-8}	(Selemani *et al.*, 2017)
σ_m :	rate at which merozoites are cleared by immune cells	1×10^{-8}	(Li *et al.*, 2011)
σ_{ir} :	rate at which infected RBCs are cleared by immune cells	1×10^{-8}	(Li *et al.*, 2011)
σ_{tr} :	rate at which blood schizonts are cleared by immune cells	1×10^{-8}	(Selemani *et al.*, 2017)
σ_{gh} :	rate at which gametocytes are cleared by immune cells	1×10^{-8}	(Austin *et al.*, 1998)
ϵ_{sh} :	proliferation rate of immune cells due to contact with sporozoites	5×10^{-5}	(Selemani *et al.*, 2017)
ϵ_{ih} :	proliferation rate of immune cells due to contact with infected HLCs	4.6×10^{-5}	(Selemani *et al.*, 2017)
ϵ_{th} :	proliferation rate of immune cells due to contact with liver schizonts	4.63×10^{-5}	(Selemani *et al.*, 2017)
ϵ_m :	proliferation rate of immune cells due to contact with merozoites	4.69×10^{-5}	(Li *et al.*, 2011)
ϵ_{ir} :	proliferation rate of immune cells due to contact with infected RBCs	2.5×10^{-5}	(Li *et al.*, 2011)
ϵ_{tr} :	proliferation rate of immune cells due to contact with blood schizonts	2.5×10^{-5}	(Selemani *et al.*, 2017)
ϵ_{gh} :	proliferation rate of immune cells due to contact with gametocytes	2.5×10^{-5}	(Selemani *et al.*, 2017)
π_{sh} :	saturation constant of sporozoites	2 000	(Selemani *et al.*, 2017)
π_{ih} :	saturation constant of infected HLCs	2 000	(Selemani *et al.*, 2017)
π_{th} :	saturation constant of liver schizonts	2 000	(Selemani *et al.*, 2017)

Continued on next page

Table 12 – *Continued from previous page*

Par	Description	Value	References
π_m :	saturation constant of merozoites	1 500	(Chiyaka *et al.*, 2008)
π_{ir} :	saturation constant of infected RBCs	2 000	(Chiyaka *et al.*, 2008)
π_{tr} :	saturation constant of blood schizonts	2 000	(Selemani *et al.*, 2017)
η_1 :	maximum rate of increase of antibodies due to presence of sporozoites	1×10^{-4}	(Selemani *et al.*, 2017)
η_2 :	maximum rate of increase of antibodies due to presence of merozoites	4×10^{-4}	(Selemani *et al.*, 2017)

We have done numerical simulations to establish the existence of malaria infection equilibrium (MIE) as stated in previous section. It is observed from Fig. 22a , Fig. 22b, Fig. 22c and Fig. 22d that each variable varies with time and reaches a constant value (i.e., a value at MIE). Therefore, Fig. 22 confirms that malaria-infection equilibrium, E_2^* for the model (5.1a) -(5.1o) exists. Now, let us deduce the stability of E_2^*.

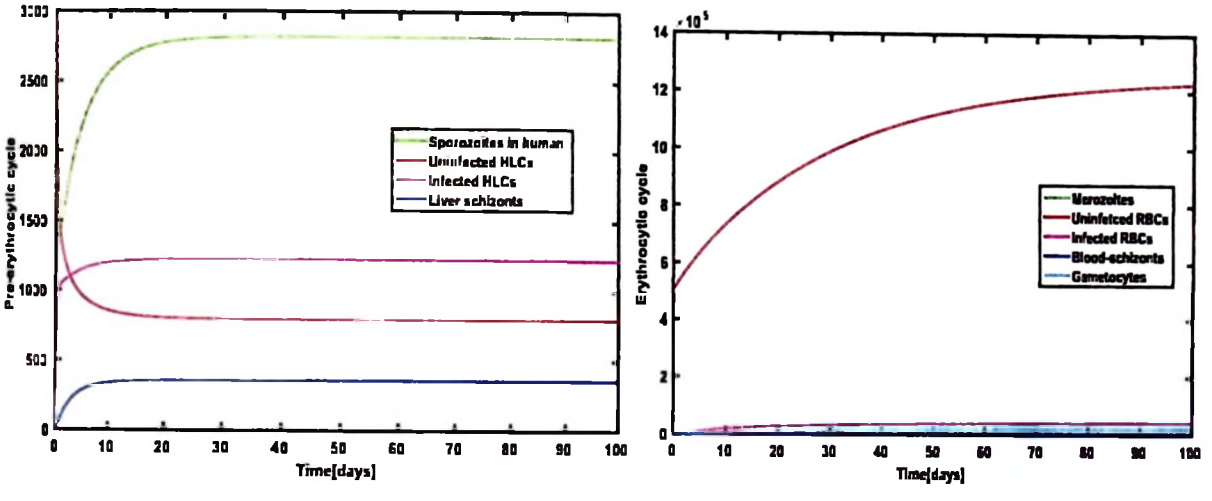

(a) Exo-erythrocytic cycle

(b) Erythrocytic cycle

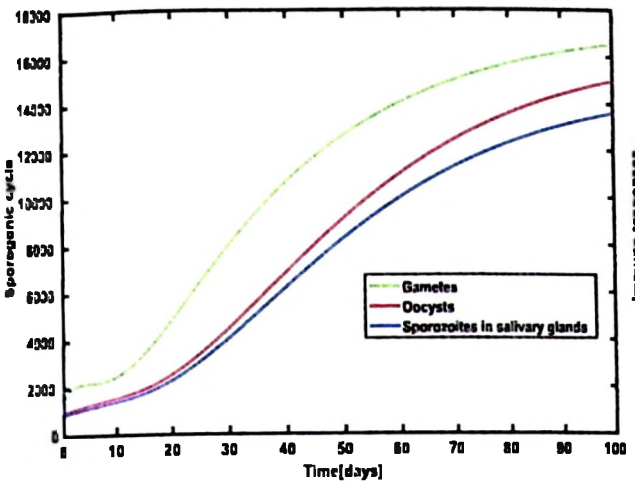

(c) Sporogonic cycle

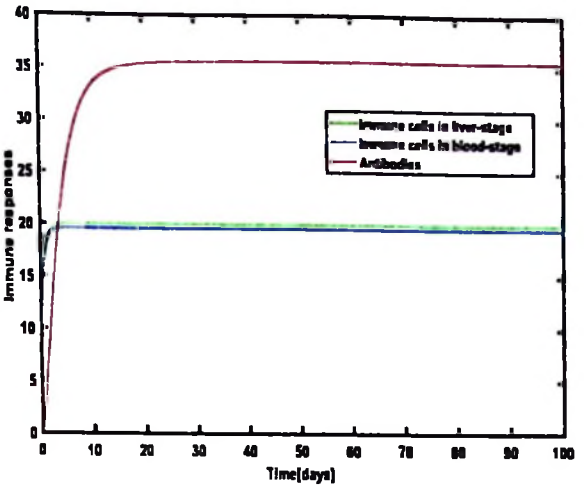

(d) immune responses

Figure 22: Time variation of variables to verify the existence of malaria infection equilibrium

Using some chosen initial values, we observe that each of state variables converges to a certain steady value (a value at MIE) (See Fig. 23). Therefore, we conclude that, malaria infection equilibrium, E_2^* is most likely to be globally asymptotically stable.

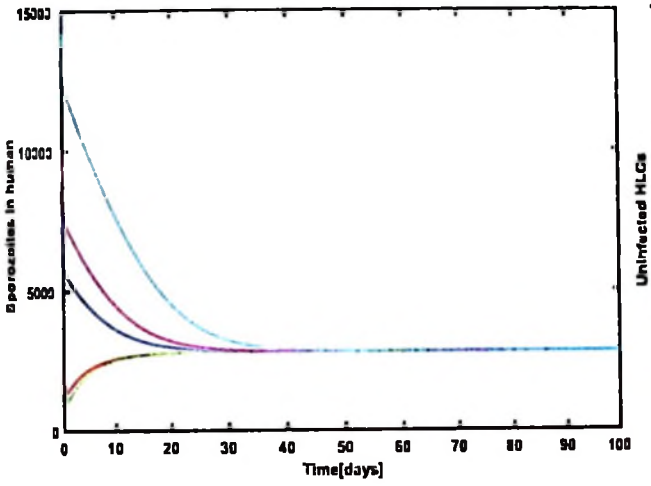

(a) $S_h^0 = 1\,000, 2\,000, 8\,000, 10\,000, 15\,000$

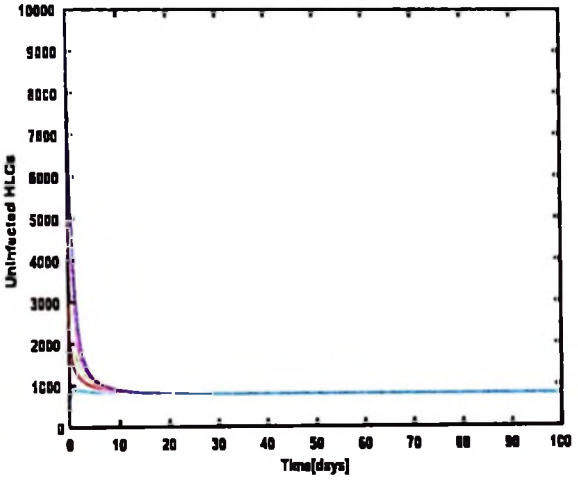

(b) $H^0 = 500, 3\,000, 5\,000, 7\,500, 10\,000$

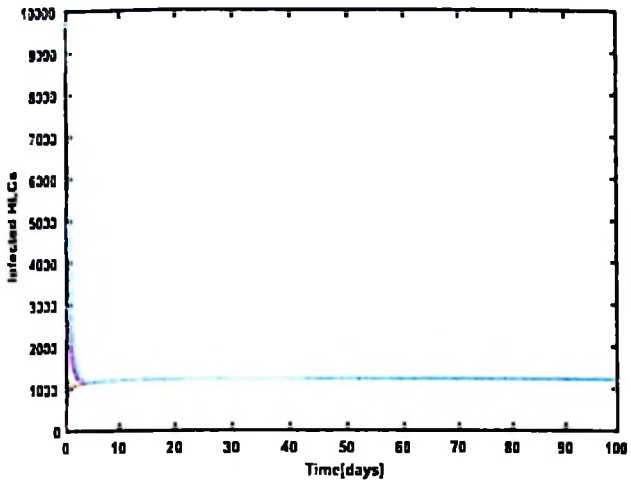

(c) $I_h^0 = 0, 500, 3\,000, 5\,000, 10\,000$

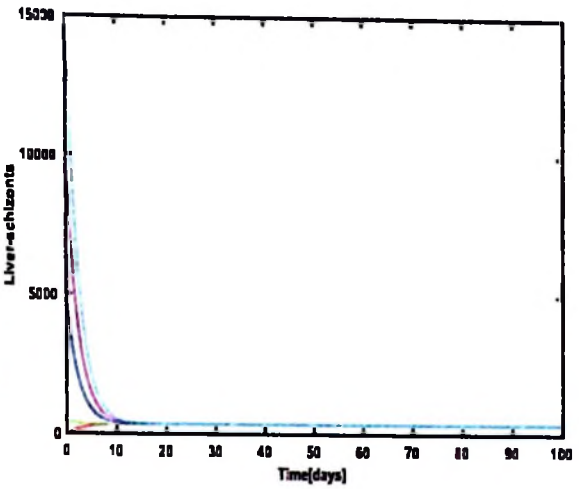

(d) $T_h^0 = 0, 500, 5\,000, 10\,000, 15\,000$

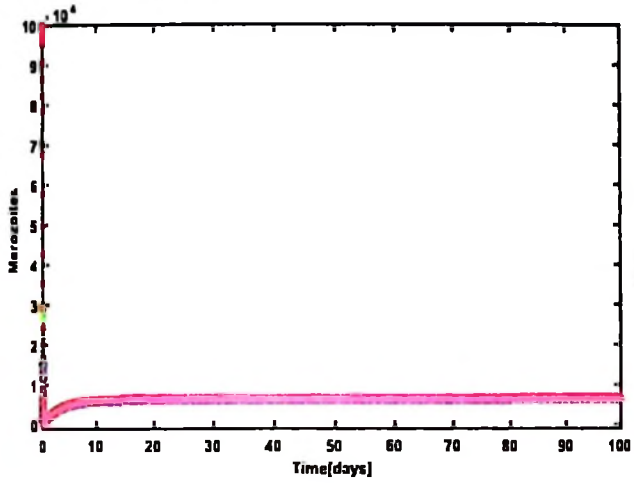

(e) $M^0 = 0, 2\,000, 15\,000, 30\,000, 100\,000$

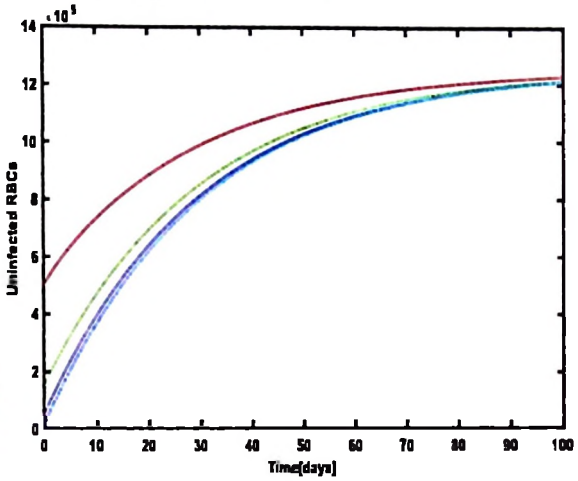

(f) $R^0 = 10\,000, 20\,000, 50\,000, 150\,000, 5\,000\,000$

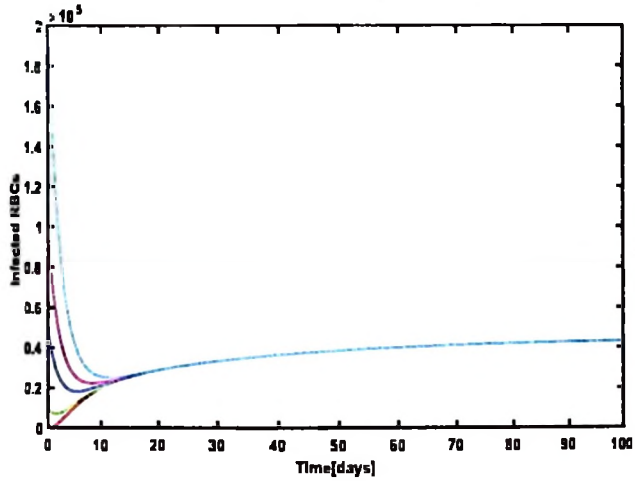

(g) $I_r^0 = 0, 10\,000, 50\,000, 100\,000, 200\,000$

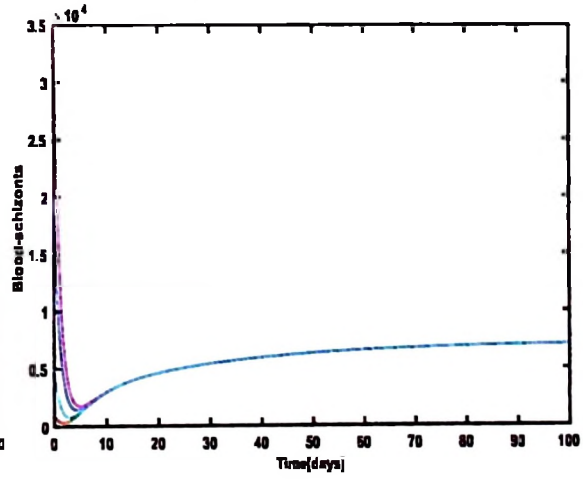

(h) $T_r^0 = 0, 1\,000, 5\,000, 20\,000, 35\,000$

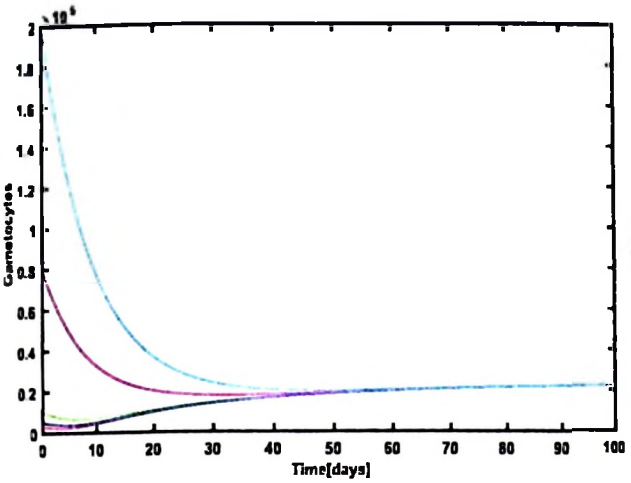

(i) $G_b^0 = 3\,000, 5\,000, 10\,000, 80\,000, 200\,000$

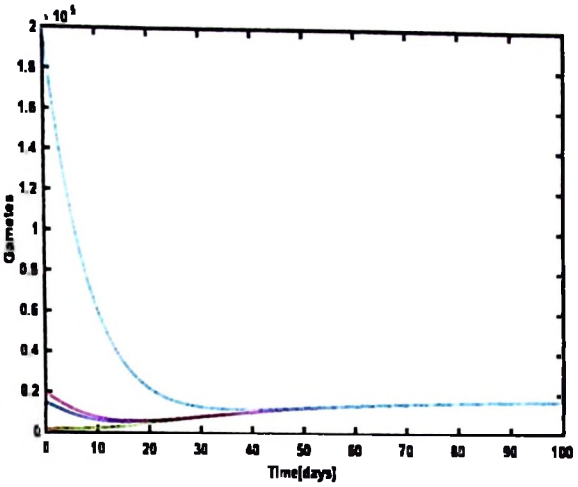

(j) $G_m^0 = 500, 1\,500, 3\,000, 15\,000, 20\,000$

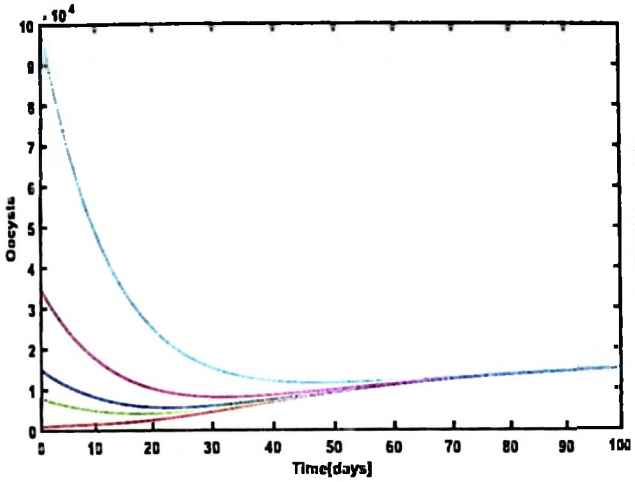

(k) $C^0 = 1\,000, 8\,000, 15\,000, 35\,000, 100;000$

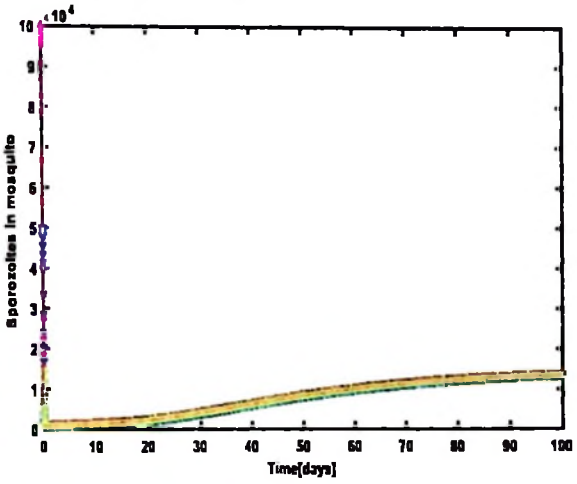

(l) $S_m^0 = 2\,000, 15\,000, 50\,000, 7\,000, 100\,000$

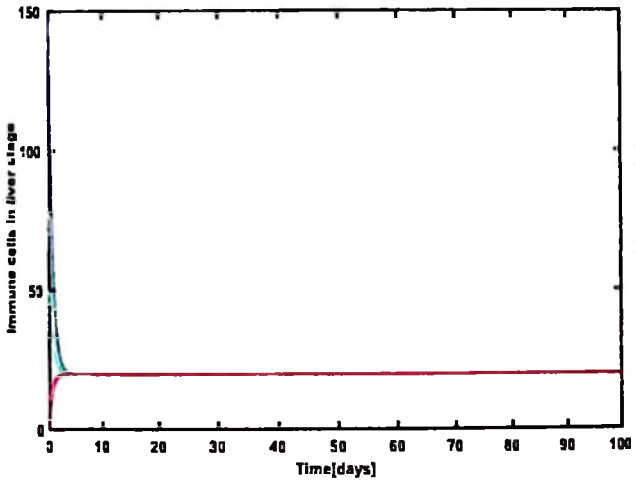

(m) $Z_1^0 = 0, 10, 50, 80, 150$

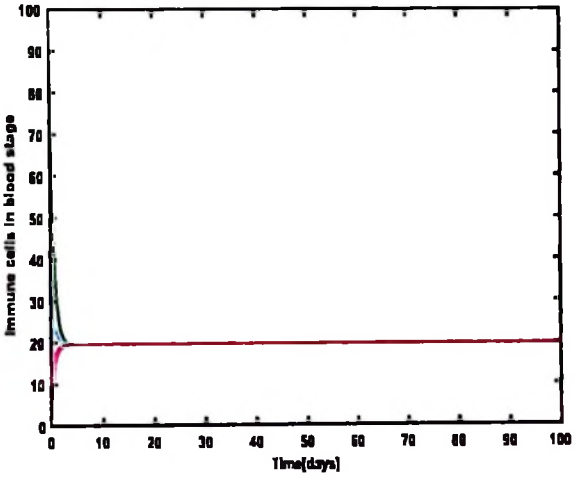

(n) $Z_2^0 = 0, 10, 35, 80, 100$

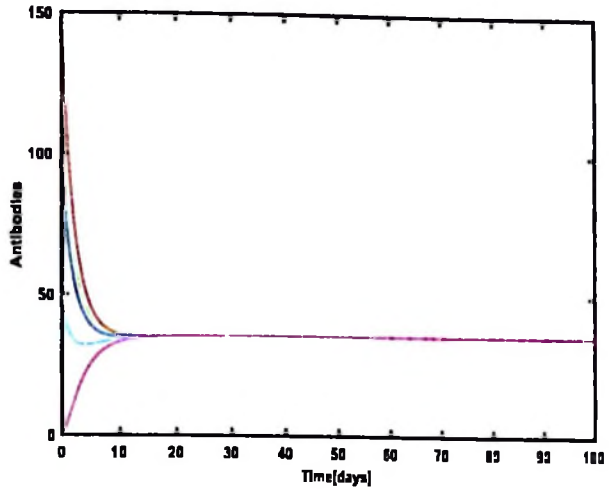

(o) $B^0 = 0, 50, 100, 120, 150$

Figure 23: Numerical simulation to show global stability of MIE of the model (5.1a)-(5.1o)

This model indicates best results compared to those of a basic model (Selemani *et al.*, 2016) and a model with effect of immune response (Selemani *et al.*, 2017) in reducing the malaria infection at erythrocytic and sporogonic stages as depicted in Fig. 24. Fig. 24a and Fig. 24b illustrate the remarkable impact of drug therapy on increasing the number of uninfected RBCs and decreasing the number infected RBCs respectively. Fig. 24c and Fig. 24d respectively portrayed that the use of drug therapy causes the a significant decrease on the number of merozoites and gametocytes while Fig. 24e and Fig. 24f indicate the effect of the drug on reducing the number of gametes and oocysts, which consequently reduce number of sporozoites in mosquito's salivary gland.

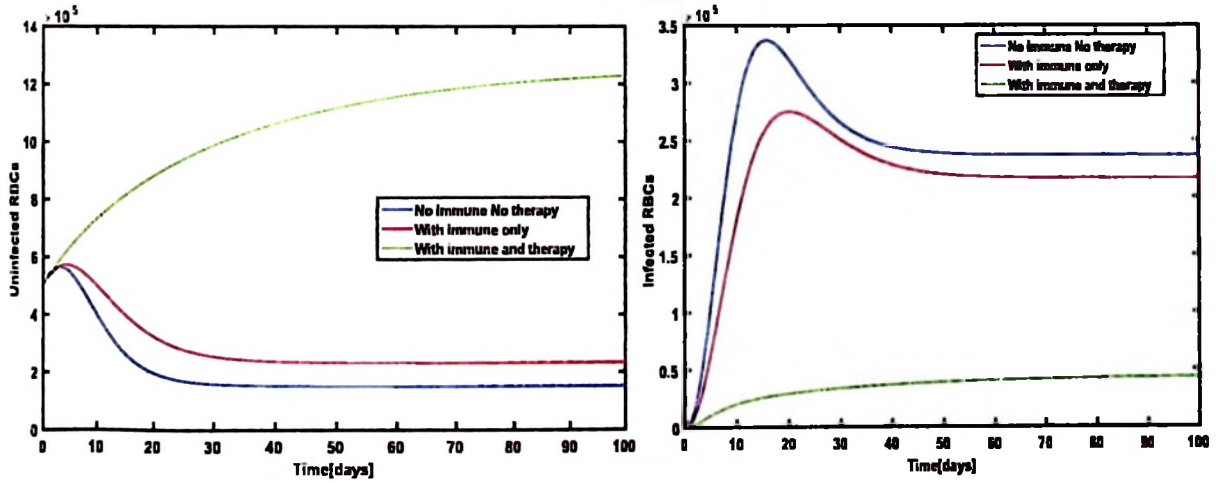

(a) Uninfected RBCs

(b) Infected RBCs

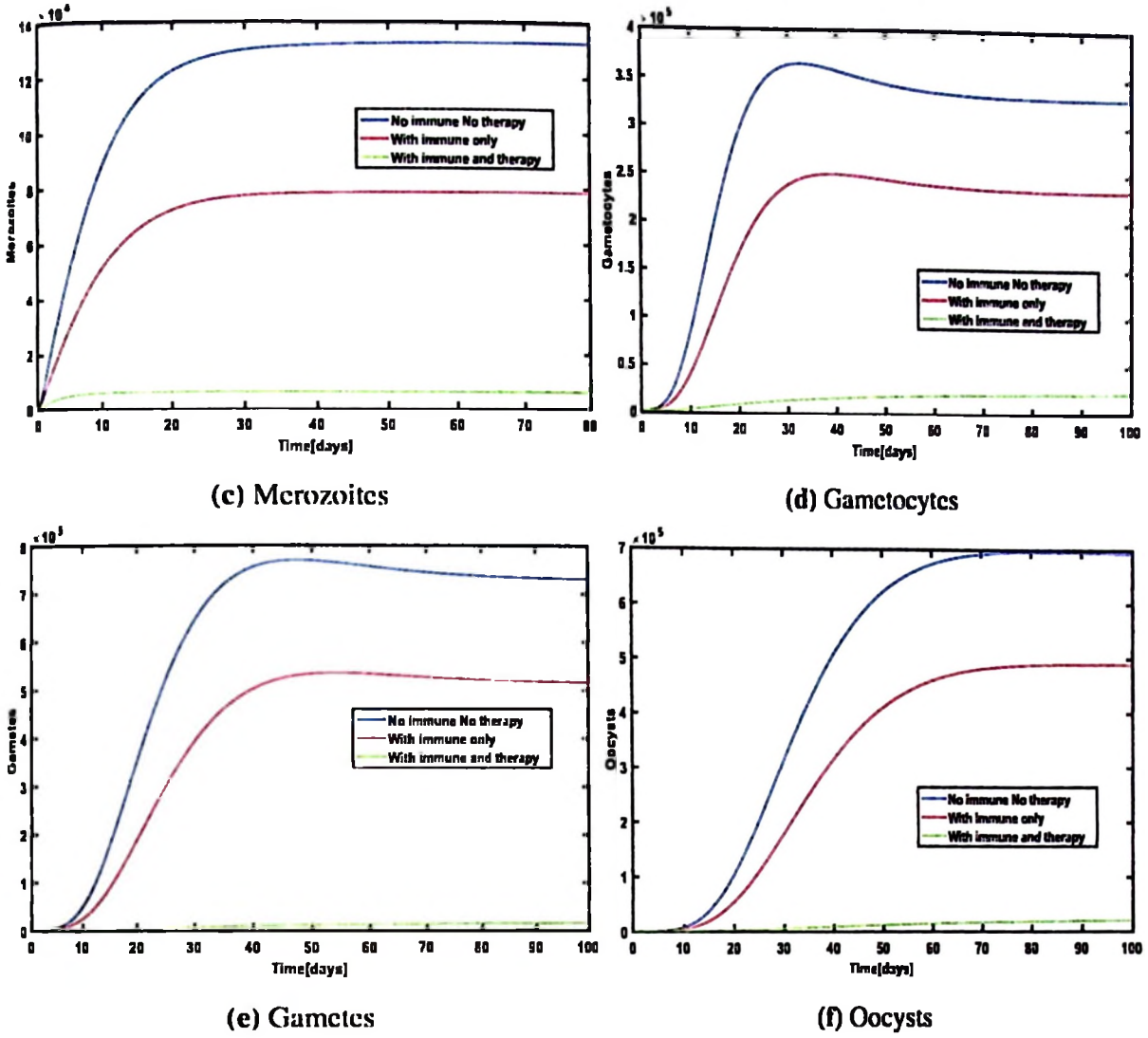

(c) Merozoites (d) Gametocytes

(e) Gametes (f) Oocysts

Figure 24: Effects of immune responses and antimalarial therapy on uninfected RBCs, infected RBCs, merozoites, gametocytes, gametes and oocysts

The exclusion of tissue schizonticidal components from the model evidently indicates that the infection is higher compared to when all drugs components were included. The number of infected RBCs and parasites (merozoites and gametocytes) increased and number of uninfected RBCs decreased markedly after exclusion of tissue schizonticides as indicated in Fig. 25. Also, the number of gametes, oocysts and sporozoites in mosquitos' salivary gland increase as it has been depicted in Fig. 26. This suggests that the tissue schizonticides has high influence in lowering the infection, and the liver stage is one of the best targets for controlling malaria using the chemotherapy, especially that the currently existing drugs target mainly the blood stage of malaria.

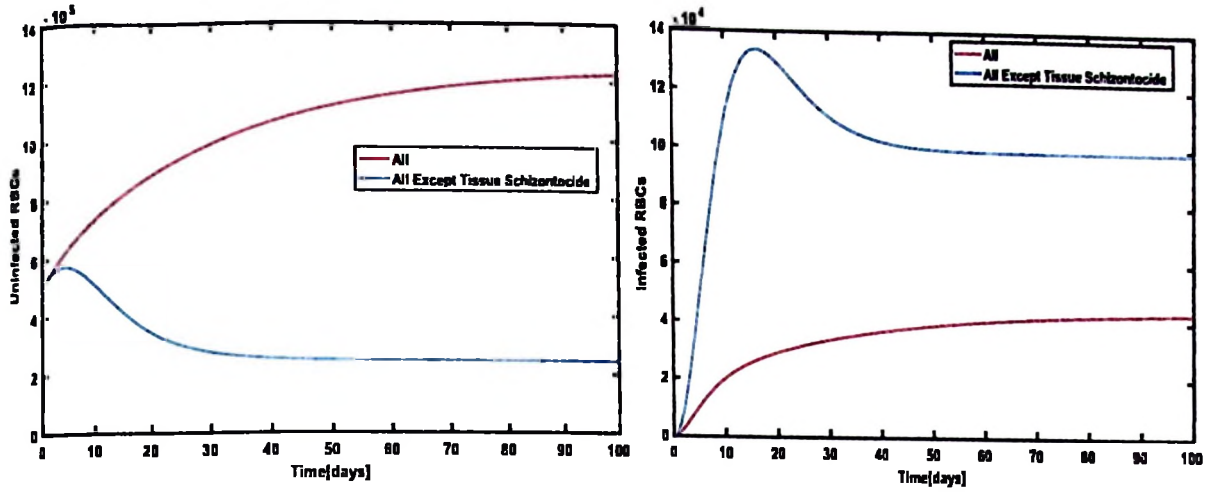

(a) Uninfected RBCs (b) Infected RBCs

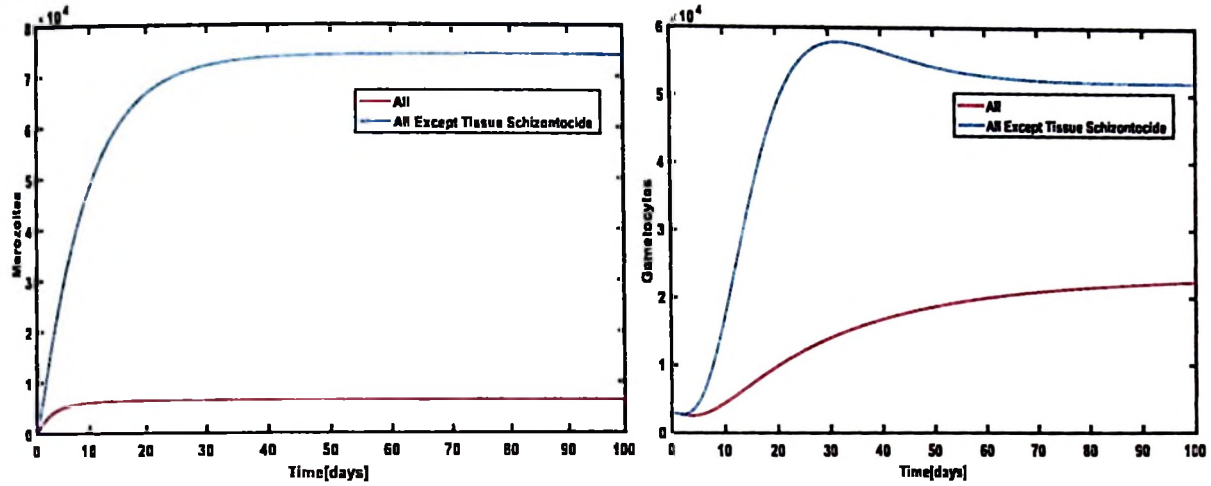

(c) Merozoites (d) Gametocytes

Figure 25: Effects of blood schizonticides, gametocytocides and sporontocides combined therapy on uninfected RBCs, infected RBCs, merozoites and gametocytes

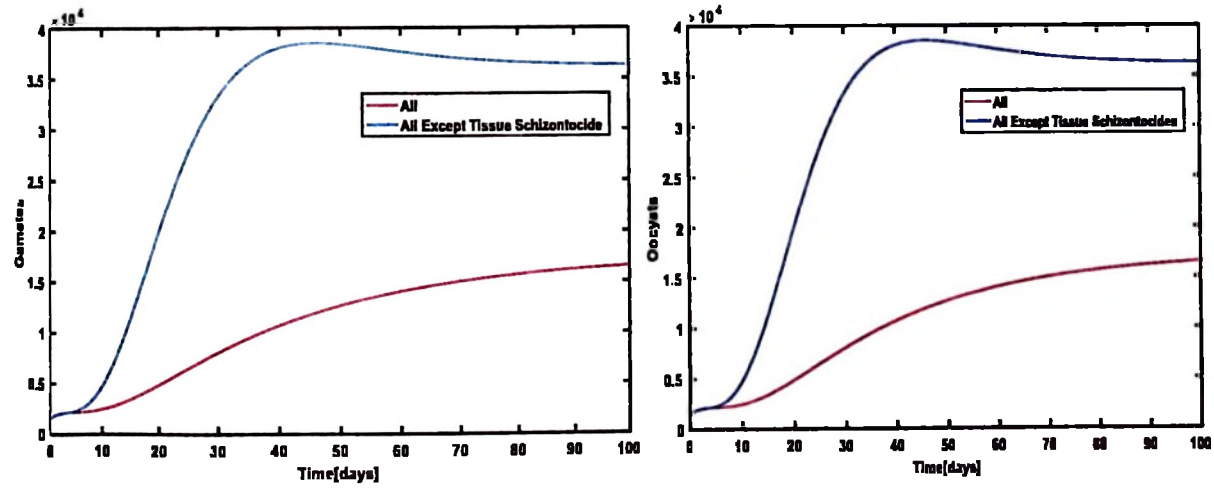

(a) Gametes (b) Oocysts

Figure 26: Effects of blood schizonticides, gametocytocides and sporontocides combined therapy on gametes and oocysts

Moreover, the effect of combined therapy of blood schizonticides with each of other two components (tissue schizonticides and gametocytocides) on reducing the number gametocytes and gametes were investigated. The results indicate that a blood schizonticide-tissue schizonticide CT is more effective in prevention of malaria as it reduces the number of gametocytes and gametes, compared to blood schizonticide-gametocytocide CT as illustrated in Fig. 27. That is to say that, the use tissue schizonticides to prevent initial erythrocytic infection is better than the use of blood schizonticides to treat and/or suppression the clinical attacks and symptoms.

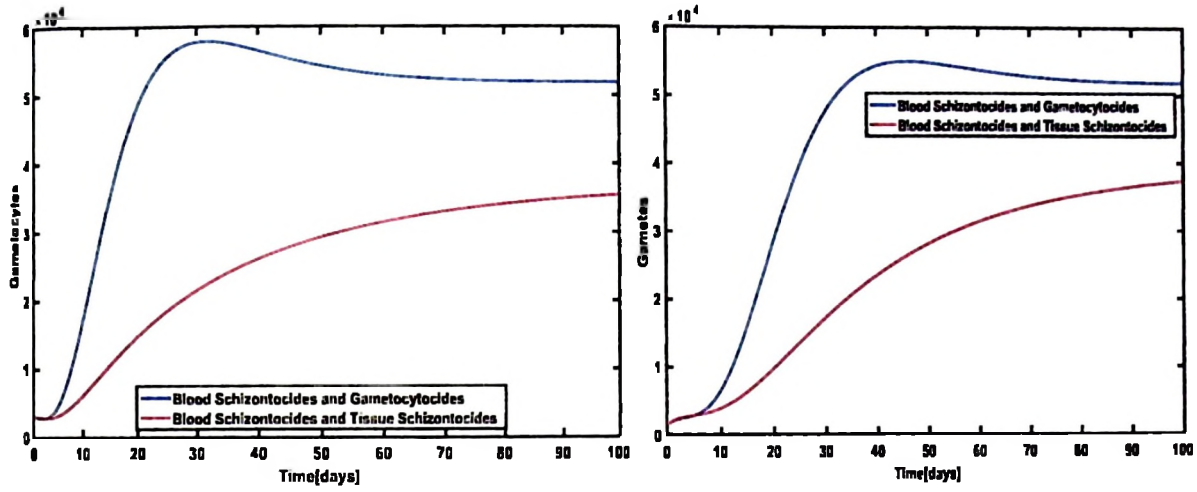

(a) Gametocytes (b) Gametes

Figure 27: Comparison on the effects of blood schizonticide-gametocytocide and blood schizonticide-tissue schizonticide CTs on gametocytes and gametes

In addition to that, the effect of blood schizonticides and its combination with tissue schizonticides on reducing number of merozoites and infected RBCs were compared, and the latter showed the better results as Fig. 28 depicts. That is, elimination of hepatic schizonts and suppression of merozoites from the liver is more efficient in reducing erythrocytic infection.

Moreover, the effect of combined therapy of blood schizonticides with each of other two components (tissue schizonticides and gametocytocides) on reducing the number gametocytes and gametes were investigated. The results indicate that a blood schizonticide-tissue schizonticide CT is more effective in prevention of malaria as it reduces the number of gametocytes and gametes, compared to blood schizonticide-gametocytocide CT as illustrated in Fig. 27. That is to say that, the use tissue schizonticides to prevent initial erythrocytic infection is better than the use of blood schizonticides to treat and/or suppression the clinical attacks and symptoms.

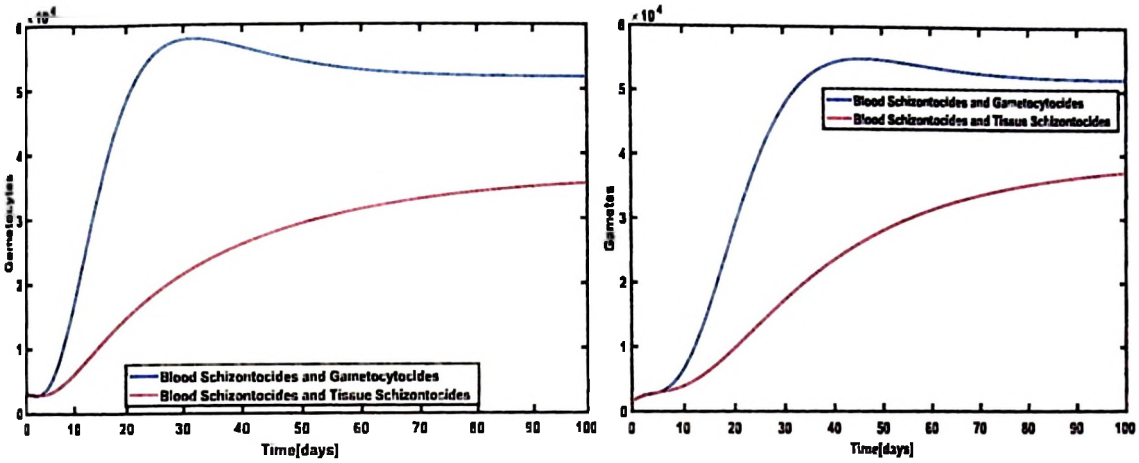

(a) Gametocytes (b) Gametes

Figure 27: Comparison on the effects of blood schizonticide-gametocytocide and blood schizonticide-tissue schizonticide CTs on gametocytes and gametes

In addition to that, the effect of blood schizonticides and its combination with tissue schizonticides on reducing number of merozoites and infected RBCs were compared, and the latter showed the better results as Fig. 28 depicts. That is, elimination of hepatic schizonts and suppression of merozoites from the liver is more efficient in reducing erythrocytic infection.

Moreover, the effect of combined therapy of blood schizonticides with each of other two components (tissue schizonticides and gametocytocides) on reducing the number gametocytes and gametes were investigated. The results indicate that a blood schizonticide-tissue schizonticide CT is more effective in prevention of malaria as it reduces the number of gametocytes and gametes, compared to blood schizonticide-gametocytocide CT as illustrated in Fig. 27. That is to say that, the use tissue schizonticides to prevent initial erythrocytic infection is better than the use of blood schizonticides to treat and/or suppression the clinical attacks and symptoms.

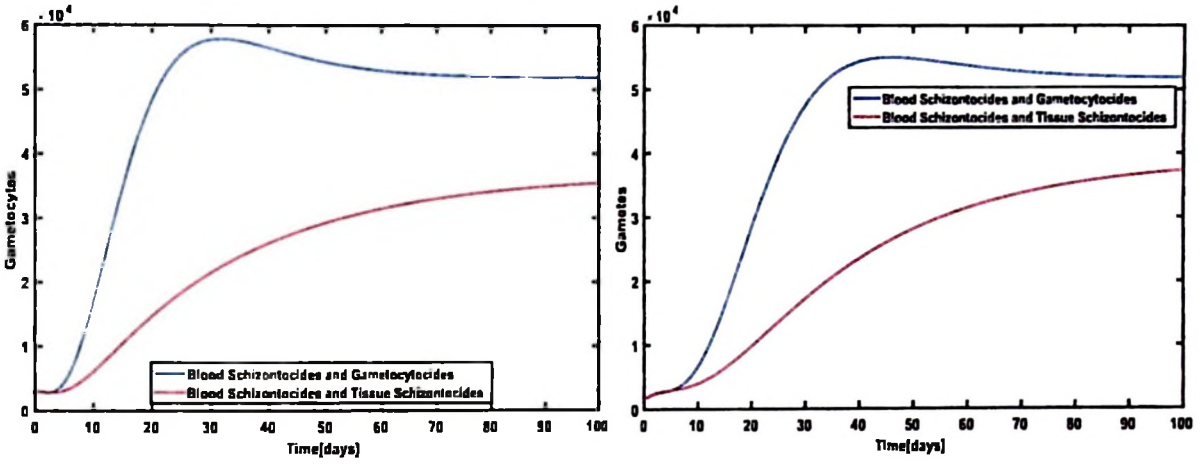

(a) Gametocytes (b) Gametes

Figure 27: Comparison on the effects of blood schizonticide-gametocytocide and blood schizonticide-tissue schizonticide CTs on gametocytes and gametes

In addition to that, the effect of blood schizonticides and its combination with tissue schizonticides on reducing number of merozoites and infected RBCs were compared, and the latter showed the better results as Fig. 28 depicts. That is, elimination of hepatic schizonts and suppression of merozoites from the liver is more efficient in reducing erythrocytic infection.

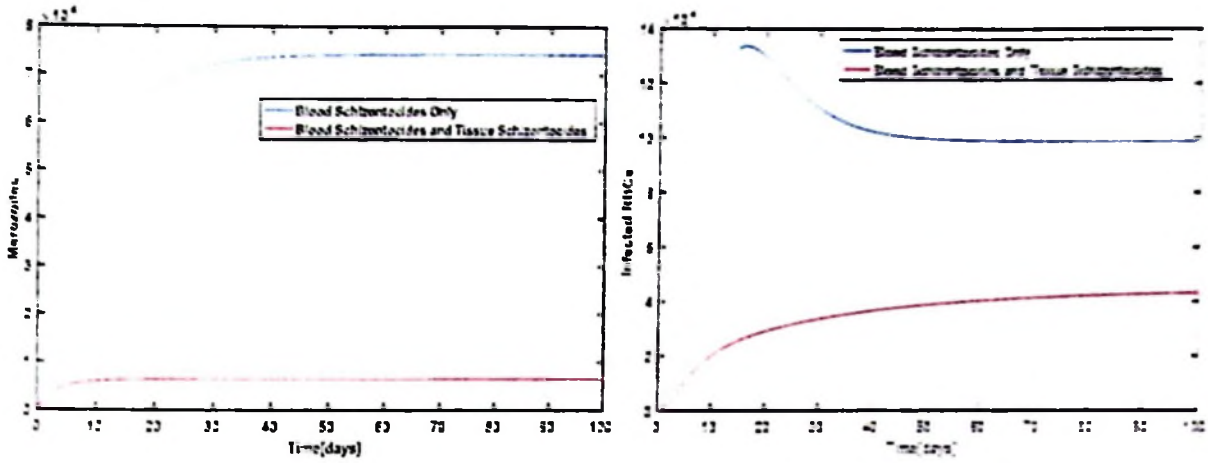

(a) Merozoites (b) Infected iRBCs

Figure 28: Comparison on the effects of blood schizonticides only and combination of blood schizonticide-tissue schizonticide on merozoites and infected iRBCs

When the effect of blood schizonticide-gametocide and blood schizonticide-sporontocide CT on reducing the number of gametes was assessed, the former indicates the superiority, as illustrated in Fig. 29. This recommends that it is better to destroy gametocytes before being ingested by a blood-seeking mosquito than to act on them after they have been sucked.

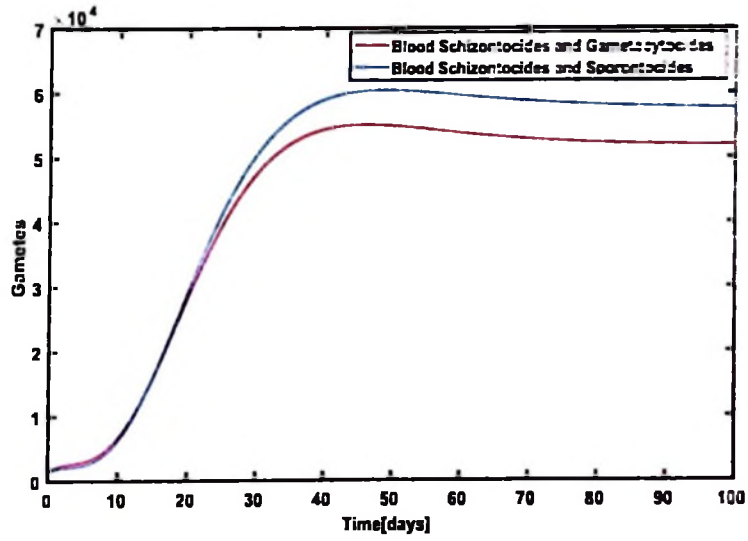

Figure 29: Comparison on the effects of blood schizonticide-gametocytocide and blood schizonticide-sporontocide CTs on gametes

Furthermore, the drug therapy (sporontocides) has shown positive results on the sporogonic stages of malaria parasites as it reduces the number of gametes that are able to undergo fusion and it eventually reduces the number of oocysts and sporozoites (See Fig. 30).

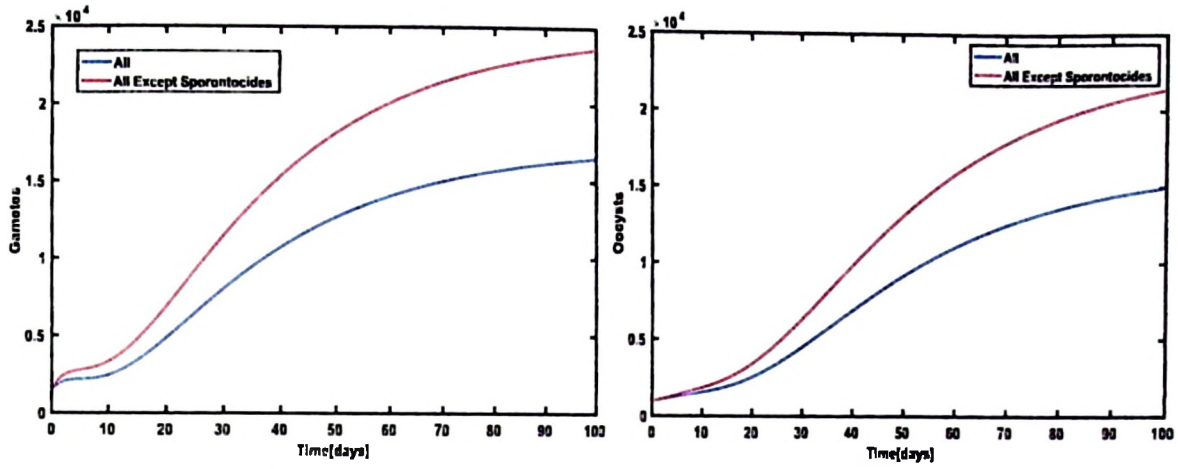

(a) Gametes (b) Oocysts

Figure 30: Effects of sporotocide on reducing the number gametes and oocysts

This suggests that, the sporontocides sucked up by mosquito in a blood meal inhibit the parasites' growth such as fusion of gametes within mosquito and hence leads to a non infective mosquito population. Consequently, it reduces onwards mosquito-human transmission.

Though the immunity has shown insignificant effect in pre-erythrocytic malaria (Selemani *et al.*, 2017), antimalarial therapy has shown a momentous effect on reducing malaria infection at this stage. Fig. 31 indicates the impact of tissue schizonticides on reducing the number of infected hepatocytes and hepatic schizonts.

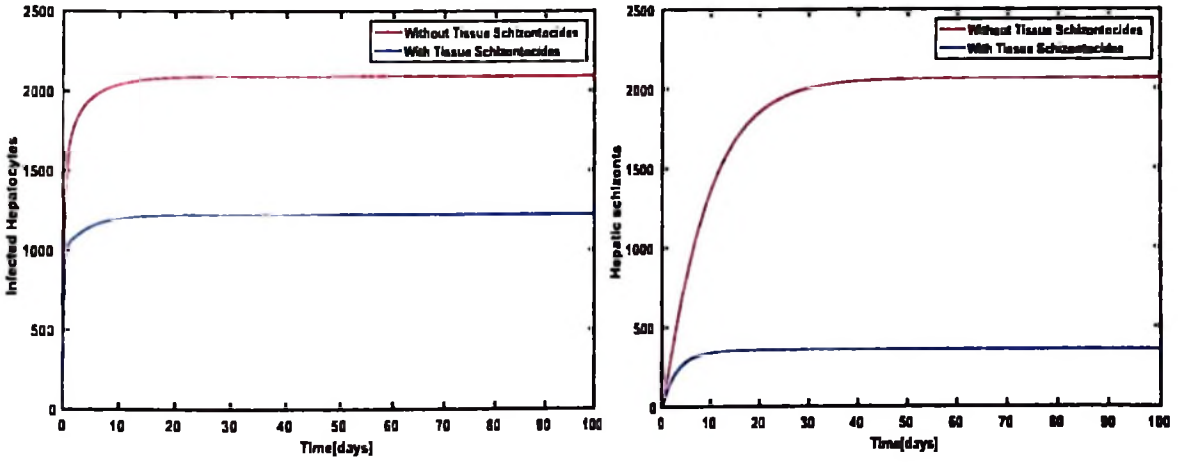

(a) Infected Hepatocytes (b) Hepatic schizonts

Figure 31: Effects of tissue schizonticides on reducing the number of infected hepatocytes and hepatic schizonts

Malaria transmission can be reduced using a CT with all four therapeutic classes of antimalarial drugs. Therefore, any CT with the following mechanisms is proposed: ability to suppress

infection (of hepatocytes from sporozoites) and destroy other infective hepatic stages, and thus prevent the initial erythrocytic infections; to act on erythrocytic asexual and sexual stages by suppressing the continuing production of, and destroying the existing parasites (merozoites and gametocytes); and to inhibit the parasites' development within an infected mosquito after gametocytes being ingested.

5.5 Conclusion

A mathematical model for the in-human host and in-human dynamics of malaria parasite with effect of immune responses and drug therapy was formulated and analyzed. The model is an extension of the work presented by Selemani *et al.* (2017), where the effect of drug therapy to destroy infected cells, schizonts and gametocytes, and suppressing merozoites' and gametocytes' production were incorporated. We also incorporated the therapy's effect to inhibit sporozoites from infecting hepatocytes and parasite's development within mosquito.

A positively invariant region, where the model is epidemiologically and mathematically well-posed was established. Using the next generation method, effective reproduction number $\mathcal{R}_e$ was computed. Existence and stability of two non-negative equilibrium points: malaria free equilibrium (MFE) and malaria infection equlibrium (MIE) were established. We also, proved that MFE is locally asymptotically stable and globally asymptotically stable (GAS) if $\mathcal{R}_e < 1$.

Additionally, it is noted that the efficacy of blood schizonticides to suppress production of merozoites from erythrocytic schizonts is higher than that of tissue schizonticides to suppress production of merozoites from hepatic schizonts. This is because τ_4, efficacy of blood schizonticides to suppress merozoites' prodcution appeared into the expression of $\mathcal{R}_e$, while τ_3, efficacy of tissue schizonticides to suppress production of merozoites does not appear.

Numerical simulations confirm that MIE exists, and is GAS irrespective of the initial values of state variables. Moreover, in comparison with the results of Selemani *et al.* (2016) and Selemani *et al.* (2017), our results revealed that inclusion of drug therapy significantly reduce infection in all stages. A remarkable decrease of infected (liver and blood) cells and parasites (at all life cycle stages) was noted. Although its components do not appear in the expression of reproduction number, tissue schizonticides manifest a marvelous effect on reducing the infection at each stage of malaria life cycle. Also, sporontocides ingested by mosquito during its blood meal indicate the effect on reducing the number of parasites within mosquito.

Based on the above results, this study proposes that a CT with all four classes of antimalarials should be developed because of its terrific effect on controlling malaria. An artemisinin derivatives-primaquine CT is proposed. This is because artemisinin derivatives are effective

against blood asexuals (blood schizonticidal activity) and gametocytes (gametocytocidal activity) for all species with exceptional of mature *P. falciparum* gametocytes. Primaquine is effective against hepatic schizonts (tissue schizonticidal activity) and gametocytes for all species (including mature gametocytes of *P. falciparum*). Moreover, the primaquine serves as sporontocide.

This work demonstrates how mathematical models are powerful tools for providing insights of complex systems. Since antimalarial drug therapies are age- and stage- specific, in subsequent work we propose the extension of the model to incorporate age structure to the parasite's and/or cells' populations.

CHAPTER SIX

General Conclusion and Recomendations

6.1 Summary

This work investigated the in-human host and in-mosquito dynamics of malaria parasite with effect of therapy. The general objective of this study was to formulate and analyze mathemtical models for in-human host and in-mosquito dynamics of malaria parasite in the entire life cycle with effects of stage-specific immune responses and drug therapy.

The general objective was achieved through three specific objectives which were to formulate and analyze: a basic mathematical model for in-human host and in-mosquito dynamics of malaria parasite; a mathematical model for in-human host and in-mosquito dynamics of malaria parasite with effect of immune responses; and, a mathematical model for in-human host and in-mosquito dynamics of malaria parasite with effect of immune responses and drug therapy. The developed models are sets of nonlinear ordinary differential equations which were analyzed using both analytical and numerical techniques.

6.2 Conclusion

A basic model developed in this work consists of twelve compartments; namely, uninfected hepatic liver cells (HLCs), infected HLCs, hepatic schizonts, merozoites, uninfected red blood cells (RBCs), infected RBCs, erythrocytic schizonts, gametocytes, gametes, oocysts, sporozoites in a mosquito in salivary glands, and sporozoites injected into a human host.

The developed model is epidemiologically and mathematically well-posed. Using the next generation method, a reproduction number was computed and found to be a function that depends only on erythrocytic parameters. This implies that the erythrocytic invasion may propagate without new infection from the liver. The impact of model parameters on control of malaria infection was assessed through the sensitivity analysis of reproduction number of the model as presented in Chapter 2. The infection rate of RBCs by merozoites, death rate of merozoites, and number of merozoites released per rupturing schizont are found be the most sensitive parameters. Despite having lower sensitivity index compared to death rate of merozoites, death rate of schizonts has greater impact on malaria control than that of merozoites. This is because each matured schizont bursts and releases an average of 16 merozoites.

Existence and stability of two non-negative equilibrium points: malaria free equilibrium (MFE) and malaria infection equilibrium (MIE) were established in Chapter 3. Using linearization of

the system. MFE is proved to be locally asymptotically stable. Moreover, by Metzler matrix theory and Lyapunov functional method, MFE and MIE are proved to be globally asymptotically stable, respectively.

In Chapter 4, an extension of the model was done in order to incorporate the effects of immunity on the malaria infection at various stages of *plasmodium*'s life cycle. Here, the effect of immune responses: to block the invasion of parasites (sporozoites and merozoites) on the uninfected cells (hepatic liver and red blood respectively), to inhibit the production of parasites (merozoites and gametocytes), and to clear of both parasites and infected cells were incorporated. Finally, the effect of antibodies on gametocytes picked-up during the blood meal was also included. In all cases, immune responses have been described using the nonlinear-bounded Michaelis-Menten-Monod function.

Analytical results show that effect of immune cells to suppress production of merozoites is higher than that of antibodies to block the invasion of sporozoites and merozoites into HLCs and RBCs respectively. Numerical simulations revealed that immunity has a significant influence on reducing infection at blood and mosquito stages only. An increase on number of uninfected RBCs, and a decrease on number of infected RBCs and free parasite (gametocytes) were noted. Also, antibodies picked-up by a mosquito during the blood meal show an influence on reducing the number of parasites within the mosquito. Moreover, longevity of immunity reduces number of parasites and infected cells in erythrocytic infection. Meaning that, as lifespan of immune cells increases the infection decreases.

A further extension to the model was made to incorporate the effect of drug therapy as shown in Chapter 5. Four therapeutic classes of antimalarial drugs namely, tissue schizonticides, blood schizonticides, gametocytocides and sporontocides were included at various stages of the *plasmodium*. The effect of drug therapy to destroy infected cells, schizonts and gametocytes; to suppress production of parasites (merozoites and gametocytes), and to inhibit sporozoites from infecting hepatocytes and parasite's development within mosquito was addressed.

Here, we deduce that the efficacy of blood schizonticides on suppressing production of merozoites is higher than that of tissue schizonticides. Numerical simulations indicate that drug therapy significantly reduces infection at all stages of *plasmodium's* life cycle. Sporontocides ingested by a mosquito during its blood meal have an effect on reducing the number of parasites within the mosquito. Although its components do not appear in the expression of reproduction number, tissue schizontocides exhibit a remarkable effect on reducing the infection at each stage of malaria life cycle.

Generally, mathematical models for in-human host and in-mosquito dynamics of malaria par-

asite developed in this work are simple presentations of complex dynamics of *plasmodium* within human host and mosquito vector. Their formulation and analysis (analytical and numerical) merely based on the predefined assumptions and chosen parameters. Despite these assumptions that have been made during the formulation for the sake of simplicity and analysis, this study provides a basic mathematical framework to explore complex dynamics of malaria parasite through its entire life cycle.

6.3 Significance of the Study

Understanding the interactions between malaria parasites, immune response and drug therapy is of great importance on development of safe and effective control strategies, and hence eradicate or reduce malaria transmission. This study has the following significances:

i) This work provides a base for further research on modelling the in-human host and in-mosquito dynamics for the entire life cycle of *plasmodium* as explained in Section 6.5.

ii) The knowledge obtained from this study can contribute to the design of safe and effective control strategies of the disease such as vaccination to stop sporozoites from infecting the hepatocytes, and a combination therapy that reduce or eliminates parasites' burden in all phases of life cycle.

iii) This study informs policy makers and stakeholders in health sector on the importance of using the combination therapy that fights malaria at various stages of *plasmodium's* life cycle to reduce burden inflicted by malaria. Therefore, this will not only save the lives of people but also will save the costs associated with persistence of malaria.

6.4 Recommendations

Based on the above results, this study proposes that the immune system should be boosted so as to improve their ability to suppress parasite's production in bloodstream. Also, causing lysis to gametocytes is of great importance in preventing parasite' development in mosquito as it may leads to a population of non-infectious mosquito: hence, reduce mosquito-human infection.

A combination therapy with all four classes of antimalarials should be developed because of its terrific effect on controlling malaria. An artemisinin derivatives-primaquine combination therapy is proposed. This is because artemisinin derivatives are effective against blood asexuals (blood schizontocidal activity) and gametocytes (gametocytocidal activity) for all species with exceptional of mature *P. falciparum* gametocytes, while primaquine is effective against hepatic schizonts (tissue schizontocidal activity) and gametocytes for all species (including mature gametocytes of *P. falciparum*). Moreover, the primaquine serves as sporontocide.

6.5 Future Work

As we pointed out in Chapter 4 that, malaria infection deteriorates with the increase in the lifespan of immune cells, therefore any mechanism that reduces the lifespan of immune cells increases the malaria infection. Therefore, this work can be extended to include the effect of immune responses and drug therapy to co-infection of malaria with another disease such as *human immunodeficiency virus* (HIV) or *Mycobacterium tuberculosis* (TB), that have a great effect on immune system.

Moreover, since antimalarial drug therapies are age- and stage- specific, we propose the extension of this work to incorporate age structure to the parasite's and/or cells' populations.

REFERENCES

Agusto, F. B., Marcus, N. and Okosun, K. O. (2012). Application of optimal control to the epidemiology of malaria. *Electronic Journal of Differential Equations.* **2012**(81): 1–22.

Anderson, R., May, R. and Gupta, S. (1989). Non-linear phenomena in hostarasite interactions. *Parasitology.* **99**(S1): S59–S79.

Artavanis-Tsakonas, K., Tongren, J. and Riley, E. (2003). The war between the malaria parasite and the immune system: Immunity, immunoregulation and immunopathology. *Clinical & Experimental Immunology.* **133**(2): 145–152.

Austin, D., White, N. and Anderson, R. (1998). The dynamics of drug action on the within-host population growth of infectious agents: Melding pharmacokinetics with pathogen population dynamics. *Journal of Theoretical Biology.* **194**(3): 313–339.

Bannister, L. and Sherman, I. (2009). Plasmodium. *In: Encyclopedia of Life Sciences (ELS).* John Wiley & Sons, Ltd: Chichester: **DOI**:10.1002/9780470015902.a0001970.pub2.

Boni, M. F., Buckee, C. O. and White, N. J. (2008). Mathematical models for a new era of malaria eradication. *PLoS Med.* **5**(11): e231.

Bullock, S. and Manias, E. (2013). *Fundamentals of pharmacology.* Pearson Higher Education AU. Frenchs Forest.

Cai, L. M., Lashari, A. A., Jung, I. H., Okosun, K. O. and Seo, Y. I. (2013). Mathematical analysis of a malaria model with partial immunity to reinfection. In: *Abstract and Applied Analysis.* Vol. 2013. Hindawi Publishing Corporation.

Cariboni, J., Gatelli, D., Liska, R. and Saltelli, A. (2007). The role of sensitivity analysis in ecological modelling. *Ecological Modelling.* **203**(1): 167–182.

Castillo-Chávez, C., Feng, Z. and Huang, W. (2002). On the computation of R_0 and its role in global stability. In: Castillo-Chávez, C, Blower, S, Van den Driessche, P, Kirschner, D and Yakubu, A.-A. (eds). *Mathematical Approaches for Emerging and Reemerging Infectious Diseases: An Introduction:* Springer. pp. 229–250.

Centers for Disease Control and Prevention (2015). Anopheles mosquitoes. `https://www.cdc.gov/malaria/about/biology/mosquitoes/`. Last accessed 12 November 2016.

Centers for Disease Control and Prevention (2016). Biology. https://www.cdc.gov/malaria/about/biology/. Accessed on 28 December 2016.

Chamwali, L. A. (2013). *The Economic burden of malaria in Tanzania*. PhD thesis. University of Dar es Salaam.

Chen, G. (2004). Stability of nonlinear systems. *Encyclopedia of RF and Microwave Engineering*.

Chitnis, N., Hyman, J. M. and Cushing, J. M. (2008). Determining important parameters in the spread of malaria through the sensitivity analysis of a mathematical model. *Bulletin of Mathematical Biology*. **70**(5): 1272–1296.

Chitnis, N., Smith, T. and Steketee, R. (2008). A mathematical model for the dynamics of malaria in mosquitoes feeding on a heterogeneous host population. *Journal of Biological Dynamics*. **2**(3): 259–285.

Chiyaka, C., Garira, W. and Dube, S. (2008). Modelling immune response and drug therapy in human malaria infection. *Computational and Mathematical Methods in Medicine*. **9**(2): 143–163.

Corradin, G. and Levitskaya, J. (2014). Priming of $CD8^+$ T cell responses to liver stage malaria parasite antigens. *Frontiers in Immunology*. **5**(527): 1–6.

Cravo, P., Culleton, R., Hunt, P., Walliker, D. and Mackinnon, M. J. (2001). Antimalarial drugs clear resistant parasites from partially immune hosts. *Antimicrobial Agents and Chemotherapy*. **45**(10): 2897–2901.

Cull, P. (1981). Global stability of population models. *Bulletin of Mathematical Biology*. **43**(1): 47–58.

Da, D. F., Churcher, T. S., Yerbanga, R. S., Yaméogo, B., Sangaré, I., Ouedraogo, J. B., Sinden, R. E., Blagborough, A. M. and Cohuet, A. (2015). Experimental study of the relationship between plasmodium gametocyte density and infection success in mosquitoes: Implications for the evaluation of malaria transmission-reducing interventions. *Experimental Parasitology*. **149**: 74–83.

Delves, M., Plouffe, D., Scheurer, C., Meister, S., Wittlin, S., Winzeler, E. A., Sinden, R. E. and Leroy, D. (2012). The activities of current antimalarial drugs on the life cycle stages of plasmodium: a comparative study with human and rodent parasites. *PLoS Med*. **9**(2): e1001169.

Iggidr, A., Kamgang, J.-C., Sallet, G. and Tewa, J.-J. (2006). Global analysis of new malaria intrahost models with a competitive exclusion principle. *SIAM Journal on Applied Mathematics*. **67**(1): 260–278.

Kajiwara, T., Sasaki, T. and Takeuchi, Y. (2015). Construction of Lyapunov functions for some models of infectious diseases in vivo: From simple models to complex models.. *Mathematical Biosciences and Engineering: MBE*. **12**(1): 117–133.

Kamgang, J. C. and Sallet, G. (2008). Computation of threshold conditions for epidemiological models and global stability of the disease-free equilibrium (DFE). *Mathematical Biosciences*. **213**(1): 1–12.

Kinyanjui, S. M. (2012). The immunology of malaria. In: Okwa, O. O. (ed). *Malaria parasites:* InTech. chapter 10, pp. 175–201.

Kiszewski, A. E. (2010). Blocking plasmodium falciparum malaria transmission with drugs: the gametocytocidal and sporontocidal properties of current and prospective antimalarials. *Pharmaceuticals*. **4**(1): 44–68.

Klein, E. (2013). Antimalarial drug resistance: A review of the biology and strategies to delay emergence and spread. *International Journal of Antimicrobial Agents*. **41**(4): 311–317.

Korobeinikov, A. (2004). Global properties of basic virus dynamics models. *Bulletin of Mathematical Biology*. **66**(4): 879–883.

Korobeinikov, A. and Maini, P. K. (2004). A Lyapunov function and global properties for sir and seir epidemiological models with nonlinear incidence. *Mathematical Biosciences and Engineering*. **1**(1): 57–60.

Labadin, J., Kon, C. and Juan, S. (2009). Deterministic malaria transmission model with acquired immunity. In: *Proceedings of the World Congress on Engineering and Computer Science*. Vol. 2. pp. 20–22.

Langhorne, J., Ndungu, F. M., Sponaas, A.-M. and Marsh, K. (2008). Immunity to malaria: more questions than answers. *Nature Immunology*. **9**(7): 725–732.

LaSalle, J. P. (1976). The stability of dynamical systems. Vol. 25. SIAM.
URL: *http://epubs.siam.org/doi/book/10.1137/1.9781611970432*

Laxminarayan, R. (2004). Act now or later? economics of malaria resistance. *The American Journal of Tropical Medicine and Hygiene*. **71**(2): 187–195.

Li, Y., Ruan, S. and Xiao, D. (2011). The within-host dynamics of malaria infection with immune response. *Mathematical Biosciences and Engineering*. **8**(4): 999–1018.

Life cycle (2015). http://www.malariasite.com/life-cycle/. Last accessed 16 November 2016.

Lungu, E. M., Kgosimore, M. and Nyabadza, F. (2007). Lecture notes: Mathematical epidemiology. http://personal.lut.fi/wiki/lib/exe/fetch.php/en/jablonska/lecturenotes.pdf. Last visited 24 August 2016.

Lutambi, A. M., Chitnis, N., Briët, O. J., Smith, T. A. and Penny, M. A. (2014). Clustering of vector control interventions has important consequences for their effectiveness: a modelling study. *PloS One*. **9**(5): e97065.

Lutambi, A. M., Penny, M. A., Smith, T. and Chitnis, N. (2013). Mathematical modelling of mosquito dispersal in a heterogeneous environment. *Mathematical Biosciences*. **241**(2): 198–216.

Mandal, S., Sarkar, R. R. and Sinha, S. (2011). Mathematical models of malaria-A review. *Malaria Journal*. **10**(202).

Mayxay, M., Chotivanich, K., Pukrittayakamee, S., Newton, P., Looareesuwan, S. and White, N. J. (2001). Contribution of humoral immunity to the therapeutic response in falciparum malaria.. *The American Journal of Tropical Medicine and Hygiene*. **65**(6): 918–923.

McQueen, P. G. and McKenzie, F. E. (2004). Age-structured red blood cell susceptibility and the dynamics of malaria infections. *Proceedings of the National Academy of Sciences of the United States of America*. **101**(24): 9161–9166.

Medicine for malaria venture (2016). Five species. http://www.mmv.org/malaria-medicines/five-species. Accessed on 31 January 2017.

Mpeshe, S. C., Luboobi, L. S. and Nkansah-Gyekye, Y. (2014*a*). Modeling the impact of climate change on the dynamics of rift valley fever. *Computational and Mathematical Methods in Medicine*. **2014**.

Mpeshe, S. C., Luboobi, L. S. and Nkansah-Gyekye, Y. (2014*b*). Stability analysis of the rift valley fever dynamical model. *Journal of Mathematical and Computational Science*. **4**(4): 740–762.

Nelson, K. E. and Williams, C. M. (2014). *Infectious disease epidemiology: theory and practice*. Jones & Bartlett Publishers. Burlington, USA.

Oaks Jr, S., Mitchell, V., Pearson, G. and Carpenter, C. (1991). Malaria: Obstacles and Opportunities. A report of the Committee for the Study on Malaria Prevention and Control:

Status Review and Alternatives Strategies. Division of International Health, Institute of Medicine. ISBN 0-309-04527-4. National Academy Press.

Onyido, A., Agbata, V., Umeanacto, P., Obiukwu, M. and Amadi, E. (2010). Malaria burden and vector abundance in a sub-urban community in the rainforest zone of Nigeria. *Nigerian Journal of Microbiology*. **24**(1): 2224–2230.

Pedro, S. A., Abelman, S., Ndjomatchoua, F. T., Sang, R. and Tonnang, H. E. (2014). Stability, bifurcation and chaos analysis of vector-borne disease model with application to rift valley fever. *PLoS ONE*. **9**(10): e108172. doi:10.1371/journal.pone.0108172.

Price, R. N. and Douglas, N. M. (2009). Artemisinin combination therapy for malaria: beyond good efficacy. *Clinical Infectious Diseases*. **49**(11): 1638–1640.

Prudêncio, M., Mota, M. M. and Mendes, A. M. (2011). A toolbox to study liver stage malaria. *Trends in Parasitology*. **27**(12): 565–574.

Selemani, M. A., Luboobi, L. S. and Nkansah-Gyekye, Y. (2016). On stability of the in-human host and in-mosquito of malaria parasites. *Asian Journal of Mathematics and Applications*. **Vol. 2016**: article ID ama0353, 23 pages.

Selemani, M. A., Luboobi, L. S. and Nkansah-Gyekye, Y. (2017). The in-human host and in-mosquito dynamics of malaria parasites with immune responses. *New Trends in Mathematical Sciences*. **5**(3): 182–202.

Singh, S., Shukla, J. and Chandra, P. (2005). Modelling and analysis of the spread of malaria: Environmental and ecological effects. *Journal of Biological Systems*. **13**(01): 1–11.

Sirimulla, S. (2007). *Drug design, molecular modelling, and QSAR studies of antimalarial mefloquine and artemisinin derivatives*. ProQuest LLC. Ann Arbor.

Smyth, J. D. and Wakelin, D. (1994). *Introduction to animal parasitology*. Cambridge University Press.

Stevenson, M. M. and Riley, E. M. (2004). Innate immunity to malaria. *Nature Reviews Immunology*. **4**(3): 169–180.

Targett, G., Drakeley, C., Jawara, M., von Seidlein, L., Coleman, R., Deen, J., Pinder, M., Doherty, T., Sutherland, C., Walraven, G. and Milligan, P. (2001). Artesunate reduces but does not prevent posttreatment transmission of plasmodium falciparum to anopheles gambiae. *Journal of Infectious Diseases*. **183**(8): 1254–1259.

WHO (2013). Factsheet on the world malaria report 2013. http://www.who.int/malaria/media/worldmalariareport2013/en. Last visited on 24 August, 2016.

WHO (2015). World malaria report 2015. http://www.who.int/malaria/publications/world-malaria-report-2015/report/en/. Last visited on 8 November, 2016.

Wickramasinghe, S. and Abdalla, S. (2000). Blood and bone marrow changes in malaria. *Best Practice & Research Clinical Haematology*. 13(2): 277–299.

Zhang, J., Jia, J. and Song, X. (2014). Analysis of an seir epidemic model with saturated incidence and saturated treatment function. *The Scientific World Journal*. 2014.

APPENDICES

Appendix A: Matlab Codes for Chapter Two

A.1. Function file for Chapter Two

```
%%%%%%%% The same function has been used in Chapter Three %%%%%%%%%%%%
function  dy=Basic_model(~,y)
dy=zeros(size(y));
%%%%%%%%%%%%%%%%%%%%%%%%%%%%%%%% Parameter Values %%%%%%%%%%%%%%%%%%%%%%%%
a=0.75; nu=20;q=0.09;r1=30000;lambda2=41500;muir=0.025;beta2=0.000002;r2
    =16;mugb=0.0000625;r3=1000; mur=0.0083;
b=150;beta1=0.001;lambda1=3000;muh=0.94;alpha1=0.1249;muth=0.029;theta=0.6;
    delta2=0.5;delta1=0.0975;%0.0975;r3=0.94
alpha2=0.145;mutr=0.185;rho=3;w=1;alpha3=0.07;mugm=0.052;delta3=0.05;muc
    =0.024;musm=40;mum=48; mush=0.0000000012;
muih=0.95;p=0.925923;
%%%%%%%%%%%%%%%%%%%%%%%%%%%%%%%% Definition of Variables %%%%%%%%%%%%%%%%%%%%%%%%
H=y(1);Ih=y(2);Th=y(3);M=y(4);R=y(5);Ir=y(6);
Tr=y(7);Gb=y(8);Gm=y(9);C=y(10);Sm=y(11);Sh=y(12);
%%%%%%%%%%%%%%%%%%%%%%%%%%%%%%%% Model Equations %%%%%%%%%%%%%%%%%%%%%%%%%%%%%%%%
dy(1)=lambda1-beta1*Sh*H-muh*H;
dy(2)=beta1*Sh*H-alpha1*Ih-muih*Ih;
dy(3)=alpha1*Ih-delta1*Th-muth*Th;
dy(4)=r1*delta1*Th+p*r2*delta2*Tr-beta2*R*M-mum*M;
dy(5)=lambda2-beta2*R*M-mur*R;
dy(6)=beta2*R*M-alpha2*Ir-muir*Ir;
dy(7)=alpha2*Ir-delta2*Tr-mutr*Tr;
dy(8)=(1-p)*r2*delta2*Tr-q*w*Gb-mugb*Gb;
dy(9)=rho*q*w*Gb-alpha3*Gm-mugm*Gm;
dy(10)=alpha3*Gm-delta3*C-muc*C;
dy(11)=r3*delta3*C-a*nu*Sm-musm*Sm;
dy(12)=a*b*nu-beta1*Sh*H-mush*Sh;
```

A.2. Effect of β_2 and μ_m on $\mathcal{R}_0$

```
%%%%%%% Effect of death rate of Merozites %%%%%%%%
%%%%%%% On number of uninfected RBCs %%%%%%%%%
clear
tspan=[0 80];
y0=[3000,0,0,2000,500000, 0,1000,3000,1500,1000,2000,2000];
hold on
%%%%%%%%%% m function K12.m is the same as Basic_model.m file %%%%%%%%%
[t,y]=ode45(@K11,tspan,y0);
plot(t,y(:,5),'r')%% Replace 5 by 6 for infected RBCs
hold on
```

```
% Replace value of mum in function K11.m file by 42, to get a function K12
[t,y]=ode45(@K12,tspan,y0);
plot(t,y(:,5),'b')% Replace 5 by 4 for Infected RBCs
hold on
% Replace value of mum in function K11.m file by 75, to get a function K13
[t,y]=ode45(@K13,tspan,y0);
plot(t,y(:,5),'g') % Replace 5 by 3 for Infected RBCs
hold on
% Replace value of mum in function K11.m file by 85, to get a function K14
[t,y]=ode45(@K14,tspan,y0);
plot(t,y(:,5),'r')% Replace 5 by 3 for Infected RBCs
legend('mu_m= 48','mu_m= 42','mu_m= 75','mu_m= 85')
xlabel('Time [days]')
ylabel('Uninfected RBCs')% Change the ylabel to respective variable
grid on
hold off
```

A.3. Effect of merozoites' death rate on RBCs

```
%%%%%%%%% Plotting to show the effect of beta2 on R0 %%%%%%%%%%%%%%%%%
clear all
 muir=0.025;delta2=0.115;r2=16; r0=5000000; p=0.925923;alpha2=0.145;
 mutr=0.185;mum=48; beta2=0:0.000001:0.0000120;
R0=beta2*r0*delta2*p*r2*alpha2./((delta2+mutr)*(alpha2+muir)*(beta2*r0+mum)
    );
plot(beta2, R0, 'r')
xlabel('Infection rate of Merozoites on RBCs, \beta_2')
ylabel('Reproduction number, {R_0}')
grid on
%%%%%%%%%%%% Plotting to show the effect of beta2 %%%%%%%%%%%%%%%%%%%%%
clear all
muir=0.025; beta2=0.000002;delta2=0.115;r2=16; r0=5000000; p=0.925923;
alpha2=0.145;mutr=0.185; mum=0:0.1:80;
R0=beta2*r0*delta2*p*r2*alpha2./((delta2+mutr)*(alpha2+muir)*(beta2*r0+mum)
    );
plot(mum, R0, 'r')
xlabel('Death rate of Merozoites, \mu_m')
ylabel('Reproduction number, {R_0}')
grid off
```

Appendix B: Matlab Codes for Chapter Three

B.1. Proving the existence of MIE for Model (3.1a)-(3.1o)

```
%%%%%%%% Plotting to Prove the Existence of MIE %%%%%%%%%%%%%%%%%%%%%%%%
%%%%%%%%%%%%%%%%%%%%%%% Figure 4.1  %%%%%%%%%%%%%%%%%%%%%%%%%%%%%%%%%%
clear;
tspan=[0 80];
%%%%%%%%%%%% Initial values of model variables %%%%%%%%%%%%%%%%%%%%%%%
y0=[3000,0,0,2000,500000, 0,1000,3000,1500,1000,2000,2000, 10,10, 0];
%%%%%%%%%%%%% Call for ODE SOLVER %%%%%%%%%%%%%%%%%%%%%%%%%%%%%%%%%%%%
[t,y]=ode45(@ImmunityOnly_model,tspan,y0);
%%%%%%%%%%%% Plotting Erythrocytic Dynamics %%%%%%%%%%%%%%%%%%%%%%%%%%
figure(1)
plot(t,y(:,4),'g',t,y(:,5),'r',t,y(:,6),'m',t,y(:,7),'b',t,y(:,8),'c')
legend('Merozoites', 'Uninfected RBCs','Infected RBCs','Blood-schizonts','
    Gametocytes')
xlabel('Time[days]')
ylabel('Erythrocytic cycle')
%%%%%%%%%%%% Plotting Pre-erythrocytic Dynamics %%%%%%%%%%%%%%%%%%%%%%%
figure(2)
plot(t,y(:,12),'g',t,y(:,1),'r',t,y(:,2),'m',t,y(:,3),'b')
legend('Sporozoites in human', 'Uninfected HCs','Infected HCs','Liver
    schizonts')
xlabel('Time[days]')
ylabel('Pre-erythrocytic cycle')
%%%%%%%%%%%%%% Plotting Sporogonic Dynamics %%%%%%%%%%%%%%%%%%%%%%%%%%%
figure(3)
plot(t,y(:,9),'g',t,y(:,10),'r',t,y(:,11),'b')
legend('Gametes', 'Oocysts','Sporozoites in salivary glands')
xlabel('Time[days]')
ylabel('Sporogonic cycle')
%%%%%%%%%%%% Plotting Dynamics of Immune Responses%%%%%%%%%%%%%%%%%%%%
figure(4)
plot(t, y(:,13),'g',t, y(:,14),'b',t,y(:,15),'r')
legend('Immune cells in liver-stage', 'Immune cells in blood-stage', '
    Antibodies')
xlabel('Time[days]')
ylabel('Immune responses')
hold off
```

B.2. Global Stability of MIE for Model (3.1a)-(3.1o)

```
%%%%%% Dynamics to prove global Asymptotic Stability of MIE %%%%%%%%%%%%
%%%%%%% Here are variations of Initial values of H only %%%%%%%%%%%%%%%
%%%%%%% Similar procedures have been used for other variables %%%%%%%%%%
clear;
%%%%%%%%%%%%%%%%%%%%%%%%%%%%%%%%%%%% H0=3000 %%%%%%%%%%%%%%%%%%%%%%%%%%%%
tspan=[0 100];
y0=[3000,0,0,2000,500000, 0,1000,3000,1500,1000,2000,2000];
[t,y]=ode45(@Basic_model,tspan,y0);
figure(1)
plot(t,y(:,1),':')
xlabel('Time[days]')
ylabel('Uninfected HLCs')
grid on
hold on
%%%%%%%%%%%%%%%%%%%%%%%%%%%%%%%%%%%% H0=5000 %%%%%%%%%%%%%%%%%%%%%%%%%%%%
tspan=[0 100];
y0=[5000,500,0,2000,500000, 0,1000,3000,1500,1000,2000,2000,10,10,0];
[t,y]=ode45(@Basic_model,tspan,y0);
figure(1)
plot(t,y(:,1),'g')
xlabel('Time[days]')
ylabel('Uninfected HLCs')
grid on
hold on
%%%%%%%%%%%%%%%%%%%%%%%%%%%%%%%%%%%%  H0=10000  %%%%%%%%%%%%%%%%%%%%%%%%%%%%
tspan=[0 100];
y0=[10000,0,0,2000,500000, 0,1000,3000,1500,1000,2000,2000,10,10,0];
[t,y]=ode45(@Basic_model,tspan,y0);
figure(1)
plot(t,y(:,1),'k')
xlabel('Time[days]')
ylabel('Uninfected HLCs')
grid on
hold on
%%%%%%%%%%%%%%%%%%%%%%%%%%%%%%%%%%%%%%%%%%%%%%%% H0=7500 %%%%%%%%%%%%%%%%%%%%%%%%%%%%%%%%%%%%%%%%%%%%
tspan=[0 100];
y0=[7500,0,0,2000,500000, 0,1000,3000,1500,1000,2000,2000,10,10,0];
[t,y]=ode45(@Basic_model,tspan,y0);
figure(1)
plot(t,y(:,1),'m')
xlabel('Time[days]')
ylabel('Uninfected HLCs')
grid on
hold on
```

```
tspan=[0 100];
y0=[500,10000,0,2000,500000, 0,1000,3000,1500,1000,2000,2000,10,10,0];
[t,y]=ode45(@Basic_model,tspan,y0);
figure(1)
plot(t,y(:,1),'-')
xlabel('Time(days)')
ylabel('Individual Hosts')
grid on
hold off
```

Appendix C: Matlab Codes for Chapter Four

C.1. Function file for Chapter Four

```
function  dy=ImmunityOnly_model(~,y)
dy=zeros(size(y));
%%%%%%%%%%%%%%%%%%%% Parameter values %%%%%%%%%%%%%%%%%%%%%%%%%%%%%%%%%%%%
a=0.75; nu=20; q=0.09; r1=30000; lambda2=41500; muir=0.025; beta2=0.000002;
r2=16;mugb=0.0000625;r3=1000; mur=0.02; b=150;beta1=0.001;lambda1=3000;
muh=0.94;alpha1=0.1249;muth=0.029;delta2=0.5;delta1=0.0975; alpha2=0.145;
mutr=0.185;rho=3;w=1;alpha3=0.07;mugm=0.052;delta3=0.05; muc=0.024;musm=40;
mum=48; mush=0.0000000012; muih=0.95;p=0.925923;c1=0.00001;c2=0.00003;
c3=0.000015;eta1=0.0001;epsilon_sh=0.0005;eta2=0.0004;epsilon_m=0.0007;
mub=0.4;sigmaih=0.000000009;epsilon_ih=0.0005;sigmath=0.00000001;
epsilon_th=0.0005;sigmair=0.00000001;epsilon_ir=0.0005;sigmatr=0.00000001;
epsilon_tr=0.0005;sigmagb=0.00000001;epsilon_gb=0.0005; sigmash
    =0.0000000009;
sigmam=0.00000001;lambdaz1=30;lambdaz2=30;gamma1=0.00005;gamma2=0.000046;
gamma3=0.0000463;gamma4=0.0000469;gamma5=0.000025;gamma6=0.000025;gamma7
    =0.000025;muz1=1.5;muz2=1.53;k1=0.035;k2=0.015;k3=0.03;
%%%%%%%%%%%%%%%%%%%% Definition of Variables
    %%%%%%%%%%%%%%%%%%%%%%%%%%%%%%%%%%%%
H=y(1);Ih=y(2);Th=y(3);M=y(4);R=y(5);
Ir=y(6);Tr=y(7);Gb=y(8);Gm=y(9);C=y(10);
Sm=y(11);Sh=y(12);Z1=y(13);Z2=y(14);B=y(15);
%%%Model equations are defind here
dy(1)=lambda1-(beta1*Sh*H)./(1+c1*B)-muh*H;
dy(2)=(beta1*Sh*H)./(1+c1*B)-alpha1*Ih-muih*Ih-(sigmaih*Z1*Ih)./(epsilon_ih
    +Ih);
dy(3)=alpha1*Ih-delta1*Th-muth*Th-(sigmath*Z1*Th)./(epsilon_th+Th);
dy(4)=(r1*delta1*Th)./(1+k1*Z1)+(p*r2*delta2*Tr)./(1+k2*Z2)-(beta2*R*M)
    ./(1+c2*B)-mum*M-(sigmam*Z2*M)./(epsilon_m+M);
dy(5)=lambda2-(beta2*R*M)./(1+c2*B)-mur*R;
dy(6)=(beta2*R*M)./(1+c2*B)-alpha2*Ir-muir*Ir-(sigmair*Z2*Ir)./(epsilon_ir+
    Ir);
dy(7)=alpha2*Ir-delta2*Tr-mutr*Tr-(sigmatr*Z2*Tr)./(epsilon_tr+Tr);
```

```
legend('All','All Except Sporontocides')
xlabel('Time[days]')
ylabel('Gametes')% Also change ylabel to 'Oocysts'
grid on
hold on
```

D.8. Effect of tissue schizonticides on infected HLCs and hepatic schizonts

```
%%% Effect of tissue schizontocides on infected hepatocytes. To observe the
%%% effect on hepatic schizonts replace 2 by 3 in an plot command.
clear
tspan=[0 100];
y01=[3000,0,0,2000,500000, 0,1000,3000,1500,1000,2000,2000,10,10,0];
y02=[3000,0,0,2000,500000, 0,1000,3000,1500,1000,2000,2000,10,10,0];
hold on
[t1,y01]=ode45(@ImmunityTherapy,tspan,y01);
% Replace values of tau1, tau2 and tau3 equal by zero in a function
% ImmunityTherapy to get a function ImmunityTherapy_Without_Tissue
[t2,y02]=ode45(@ImmunityTherapy_Without_Tissue,tspan,y02);
figure(1)
plot(t1,y01(:,2),'r',t2,y02(:,2),'b')
legend('Without Tissue Schizontocides', 'With Tissue Schizontocides')
xlabel('Time[days]')
ylabel('Infected HLCs')% Also change ylabel to 'Hepatic schizonts'
grid on
hold on
```

```
xlabel('Time[days]')
ylabel('Gametocytes')
grid on
hold on
```

D.6. Comparison of blood schizonticidal-gametocytocidal and blood schizonticidal-sporontocidal combination therapies

```
% Comparison of effect of blood schizonticidal-gametocytocidal and blood
% schizonticidal-sporontocidal combination therapies on gametes.
clear
tspan=[0 100];
y01=[3000,0,0,2000,500000, 0,1000,3000,1500,1000,2000,2000,10,10,0];
y02=[3000,0,0,2000,500000, 0,1000,3000,1500,1000,2000,2000,10,10,0];
hold on
% Replace values of taul, tau2, tau3 and tau9 equal by zero in a function
% ImmunityTherapy to get a function Blood_Gametocytocides
[t1,y01]=ode45(@Blood_Gametocytocides,tspan,y01);
% Replace values of taul, tau2 tau3, tau7 and tau8 equal by zero in a
    function
% ImmunityTherapy to get a function Blood_Sporontocides
[t2,y02]=ode45(@Blood_Sporontocides,tspan,y02);
figure(1)
plot(t1,y01(:,9),'r',t2,y02(:,9),'b')
legend('Blood Schizontocides and Gametocytocides','Blood Schizontocides and
    Sporontocides')
xlabel('Time[days]')
ylabel('Gametes')
grid on
hold on
```

D.7. Effect of Sporontocides on gametes and oocysts

```
%%% Effect of sporontocides on gametes. To observe the effect on oocysts
   replace 9
%%% by 10 in an plot command.
clear
tspan=[0 100];
y01=[3000,0,0,2000,500000, 0,1000,3000,1500,1000,2000,2000,10,10,0];
y02=[3000,0,0,2000,500000, 0,1000,3000,1500,1000,2000,2000,10,10,0];
hold on
[t1,y01]=ode45(@ImmunityTherapy,tspan,y01);
% Replace values of taul, tau2 and tau3 equal by zero in a function
% ImmunityThepary to get a function WithoutSporontocide
[t2,y02]=ode45(@WithoutSporontocide,tspan,y02);
figure(1)
plot(t1,y01(:,9),'r',t2,y02(:,9),'b')
```

D.4 Effect of blood tissue schizonticide

```
% Effect of blood schizonticidal, gametocidal and sporontocidal combination
% therapy. A plot by codes in this script shows effect on parasites. For
% other variables replace 4 in plot command by their corresponding equation
    number. That is, 5 for uninfected RBCs, 6 for infected RBCs, 8 for
    gametocytes, 9 for gametes and 10 for oocysts,
clear
tspan=[0 100];
y01=[3000,0,0,2000,500000, 0,1000,3000,1500,1000,2000,2000,10,10,0];
y02=[3000,0,0,2000,500000, 0,1000,3000,1500,1000,2000,2000,10,10,0];
hold on
[t1,y01]=ode45(@ImmunityTherapy,tspan,y01);
% Replace values of tau1, tau2 and tau3 equal to zero in a function
% ImmunityTherapy to get a function ImmunityTherapy_Without_Tissue
[t2,y02]=ode45(@ImmunityTherapy_Without_Tissue,tspan,y02);
figure(1)
plot(t1,y01(:,4),'r',t2,y02(:,4),'b')
legend('With Blood Schizontocides', 'With Tissue Schizonticides')
xlabel('Time (days)')
ylabel('Number of Cells')
grid on
hold on
```

D.5 Comparison of blood schizonticidal-gametocytocidal and blood schizonticidal-tissue schizonticidal combination therapies

```
% Comparison of blood schizonticidal-tissue schizonticidal and gametocidal
    and sporontocidal combination
% treatments. Given in this script gives a plot to show effect on gametocytes
    . For other variables replace 4 in plot command by their corresponding
    equation number. That is, 5 for uninfected RBCs, 6 for infected RBCs, 8
    for gametocytes, 9 for gametes and 10 for oocysts,
clear
tspan=[0 100];
y01=[3000,0,0,2000,500000, 0,1000,3000,1500,1000,2000,2000,10,10,0];
y02=[3000,0,0,2000,500000, 0,1000,3000,1500,1000,2000,2000,10,10,0];
hold on
% Replace values of tau1, tau2, tau3 and tau4 equal by zero in a function
% ImmunityTherapy to get a function Blood_Gametocytocides
[t1,y01]=ode45(@Blood_Gametocytocides,tspan,y01);
% Replace values of tau1, tau2 and tau4 equal by zero in a function
% ImmunityTherapy to get a function Blood_Tissue
[t2,y02]=ode45(@Blood_Tissue,tspan,y02);
figure(2)
plot(t1,y01(:,8),'r',t2,y02(:,8),'b')
legend('Blood and Gametocytocides','Blood Schizontocides and
```

```
y0=[7500,0,0,2000,500000, 0,1000,3000,1500,1000,2000,2000,10,10,0];
[t,y]=ode45(@ImmunityTherapy,tspan,y0);
figure(1)
plot(t,y(:,1),'r')
xlabel('Time[days]')
ylabel('Uninfected RBCs')
grid on
hold on
%%%%%%%%%%%%%%%%%%%%%%%%%%%%%% H0=100 %%%%%%%%%%%%%%%%%%%%%%%%%%%%%%
tspan=[0 100];
y0=[500,10000,0,2000,500000, 0,1000,3000,1500,1000,2000,2000,10,10,0];
[t,y]=ode45(@ImmunityTherapy,tspan,y0);
figure(1)
plot(t,y(:,1),'c')
xlabel('Time[days]')
ylabel('Uninfected RBCs')
grid on
hold off
```

D.3 Effect of immunity and therapy o reducing infections

```
%%%%%%%%% Effect of Immunity and Therapy on uninfected RBCs %%%%%%%%%%
clear
tspan=[0 100];
y01=[3000,0,0,2000,500000, 0,1000,3000,1500,1000,2000,2000];
y02=[3000,0,0,2000,500000, 0,1000,3000,1500,1000,2000,2000,10,10,0];
y03=[3000,0,0,2000,500000, 0,1000,3000,1500,1000,2000,2000,10,10,0];
[t1,y01]=ode45(@Basic_model,tspan,y01);
[t2,y02]=ode45(@ImmunityOnly_model,tspan,y02);
[t3,y03]=ode45(@ImmunityTherapy_model,tspan,y03);
hold on
figure(1)
plot(t1,y01(:,5),'b',t2,y02(:,5),'r',t3,y03(:,5),'g')
% To investigate effect on other variables, replace 5 by 6 (infected RBCs),
% 4 (for Merozoites), 8 (Gametocytes), 9 (for gametes), 10 (for oocysts)
% and 12 (for sporozoites in salivary
legend('No immune No therapy','With immune only', 'With immune and therapy'
    )
xlabel('Time[days]')
ylabel('Uninfected RBCs')
grid on
hold on
```

```
dy(11)=r3*delta3*C-a*nu*Sm-musm*Sm;
dy(12)=a*b*nu-(beta1*Sh*H)./(1+c1*B)-mush*Sh-(sigmash*Z1*Sh)./(pi_sh+Sh);
dy(13)=lambdaz1+((epsilon_sh*Sh)./(pi_sh+Sh)+(epsilon_ih*Ih)./(pi_ih+Ih)+(
    epsilon_th*Th)./(pi_th+Th))*Z1-muz1*Z1;
dy(14)=lambdaz2+((epsilon_m*M)./(pi_m+M)+(epsilon_ir*Ir)./(pi_ir+Ir)+(
    epsilon_tr*Tr)./(pi_tr+Tr)+(epsilon_gb*Gb)./(pi_gb+Gb))*Z2-muz2*Z2;
dy(15)=(eta1*Sh*Z1)./(pi_sh+Sh)+(eta2*M*Z2)./(pi_m+M)-mub*B;
```

D.2. Global Stability of MIE for Model (5.1a)-(5.1o)

```
%%%%% Dynamics to prove global Asymptotic Stability of MIE %%%%%%%%%%%%%
%%%%%%% Here are variations of initial values of H only %%%%%%%%%%%%%%%
%%%%%%% Similar procedures have been used for other variables %%%%%%%%%
clear;
%%%%%%%%%%%%%%%%%%%%%%%%%%%%%%%%% H0=3000 %%%%%%%%%%%%%%%%%%%%%%%%%%%%
tspan=[0 100];
y0=[3000,0,0,2000,500000, 0,1000,3000,1500,1000,2000,2000,10,10,0];
[t,y]=ode45(@ImmunityTherapy,tspan,y0);
figure(1)
plot(t,y(:,1),'r')
xlabel('Time[days]')
ylabel('Uninfected HLCs')
grid on
hold on
%%%%%%%%%%%%%%%%%%%%%%%%%%%%%%%% H0=5000 %%%%%%%%%%%%%%%%%%%%%%%%%%%%
tspan=[0 100];
y0=[5000,500,0,2000,500000, 0,1000,3000,1500,1000,2000,2000,10,10,0];
[t,y]=ode45(@ImmunityTherapy,tspan,y0);
figure(1)
plot(t,y(:,1),'g')
xlabel('Time[days]')
ylabel('Uninfected HLCs')
grid on
hold on
%%%%%%%%%%%%%%%%%%%%%%%% H0=10000 %%%%%%%%%%%%%%%%%%%%%%%%%%%%%%%%
tspan=[0 100];
y0=[10000,0,0,2000,500000, 0,1000,3000,1500,1000,2000,2000,10,10,0];
[t,y]=ode45(@ImmunityTherapy,tspan,y0);
figure(1)
plot(t,y(:,1),'b')
xlabel('Time[days]')
ylabel('Uninfected HLCs')
grid on
hold on
%%%%%%%%%%%%%%%%%%%%%%%%%%%%%%%% H0=7500 %%%%%%%%%%%%%%%%%%%%%%%%%%%%%%%%
tspan=[0 100];
```

```
hold off
```

Appendix D: Matlab Codes for Chapter Five

D.1. Function File for Chapter Five

```
function  dy=ImmunityTherapy_model(~,y)
dy=zeros(size(y));
%%%%%%%%%%%%%%%%%%%%%%%% Parameter Values %%%%%%%%%%%%%%%%%%%%%%%%%%%%%
a=0.75; nu=20;q=0.09;r1=30000;lambda2=41500;muir=0.025;beta2=0.000002;r2
    =16;mugb=0.0000625;
r3=1000; mur=0.02; alpha2=0.145;mutr=0.185;rho=3;w=1;alpha3=0.07;mugm
    =0.052;delta3=0.05;
muc=0.024;musm=40;mum=48; mush=0.0000000012;muih=0.95;p=0.925923;c1
    =0.00001;c2=0.00003;
eta1=0.4;pi_sh=2000;eta2=0.6;pi_m=1500;mub=0.4;sigmaih=0.000000009;pi_ih
    =2000;sigmath=0.00000001;
pi_th=2000;sigmair=0.00000001;pi_ir=2000; sigmatr=0.00000001; pi_tr=2000;
    sigmagb=0.00000001;pi_gb=2000;
sigmash=0.0000000009;sigmam=0.00000001;lambdaz1=30;lambdaz2=30;epsilon_sh
    =0.00005;epsilon_ih=0.000046;
epsilon_th=0.0000463;epsilon_m=0.0000469;epsilon_ir=0.000025;epsilon_tr
    =0.000025;epsilon_gb=0.000025;
muz1=1.5;muz2=1.53 ;k1=0.035;k2=0.015;k3=0.03;tau1=0.25;tau2=0.3;tau3=0.5;
    tau4=0.5;tau5=0.01;tau6=0.2;
tau7=0.3;tau8=0.01;tau9=0.3;
%%%%%%%%%%%%%%%%%%%%% Defition of Model Variables %%%%%%%%%%%%%%%%%%
H=y(1);Ih=y(2);Th=y(3);M=y(4);R=y(5);
Ir=y(6);Tr=y(7);Gb=y(8);Gm=y(9);C=y(10);
Sm=y(11);Sh=y(12);Z1=y(13);Z2=y(14);B=y(15);
%%%%%%%%%%%%%%%%%%%%%%%%%%%%Model Equations
    %%%%%%%%%%%%%%%%%%%%%%%%%%%%%%%%%%%%%%%%%
dy(1)=lambda1-(beta1*Sh*H)./(1+c1*B)-muh*H;
dy(2)=(1-tau1)*(beta1*Sh*H)./(1+c1*B)-(alpha1+muih+tau2)*Ih-(sigmaih*Z1*Ih)
    ./(pi_ih+Ih);
dy(3)=alpha1*Ih-(delta1+muth+tau2)*Th-(sigmath*Z1*Th)./(pi_th+Th);
dy(4)=(1-tau3)*(r1*delta1*Th)./(1+k1*Z1)+(1-tau4)*(p*r2*delta2*Tr)./(1+k2*
    Z2)-(beta2*R*M)./(1+c2*B)-(mum+tau5)*M-(sigmam*Z2*M)./(pi_m+M);
dy(5)=lambda2-(beta2*R*M)./(1+c2*B)-mur*R;
dy(6)=(beta2*R*M)./(1+c2*B)-(alpha2+muir+tau6)*Ir-(sigmair*Z2*Ir)./(pi_ir+
    Ir);
dy(7)=alpha2*Ir-(delta2+mutr+tau6)*Tr-(sigmatr*Z2*Tr)./(pi_tr+Tr);
dy(8)=(1-tau7)*((1-p)*r2*delta2*Tr)./(1+k2*Z2)-(q*w+mugb+tau8)*Gb-(sigmagb*
    Z2*M)./(pi_gb+Gb);
dy(9)=(1-tau9)*(rho*q*w*Gb)./(1+k3*B)-alpha3*Gm-mugm*Gm;
dy(10)=alpha3*Gm-delta3*C-muc*C;
```

```
dy(8)=((1-p)*r2*delta2*Tr)./(1+k2*Z2)-q*w*Gb-mugb*Gb-(sigmagb*Z2*M)./(
    epsilon_gb+Gb);
dy(9)=(rho*q*w*Gb)./(1+k3*B)-alpha3*Gm-mugm*Gm;
dy(10)=alpha3*Gm-delta3*C-muc*C;
dy(11)=r3*delta3*C-a*nu*Sm-musm*Sm;
dy(12)=a*b*nu-(beta1*Sh*H)./(1+c1*B)-mush*Sh-(sigmash*Z1*Sh)./(epsilon_sh+
    Sh);
dy(13)=lambdaz1+((gamma1*Sh)./(epsilon_sh+Sh)+(gamma2*Ih)./(epsilon_ih+Ih)
    +(gamma3*Th)./(epsilon_th+Th))*Z1-muz1*Z1;
dy(14)=lambdaz2+((gamma4*M)./(epsilon_m+M)+(gamma5*Ir)./(epsilon_ir+Ir)+(
    gamma6*Tr)./(epsilon_tr+Tr)+(gamma7*Gb)./(epsilon_gb+Gb))*Z2-muz2*Z2;
dy(15)=(eta1*Sh*Z1)./(epsilon_sh+Sh)+(eta2*M*Z2)./(epsilon_m+M)-mub*B;
```

C.2. Effect of immunity on RBCs, merozoites and gametocytes

```
%%%%%%%% Showing effect of immunity of Reducing Infection %%%%%%%%%%
clear
tspan=[0 80];
y01=[3000,0,0,2000,500000, 0,1000,3000,1500,1000,2000,2000];
y02=[3000,0,0,2000,500000, 0,1000,3000,1500,1000,2000,2000,10,10,0];
[t1,y01]=ode45(@Basic_model,tspan,y01);
[t2,y02]=ode45(@ImmunityOnly_model,tspan,y02);
hold on
%%%%%%%%%%% Effect of immunity on unfected RBCs %%%%%%%%%%%%%%%%%%
figure(1)
plot(t1,y01(:,5),'b',t2,y02(:,5),'r')
legend('without immune','with immune')
xlabel('Time[days]')
ylabel('Uninfected RBCs')
grid on
hold on
%%%%%%%%%%% Effect of immunity on Merozoites %%%%%%%%%%%%%%%%%%
figure(2)
plot(t1,y01(:,4),'b',t2,y02(:,4),'r')
legend('without immune','with immune')
xlabel('Time[days]')
ylabel('Merozoites')
grid on
hold on
%%%%%%%%%% Effect of immunity on gametocytes %%%%%%%%%%%%%%%%%%
figure(3)
plot(t1,y01(:,8),'b',t2,y02(:,8),'r')
legend('without immune','with immune')
xlabel('Time[days]')
ylabel('Gametocytes')
grid on
```

```
hold on
%%%%%%%%%%% Effect of Immunity on Gametes %%%%%%%%%%%%%%%%%%
figure(4)
plot(t1,y01(:,8),'[illegible]',t2,y02(:,8),'[illegible]')
legend('without immune','with immune')
xlabel('Time[days]')
ylabel('Gametocytes')
grid on
hold on
```

C.3. Effect of immune responses' life span on RBCs, merozoites and gametocytes

```
% %%%%% Effect of life span of Immune Cells %%%%%%%%
%%%%%%%% on number of infected RBCs %%%%%%%%%
clear
tspan=[0 80];
y0=[3000,0,0,2000,500000, 0,1000,3000,1500,1000,2000,2000,10,10,0];
hold on
%%% A function J11 is obtained when we take muz1=1.50;muz2=1.50 in Function
    ImmunityOnly_model %%%
[t,y]=ode45(@J11,tspan,y0); %Replace 6 by 4 (merozoites),5 (Uninfected RBCs
  ), 8 (Gametocytes)
plot(t,y(:,6),'[illegible]') %Replace 6 by 4 (merozoites),5 (Uninfected RBCs), 8 (
  Gametocytes)
hold on
%%% A function J12 is obtained when we take muz1=1.25;muz2=1.25 in Function
    ImmunityOnly_model %%%
[t,y]=ode45(@J12,tspan,y0);
plot(t,y(:,6),'[illegible]')% Replace 6 by 4 (merozoites),5 (Uninfected RBCs), 8 (
  Gametocytes)
%%% A function J13 is obtained when we take muz1=1.00;muz2=1.00 in Function
    ImmunityOnly_model %%%
[t,y]=ode45(@J13,tspan,y0);
plot(t,y(:,6),'g') %Replace 6 by 4 (merozoites),5 (Uninfected RBCs), 8 (
  Gametocytes)
hold on
%%% A function J14 is obtained when we take muz1=0.75;muz2=0.75 in Function
    ImmunityOnly_model %%%
[t,y]=ode45(@J14,tspan,y0);
plot(t,y(:,6),'[illegible]')% Replace 6 by 4 (merozoites),5 (Uninfected RBCs), 8 (
  Gametocytes)
legend('\mu_{z}_1=1.50, \mu_{z}_2=1.50','\mu_{z}_1=1.25, \mu_{z}_2=1.25','\
  mu_{z}_1=1.00, \mu_{z}_2=1.00','\mu_{z}_1=0.75, \mu_{z}_2=0.75')
xlabel('Time[days]')
ylabel('Infected RBCs')%% Change the ylabel to respective variable
grid on
```